THE ROLE OF MITOCHONDRIA IN DIRECT NEURONAL REPROGRAMMING AND ITS RELEVANCE FOR DISEASE

Giovanna Rose Sonsalla

Graduate School of Systemic Neurosciences

LMU Munich

Dissertation der
Graduate School of Systemic Neurosciences der
Ludwig-Maximilians-Universität München

May 28th, 2021

Supervisor
Prof. Dr. Magdalena Götz
Head of Department of Physiological Genomics
BioMedical Center - BMC
Ludwig-Maximilians-Universität München

Institute of Stem Cell Research
Helmholtz Zentrum München

First Reviewer: Prof. Dr. Magdalena Götz
Second Reviewer: Dr. Silvia Cappello
External Reviewer: Prof. Dr. Alessandro Prigione

Date of Submission: 28.05.2021
Date of Defense: 09.09.2021

Index

Abstract

Cell reprogramming methods have been studied extensively in recent years as a strategy to replace the neuronal cells lost in injury or disease. Much progress has been made regarding the direct conversion of murine astrocytes and fibroblasts into neurons, however, there are still many limitations that need to be overcome before these strategies can be relevant for clinical applications. One of the major reprogramming hurdles recently identified is the metabolic switch from glycolysis to oxidative phosphorylation (oxphos) that occurs as astrocytes adopt a neuronal identity. The forced cellular transition requires remodeling of the metabolic machinery, leading to increased stress and cell death. In order to overcome this impediment to efficient reprogramming, my PhD projects focused on further understanding the changes in mitochondrial metabolism during reprogramming, and alleviating the stress associated with this change. One of my projects investigated the conversion of murine astrocytes into neurons and delved into the mitochondrial proteome of astrocytes and neurons. Unique pathways for each cell type were discovered, and by upregulating neuron-enriched proteins in murine astrocytes undergoing reprogramming, a significant improvement in the efficiency of the conversion process was obtained. My second project analyzed the role of the mitochondria during neuronal reprogramming in human astrocytes and fibroblasts. Functional oxphos metabolism was shown to be necessary for human neuronal conversion as well, as cells with a mitochondrial deficiency were significantly hindered in their reprogramming ability. The unfolded protein response (UPR) pathway of the endoplasmic reticulum was shown to have a novel role in direct neuronal reprogramming, and inhibition of this pathway could increase reprogramming efficiency even in cells with a mitochondrial deficiency in Complex I of the electron transport chain. Therefore, the aim of my thesis was to improve the current strategies for neuronal replacement by untangling the mechanisms related to the metabolic shift and identifying viable treatments for increasing conversion efficiency.

Introduction

1. Introduction

The Central Nervous System (CNS) is composed of the brain and the spinal cord, and it is responsible for integrating information and directing activity across the body. Although the CNS is a very impressive and well-orchestrated system, the complexity and careful balancing of its many components provides ample opportunity for things to go awry. The failure of the system can be clearly seen in neurodegenerative diseases, which are increasing in prevalence worldwide and result in a tremendous strain on society through the disease-related health costs (Chen et al., 2016; Gan et al., 2018). Therefore, further understanding the mechanisms underlying these diseases and swiftly discovering viable treatments is imperative. Although some of the same elements are found in both acute traumatic brain injury and chronic injury (disease), for the purpose of this thesis the focus will be on chronic disorders.

The loss of functional neurons is one of the hallmarks of neurodegenerative diseases, resulting largely from the reduction of oxygen and metabolic substrates (Gan et al., 2018). Neurons are especially susceptible to sub-optimal environments due to their high energy requirements (Harris et al., 2012). A steady flow of glucose and oxygen is required for proper brain function, and although accounting for only 2% of all body mass, the high metabolic demand of the brain cellular environment causes it to consume 20% of the metabolic energy (Dienel, 2019). In order to help meet these high energy demands, glial cells such as oligodendrocytes and astrocytes play crucial roles due to their metabolic resilience and plasticity (Amaral et al., 2013; Magistretti & Allaman, 2015; Morita et al., 2019). Indeed, the majority of astrocytes have endfeet that cover brain vessels, and thus are able to exert control of the nutrients and substrates that flow from the periphery across the blood-brain-barrier (BBB) (Mathiisen et al., 2010). Astrocytes are a prominent glia cell in the mammalian brain, comprising 20-40% of all glia cells and being responsible for a myriad of functions (Liddelow & Barres, 2017; Verkhratsky & Nedergaard, 2018). These tasks range from the regulation of cerebral metabolism and blood flow (Attwell et al., 2010; Iadecola & Nedergaard, 2007) to neurotransmission and neurodevelopment (Chung et al., 2015).

The complicated interaction between neurons and astrocytes adds further complexity to the therapeutic strategies for neurodegenerative diseases. One of the most promising options to replace the loss of functional neurons is to directly reprogram other somatic cell types into

neurons (Gascón et al., 2017; Lu & Yoo, 2018; Masserdotti et al., 2015). Indeed, the direct neuronal reprogramming of both murine and human fibroblasts (Pang et al., 2011; Vierbuchen et al., 2010) and glial cells (Berninger et al., 2007; Heinrich et al., 2010) has been achieved. However, as will be discussed in more detail later, there are still many obstacles that hamper complete maturation of the induced neurons, as well as prevent a high reprogramming efficiency. In particular, the metabolic barriers to reprogramming are not well understood (Gascón et al., 2017). A greater understanding of mitochondrial metabolism is not only relevant for neuronal conversion, but is also imperative for directly treating disease pathology, as disruptions to energy generation and increased oxidative damage are common characteristics of disease (Watts et al., 2018).

I will first introduce the very different metabolic profile of neurons and astrocytes, and then examine the molecular and functional reasons underlying their differences. I will discuss that in spite of these differences, the roles of neurons and astrocytes in the CNS are extremely interconnected and they cooperate synergistically. I shall then consider the effect of mitochondrial dysfunction on neuron and astrocyte function, and its role in neurodegenerative diseases. Next, I will discuss the therapeutic strategy of direct neuronal reprogramming, and the hurdle of the metabolic switch during forced cell fate conversion. I will conclude by considering patients suffering from a mitochondrial disorder and examine what can be learned from these patients to further understand and alleviate the metabolic disruptions that occur in numerous diseases.

1.1 Metabolism in the CNS: focus on astrocytes and neurons

One of the predominant sources of energy for cells in the brain is glucose (Mergenthaler et al., 2013). Glucose is used for the generation of building blocks for biosynthesis and reducing equivalents for powering redox reactions. Many metabolic intermediates of glucose, such as lactate, pyruvate, acetate, and glutamate, can be further processed to generate energy (Zielke et al., 2009). As will become clear below, the different cell types in the brain preferentially send glucose down different pathways as they balance their bioenergetic demands with their antioxidant needs. The synergistic interactions of different cell types, especially neurons and glia, allow them to maintain their delicate metabolic homeostasis.

The two major pathways used by cells to generate energy through glucose metabolization are oxidative phosphorylation (oxphos) and glycolysis. Both pathways utilize glucose to form adenosine-5′-triphosphate (ATP), which is a main energy currency in the brain. However, one molecule of glucose processed through the glycolytic pathway only generates 2 ATP molecules, whereas oxphos yields 36 molecules of ATP (Camandola & Mattson, 2017). Astrocytes are able to flexibly use both pathways for energy generation, whereas neurons rely more on the oxphos pathway to meet their high energy demands (Bélanger et al., 2011; Kasischke et al., 2004). Despite the strikingly lower metabolic efficiency demonstrated by glycolysis, the pathway compensates by providing reducing equivalents such as reduced nicotinamide adenine dinucleotide (NADH) and reduced flavin adenine dinucleotide ($FADH_2$), which are essential for oxphos function and many other metabolic reactions (Camandola & Mattson, 2017). Notwithstanding their differences, neurons and astrocytes actually have complementary metabolic profiles, as will be discussed in more detail below. The main glucose metabolic pathways and their different roles in neurons and astrocytes will be introduced in more detail first, before synergistic activity is described.

1.1.1 Glucose metabolic pathways

Before glucose can be metabolized, it enters neurons, glia, and endothelial cells through their respective glucose transporters (GLUTs) (Thorens & Mueckler, 2010). The enzyme hexokinase (HK) then proceeds to phosphorylate glucose and produce glucose-6-phosphate (G6P), which can be utilized by different metabolic pathways (Mergenthaler et al., 2013). As can be seen in Figure 1, the main routes for G6P to traverse include (1) glycogenesis, (2) the pentose phosphate pathway (PPP), and (3) glycolysis with the downstream choices of either (a) mitochondrial metabolism in the form of oxphos, or (b) lactate production. Both neurons and astrocytes can utilize PPP and glycolysis, however, only astrocytes can take advantage of the first pathway, glycogenesis, and store glucose energy in the form of glycogen (Camandola & Mattson, 2017).

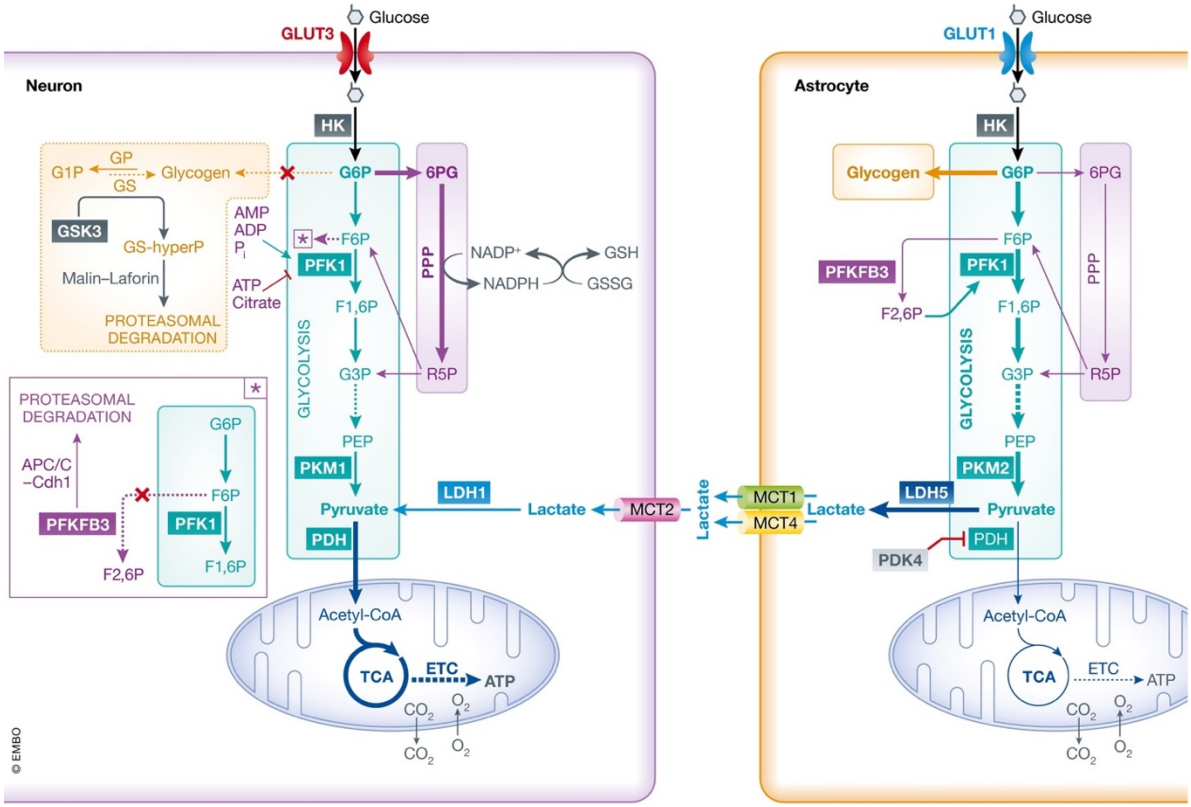

Figure 1. *Schematic overview of the different glucose metabolic pathways, highlighting the differences between neurons and astrocytes*. (Camandola & Mattson, 2017; License Number: 5076090684520)

Throughout the body, glycogen is mainly localized to the skeletal muscle and liver where it appears at much higher concentrations than in the brain (Nelson et al., 1968). However, despite its relatively low concentrations, brain glycogen has been shown to be instrumental in aiding astrocyte support to neurons (Brown, 2004; Swanson & Choi, 1993). Glycogen phosphorylase (GP) is present mainly in astrocytes, which contain both the skeletal muscle and brain isoforms of the enzyme (Pfeiffer-Guglielmi et al., 2003). The presence of two isozymes in astrocytes indicates the cells' ability to manipulate glycogen in response to extracellular as well as intracellular signals. In contrast, neurons contain GP to a much lower percent, and then only the brain isoform (Pfeiffer-Guglielmi et al., 2003). Furthermore, although neurons contain muscle glycogen synthase (MGS), and thus have the ability to synthesize glycogen, the MGS enzyme has reduced activity in these cells due to proteasomal degradation and the prevalence of its phosphorylated state (Vilchez et al., 2007). Astrocytes are therefore able to store glycogen as a future energy source, which is instrumental during periods of heightened activity, considering that astrocytes can break glycogen down into lactate and provide it to neighboring neurons (Pellerin & Magistretti, 1994; Rich et al., 2019). Indeed, a distinct functional role for

the energy produced through glycogenesis has been shown *in vitro* (Sickmann et al., 2009), as well as *in vivo* (Gibbs et al., 2006; Suzuki et al., 2011).

The PPP branch is distinct from the other pathways because it does not generate ATP but instead uses G6P to furnish the cell with ribose 5-phosphate (R5P) and reduced nicotinamide adenine dinucleotide phosphate (NADPH) (Bélanger et al., 2011). The redox energy from NADPH is essential for the synthesis of non-essential amino acids and fatty acids, while R5P is used as a main component for nucleotide biosynthesis (Bélanger et al., 2011). In addition, NADPH is used to regenerate the antioxidant glutathione, thus providing protection for the cell against oxidative stress (Bolaños et al., 2010). Therefore, glucose is sent down different pathways depending on the specific needs of the different cell types, as both the ATP energy demands, and the antioxidant needs of the cell need to be met. The cell-specific metabolic profiles of astrocytes and neurons will continue to be examined as the other glucose metabolism pathways are introduced.

The third option, glycolysis, turns G6P into pyruvate through multiple reactions catalyzed by 10 different enzymes. The glycolytic reactions also generate two molecules of ATP, as mentioned previously, and essential cofactors such as NADH, $FADH_2$, and coenzyme A (CoA). The ability of astrocytes to flexibly use glycolysis is supported by their high expression of 6-phosphofructo-2-kinase/fructose-2,6-bisphosphatase 3 (PFKFB3) (Herrero-Mendez et al., 2009). The glycolytic pathway is stimulated by PFKFB3 because it generates a main driver of the pathway, fructose-2,6-bisphosphate (fructose-2,6-BP). Conversely, neurons are limited in their use of glycolysis, because PFKFB3 is constantly undergoing proteasome degradation and, as a result, is only present at low levels (Herrero-Mendez et al., 2009). The pyruvate generated through glycolysis can then be used in two different ways depending on the metabolic requirements of the cell and the presence of oxygen.

In aerobic conditions where oxygen is present, pyruvate is transported to the mitochondria and converted into acetyl coenzyme A (acetyl-CoA). Pyruvate follows this pathway preferentially in neurons, because the enzyme pyruvate dehydrogenase (PD) that converts pyruvate into acetyl-CoA is present in neurons to a greater degree in its active form (Itoh et al., 2003; Zhang et al., 2014). In contrast, astrocytes highly express pyruvate dehydrogenase kinase isoform 4 (PDK4), which phosphorylates and consequently inhibits the activity of PD. Therefore, the fraction of inactive PD is higher in astrocytes, leading to a reduced production of acetyl-CoA

from pyruvate (Itoh et al., 2003; Zhang et al., 2014). Regardless, once acetyl-CoA is produced, the tricarboxylic acid (TCA) cycle within the mitochondria uses it to generate even more of the energetic cofactors mentioned above, NADH and $FADH_2$. The TCA cycle also provides many amino acids and lipids to the cell (Akram, 2014). The reduced cofactors NADH and $FADH_2$ are then used along with oxygen to power the metabolic machinery of oxphos, known as the electron transport chain (ETC), composed of five complexes present at the inner mitochondrial membrane (IMM) (Wilson, 2017). Electrons are passed from NADH and $FADH_2$ through the different ETC complexes, and this in turn powers the transfer of protons (H^+) across the IMM. The resulting electrochemical gradient is then able to propel the synthesis of ATP by Complex V, ATP synthase (Wilson, 2017). The ETC will be discussed later in more detail.

In anaerobic conditions, pyruvate is diverted from the TCA cycle and is instead used for lactate production. In astrocytes, instead of sending pyruvate through to the mitochondria the cells prefer to convert pyruvate into lactate using the lactate dehydrogenase 5 (LDH5) enzyme (Magistretti & Allaman, 2018). Not only do astrocytes have a lower activity of PD and subsequent reduced generation of acetyl-CoA as mentioned above, but astrocytes also express much higher levels of LDH5 than neurons (Bittar et al., 1996). The LDH5 form of LDH favors converting pyruvate into lactate, whereas the LDH1 enzyme found more often in neurons prefers to convert lactate into pyruvate (Bittar et al., 1996). The pyruvate produced through glycolysis can thus either be directly channeled to the oxphos pathway for energy generation or converted into lactate. Interestingly, astrocytes can provide lactate to neighboring neurons during times of high activity as a method of metabolic support (Pellerin & Magistretti, 1994).

As has become apparent, energy generation varies greatly between astrocytes and neurons. Astrocytes have more flexibility to meet their metabolic needs, whereas neurons funnel glucose preferentially through the PPP branch and supplement their oxphos machinery with lactate from neighboring astrocytes. Indeed, when oxphos was inhibited in primary cultures of rat cells, astrocytes were able to recover their ATP levels through the glycolytic pathway, whereas neurons failed to recover (Almeida et al., 2001). Even *in vivo*, when astrocytes were unable to use oxphos as a form of energy production, there was no evidence of their survival being affected (Supplie et al., 2017). To understand the mechanisms underlying these results, it has been shown that when oxidative respiration is inhibited, astrocytes can compensate by upregulating glycolysis activator 6-phosphofructo-1-kinase (PFK1), whereas neurons are unable to compensate in a similar fashion (Almeida et al., 2004). However, the failure of

neurons to utilize glycolysis to the same extent as astrocytes is not a failure of the system. In contrast, when glycolysis in neurons was enhanced through transfection with the glycolytic driver PFKFB3, it actually led to increased oxidative stress and ultimately neuronal cell death through apoptosis (Herrero-Mendez et al., 2009). The bioenergetic differences between astrocytes and neurons can even be distinguished in terms of their ETC subunit assembly, as the Complex I supercomplexes more often found in neurons were correlated with their reduced reactive oxygen species (ROS) production compared to astrocytes (Lopez-Fabuel et al., 2016). Therefore, the preferred energy generation pathways are carefully chosen based on the neuroprotective abilities of the cell.

1.1.2 Alternative metabolic pathways

Although the metabolism of glucose is a main source of energy, the complexity and high energy demand of the mammalian brain necessitate alternative routes of energy production. Fatty acid oxidation is one such track, which accounts for up to 20% of brain energy requirements (Panov et al., 2014). It is postulated that fatty acid oxidation occurs primarily in astrocytes as an extra source of ATP generation that allows them to further metabolically support neurons. As was mentioned previously, astrocytes are able to produce lactate from pyruvate and provide the lactate to neurons, rather than allowing pyruvate to be converted into acetyl-CoA, enter the TCA cycle and subsequently generate ATP through oxphos. In order to still obtain enough ATP to maintain their cellular functions, astrocytes need another option to power their oxphos pathway. Indeed, in astrocytes, fatty acids are the favored substrate for producing acetyl-CoA, which they accomplish by undergoing β-oxidation (Panov et al., 2014). One of the reasons β-oxidation of fatty acids is not as prominent in neuronal cells is because this pathway has multiple sites of ROS generation, and thus challenges the low oxidative stress threshold of neurons (Perevoshchikova et al., 2013; Schönfeld & Reiser, 2013).

Another additional metabolic substrate for ATP generation is glutamate, which can also be processed and fed into the TCA cycle (McKenna, 2007; Schousboe, 2019). Traditionally, glutamate is viewed as a main excitatory neurotransmitter in the brain that is essential for cell signaling. During neurotransmission, glutamate released into the synapse stimulates activity on the post-synaptic neurons and is then cleared from the extracellular space by astrocytes. Glutamate is subsequently converted into glutamine by astrocytes and transferred to neighboring neurons, where it can be deamidated back to glutamate and used for further

neurotransmission. Alternatively, glutamate can be transformed to α-ketoglutarate and enter the TCA cycle (McKenna, 2013; McKenna et al., 2016). Astrocytes can utilize glutamate as a substrate for the TCA cycle (Nissen et al., 2015), but neurons have also been shown to employ this metabolic option, which can be crucial for preventing glutamate accumulation and the resultant excitotoxicity (Divakaruni et al., 2017).

Therefore, although similar metabolic energy pathways are present in both astrocytes and neurons, their cell-specific functions cause them to preferentially utilize select avenues, which is enforced by the expression of specific enzymes and transporters in each cell type. Neurons favor the PPP pathway over the glycolytic pathway and are unable to utilize the third option of storing glucose as glycogen. The end compound of pyruvate obtained directly through glycolysis, or indirectly in the form of lactate provided by astrocytes, is then funneled into the oxphos energy pathway in the mitochondria. In contrast, the metabolic profile of astrocytes shows greater flexibility, as they are able to use glucose for glycogen synthesis and subsequent energy storage, and when oxphos is blocked they are better able to compensate with the glycolytic pathway for energy generation.

1.2 Astrocyte and neuron interaction

It was shown more than 30 years ago (Rosenberg & Aizenman, 1989), and has been demonstrated consistently in the years following (Mederos et al., 2018; Wade et al., 2011), that astrocytes provide essential support to neurons through a variety of crosstalk mechanisms. Astrocytes protect neurons against excitotoxicity (Rothstein et al., 1996) and oxidative stress (Drukarch et al., 1998), as well as provide transmitophagy (Davis et al., 2014; Morales et al., 2020). A more novel method of support was recently proposed, whereby astrocytes provide functional mitochondria to neurons in a mouse model of ischaemic stroke (Hayakawa et al., 2016) or following traumatic brain injury (Ren et al., 2021); although this is still debated (Berridge et al., 2016).

This neuroglia interplay is especially essential for buffering the relatively low toxicity threshold of neurons. For example, fatty acids generated by neurons during periods of high activity can be transferred to astrocytes, where they are subsequently broken down and, as a result, do not become toxic to the neuronal cells (Ioannou et al., 2019). Besides removing toxic

elements, astrocytes can also directly boost the antioxidant defense of neurons (Jimenez-Blasco et al., 2015). For instance, neurons tend to oxidize glucose through PPP to regenerate glutathione and accordingly protect themselves against oxidative damage. However, in times of high activity, astrocytes themselves will provide glutathione precursors to neurons, thereby providing them an alternative way to counter ROS (Jimenez-Blasco et al., 2015).

A form of neurometabolic coupling has also been proposed, known as the astrocyte-neuron lactate shuttle (ANLS) hypothesis (Magistretti & Allaman, 2015; Pellerin et al., 1998). This model suggests that upon feedback from neurons, such as through neurotransmitter release, astrocytes release lactate into the extracellular space, whereby neurons can uptake the lactate to meet their energy needs, especially during periods of heightened activity. Neurons can convert lactate back into pyruvate and then channel pyruvate directly into their oxphos pathway, which is more energy conserving than producing pyruvate through the multiple steps of glycolysis. As was mentioned previously, astrocytes can provide the lactate either by breaking down their stored glycogen (Dringen et al., 1993; Rich et al., 2019) or by having their aerobic glycolysis stimulated (Pellerin & Magistretti, 1994).

It is clear that astrocytes have a prominent role in the neurometabolic coupling throughout the human brain. These tight connections mean that astrocytes not only provide support to neighboring neurons but can also cause negative effects when the astrocytes themselves are dysfunctional. For example, when the mitochondria of glial cells were inhibited using fluorocitrate, the adjoining neurons had increased vulnerability to excitotoxicity (Voloboueva et al., 2007). Thus, the investigation of disease pathophysiology should not only be focused on neurons, but also consider other cell types to properly address the glitches in these interconnected networks. One common attribute of disorders that is becoming increasingly evident and affects cell populations throughout the brain is mitochondrial dysfunction.

1.3 Mitochondrial dysfunction and its role in neurodegeneration

Mitochondria have been linked to aging and neurodegeneration, and thus are viewed as one of the early hallmarks of age-related disorders (Koopman et al., 2012). Mitochondrial dysfunction has indeed been identified in various pathological conditions as an early occurrence contributing to the disease progression, including diabetes (Kim et al., 2008), cancer (Porporato

et al., 2018), and multiple sclerosis (de Barcelos et al., 2019). Furthermore, impaired mitochondria function has also been implicated in many neurodegenerative diseases (Mishra & Chan, 2014; Srivastava, 2017; Stanga et al., 2020), such as at the early stages of Alzheimer's disease (AD) pathogenesis (Yao et al., 2009). The pathological effects of the APOE4 risk gene for AD have been shown to include mitochondria dynamics, as the mitochondria of astrocytes in APOE4 transgenic mice demonstrated reduced mitophagy and mitochondrial fission (Schmukler et al., 2020). Impaired mitochondrial dynamics were also demonstrated in a tau mouse model of AD (Kandimalla et al., 2018). In multiple sclerosis (MS), it was established that mitochondrial dysfunction specifically in astrocytes is a key cause of the neurological dysfunction found in that disease (Sadeghian et al., 2016). In particular, the relationship of the mitochondria with inflammation signaling, such as through the generation of ROS, has been tied to various pathologies (Missiroli et al., 2020).

One of the other main connections between neurodegenerative diseases and mitochondria is oxidative stress. Impaired mitochondrial function can lead to increased levels of oxidative stress, which is a common characteristic of neurodegenerative diseases (Lin & Beal, 2006; Xie et al., 2013). Mitochondrial dysfunction has certainly been implicated in various diseases, but even in healthy aging it has been shown that both neuronal and glial mitochondrial metabolism is reduced and altered (Boumezbeur et al., 2010). The metabolic networks connecting astrocytes across brain regions partially explain the spread of damage that occurs in most disorders, as was shown in a glaucoma mouse model (Cooper et al., 2020). Furthermore, the neurometabolic coupling between astrocytes and neurons that was previously described has been shown to be instrumental in disease pathology. For example, in a mouse model of Huntington's disease (HD), region-specific metabolite analysis revealed that a reduced amount of glucose, as well as its amino acid precursors, were present in the mouse striatum compared to the cerebellum (Polyzos et al., 2019). The astrocytes in the HD striatum subsequently compensated for the reduced glucose levels by relying more on fatty acid oxidation to obtain energy. The resulting increase of ROS levels then oxidatively damaged the nearby neurons and might have partially accounted for the neuronal death observed in the disease (Polyzos et al., 2019). Metabolic reprogramming might thus be a viable therapeutic option to counteract the mitochondrial deficiencies observed in various diseases.

1.4 Direct neuronal reprogramming

It was accepted as a universal doctrine that once cells had obtained a fully differentiated cell fate their developmental potency was lost. However, it was then discovered that somatic cells could regain their pluripotent potential under the influence of four transcription factors (Oct4, Sox2, Klf4, and c-Myc) (Okita et al., 2007; Takahashi & Yamanaka, 2006). The pluripotent reprogramming was initially successfully achieved in mouse cells (Wernig et al., 2007), and then subsequently in human cells (Takahashi et al., 2007). Many doors were opened as the reprogramming potential was thereafter investigated in many different types of somatic cells (Vierbuchen & Wernig, 2011). Induced pluripotent stem cells (iPSCs) are an invaluable method for disease modelling (Sharma et al., 2020; Singh et al., 2015) and their ability to generate specific human cell types *in vitro* can also be used in transplantation therapies (Kondo et al., 2014; Nagoshi & Okano, 2018; Windrem et al., 2017). Another advantageous reprogramming tool is the ability to directly change the identity of a fully differentiated cell type into another, thus bypassing the pluripotent state. In particular, direct neuronal reprogramming is of special interest as a therapeutic tool for the many neurodegenerative diseases.

Understanding the role of transcription factors in endogenous neurogenesis paved the way for unlocking their use in direct neuronal reprogramming. The initiation of neuronal lineage development is controlled by a few proneural genes that belong to the basic helix-loop-helix (bHLH) family of transcription factors, and these factors specifically bind DNA sequences that have an E-box motif (Bertrand et al., 2002). Achaete-scute homolog 1 (Ascl1) and Neurogenin2 (Neurog2) are two well-known and extensively studied examples of proneural bHLH transcription factors. For example, overexpression of Ascl1 in the developing chick neural tube (Nakada et al., 2004) and murine cerebral cortex (Cai et al., 2000) led to the generation of neurons. Conversely, mice expressing a null allele of Ascl1 had a reduction of olfactory neuroepithelium (Guillemot et al., 1993) and neural progenitors in the ventral telencephalon (Casarosa et al., 1999). Neurog2, on the other hand, has been shown to be essential for the generation of sensory cranial ganglia neural progenitors (Fode et al., 1998). The importance of the Neurog family of transcription factors in maintaining dorsal-ventral neural specification was demonstrated in Neurog mutant embryos (Fode et al., 2000). Without the usual presence of Neurog in the dorsal domain, Ascl1 expression would extend out from

its ventral region and infiltrate the dorsal territory (Fode et al., 2000). Therefore, Neurog2 and Ascl1 have important and distinct roles in the initiation of neuronal specification and regionalization in the developing brain.

The direct switch to a neuronal cell fate was first accomplished using postnatal mouse astroglial cells *in vitro* (Heins et al., 2002). The transcription factor Pax6 was used initially, and then neuronal subtype specificity was explored by using Neurog2, Ascl1, and Dlx2 (Heinrich et al., 2010, 2011). Human and murine fibroblasts have also been successfully converted into neurons using a variety of different transcription factors (Colasante et al., 2015; Pang et al., 2011; Vierbuchen et al., 2010; Wapinski et al., 2017). Not just transcription factors, but also small molecule cocktails have been utilized for direct neuronal reprogramming (Gao et al., 2017; Li et al., 2015; Yang et al., 2019; Yin et al., 2019; Zhang et al., 2015). For therapeutic applications, direct neuronal reprogramming is often aimed at endogenous cells in the brain, such as glia cells (Berninger et al., 2007; Blum et al., 2011; Hu et al., 2019; Masserdotti et al., 2015; Rivetti Di Val Cervo et al., 2017) and pericytes (Karow et al., 2012, 2018; Liang et al., 2018). The subtype specificity of the reprogrammed neurons has been further explored in order to replace the relevant populations of cells that are lost in various neurodegenerative diseases. For example, with the aim of potentially transplanting healthy dopaminergic neurons into the brain of a Parkinson's disease (PD) patient, murine and human fibroblasts have been successfully converted into dopaminergic neurons (Caiazzo et al., 2011; Liu et al., 2012; Pfisterer et al., 2011). The investigation of disease pathology has also been possible through direct reprogramming strategies, and this form of disease modeling has been utilized for both PD (Lee et al., 2019) and AD (Hu et al., 2015), among others (Drouin-Ouellet et al., 2017). Neuronal reprogramming was successfully achieved not only *in vitro*, but also *in vivo*, specifically in the mouse brain (Buffo et al., 2005; Gascón et al., 2016; Heinrich et al., 2014; Liu et al., 2021; Mattugini et al., 2019).

The field of direct neuronal reprogramming has expanded its knowledge base over time, with more work focusing on the potential hurdles to reprogramming and understanding the underlying cascades involved in the process. It was determined that Ascl1 and Neurog2 activate very distinct neurogenic cascades when transduced in murine astrocytes (Masserdotti et al., 2015). Furthermore, the efficacy of the transcription factors has been shown to be context dependent and strongly affected by the starting cell population. For example, Neurog2 exhibits poor neuronal reprogramming efficiency when applied to murine embryonic fibroblasts

(Chanda et al., 2014), but in contrast is very effective in reprogramming murine postnatal astrocytes (Masserdotti et al., 2015). The reprogramming of somatic cells into neurons is influenced by the accessibility of target genes, as was shown with Ascl1 and its ability to access closed chromatin targets in fibroblasts (Wapinski et al., 2013). Not only epigenetic hurdles, but also metabolic differences between cells can greatly influence the viability and efficiency of reprogramming (Gascón et al., 2016; Russo et al., 2021).

As was mentioned previously, certain metabolic states are required for each cell type in order to support the cell-specific functions that are performed. The localization of different cell types on the spectrum of glycolysis to oxphos based on their metabolic preferences is demonstrated in Figure 2. Therefore, when cell fate conversion occurs, such as in direct neuronal reprogramming, a parallel switch in metabolic identity must also take place. Indeed, even during the differentiation of neurons from iPSCs a shifted metabolic profile to favor oxphos for energy generation was detected (Fang et al., 2016; Zheng et al., 2016). This metabolic switch was also shown to be essential for direct neuronal reprogramming, for when oxphos was blocked by treating the cells with Oligomycin A, the resultant glycolytic-dependent astrocytes were no longer able to transform into neurons (Gascón et al., 2016). During successful neuronal reprogramming, increased oxidative stress was observed as the cells changed their metabolic components to favor oxphos and thus more ROS was generated by the ETC. Interestingly, it was shown that by treating cells with anti-oxidative compounds the success of reprogramming increased dramatically both *in vitro* and *in vivo* (Gascón et al., 2016). These results imply that by alleviating the stress occurring during the metabolic switch of cell fate change the success of reprogramming can be greatly improved.

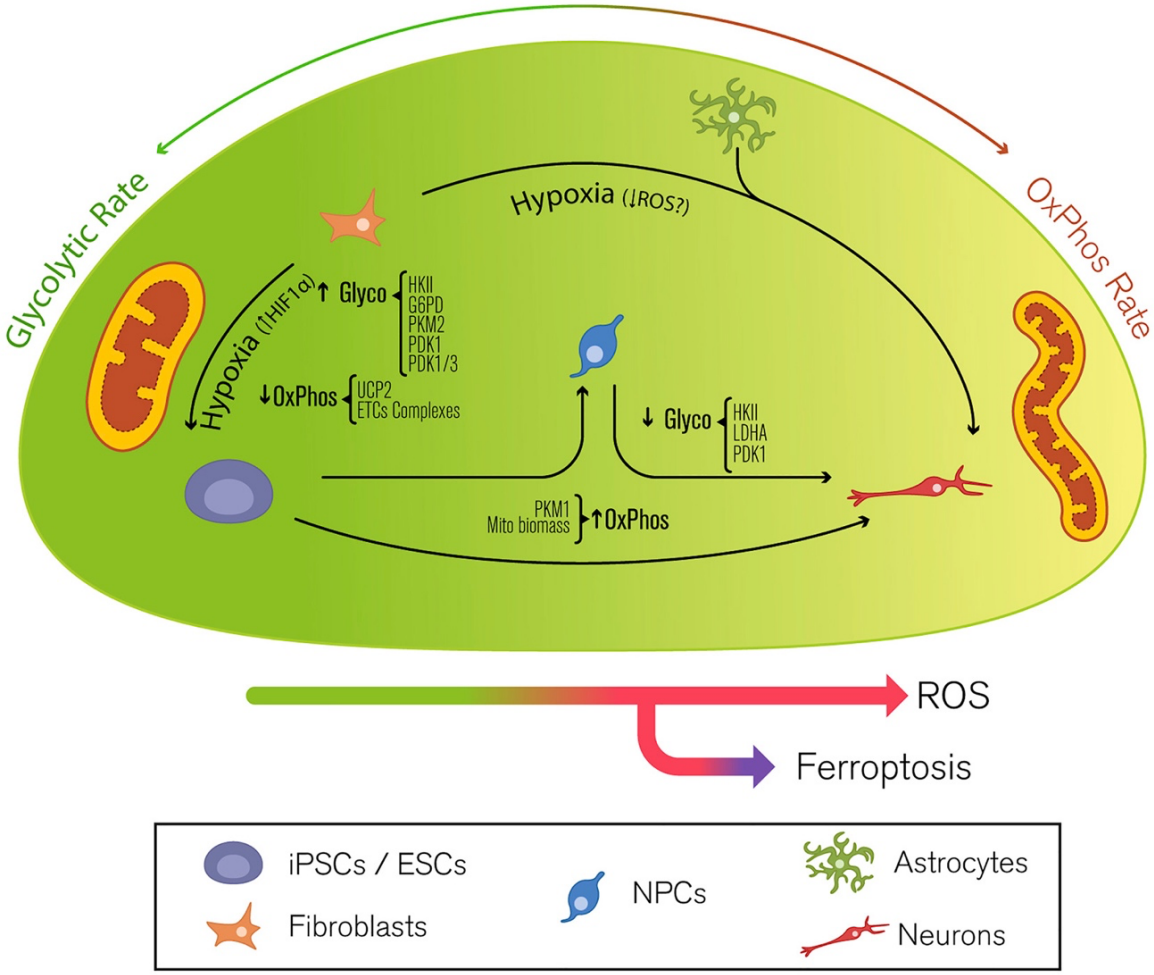

Figure 2. *Schematic of the metabolic profiles of different cell types, and the subsequent changes in metabolism that must occur during cell fate transition.* (Gascón et al., 2017; License Number: 5076091092613)

1.5 Complex I deficiency: NDUFS4-mutation

In order to improve the therapeutic potential of direct neuronal reprogramming, it is imperative to further increase the reprogramming efficiency and the viability of reprogrammed neurons. Successful metabolic conversion is a main hurdle to reprogramming that is still not well understood. One option to further understand and thus improve the switch from glycolytic to oxphos metabolism is to study patients who have mitochondrial deficiencies. However, before discussing mitochondrial disorders, the oxphos machinery will first be described in more detail. As mentioned previously, the oxphos metabolic pathway in the mitochondria is comprised of five multi-subunit complexes embedded in the IMM (Letts & Sazanov, 2017). The reduced electron carriers NADH and $FADH_2$ transfer electrons to Complex I (CI) and Complex II (CII), respectively. The electrons are then passed down the other complexes in the electron transport

chain, enabling said complexes to pump protons from the matrix to the intermembrane space. The resulting electrochemical proton gradient across the membrane causes protons to naturally flow back into the matrix through the Complex V (ATP synthase) pore and thereby generate ATP (Letts & Sazanov, 2017). The electrochemical gradient is not only important for the production of cellular energy in the form of ATP but is also critical for other mitochondrial functions such as calcium homeostasis and apoptosis (Koopman et al., 2013). Therefore, when there are issues with the performance of the ETC, it has deleterious consequences for the various essential functions of the mitochondria within the cell. Indeed, oxphos deficiencies are often associated with severe phenotypes in the patients, including neurodegeneration (Koopman et al., 2013).

Mitochondrial diseases are associated with deficiencies in key mitochondrial functions, such as oxphos, although they are very heterogenous, both in their clinical presentation and genetic basis (Gusic & Prokisch, 2021; Tan et al., 2020). Indeed, since mitochondrial proteins are encoded by both nuclear DNA (nDNA) and mitochondrial DNA (mtDNA), mutations can occur in both genomes (Schlieben & Prokisch, 2020). The wide range of mitochondrial disorder phenotypes makes diagnosis difficult, although some specific syndromes have been defined, such as Leber's hereditary optic neuropathy (LHON), Leigh's syndrome (LS), and mitochondrial encephalopathy, lactic acidosis and stroke-like episodes (MELAS) (Baertling et al., 2014; Rahman et al., 1996; Schlieben & Prokisch, 2020). As was mentioned previously, mitochondrial defects are also involved in the pathogenesis of various diseases, including AD and PD, as well as amyotrophic lateral sclerosis (Filosto et al., 2011; Lin & Beal, 2006; Stanga et al., 2020). Mitochondria dysfunction can even be an early hallmark of neurodegenerative diseases, as increased oxidative damage was detected in patients with mild dementia (Keller et al., 2005). The most common defects of mitochondrial metabolism are mutations in CI of the ETC (Distelmaier et al., 2009a; Smeitink et al., 2001a; Smeitink et al., 2001b). Human NADH:ubiquinone oxidoreductase, also known as CI, is the largest multi-subunit complex of the ETC and is encoded by both nuclear DNA (nDNA) and mitochondrial DNA (mtDNA) (Smeitink et al., 2001a). CI is located on the inner mitochondrial membrane and is responsible for oxidizing NADH to NAD^+ and passing the resulting electrons onto CIII (Friedrich & Böttcher, 2004). Four protons are also translocated from the mitochondrial matrix to the intermembrane space, thus supporting the proton motive force across the membrane (Friedrich & Böttcher, 2004). Structural analysis revealed that CI is composed of a hydrophobic

membrane arm that inhabits the IMM and a peripheral arm that extends into the mitochondrial matrix, forming an L shape (Clason et al., 2010; Wirth et al., 2016).

One common mutation in the mammalian CI occurs in the 18kDa nuclear-encoded subunit NDUFS4 (NADH dehydrogenase [ubiquinone] iron-sulfur protein 4), an accessory subunit of the peripheral arm of CI (Breuer et al., 2013; Van Den Heuvel et al., 1998). The NDUFS4 gene is important for the assembly of a functional complex, as evidenced by the lack of complete CI detected in patients with NDUFS4 mutations (Petruzzella et al., 2001; Scacco et al., 2003). Indeed, compared to the fully assembled CI at ~980kDa, the much smaller ~800kDa subcomplex detected in an NDUFS4-mutant patient indicates that multiple subunits are unable to bind and complete the assembly (Lazarou et al., 2007). Therefore, NDUFS4 most likely plays an essential role in the final assembly stages of CI (Vogel et al., 2007). A regulatory role for NDUFS4 is also possible, as it has been shown that cAMP-dependent protein kinase (PKA) phosphorylates NDUFS4 and this process is the manner by which CI is activated by cAMP (Papa et al., 2012).

NDUFS4-mutant patients have a variety of symptoms, which occur shortly after birth, and many patients die within the first few years of life (Fiedorczuk & Sazanov, 2018). The patients' phenotype is characterized by infantile-onset Leigh syndrome (LS), lactic acidosis and encephalomyopathy (Fiedorczuk & Sazanov, 2018). Tissues with high energy demand are particularly affected by mitochondrial dysfunction, and as a result cardiac, muscular, and neural pathologies are common clinical features. Indeed, the patients exhibit abnormal ocular movements, muscular hypotonia, cardiomyopathy, and respiratory failure (Budde et al., 2003; Ortigoza-Escobar et al., 2016). In accordance with these symptoms, the patients present with lesions in the basal ganglia and brainstem (Ortigoza-Escobar et al., 2016).

Skin fibroblasts from NDUFS4-mutant patients analyzed by blue native polyacrylamide gel electrophoresis (BN-PAGE) demonstrated partially assembled 830kDa subcomplexes but an absence of fully assembled CI (Assouline et al., 2012). Concomitant with the lack of complete CI, spectrophotometric analysis revealed reduced CI enzyme activity in patient skin fibroblasts and muscle tissue (Assouline et al., 2012). The low level of CI activity, that can still be detected in patient tissues despite being only partially assembled, can be explained by the formation of supercomplexes between CI and CIII (Calvaruso et al., 2012). The stabilization that CIII gives to CI is especially relevant for allowing the NADH dehydrogenase module to properly

associate with the complex (Calvaruso et al., 2012). When the mitochondrial ROS production in human fibroblasts was measured using a mitochondria-targeted superoxide detector (MitoSOX Red), NDUFS4-deficient fibroblasts displayed increased ROS levels compared to controls (Melcher et al., 2017). Considering that increased ROS can have detrimental effects on cell function, reducing ROS levels was investigated as a possible therapeutic strategy. Co-culturing with mesenchymal stem cells (MSCs) reduced the ROS levels of patient cells back to control cell levels. Interestingly, even with normalized ROS levels there was no detectable recovery of CI assembly or activity in the patient cells (Melcher et al., 2017). The separation of ROS from the bioenergetic effects of deficient CI activity was further demonstrated when investigating NDUFS4-mutations in heart tissue. Mice with a heart-specific NDUFS4-mutation had severe cardiomyopathy and CI activity was reduced by ~50% (Chouchani et al., 2014). However, there was no increase in hydrogen peroxide levels in the heart or markers of oxidative damage, indicating that the cardiac dysfunction was primarily due to the reduced CI activity and not ROS influences (Chouchani et al., 2014).

In order to further understand the disease progression and to develop therapeutic strategies, a Ndufs4 knockout (KO) mouse model was developed (Kruse et al., 2008). The KO mice are similar to wild type (WT) mice for the first four weeks, but after postnatal day(P)35 the mice start to exhibit motor dysfunction and they die by ~P50. Reduced CI activity and the presence of fewer fully assembled CI was confirmed in the KO mice. Overall, the mice seemed to resemble the human CI deficiencies (Kruse et al., 2008). Although the full body KO mouse model partially represents the human mitochondrial encephalomyopathy, other mouse models have also been developed that target specific cell populations. For example, Ndufs4 was selectively knocked out in neurons and glia, referred to as the NesKO mouse model (Quintana et al., 2010). Interestingly, this restricted KO led to a very similar phenotype as the full KO mouse model, indicating the important role of the CNS in disease progression (Quintana et al., 2010). In order to further understand the role CI dysfunction has in the basal ganglia and striatum, a mouse line was generated that targeted the Ndufs4 knockout to medium spiny neurons (MSN KO mice) (Chen et al., 2017). Although the mice exhibited a progressive motor impairment, no reactive gliosis or neuronal cell death was detected. The inflammation observed in the other KO models could thus be due to the axons projecting to the striatum, since the MSNs by themselves do not seem to elicit such a reaction (Chen et al., 2017). Another conditional deletion of Ndusf4, this time in dopaminergic neurons (Ndufs4 cKO), also did not cause neuronal cell death (Choi et al., 2017). In this case, there were no motor impairments but

there was impaired cognitive function and a reduced amount of dopamine in the brain (Choi et al., 2017). To sum up, mouse models of CI-deficiency can be instrumental in further untangling the cell-specific contributions to mitochondrial disease. However, mouse models still do not properly recapitulate the human disease pathogenesis (Lorenz et al., 2017; Tzoulis et al., 2014), and thus the influence of mitochondrial mutations on different human cell types still needs to be further investigated.

Models for studying mitochondrial disease in humans have been revolutionized with the discovery of iPSC reprogramming. Patient-specific phenotypes can now be more accurately represented, and their disease mechanisms investigated, which not only allows for a greater understanding of the disease pathogenesis but also provides the opportunity for drug screening (Inak et al., 2017). These iPSC disease-modeling strategies allow for, in particular, the study of cells from tissues that are not easily accessible, such as the human brain (Mertens et al., 2016). Indeed, iPSC-derived neural progenitor cells (NPCs) have been used successfully as a cellular model system for mitochondrial disease that not only portrays the mutant phenotypes but can also be rescued upon drug treatment (Liang et al., 2020; Lorenz et al., 2017). The pathogenic phenotype of neuronal cells, specifically in LS, was successfully investigated using patient iPSC reprogramming (Galera-Monge et al., 2020). Altered bioenergetics could be detected in iPSC-derived neural cells from a LS patient, as well as compromised mitochondrial calcium regulation (Galera-Monge et al., 2020). The course of neuronal development has also recently been studied in patients with a mitochondrial mutation, specifically in the protein SURF1, which is involved in the assembly of CIV (Inak et al., 2021). Interestingly, aberrant neuronal maturation could be detected in SURF1-mutant patient cells in both 2D, as well as 3D organoid, culture models. Diminished neurite outgrowth was additionally observed in NPCs from patients with mutations in NDUFS4, which as discussed previously, is another common LS-associated mutation. Therefore, impaired neuronal morphogenesis is potentially a consistent pathogenic feature across LS (Inak et al., 2021). The underlying cause for the defective neuronal differentiation could be explained by the negative impact of these mitochondrial mutations on the oxphos metabolic pathway. Indeed, NPCs from patients with other mutations related to LS demonstrated altered bioenergetics, and more specifically, an enhanced dependence on glycolysis (Ma et al., 2015). Cells from patients with a SURF1 mutation also exhibited defects already at the NPC stage, including the inability to shift their metabolism from a glycolytic progenitor state into the oxphos metabolism preferred by mature neuronal cells (Inak et al., 2021). These results further corroborate the importance of being able

to utilize the oxphos metabolic machinery in order to successfully obtain a neuronal fate. Therefore, iPSC technology is instrumental for studying human mitochondrial disease, especially the CNS pathogenesis.

In conclusion, investigating patients with mitochondrial disorders can reveal new therapeutic strategies not only for treating the mitochondrial dysfunction that is an early hallmark of many diseases, but can also be used for analyzing the metabolic switch that occurs during direct neuronal reprogramming.

1.6 Aim of the thesis

The overall aim of my PhD studies was to investigate the underlying mechanisms, and in particular the metabolic switch, that influence the ability of a cell to directly convert into a neuronal fate. Although direct neuronal reprogramming is a promising tool for replacing the functional neurons lost in neurodegenerative disease, further optimization is required to make it a viable treatment in human patients. Thus, the identification and mitigation of reprogramming barriers not only in murine reprogramming, but also in human cell reprogramming, is imperative.

The first aim of my PhD research was to study the influence of the mitochondria during neuronal reprogramming, especially in regard to the known metabolic shift. To this end, the mitochondrial proteome of murine astrocytes and neurons was explored, and their respective mitochondria structure was analyzed. The distinct mitochondrial composition of the two cell types was then used to determine the extent of metabolic programming that occurs during forced neuronal fate acquisition. Additionally, the manipulation of neuron-enriched mitochondrial proteins and their effect on the reprogramming efficiency were investigated.

For the focus of my second aim, I examined the role of mitochondrial metabolism in human cells during neuronal reprogramming, as well as the influence of mitochondrial mutations on different cell types. The ability of NDUFS4-mutant iPSCs to be differentiated into astrocytes *in vitro* was first investigated, and their phenotype compared to cells from control donors. Then the relative proficiency of the glial cells from both donors to reprogram into neurons, and the

contribution of the mitochondrial deficiency on reprogramming, was determined. Finally, various treatments were tested to alleviate cell stress during reprogramming, as well as to address the mitochondrial dysfunction, leading to the discovery of a novel limiting pathway in neuronal reprogramming.

Results

2. Results

2.1 Aim of the Study I

The aim of the first study was to investigate and compare the mitochondrial metabolism between astrocytes and neurons and determine how manipulation of cell-type-specific-enriched mitochondrial proteins can influence direct neuronal reprogramming.

CRISPR-Mediated Induction of Neuron-Enriched Mitochondrial Proteins Boosts Direct Glia-to-Neuron Conversion

Gianluca L Russo, ***Giovanna Sonsalla***, Poornemaa Natarajan, Christopher T Breunig, Giorgia Bulli, Juliane Merl-Pham, Sabine Schmitt, Jessica Giehrl-Schwab, Florian Giesert, Martin Jastroch, Hans Zischka, Wolfgang Wurst, Stefan H Stricker, Stefanie M Hauck, Giacomo Masserdotti and Magdalena Götz

For this paper I conducted the time course analysis of the changes in specific mitochondrial proteins during astrocyte to neuron reprogramming. I was also involved in the review and editing of the manuscript.

The paper is published in Cell Stem Cell, 4 March 2021, pages 524–534.e7.

https://doi.org/10.1016/j.stem.2020.10.015

Note that due to elevated number of pages Supplementary Table 1 and Supplementary Table 2 are not included in the PDF version of this thesis but are available as separate excel files.

Cell Stem Cell

Short Article

CRISPR-Mediated Induction of Neuron-Enriched Mitochondrial Proteins Boosts Direct Glia-to-Neuron Conversion

Graphical Abstract

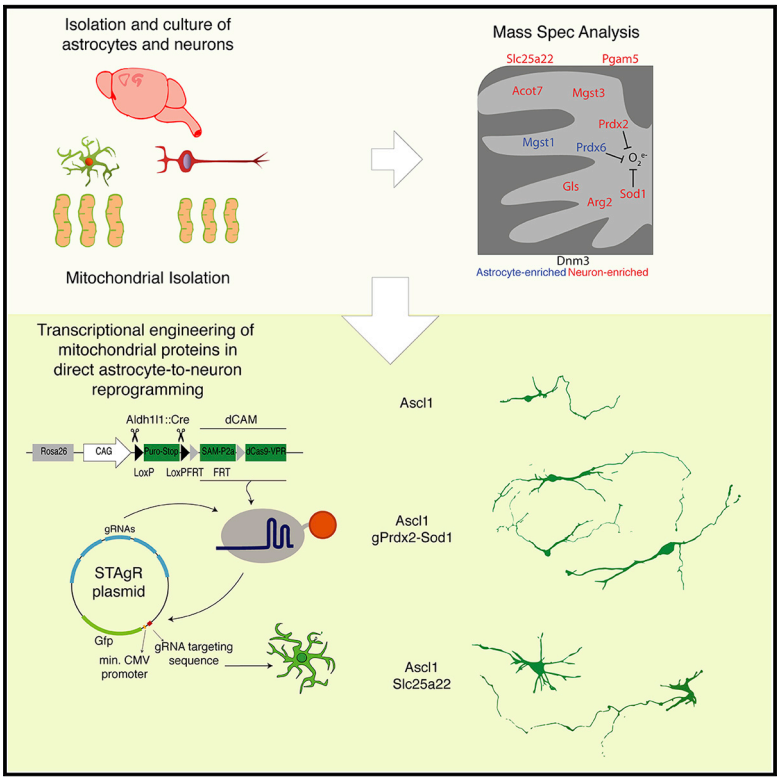

Highlights

- Mitochondrial proteomes of cortical astrocytes and neurons are distinct
- Astrocyte-enriched mitochondrial proteins are downregulated late in neuronal conversion
- Neuron-enriched mitochondrial proteins are upregulated late in neuronal conversion
- Early induction of neuronal mitochondrial proteins improves neuronal reprogramming

Authors

Gianluca L. Russo, Giovanna Sonsalla, Poornemaa Natarajan, ..., Stefanie M. Hauck, Giacomo Masserdotti, Magdalena Götz

Correspondence

magdalena.goetz@helmholtz-muenchen.de

In Brief

Russo et al. identify mitochondrial proteins enriched in neurons or astrocytes. Astrocyte-enriched mitochondrial proteins are often only partially downregulated during astrocyte-to-neuron direct reprogramming. Neuron-enriched ones are upregulated late and mainly in reprogrammed neurons. CRISPRa-mediated early induction of neuron-enriched mitochondrial proteins boosts direct neuronal reprogramming speed and efficiency.

Russo et al., 2021, Cell Stem Cell *28*, 524–534
March 4, 2021
https://doi.org/10.1016/j.stem.2020.10.015

CellPress

CellPress
OPEN ACCESS

Cell Stem Cell

Short Article

CRISPR-Mediated Induction of Neuron-Enriched Mitochondrial Proteins Boosts Direct Glia-to-Neuron Conversion

Gianluca L. Russo,[1,2,3] Giovanna Sonsalla,[1,2,3,15] Poornemaa Natarajan,[1,2,3,15] Christopher T. Breunig,[4,5] Giorgia Bulli,[1,2] Juliane Merl-Pham,[6] Sabine Schmitt,[7] Jessica Giehrl-Schwab,[8] Florian Giesert,[8,9] Martin Jastroch,[10] Hans Zischka,[7,11] Wolfgang Wurst,[8,9,12] Stefan H. Stricker,[4,5] Stefanie M. Hauck,[6,16] Giacomo Masserdotti,[1,2,16] and Magdalena Götz[1,2,13,14,16,*]

[1]Physiological Genomics, Biomedical Center (BMC), Ludwig-Maximilians-Universität (LMU), Planegg-Martinsried, Germany
[2]Institute for Stem Cell Research, Helmholtz Center Munich, BMC LMU, Planegg-Martinsried, Germany
[3]Graduate School of Systemic Neurosciences, BMC, LMU, Planegg-Martinsried, Germany
[4]MCN Junior Research Group, Munich Center for Neurosciences, BMC, LMU, Planegg-Martinsried, Germany
[5]Epigenetic Engineering, Institute of Stem Cell Research, Helmholtz Zentrum, Planegg-Martinsried, Germany
[6]Research Unit Protein Science, Helmholtz Center Munich, Neuherberg, Germany
[7]Institute of Toxicology and Environmental Hygiene, School of Medicine, Technical University Munich (TUM), Munich, Germany
[8]Institute of Developmental Genetics, Helmholtz Center Munich, Neuherberg, Germany
[9]Developmental Genetics, TUM, Munich-Weihenstephan, Germany
[10]Department of Molecular Biosciences, The Wenner-Gren Institute, The Arrhenius Laboratories F3, Stockholm University, Stockholm, Sweden
[11]Institute of Molecular Toxicology and Pharmacology, Helmholtz Center Munich, Neuherberg, Germany
[12]German Center for Neurodegenerative Diseases (DZNE) Site Munich, Munich, Germany
[13]Excellence Cluster of Systems Neurology (SYNERGY), Munich, Germany
[14]Lead Contact
[15]These authors contributed equally
[16]These authors contributed equally
*Correspondence: magdalena.goetz@helmholtz-muenchen.de
https://doi.org/10.1016/j.stem.2020.10.015

SUMMARY

Astrocyte-to-neuron conversion is a promising avenue for neuronal replacement therapy. Neurons are particularly dependent on mitochondrial function, but how well mitochondria adapt to the new fate is unknown. Here, we determined the comprehensive mitochondrial proteome of cortical astrocytes and neurons, identifying about 150 significantly enriched mitochondrial proteins for each cell type, including transporters, metabolic enzymes, and cell-type-specific antioxidants. Monitoring their transition during reprogramming revealed late and only partial adaptation to the neuronal identity. Early dCas9-mediated activation of genes encoding mitochondrial proteins significantly improved conversion efficiency, particularly for neuron-enriched but not astrocyte-enriched antioxidant proteins. For example, Sod1 not only improves the survival of the converted neurons but also elicits a faster conversion pace, indicating that mitochondrial proteins act as enablers and drivers in this process. Transcriptional engineering of mitochondrial proteins with other functions improved reprogramming as well, demonstrating a broader role of mitochondrial proteins during fate conversion.

INTRODUCTION

The ability to regenerate lost neurons after an injury or in neurodegenerative disease is still a key challenge in the field of regenerative medicine. Among different therapeutic approaches (Barker et al., 2018; Grade and Götz, 2017), direct conversion of local glia into neurons has become a viable option to replace functional neurons (Vignoles et al., 2019). Because direct neuronal conversion is dramatically hindered by increased generation of reactive oxygen species (ROS) during the process, Bcl2 or pharmacological application of antioxidants could drastically improve neuronal generation *in vitro* and *in vivo* (Gascón et al., 2016). At the same time, neurons rely on oxidative phosphorylation (OxPhos) (Harris et al., 2012; Herrero-Mendez et al., 2009), so an increase in mitochondrial activity is required during neuronal conversion. Mitochondria perform a plethora of additional functions (Spinelli and Haigis, 2018), and specific mitochondrial proteins may be required to implement the cell-type-specific metabolic needs (Calvo and Mootha, 2010; Folmes et al., 2012; Pagliarini et al., 2008). Because changes in

CellPress
OPEN ACCESS

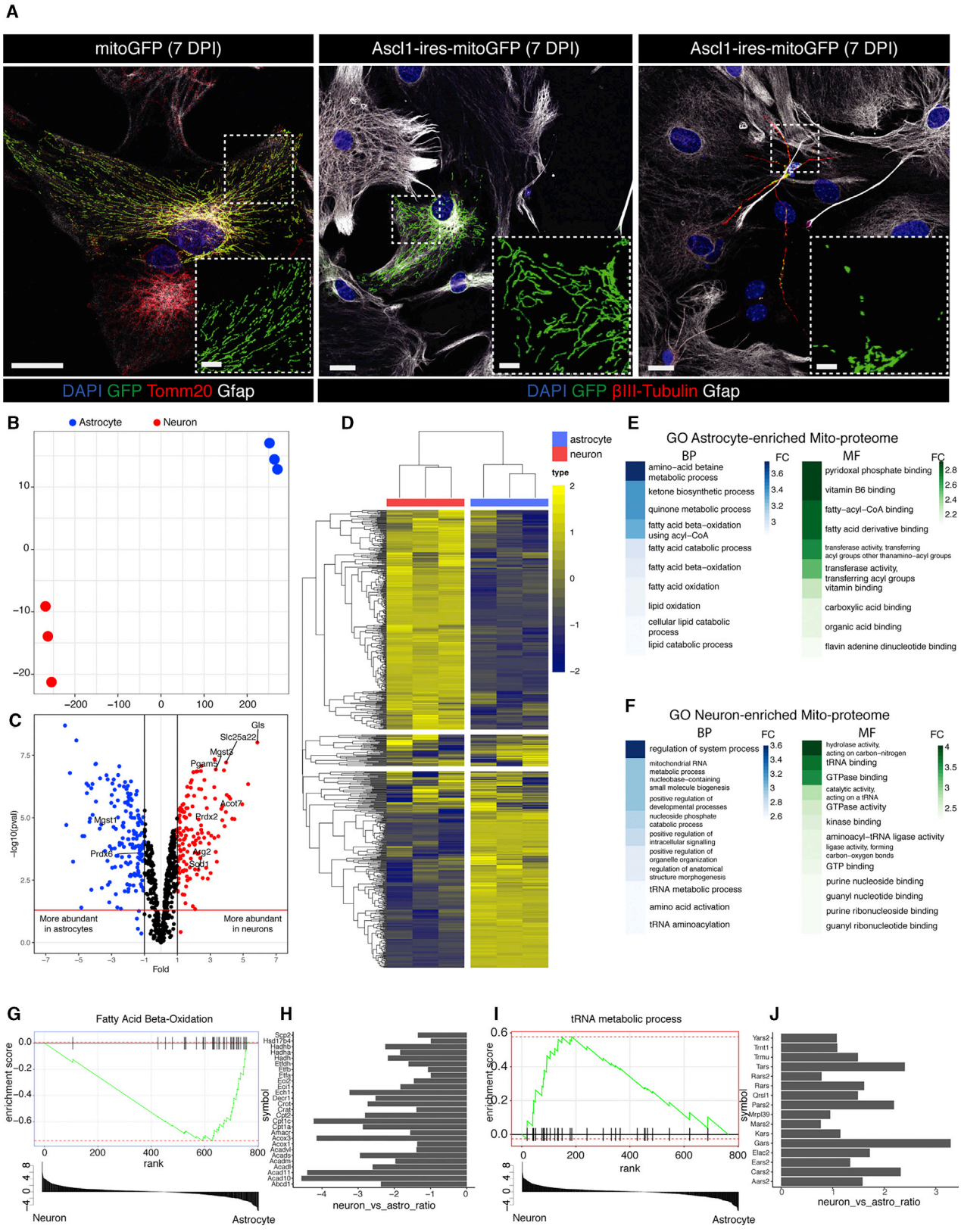

(legend on next page)

mitochondrial proteins have not yet been investigated in neuronal reprogramming, we assessed the similarities and differences in mitochondrial composition for cultured neurons and astrocytes and aimed to improve mismatching during reprogramming by regulating the respective genes by CRISPRa (clustered regularly interspaced short palindromic repeat activation)-mediated transcriptional engineering.

RESULTS

Mitochondrial Morphology Changes during Cortical Astrocyte-to-Neuron Reprogramming *In Vitro*

We first monitored morphological changes of mitochondria during reprogramming. Astrocytes isolated from postnatal day 5 (P5) murine cerebral cortex (Heinrich et al., 2011) were transduced with a retrovirus encoding mitochondrion-targeted green fluorescent protein (*mitoGFP*) with or without the reprogramming proneural factor Achaete-scute homolog 1 (*Ascl1-ires-mitoGFP*, ires [intra ribosome entry site]), shown previously to reprogram astrocytes into GABAergic neurons (Heinrich et al., 2010; Masserdotti et al., 2015). MitoGFP co-localized with Tomm20, a pan-mitochondrial marker protein, revealing an elongated and ramified mitochondrial network in astrocytes (Figure 1A, left panel). This was maintained in Ascl1-transduced astrocytes failing to reprogram (positive for the astroglial protein glia fibrillary acidic protein [Gfap], negative for neuron-specific βIII-tubulin; Figure 1A, center panel), whereas successfully converted neuronal cells (βIII-tubulin+, Gfap−) had smaller mitochondria with shorter and rounder morphology (Figure 1A, right panel). These data are in line with neurons *in vivo* possessing smaller mitochondria and higher fission properties (Misgeld and Schwarz, 2017), whereas astrocytes have more elongated mitochondria and fusion events (Motori et al., 2013). To gain a better understanding of mitochondrial restructuring during the reprogramming process, we investigated the proteins that mediate morphological and functional changes in mitochondria.

Astrocytes and Neurons Differ in Mitochondrial Structure and Function *In Vitro*

To determine the comprehensive mitochondrial proteome of neurons and astrocytes, we chose highly pure neuronal cultures derived from embryonic day 14 (E14) cerebral cortex, cultured for 7 days (Walcher et al., 2013); i.e., young neurons comparable with reprogrammed neurons at 7 days post-transduction (DPT) in reprogramming) and primary cultures of astrocytes as used in direct neuronal reprogramming. Functional bio-energetic differences of neurons and astrocytes from these cultures were confirmed by Seahorse analysis (Figures S1A–S1C). A cell fractionation-based method (Schmitt et al., 2013) enriched mitochondria, as assessed by western blot (Figure S1D) and electron microscopy (EM) (Figure S1E), and functional assays confirmed the isolation of intact mitochondria from both cell types (Figures S1F and S1G). EM confirmed the cell-type-specific differences in mitochondrial morphology (Figures 1A and 1E) and also revealed some other organelles in the neuronal samples, probably because small mitochondria are tightly linked to the cytoskeleton in the thin neuronal processes and the endoplasmic reticulum (ER) (Fecher et al., 2019).

Astrocytes and Neurons Exhibit Profound Differences in Their Mitochondrial Proteome

We then used liquid chromatography-tandem mass spectrometry (LC-MS/MS) to identify proteins in neuronal and astrocytic mitochondria. A *t*-distributed stochastic neighbor embedding (t-SNE) plot for all identified proteins normalized for abundance (Figures S1J; normalization in Figure S1H) or mitochondrion-specific proteins (Figure 1B; normalization in Figure S1K), as classified by MitoCarta 2.0 (Table S1; Calvo et al., 2016), revealed clear separation of neurons and astrocytes. Unsupervised cluster analysis confirmed the cell type dependent similarity, considering whole proteins (Figure S1I) or only mitochondrial proteins (Figure S1L). Overall, we detected 757 (±1) mitochondrial proteins in astrocytes and 738 (±1) in neurons (Figures S1M and S1N) of which 164 (22%) were more abundant in astrocytes and 141 (19%) more abundant in neurons ($p < 0.05$ and 2-fold enrichment; Figure 1C; Table S1), with high reproducibility across samples (Figure 1D). Thus, about a fifth of the mitochondrial proteome differs significantly between these cell types. Western blotting of whole-cell lysates from independent cultures confirmed enrichment of Sfxn5 and Cpox in astrocytes (Figure S1O, left and center panel) and glutaminase (Gls) in neurons (Figure S1O, right panel).

Gene Ontology (GO) term analysis of mitochondrial proteins significantly enriched in astrocytes (Figure 1E, left panel; top 10 enriched biological processes [BPs]; Fisher's exact test < 0.01; see Table S2A for a complete list) revealed terms such as fatty acid catabolic process, fatty acid β-oxidation, and lipid catabolic process, also relevant pathways for astrocytes *in vivo* (van Deijk et al., 2017). This was supported by the analysis of molecular function (MF) GO terms (Figure 1E, right panel; Table

Figure 1. Astrocytes and Neurons Differ in Mitochondrial Structure and Proteome

(A) Micrograph of mitochondrial morphology in control (mitoGFP) astrocytes (left panel), Ascl1-non-reprogrammed astrocytes (center panel), and Ascl1-induced neurons (right panel, Ascl1-mitoGFP), 7 DPI. Scale bars, 20 μm and 6 μm (insets).

(B) *t*-SNE plot of samples considering only mitochondrial proteins.

(C) Volcano plot of mitochondrial proteins with $\log_2$ ratio of abundance of neurons/astrocytes (x axis) and the $-\log_{10}$ of the corresponding significance value (p value, y axis); 2-fold changes (vertical lines), significance cutoff p = 0.05 (horizontal line). Proteins significantly more abundant in astrocytes are shown in blue and more abundant in neurons in red. Names highlight proteins covered in this study.

(D) Unsupervised heatmap cluster analysis of all detected mitochondrial proteins. Astrocytes, blue; neurons, red. n = 3 for each group. The color scale indicates *Z* score.

(E and F) GO terms of the top 10 biological processes (BPs; blue, left panels) and molecular functions (MFs; green, right panels) for astrocyte-enriched (E) and neuron-enriched (F) mitochondrial proteins. The color bar represents the fold change compared with the expected number of genes for each term. Terms were considered if exact Fisher test < 0.01.

(G–J) Examples of 2 terms identified by gene set enrichment analysis (GSEA) (G and I) and barplots (H and J) of the main genes associated with the respective terms (in G or I).

S2A), including terms such as fatty-acyl-coenzyme A (CoA) binding, in line with a recent study of mitochondria of Bergmann glia from adult mice (Fecher et al., 2019). Likewise, gene set enrichment analysis (GSEA) identified fatty acid β-oxidation-related proteins in astrocytes (Figure 1G; Table S2E), comprising key regulators such as Acads, Cpt1a, and Cpt2 (Figure 1H; Tables S1 and S2E).

To explore the functional relevance of the fatty acid β-oxidation pathway in direct reprogramming, we blocked this pathway using etomoxir, an inhibitor of Cpt1a (Jernberg et al., 2017), early during the conversion process (Figure S2A). Medium to high doses of etomoxir (25 μM and 100 μM, respectively) improved reprogramming compared to the control (no etomoxir) upon Ascl1 (Figures S2B and S2C) or Neurogenin2 (Neurog2) expression (Figures S2D and S2E). Interestingly, co-treatment with α-tocotrienol, an analog of the ROS scavenger vitamin E, reduced Ascl1-mediated reprogramming efficiency, suggesting that the positive effect of etomoxir might be partly due to an increase in ROS, as shown previously (O'Connor et al., 2018). Thus, β-oxidation is a general hurdle in glia-to-neuron reprogramming.

GO terms significant for neuron-enriched mitochondrial proteins were associated with RNA metabolism and function (BP in Figure 1F, left panel, and Table S2C; MF in Figure 1F, right panel, and Table S2D) and further supported by GSEA (Figures 1I and 1J, tRNA metabolic process; full list in Table S2E). This highlights the notion that tRNA biogenesis is an important activity in neuronal mitochondria and its dysfunction is associated with neurodevelopmental disease (Schaffer et al., 2019). Among neuron-enriched mitochondrial proteins, we also detected Gls, the enzyme regulating glutamine metabolism and glutamate neurotransmitter levels (Márquez et al., 2009), and ATP citrate lysate (Acly), involved in production of cytosolic acetyl-CoA (Lin et al., 2013; Table S1).

Enrichment of the mitochondrial fusion protein Mitofusin 1 (Mfn1) in astrocytes is in line with the presence of more elongated mitochondria in such cells (Figure 1A), whereas the fission master regulator Dynamin-related protein (Dnm1l, also known as Drp1) is more prevalent in the neuronal mitochondrial proteome (Table S1). Interestingly, the antioxidant proteins Gpx1, Gpx4, Prdx6, and Mgst1 were more enriched in astrocytes (Table S1), whereas Mgst3, Prdx2, and Sod1 were more abundant in neurons (Table S1), suggesting that different members of antioxidant protein families (e.g., peroxiredoxins and microsomal glutathione S-transferases) are enriched in specific cell types. This raised the intriguing question of whether these proteins (Prdx2 and Prdx6 or Mgst1 and Mgst3) are functionally similar and only expressed in a cell-type-specific manner or whether the neuron-enriched antioxidant proteins may be specifically required in neurons and, hence, during the direct conversion process.

We also compared our data with mitochondrial proteins isolated from adult murine cerebellum (Purkinje cells, granule cells, and astrocytes; Fecher et al., 2019). Despite the very different experimental conditions (*in vivo* versus *in vitro*, adult versus postnatal, cerebellum versus cortex, immunoprecipitation [IP]-based versus fractionation-based-method), we found 117 proteins enriched in both astrocyte-derived samples; i.e., 60% of all mitochondrial proteins identified by Fecher et al. (2019) were also present in our astrocyte-enriched mitochondrial proteome (Figure S1P). Likewise, 46% of neuron-enriched mitochondria identified by Fecher et al. (2019) were common to our neuronal dataset (Figure S1Q).

Thus, the mitochondrial proteome already differs profoundly in astrocytes and neurons *in vivo* and *in vitro*, comprising broad categories of protein functions from metabolism to tRNA synthesis and mitochondrial translation.

Mitochondrial Protein Changes during Astrocyte-to-Neuron Reprogramming

To determine whether and when astrocytes downregulate their characteristic mitochondrial proteins and express neuron-enriched ones during reprogramming, we chose differentially enriched functionally relevant candidates detectable by immunostaining (Table S1). The immunofluorescence intensity of the candidates was quantified and normalized to the signal intensity of the pan-mitochondrial protein Tomm20, preventing any bias of the total mitochondrial mass on quantification.

Sfxn5, a mitochondrial transporter of citrate (Miyake et al., 2002), an essential intermediate of the tricarboxylic acid cycle (TCA), was enriched in astrocyte-derived mitochondria (Table S1). Accordingly, its level was much higher in astrocytes or DsRed-transduced controls than in reprogrammed neurons (Figures 2A, 2B, and 2D). During *Ascl1*-mediated reprogramming, Sfxn5 was similar to control astrocytes at early stages (Figures 2A and 2D), whereas βIII-tubulin+ reprogrammed neurons had significantly lower levels (Figures 2B and 2D). Notably, Sfxn5 and Tomm20 showed a greater colocalization in *Ascl1*-transduced cells at 1 than 7 DPT (Figure 2C), supporting the notion that Sfxn5 is mitochondrially localized in astrocytes and disappears in induced neurons (iNeurons). Likewise, the astrocyte-enriched mitochondrial protein Cpox (Mori et al., 2013), highly expressed in astrocytes (Figures S3A, S3B, and S3D) was downregulated significantly in Ascl1-transduced cells (Figures S3B and S3D, center panel), but to a lower degree in *Ascl1*-transduced astrocytes than in *Ascl1*-iNeurons (Figures S3C and S3D). These data show a relatively late (5–7 DPT) regulation of Sfxn5 and Cpox. The lack of downregulation in reprogramming-resistant astrocytes prompts the suggestion that this may contribute to failure of reprogramming.

Among neuron-enriched mitochondrial proteins, we examined Prdx2, which catalyzes the reduction of peroxides and, hence, protects against oxidative stress (Boulos et al., 2007). Prdx2 was not detected in astrocytes (Figures 2E, 2F, and 2H), while *Ascl1*-transduced cells had some Prdx2 signal at 3 DPT, with the strongest increase at 5–7 DPT in *Ascl1*-iNeurons (Figures 2F and 2H). At 7 DPT, Prdx2 reached a level similar to that observed in primary neurons (Figure 2H) and co-localized with Tomm20 (Figure 2G). Similarly, Gls, fundamental for glutamate production and glutamate and GABA transmitter levels as well as neuronal differentiation (Velletri et al., 2013), showed the strongest expression in iNeurons (5–7 DPT; Figures S3F and S3H), where it colocalized with Tomm20 (Figure S3G). Notably, its upregulation started earlier, at 1 DPT (Figure S3H), but did not reach the levels of primary cortical neurons (Figure S3H, right panel).

Mitochondrial proteins enriched in astrocytes (Sfxn5 and Cpox) or neurons (Prdx2 and Gls) change relatively late during

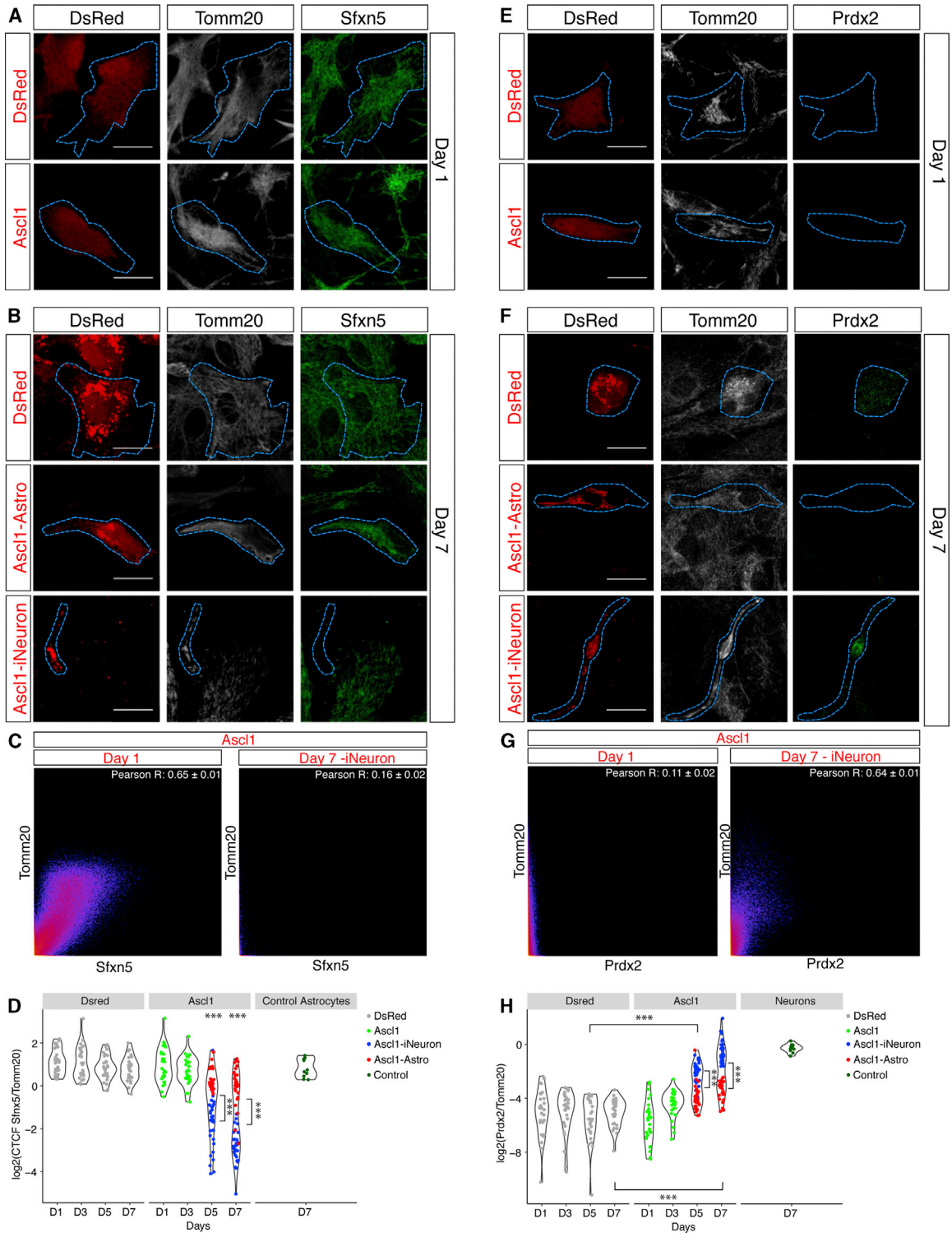

Figure 2. Mitochondrial Protein Changes during Astrocyte-to-Neuron Reprogramming

(A, B, E, and F) Micrographs showing immunostaining in astrocytes transduced with DsRed or Ascl1-ires-DsRed as indicated. Scale bars, 20 μm.

(C and G) Examples of scatterplots of the pixel intensity correlation between Tomm20 and Sfxn5 (C) or Prdx2 (G) in Ascl1-transduced cells on day 1 (left panel) and in reprogrammed cells on day 7 (right panel). Pearson's coefficient as average of 3 cells/biological replicate; n = 3 biological replicates.

(D and H) Violin plots of the $\log_2$ ratio of the intensity of the expression of Sfxn5 (D) or Prdx2 (H) normalized to Tomm20 intensity over time. Each dot represents 1 cell. 10 cells analyzed/biological replicate/condition/day. n = 3 biological replicates; ***$p \leq 0.001$.

CellPress
OPEN ACCESS

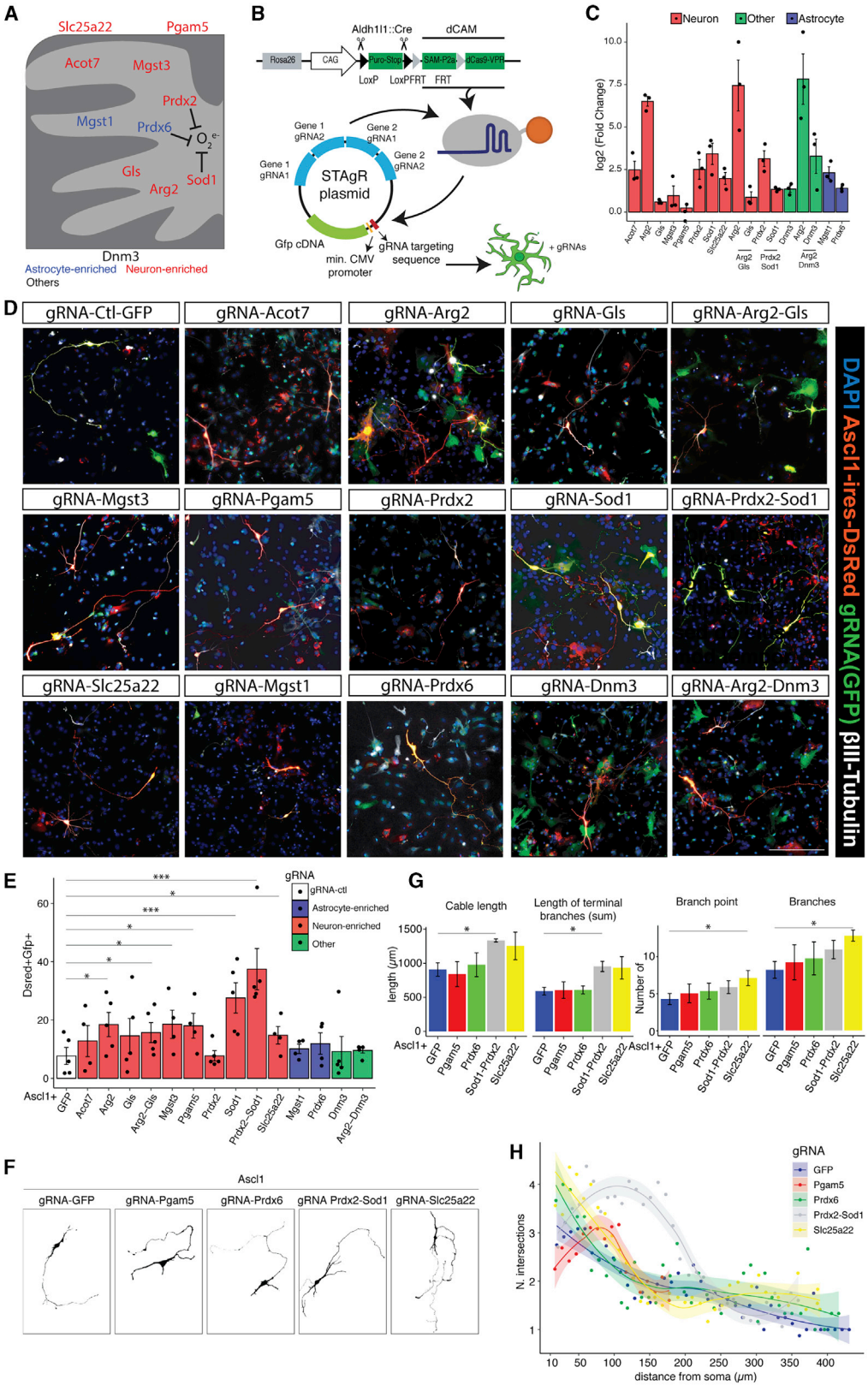

(legend on next page)

neuronal reprogramming. Remarkably, the changes correlated with the degree of conversion, prompting the hypothesis that they may be functionally relevant.

CRISPRa-Mediated Induction of Neuron-Enriched Mitochondrial Proteins Improves the Efficiency of Direct Neuronal Reprogramming

To test the above prediction, we chose 8 candidates enriched in neuronal mitochondria (Figures S4A and S4B; Table S1; Fecher et al., 2019): Sod1 and Prdx2 for their antioxidant activity in neurons (Liu et al., 2020; Rosen, 1993), acyl-CoA thioesterase 7 (Acot7), arginase 2 (Arg2), Gls, microsomal Gst3 (Mgst3), mitochondrial serine/threonine protein phosphatase (Pgam5), and solute carrier 25 member 22 (Slc25a22) (Figure 3A). Among astrocyte-enriched antioxidant mitochondrial proteins, we selected Prdx6 (Fisher, 2011) and the microsomal glutathione S-transferase Mgst1, a member of the membrane-associated proteins in eicosaonid and glutathione metabolism (MAPEG) family, as Mgst3 (Bresell et al., 2005). Dynamin 3 (Dnm3) was included as a protein with mitochondrion-unrelated functions (Gu et al., 2010; Figure 3A).

Quantitative RT-PCR from cells isolated by fluorescence-activated cell sorting (FACS) 48 h after transfection of the dCas9-VPR coding plasmid (Breunig et al., 2018b) and non-targeting control gRNAs or gRNAs designed to target the promoter region of the above candidates showed different levels of induction (Figure 3C; *Arg2*, ~94-fold; *Acot7*, *Prdx2*, *Sod1*, *Slc25a22*, *Dnm3*, *Mgst1*, and *Prdx6*, ~ 5-fold; *Gls*, *Mgst3*, and *Pgam5*, ~2-fold). Multiple gRNAs targeting different genes (e.g., Arg2+-Gls) did not alter the induction levels of their specific targets, and no significant induction was detectable for six putative off targets of each gRNA (Figure S4C).

gRNAs for the selected candidates were cloned in a plasmid with a GFP reporter module whose activation depends on the presence of the self-transcribed gRNAs (e.g., for Sod1) and dCas9-CAM (Figure 3B). Then, primary cultures of astrocytes, obtained by crossing a transgenic mouse line in which the dCas9 gene is fused to three transactivating domains (VP64, p65, and RTA[R transactivator]) and SAM (synergistic activator Mediator) components (dCAM) (Chavez et al., 2015; Konermann et al., 2015; STAR Methods) with the astrocyte-specific Aldh1l1:-Cre mouse line (Tien et al., 2012; Figure 3B), were co-transfected with the constructs for *Ascl1-ires-DsRed* and the control STAgR-GFP (*gRNA-GFP*) or gene-specific gRNA, and neuronal conversion was examined 8 DPT. Strikingly, the induction of many, but not all, genes coding for neuron-enriched mitochondrial proteins improved the reprogramming efficiency (Figures 3D and 3E). Induction of *Sod1* resulted in the highest reprogramming efficiency alone or in combination with *Prdx2* (Figure 3D and 3E; Figure S4D). In addition, induction of *Arg2* and *Mgst3* as well as *Pgam5* and *Slc25a22*, which do not have any reported antioxidant activity, significantly improved the conversion efficiency (Figures 3D and 3E). Remarkably, the induction of genes coding for astrocyte-enriched mitochondrial proteins, even with antioxidant function (*Mgst1* and *Prdx6*), was not beneficial for reprogramming, like *Dnm3* (Figures 3D and 3E). This highlights the need for neuron-enriched antioxidants (e.g., Sod1 and Mgst3) and shows that members of the same family (e.g., Mgst1 and Mgst3) are clearly not functionally redundant. The expression of neuron-enriched candidates also resulted in a more complex morphology of iNeurons, with more neurite outgrowth in Ascl1-Sod1+Prdx2-co-expressing neurons and more branches in Ascl1-Slc25a22-co-expressing neurons (Figures 3F and 3G).

These data suggest that neuron-specific mitochondrial proteins are particularly important during the conversion process and that their earlier and/or higher expression improves reprogramming.

CRISPRa-Mediated Induction of Prdx2 and Sod1 Improves Neuronal Reprogramming by Faster Conversion into Neurons with a Longer Lifespan

To investigate the effect of the early activation of mitochondrial proteins on neuronal conversion, we followed single cells by live imaging as described before (Costa et al., 2011), from 28 h after the transfection for 6 days with GFP/DsRed pictures taken every 4 h (Figure 4A; Figure S2F; Video S1). *Ascl1-Prdx2-Sod1*-co-transfected cells with neuron-like morphology (smaller cell soma and processes longer than 3× the soma length; Gascón et al., 2016) were already increased significantly at 75 h compared with *Ascl1*-only cells (Figure 4B). *Prdx2* and *Sod1* co-activation significantly increased the lifespan of all tracked cells (Figure 4C), mainly because of an increased lifespan of the converted neurons (Figures 4E and 4F), but not of non-reprogrammed astrocytes (Figure 4D), consistent with the cell-type-specific role of antioxidants. Measuring the conversion speed (when cells first acquire a neuron-like morphology) showed a bi-phasic distribution in *Ascl1*-transfected cells (Figure 4G). Cells turning into neurons fast (red dots) typically died before the end of the experiment, whereas those that reprogrammed at a slower pace (blue dots) survived until the end of the video session at 6 DPT (Figure 4G). This was remarkably different in *Ascl1-Prdx2-Sod1*-expressing cells: many cells

Figure 3. CRISPRa-Mediated Activation of Neuron-Enriched Mitochondrial Proteins Improves Neuronal Reprogramming

(A and B) Schemes of the selected candidates in mitochondria and the dCas9-CAM-STAgR (string assembly gRNA) system employed here.

(C) Real-time quantitative PCR (qPCR) of the candidates in dCas9-CAM gene-specific gRNA-expressing cells. Data are shown as $\log_2$ fold change over the gRNA scramble control (mean ± SEM). n = 3 for each group.

(D) Micrographs showing reprogrammed cells (βIII-tubulin$^+$-DsRed$^+$-GFP$^+$) upon co-transfection of Ascl1-ires-DsRed (red) and different STAgR constructs (green). Scale bar, 100 μm.

(E) Reprogramming efficiency as the percentage of βIII-tubulin$^+$/DsRed$^+$/GFP$^+$ at 7 DPT. Data are shown as mean ± SEM. *p < 0.05, ***p < 0.001. n = 5 per experimental condition.

(F) Examples of the morphology of reprogrammed neurons co-expressing Ascl1 and the indicated gRNAs.

(G) Morphological analysis of reprogrammed neurons upon induction of selected candidates (x axis). Data are shown as mean ± SEM. Paired t test, *p ≤ 0.05; n = 4 biological replicates.

(H) Sholl analysis of reprogrammed neurons co-expressing Ascl1 and the indicated candidates. Data are shown as mean ± SEM. Paired t test, *p ≤ 0.05; n = 4 biological replicates.

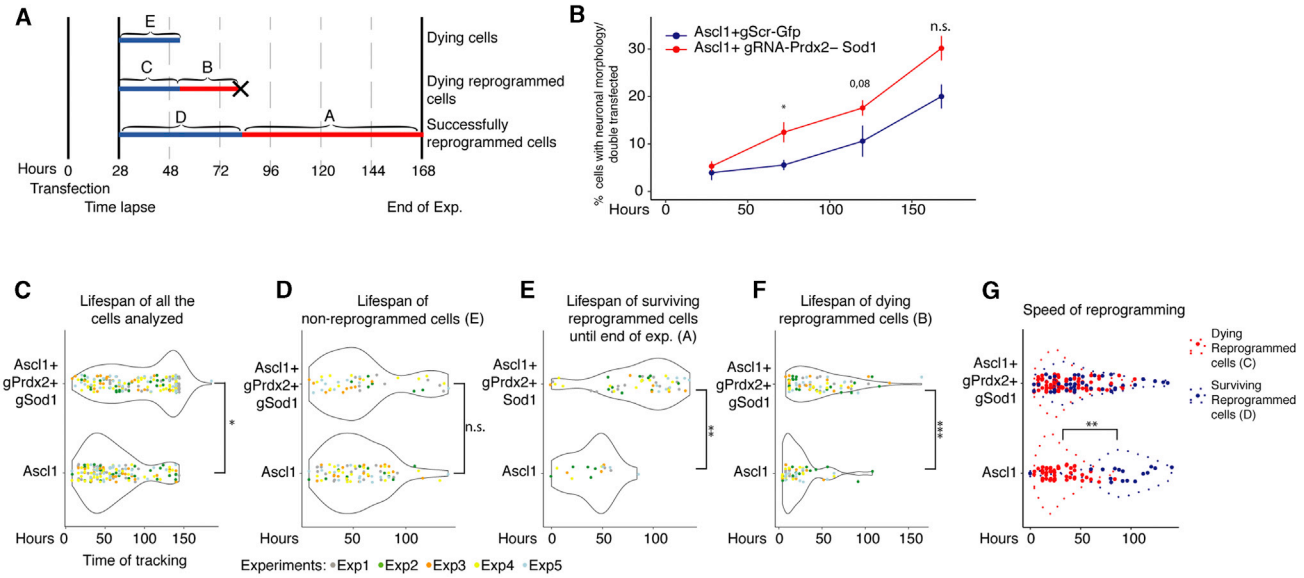

Figure 4. Continuous Single-Cell Live Imaging Reveals Several Roles of Prdx2-Sod1 Activation in Neuronal Reprogramming

(A) Scheme of continuous live imaging and the analysis performed.

(B) Time course analysis of the percentage of cells acquiring neuronal morphology over double-transfected cells at the indicated time points. Data are shown as mean ± SEM. *p ≤ 0.05. n = 3 biological replicates for each group.

(C and D) Violin plot showing the lifespan of all cells analyzed irrespective of their final identity (C) and cells that died without converting (D), following expression of *Ascl1-gRNA-GFP* or *Ascl1-gRNA-Prdx2-Sod1*. n = 5 biological replicates for each group. *p ≤ 0.05

(E–G) Violin plots showing the lifespan (E and F) and speed of reprogramming (G) upon expression of *Ascl1-gRNA-GFP* or *Ascl1-gRNA-Prdx2-Sod1*. n = 5 biological replicates (color-coded) for each group. *p ≤ 0.05, **p ≤ 0.01, ***p ≤ 0.001.

reprogrammed fast and survived until the end of the experiment (Figure 4G). Importantly, this is not due to improved survival of the fast-converting cells that would die under the *Ascl1*-only condition because a similar number of cells converting fast and dying (blue dots and curve in Figure 4G) was observed among *Ascl1-Prdx2-Sod1* cells. Rather, many more cells were recruited for reprogramming under the *Ascl1-Prdx2-Sod1* condition and in a fast manner (Figure 4G). We therefore conclude that activation of these neuron-enriched mitochondrial proteins speeds up the conversion process in addition to its role in protecting neurons from cell death.

DISCUSSION

Here we describe the comprehensive mitochondrial proteomes of cortical astrocytes and neurons that show quantitative differences in a fifth of the identified proteins. The functional relevance of these differences is shown by the fact that cells failing to upregulate neuron-enriched mitochondrial proteins often do not reprogram; activating their expression improved the reprogramming efficiency, and astrocyte-enriched mitochondrial proteins, even with known antioxidant function, have no such effects.

Astrocyte Metabolism and Its Influence on Neuronal Reprogramming

Astrocytes share similarities with neural stem cells (NSCs) (Götz et al., 2015). For example, we and others (Fecher et al., 2019) found the mitochondrial proteome of astrocytes to be enriched for the GO terms lipid metabolism and fatty acid β-oxidation, also highly represented in neural stem cells (NSCs) and downregulated during adult neurogenesis (Knobloch et al., 2017; Llorens-Bobadilla et al., 2015). Despite the fast transcriptional changes at early stages of reprogramming (Gascón et al., 2016; Masserdotti et al., 2015), genes associated with lipid metabolism (e.g., *Cpt1a*) are not yet downregulated after 48 h (Gascón et al., 2016; Masserdotti et al., 2015), suggesting slow metabolic conversion, a limiting factor in induced pluripotent stem cell (iPSC) reprogramming (Wu et al., 2016). Accordingly, etomoxir-mediated reduction of fatty acid β-oxidation improved neuronal reprogramming (Figure S3), indicating that the manipulation of specific metabolic pathways might substantially contribute to remove hurdles during the conversion. The addition of ROS scavenger reduced the reprogramming efficiency combined with etomoxir, suggesting potential beneficial effects of ROS under this condition. It will be interesting to determine the level of ROS above which it shows deleterious effects.

Early Activation of Neuron-Enriched Mitochondrial Proteins with a Wide Functional Spectrum Improves Astrocyte-to-Neuron Conversion

The comprehensive mitochondrial proteome revealed cell-type-specific enrichment of antioxidant proteins; e.g., Mgst1 and Mgst3 were enriched in the mitochondrial proteome of astrocytes and neurons, respectively. Remarkably, early CRISPRa-mediated induction of the latter, but not the former, improved direct neuronal conversion, demonstrating the key functional role of cell-type-specific but similar antioxidant proteins. Sod1 activation had the most potent effect, in line with its functional relevance in neurodegeneration (Kaur et al., 2016). However, other mitochondrial proteins with antioxidant functions, such

as Prdx6 and Prdx2 (enriched in astrocytes and neurons, respectively) did not improve reprogramming, showing that only some antioxidants perform highly cell-type-specific functions relevant in direct neuronal reprogramming.

The early activation of neuron-enriched mitochondrial proteins without any reported antioxidant activity also significantly increased direct reprogramming efficiency. Pgam5, a mitochondrial phosphatase that associates with the RIP1/RIP3/MLKL (Mixed lineage kinase domain-like pseudokinase) complex, doubled *Ascl1*-induced reprogramming efficiency, possibly by inhibiting necroptosis (Gascón et al., 2016; Lu et al., 2016). In addition, Pgam5 regulates mitochondrial homeostasis and dynamics by dephosphorylating Drp1, BCL-xL (B-cell lymphoma extra large), and FUNDC1 (Ma et al., 2020), a key process for neuronal function and survival (Lu et al., 2014). Likewise, the mitochondrial glutamate transporter Slc25a22, which also improved reprogramming by 2-fold, is important for brain function (Cohen et al., 2014; Molinari et al., 2005, 2009; Poduri et al., 2013) by regulating glutamate levels (Goubert et al., 2017).

Conversely, the activation of Gls did not significantly improve reprogramming, suggesting that glutamate biogenesis does not have a major role in this process. Likewise, the activation of a non-mitochondrial protein, Dnm3, expressed at similar levels in astrocytes and neurons, had no effect. These results confirm our cutoff criteria and highlight a potent role of only some neuron-enriched mitochondrial proteins in direct conversion by influencing several functional pathways.

Notably, astrocyte-enriched mitochondrial proteins, like Sfnx5 and Cpox, were only partially downregulated in reprogramming and maintained a higher expression in cells that failed to convert. This indicates that these cells face a "confused" metabolic state that may hinder reprogramming and highlights the importance to further ease the metabolic transition for proper conversion. Indeed, "on-memory" genes not shut off during reprogramming from the original starter cell limit the conversion process (Hormanseder et al., 2017).

Neuron-Enriched Mitochondrial Protein Activation as an Enabler and Driver in Reprogramming

Most improvement in reprogramming efficiency was achieved by early expression of the neuron-enriched mitochondrial proteins Sod1 and Prdx2: they increased recruitment of more cells into the conversion process and improved survival only of reprogrammed neurons and their differentiation. Thus, early activation of these neuron-enriched mitochondrial antioxidants protects neurons, but not astrocytes, against aberrant ROS levels (Gascón et al., 2016).

Remarkably, *Ascl1*-expressing cells showed a significant difference in conversion speed between neurons that survive and those that do not survive for 6 days, with the former converting much slower. This is reminiscent of natural neurogenesis, where the transition from progenitors to neurons often occurs more gradually via intermediate progenitors (Khacho et al., 2016; Llorens-Bobadilla et al., 2015), suggesting the need for a period of adaptation to support the new identity. Surprisingly, the expression of *Prdx2* and *Sod1* speeds up the conversion process in cells surviving until the end of the time lapse, similarly to co-expression of Bcl2 (Gascón et al., 2016). Thus, different mitochondrion-dependent pathways may speed up the conversion rate by improving cell survival and/or protecting against ROS damage. We therefore propose that failure or late activation of neuron-enriched mitochondrial proteins may impair the conversion process at several levels, ultimately causing cells to die. Importantly, this occurs despite the expression of a multitude of antioxidant and metabolic proteins present in astrocytes. Thus, direct neuronal reprogramming sheds new light on the function of cell-type-enriched mitochondrial proteins.

Limitations of Study

Clearly, it would be desirable to follow the mitochondrial proteome in a comprehensive manner during the reprogramming process, which will be made easier by newly developed mouse lines with tagged mitochondrial proteins (Fecher et al., 2019), also in the murine brain *in vivo* or human cells *in vitro*. Ideally, these could be compared with fully differentiated neurons; here we choose culture conditions and time points to match the reprogramming protocol.

STAR★METHODS

Detailed methods are provided in the online version of this paper and include the following:

- KEY RESOURCES TABLE
- RESOURCE AVAILABILITY
  - Lead Contact
  - Materials Availability
  - Data and Code Availability
- EXPERIMENTAL MODEL AND SBJECT DETAILS
  - Wild-type mice (Primary Cell culture, Proteomics, IHC)
  - Aldh1-Cre and Cre-inducible dCas9-VPR mice
  - Primary cultures of cortical astrocytes
  - Cells undergoing direct neuronal conversion
  - Primary cultures of cortical neurons
- METHOD DETAILS
  - Transfection and Transduction
  - Fluorescence-activated Cell Sorting
  - Mitochondria isolation
  - Characterization of isolated mitochondria
  - Seahorse experiments
  - Proteome analysis
  - Western Blot Analysis
  - Immunocytochemistry
  - RNA extraction, retro-transcription and Real Time Quantitative PCR (qRT-PCR)
  - STAgR cloning
  - Live-Imaging Microscopy
- QUANTIFICATION AND STATISTICAL ANALYSIS

SUPPLEMENTAL INFORMATION

Supplemental Information can be found online at https://doi.org/10.1016/j.stem.2020.10.015.

ACKNOWLEDGMENTS

Particular thanks go to Caroline Fecher and Thomas Misgeld (Technical University of Munich) for providing the antibodies against Sfxn5 and Gls and sharing their proteome data and expertise about mitochondria. We are very

grateful to Tatiana Simon (BMC, Munich) and Andrea Steiner-Mezzadri (Helmholtz Center Munich) for technical assistance, Daniel Brandt for technical support with the Seahorse analyzer, Uli Ohmayer for initial proteomic analysis, Andreas Beyerlein and Hannah Busen from Core Facility Statistical Consulting (all from Helmholtz Center Munich), Tobias Straub (Bioinformatic Core Facility of the BMC, LMU, Munich) and Pawel Smialowski (Helmholtz Zentrum, Munich) for help with R coding, Tamas Schauer for advice regarding DHARMa, and Nicola Mattugini for comments on the manuscript. This work was funded by the Fondation Rodger de Spoelberch, the German Research Foundation (SFB870 and SPP1757), the advanced ERC ChroNeuroRepair and ERAnet (to M.G.), SPP2127 (to S.M.H.), and ExNet-0041-Phase2-3 (SyNergy-HMGU) and AMPro Project (Aging and Metabolic Programming) network funds of the Helmholtz Association (to W.W.).

AUTHOR CONTRIBUTIONS

M.G. conceived and designed the project. G.L.R. and G.M. shaped the project, and G.L.R. performed experiments and analysis. G.S. contributed to the time course analysis. P.N. performed and analyzed the experiment with etomoxir, gRNA, and continuous live imaging. C.T.B. and S.H.S. provided CRISPR-Cas expertise and developed and designed the STAgR approach, and C.T.B. helped with cloning of the constructs. G.B. performed western blots. J.M.-P. and S.M.H. provided proteomics expertise and performed experiments and analysis. S.S. and H.Z. performed mitochondrial isolation and electron microscopy. J.G.-S., F.G., and W.W. generated and provided dCAM transgenic mice. M.J. provided expertise regarding metabolism and Seahorse analysis. G.M. analyzed the data; provided expertise and training of G.L.R., G.S., P.N., and G.B. regarding reprogramming; and co-directed the project together with M.G. G.L.R., G.M., and M.G. wrote the manuscript, and all authors contributed corrections and comments.

DECLARATION OF INTERESTS

The authors declare no competing interests.

Received: August 5, 2019
Revised: August 11, 2020
Accepted: August 20, 2020
Published: November 16, 2020; corrected online: December 2, 2020

REFERENCES

Barker, R.A., Götz, M., and Parmar, M. (2018). New approaches for brain repair-from rescue to reprogramming. Nature *557*, 329–334.

Boulos, S., Meloni, B.P., Arthur, P.G., Bojarski, C., and Knuckey, N.W. (2007). Peroxiredoxin 2 overexpression protects cortical neuronal cultures from ischemic and oxidative injury but not glutamate excitotoxicity, whereas Cu/Zn superoxide dismutase 1 overexpression protects only against oxidative injury. J. Neurosci. Res. *85*, 3089–3097.

Bresell, A., Weinander, R., Lundqvist, G., Raza, H., Shimoji, M., Sun, T.H., Balk, L., Wiklund, R., Eriksson, J., Jansson, C., et al. (2005). Bioinformatic and enzymatic characterization of the MAPEG superfamily. FEBS J. *272*, 1688–1703.

Breunig, C.T., Durovic, T., Neuner, A.M., Baumann, V., Wiesbeck, M.F., Köferle, A., Götz, M., Ninkovic, J., and Stricker, S.H. (2018a). One step generation of customizable gRNA vectors for multiplex CRISPR approaches through string assembly gRNA cloning (STAgR). PLoS ONE *13*, e0196015.

Breunig, C.T., Neuner, A.M., Giehrl-Schwab, J., Wurst, W., Götz, M., and Stricker, S.H. (2018b). A Customizable Protocol for String Assembly gRNA Cloning (STAgR). J. Vis. Exp. (142), e58556.

Calvo, S.E., and Mootha, V.K. (2010). The mitochondrial proteome and human disease. Annu. Rev. Genomics Hum. Genet. *11*, 25–44.

Calvo, S.E., Clauser, K.R., and Mootha, V.K. (2016). MitoCarta2.0: an updated inventory of mammalian mitochondrial proteins. Nucleic Acids Res. *44* (D1), D1251–D1257.

Chavez, A., Scheiman, J., Vora, S., Pruitt, B.W., Tuttle, M., P R Iyer, E., Lin, S., Kiani, S., Guzman, C.D., Wiegand, D.J., et al. (2015). Highly efficient Cas9-mediated transcriptional programming. Nat. Methods *12*, 326–328.

Cohen, R., Basel-Vanagaite, L., Goldberg-Stern, H., Halevy, A., Shuper, A., Feingold-Zadok, M., Behar, D.M., and Straussberg, R. (2014). Two siblings with early infantile myoclonic encephalopathy due to mutation in the gene encoding mitochondrial glutamate/H+ symporter SLC25A22. Eur. J. Paediatr. Neurol. *18*, 801–805.

Costa, M.R., Ortega, F., Brill, M.S., Beckervordersandforth, R., Petrone, C., Schroeder, T., Götz, M., and Berninger, B. (2011). Continuous live imaging of adult neural stem cell division and lineage progression in vitro. Development *138*, 1057–1068.

Fecher, C., Trovò, L., Müller, S.A., Snaidero, N., Wettmarshausen, J., Heink, S., Ortiz, O., Wagner, I., Kühn, R., Hartmann, J., et al. (2019). Cell-type-specific profiling of brain mitochondria reveals functional and molecular diversity. Nat. Neurosci. *22*, 1731–1742.

Ferreira, T.A., Blackman, A.V., Oyrer, J., Jayabal, S., Chung, A.J., Watt, A.J., Sjöström, P.J., and van Meyel, D.J. (2014). Neuronal morphometry directly from bitmap images. Nat. Methods *11*, 982–984.

Fisher, A.B. (2011). Peroxiredoxin 6: a bifunctional enzyme with glutathione peroxidase and phospholipase A_2 activities. Antioxid. Redox Signal. *15*, 831–844.

Folmes, C.D., Dzeja, P.P., Nelson, T.J., and Terzic, A. (2012). Metabolic plasticity in stem cell homeostasis and differentiation. Cell Stem Cell *11*, 596–606.

Gascón, S., Murenu, E., Masserdotti, G., Ortega, F., Russo, G.L., Petrik, D., Deshpande, A., Heinrich, C., Karow, M., Robertson, S.P., et al. (2016). Identification and Successful Negotiation of a Metabolic Checkpoint in Direct Neuronal Reprogramming. Cell Stem Cell *18*, 396–409.

Gibson, D.G. (2011). Enzymatic assembly of overlapping DNA fragments. Methods Enzymol. *498*, 349–361.

Götz, M., Sirko, S., Beckers, J., and Irmler, M. (2015). Reactive astrocytes as neural stem or progenitor cells: In vivo lineage, In vitro potential, and Genome-wide expression analysis. Glia *63*, 1452–1468.

Goubert, E., Mircheva, Y., Lasorsa, F.M., Melon, C., Profilo, E., Sutera, J., Becq, H., Palmieri, F., Palmieri, L., Aniksztejn, L., and Molinari, F. (2017). Inhibition of the Mitochondrial Glutamate Carrier SLC25A22 in Astrocytes Leads to Intracellular Glutamate Accumulation. Front. Cell. Neurosci. *11*, 149.

Grade, S., and Götz, M. (2017). Neuronal replacement therapy: previous achievements and challenges ahead. NPJ Regen. Med. *2*, 29.

Gu, C., Yaddanapudi, S., Weins, A., Osborn, T., Reiser, J., Pollak, M., Hartwig, J., and Sever, S. (2010). Direct dynamin-actin interactions regulate the actin cytoskeleton. EMBO J. *29*, 3593–3606.

Harris, J.J., Jolivet, R., and Attwell, D. (2012). Synaptic energy use and supply. Neuron *75*, 762–777.

Hartfuss, E., Galli, R., Heins, N., and Götz, M. (2001). Characterization of CNS precursor subtypes and radial glia. Dev. Biol. *229*, 15–30.

Hartig, F., and Lohse, L. (2020). DHARMa: Residual Diagnostics for Hierarchical (Multi-Level/Mixed) Regression Models. R package version 0.3.2.0. https://cran.r-project.org/web/packages/DHARMa/index.html.

Heinrich, C., Blum, R., Gascón, S., Masserdotti, G., Tripathi, P., Sánchez, R., Tiedt, S., Schroeder, T., Götz, M., and Berninger, B. (2010). Directing astroglia from the cerebral cortex into subtype specific functional neurons. PLoS Biol. *8*, e1000373.

Heinrich, C., Gascón, S., Masserdotti, G., Lepier, A., Sanchez, R., Simon-Ebert, T., Schroeder, T., Götz, M., and Berninger, B. (2011). Generation of subtype-specific neurons from postnatal astroglia of the mouse cerebral cortex. Nat. Protoc. *6*, 214–228.

Heins, N., Malatesta, P., Cecconi, F., Nakafuku, M., Tucker, K.L., Hack, M.A., Chapouton, P., Barde, Y.A., and Götz, M. (2002). Glial cells generate neurons: the role of the transcription factor Pax6. Nat. Neurosci. *5*, 308–315.

Herrero-Mendez, A., Almeida, A., Fernández, E., Maestre, C., Moncada, S., and Bolaños, J.P. (2009). The bioenergetic and antioxidant status of neurons is controlled by continuous degradation of a key glycolytic enzyme by APC/C-Cdh1. Nat. Cell Biol. *11*, 747–752.

Hormanseder, E., Simeone, A., Allen, G.E., Bradshaw, C.R., Figlmuller, M., Gurdon, J., and Jullien, J. (2017). H3K4 Methylation-Dependent Memory of

Somatic Cell Identity Inhibits Reprogramming and Development of Nuclear Transfer Embryos. Cell Stem Cell *21*, 135–143.e6.

Jernberg, J.N., Bowman, C.E., Wolfgang, M.J., and Scafidi, S. (2017). Developmental regulation and localization of carnitine palmitoyltransferases (CPTs) in rat brain. J. Neurochem. *142*, 407–419.

Kaur, S.J., McKeown, S.R., and Rashid, S. (2016). Mutant SOD1 mediated pathogenesis of Amyotrophic Lateral Sclerosis. Gene *577*, 109–118.

Khacho, M., Clark, A., Svoboda, D.S., Azzi, J., MacLaurin, J.G., Meghaizel, C., Sesaki, H., Lagace, D.C., Germain, M., Harper, M.E., et al. (2016). Mitochondrial Dynamics Impacts Stem Cell Identity and Fate Decisions by Regulating a Nuclear Transcriptional Program. Cell Stem Cell *19*, 232–247.

Knobloch, M., Pilz, G.A., Ghesquière, B., Kovacs, W.J., Wegleiter, T., Moore, D.L., Hruzova, M., Zamboni, N., Carmeliet, P., and Jessberger, S. (2017). A Fatty Acid Oxidation-Dependent Metabolic Shift Regulates Adult Neural Stem Cell Activity. Cell Rep. *20*, 2144–2155.

Konermann, S., Brigham, M.D., Trevino, A.E., Joung, J., Abudayyeh, O.O., Barcena, C., Hsu, P.D., Habib, N., Gootenberg, J.S., Nishimasu, H., et al. (2015). Genome-scale transcriptional activation by an engineered CRISPR-Cas9 complex. Nature *517*, 583–588.

Korotkevich, G., Sukhov, V., and Sergushichev, A. (2019). Fast gene set enrichment analysis. bioRxiv. https://doi.org/10.1101/060012.

Lin, R., Tao, R., Gao, X., Li, T., Zhou, X., Guan, K.L., Xiong, Y., and Lei, Q.Y. (2013). Acetylation stabilizes ATP-citrate lyase to promote lipid biosynthesis and tumor growth. Mol. Cell *51*, 506–518.

Liu, J., Su, G., Gao, J., Tian, Y., Liu, X., and Zhang, Z. (2020). Effects of Peroxiredoxin 2 in Neurological Disorders: A Review of its Molecular Mechanisms. Neurochem. Res. *45*, 720–730.

Llorens-Bobadilla, E., Zhao, S., Baser, A., Saiz-Castro, G., Zwadlo, K., and Martin-Villalba, A. (2015). Single-Cell Transcriptomics Reveals a Population of Dormant Neural Stem Cells that Become Activated upon Brain Injury. Cell Stem Cell *17*, 329–340.

Lu, W., Karuppagounder, S.S., Springer, D.A., Allen, M.D., Zheng, L., Chao, B., Zhang, Y., Dawson, V.L., Dawson, T.M., and Lenardo, M. (2014). Genetic deficiency of the mitochondrial protein PGAM5 causes a Parkinson's-like movement disorder. Nat. Commun. *5*, 4930.

Lu, W., Sun, J., Yoon, J.S., Zhang, Y., Zheng, L., Murphy, E., Mattson, M.P., and Lenardo, M.J. (2016). Mitochondrial Protein PGAM5 Regulates Mitophagic Protection against Cell Necroptosis. PLoS ONE *11*, e0147792.

Ma, K., Zhang, Z., Chang, R., Cheng, H., Mu, C., Zhao, T., Chen, L., Zhang, C., Luo, Q., Lin, J., et al. (2020). Dynamic PGAM5 multimers dephosphorylate BCL-xL or FUNDC1 to regulate mitochondrial and cellular fate. Cell Death Differ. *27*, 1036–1051.

Márquez, J., Tosina, M., de la Rosa, V., Segura, J.A., Alonso, F.J., Matés, J.M., and Campos-Sandoval, J.A. (2009). New insights into brain glutaminases: beyond their role on glutamatergic transmission. Neurochem. Int. *55*, 64–70.

Masserdotti, G., Gillotin, S., Sutor, B., Drechsel, D., Irmler, M., Jørgensen, H.F., Sass, S., Theis, F.J., Beckers, J., Berninger, B., et al. (2015). Transcriptional Mechanisms of Proneural Factors and REST in Regulating Neuronal Reprogramming of Astrocytes. Cell Stem Cell *17*, 74–88.

Misgeld, T., and Schwarz, T.L. (2017). Mitostasis in Neurons: Maintaining Mitochondria in an Extended Cellular Architecture. Neuron *96*, 651–666.

Miyake, S., Yamashita, T., Taniguchi, M., Tamatani, M., Sato, K., and Tohyama, M. (2002). Identification and characterization of a novel mitochondrial tricarboxylate carrier. Biochem. Biophys. Res. Commun. *295*, 463–468.

Molinari, F., Raas-Rothschild, A., Rio, M., Fiermonte, G., Encha-Razavi, F., Palmieri, L., Palmieri, F., Ben-Neriah, Z., Kadhom, N., Vekemans, M., et al. (2005). Impaired mitochondrial glutamate transport in autosomal recessive neonatal myoclonic epilepsy. Am. J. Hum. Genet. *76*, 334–339.

Molinari, F., Kaminska, A., Fiermonte, G., Boddaert, N., Raas-Rothschild, A., Plouin, P., Palmieri, L., Brunelle, F., Palmieri, F., Dulac, O., et al. (2009). Mutations in the mitochondrial glutamate carrier SLC25A22 in neonatal epileptic encephalopathy with suppression bursts. Clin. Genet. *76*, 188–194.

Mori, M., Gotoh, S., Taketani, S., Hiai, H., and Higuchi, K. (2013). Hereditary cataract of the Nakano mouse: Involvement of a hypomorphic mutation in the coproporphyrinogen oxidase gene. Exp. Eye Res. *112*, 45–50.

Motori, E., Puyal, J., Toni, N., Ghanem, A., Angeloni, C., Malaguti, M., Cantelli-Forti, G., Berninger, B., Conzelmann, K.K., Götz, M., et al. (2013). Inflammation-induced alteration of astrocyte mitochondrial dynamics requires autophagy for mitochondrial network maintenance. Cell Metab. *18*, 844–859.

O'Connor, R.S., Guo, L., Ghassemi, S., Snyder, N.W., Worth, A.J., Weng, L., Kam, Y., Philipson, B., Trefely, S., Nunez-Cruz, S., et al. (2018). The CPT1a inhibitor, etomoxir induces severe oxidative stress at commonly used concentrations. Sci. Rep. *8*, 6289.

Pagliarini, D.J., Calvo, S.E., Chang, B., Sheth, S.A., Vafai, S.B., Ong, S.E., Walford, G.A., Sugiana, C., Boneh, A., Chen, W.K., et al. (2008). A mitochondrial protein compendium elucidates complex I disease biology. Cell *134*, 112–123.

Poduri, A., Heinzen, E.L., Chitsazzadeh, V., Lasorsa, F.M., Elhosary, P.C., LaCoursiere, C.M., Martin, E., Yuskaitis, C.J., Hill, R.S., Atabay, K.D., et al. (2013). SLC25A22 is a novel gene for migrating partial seizures in infancy. Ann. Neurol. *74*, 873–882.

Rosen, D.R. (1993). Mutations in Cu/Zn superoxide dismutase gene are associated with familial amyotrophic lateral sclerosis. Nature *364*, 362.

Schaffer, A.E., Pinkard, O., and Coller, J.M. (2019). tRNA Metabolism and Neurodevelopmental Disorders. Annu. Rev. Genomics Hum. Genet. *20*, 359–387.

Schmitt, S., Saathoff, F., Meissner, L., Schropp, E.M., Lichtmannegger, J., Schulz, S., Eberhagen, C., Borchard, S., Aichler, M., Adamski, J., et al. (2013). A semi-automated method for isolating functionally intact mitochondria from cultured cells and tissue biopsies. Anal. Biochem. *443*, 66–74.

Spinelli, J.B., and Haigis, M.C. (2018). The multifaceted contributions of mitochondria to cellular metabolism. Nat. Cell Biol. *20*, 745–754.

Tien, A.C., Tsai, H.H., Molofsky, A.V., McMahon, M., Foo, L.C., Kaul, A., Dougherty, J.D., Heintz, N., Gutmann, D.H., Barres, B.A., and Rowitch, D.H. (2012). Regulated temporal-spatial astrocyte precursor cell proliferation involves BRAF signalling in mammalian spinal cord. Development *139*, 2477–2487.

van Deijk, A.F., Camargo, N., Timmerman, J., Heistek, T., Brouwers, J.F., Mogavero, F., Mansvelder, H.D., Smit, A.B., and Verheijen, M.H. (2017). Astrocyte lipid metabolism is critical for synapse development and function in vivo. Glia *65*, 670–682.

Velletri, T., Romeo, F., Tucci, P., Peschiaroli, A., Annicchiarico-Petruzzelli, M., Niklison-Chirou, M.V., Amelio, I., Knight, R.A., Mak, T.W., Melino, G., and Agostini, M. (2013). GLS2 is transcriptionally regulated by p73 and contributes to neuronal differentiation. Cell Cycle *12*, 3564–3573.

Vignoles, R., Lentini, C., d'Orange, M., and Heinrich, C. (2019). Direct Lineage Reprogramming for Brain Repair: Breakthroughs and Challenges. Trends Mol. Med. *25*, 897–914.

Walcher, T., Xie, Q., Sun, J., Irmler, M., Beckers, J., Öztürk, T., Niessing, D., Stoykova, A., Cvekl, A., Ninkovic, J., and Götz, M. (2013). Functional dissection of the paired domain of Pax6 reveals molecular mechanisms of coordinating neurogenesis and proliferation. Development *140*, 1123–1136.

Wiśniewski, J.R., Zougman, A., Nagaraj, N., and Mann, M. (2009). Universal sample preparation method for proteome analysis. Nat. Methods *6*, 359–362.

Wu, J., Ocampo, A., and Belmonte, J.C.I. (2016). Cellular Metabolism and Induced Pluripotency. Cell *166*, 1371–1385.

Zhang, X., Smits, A.H., van Tilburg, G.B., Ovaa, H., Huber, W., and Vermeulen, M. (2018). Proteome-wide identification of ubiquitin interactions using UbIA-MS. Nat. Protoc. *13*, 530–550.

Zischka, H., Larochette, N., Hoffmann, F., Hamöller, D., Jägemann, N., Lichtmannegger, J., Jennen, L., Müller-Höcker, J., Roggel, F., Göttlicher, M., et al. (2008). Electrophoretic analysis of the mitochondrial outer membrane rupture induced by permeability transition. Anal. Chem. *80*, 5051–5058.

STAR★METHODS

KEY RESOURCES TABLE

REAGENT or RESOURCE	SOURCE	IDENTIFIER
Antibodies		
Rabbit anti-CS	Novus Biologicals	NBP2-13878
Rabbit anti-VDAC	Cell Signaling	Cat# 4866; RRID: AB_2272627
Goat anti-ANT	Santa Cruz	Cat# sc.9299; RRID: AB_671086
Total Oxphos Rodent Ab cocktail	Abcam	Cat# ab110413; RRID: AB_2629281
Mouse anti-β-III-Tubulin	Sigma-Aldrich	Cat# T8660; RRID: AB_477590
Mouse anti-GFAP	Dako	Cat# Z0334; RRID: AB_100013482
Rabbit anti-GFAP	Sigma-Aldrich	Cat# G3893; RRID: AB_477010
Rat anti-RFP	Chromotek	Cat# 5F8; RRID: AB_2336064
Rabbit anti-RFP	Rockland	Cat# 600-401-379; RRID: AB_2209751
Chicken anti-GFP	Aves Labs	Cat# GFP-1020; RRID: AB_10000240
Rabbit anti-CPOX	Abcam	Cat# Ab169766
Rabbit anti-Prdx2	Abcam	Cat# Ab109367; RRID: AB_10862524
Rabbit anti-Gls	Proteintech	Cat# 20170-1-AP; RRID: AB_10665373
Rabbit anti-Sfxn5	Abcam	Cat# Ab172971
Anti-Aldh1l1	Merck Millipore	Cat# MABN495; RRID: AB_2687399
Anti-Tomm20	Abnova	CAt# H00009804-M01; RRID: AB_1507602
Anti-Mouse-HRP linked	Invitrogen	Cat#626520; RRID: AB_2533947
Anti-Mouse, HRP linked	Cell Signaling	Cat# 7076; RRID: AB_330924
Anti-Rabbit, HRP linked	Cell Signaling	Cat# 7074; RRID: AB_2099233
Anti-Rabbit, HRP, linked	GE Healthcare	Cat#NA934; RRID: AB_2722659
Anti-Goat, HRP linked	Santa Cruz	Cat# sc-2020; RRID: AB_631728
Anti-Mouse Alexa Fluor 488	Molecular Probes	Cat# A-21202; RRID: AB_141607
Anti-Chicken Alexa Fluor 488	Thermo Fisher	Cat# A-11039; RRID: AB_2534096
Anti-Rat Cy3	Dianova	Cat# 112-165-167; RRID: AB_2338251
Anti-Mouse IgG2b 633	Innovative Research	Cat# A21146; RRID: AB_1500899
Anti-Mouse IgG1 647	Molecular Probes	Cat# A21240; RRID: AB_141658
Anti-Rabbit Alexa Fluor 488	Molecular Probes	Cat# A21206; RRID: AB_141708
Anti-Mouse IgG1 Biotin	Southernbiotech	Cat# 1070-08; RRID: AB_2794413
Streptavidin Alex Fluor 405	Thermo Fisher	Cat# S32351
Bacterial and Virus Strains		
RV CAG-Neurog2-ires-DsRedExpress2	Gascón et al., 2016	N/A
RV CAG-Ascl1-ires-DsRed	Gascón et al., 2016	N/A
RV CAG-DsRedExpress2	Gascón et al., 2016	N/A
RV CAG-mitoGFP	This study	N/A
RV CAG-Ascl1-ires-mitoGFP	This study	N/A
RV CAG-Ascl1-ires-mitoRFP	This study	N/A
Chemicals, Peptides, and Recombinant Proteins		
EGF	GIBCO	Cat# PHG0311
bFGF	GIBCO	Cat# 13256029
Poly-D-Lysine	Sigma-Aldrich	Cat# P0899
B27	GIBCO	Cat# 17504044
HBSS medium	Thermo Fisher	Cat# 24020117
HEPES	Thermo Fisher	Cat# 15630080
DMEM/F12	Thermo Fisher	Cat# 10565018

(*Continued on next page*)

Continued

REAGENT or RESOURCE	SOURCE	IDENTIFIER
trypsin/EDTA 0,25%	Thermo Fisher	Cat# 25200056
Neurobasal Medium	GIBCO	Cat# 21103149
Glucose	GIBCO	Cat# A2494001
GluataMAX	GIBCO	Cat# 35050061
OptiMEM – GlutaMAX	Thermo Fisher	Cat# 51985-026
EGTA	Sigma-Aldrich	Cat# E3889
Lipofectamine 2000	Thermo Fisher	Cat# 11668019
Rhodamine 123	Thermo Fisher	Cat# R302
Oligomycin A	Sigma-Aldrich	Cat# 73351
FCCP	Sigma-Aldrich	Cat# C2920
Rotenone	Sigma-Aldrich	Cat# R8875
Antimycin A	Sigma-Aldrich	Cat# A8674
2-Deoxy-D-glucose	Sigma-Aldrich	Cat# D8375
Triton X-100	Sigma-Aldrich	Cat# T9284
Etomoxir	Sigma-Aldrich	Cat# E1905
Bovine Serum Albumine (BSA)	Sigma-Aldrich	Cat# A9418
Critical Commercial Assays		
Arcturus PicoPure RNA Isolation Kit	Thermo Fisher	Cat# 12204-01
Bradford Protein Assay Kit	BioRad	Cat# 5000201
First Strand cDNA Synthesis Kit	Thermo Fisher	Cat# K1621
PowerUp SYBR Green Master Mix	Thermo Fisher	Cat# A25742
Agencourt AMPure XP	Beckman Coulter	Cat# 10136224
RC DC Protein assay	BioRad	N/A
Deposited Data		
mitoProteomic data, identifier: PXD014886	This study	https://www.ebi.ac.uk/pride
Experimental Models: Organisms/Strains		
C57BL/6	LMU animal Facility	N/A
Aldh1l1-Cre	LMU animal Facility	N/A
Rosa26-LoxP-Stop-LoxP-dCAM	HMGU	N/A
Oligonucleotides		
See Methods S1	This study	N/A
Recombinant DNA		
STAgR_Neo	Addgene	RRID:Addgene_102992
STAGR_gRNAScaffold_hU6	Addgene	RRID:Addgene_102843
STAGR_gRNAScaffold_hH1	Addgene	RRID:Addgene_102841
STAGR_gRNAScaffold_h7SK	Addgene	Addgene_102841
STAGR_gRNAScaffold_mU6	Addgene	RRID:Addgene_102844
pCDNA-miniCMV-GFP	This study	N/A
STAgR_cntrl	This study	N/A
STAgR_Acot7	This study	N/A
STAgR_Arg2	This study	N/A
STAgR_Gls	This study	N/A
STAgR_Mgst3	This study	N/A
STAgR_Pgam5	This study	N/A
STAgR_Sod1	This study	N/A
STAgR_Slc25a22	This study	N/A
STAgR_Dnm3	This study	N/A
STAgR_Mgst1	This study	N/A
STAgR_Prdx6	This study	N/A

(*Continued on next page*)

Continued

REAGENT or RESOURCE	SOURCE	IDENTIFIER
STAgR_Arg2-Gls (A-G)	This study	N/A
STAgR_Prdx2-Sod1 (P-S)	This study	N/A
STAgR_Arg2-Dnm3 (A-D)	This study	N/A
Software and Algorithms		
ZEN software	Zeiss	https://www.zeiss.com/microscopy/en_us/products/microscope-software/zen.html RRID:SCR_013672
ImageJ	ImageJ	https://imagej.net/Downloads RRID: SCR_003070
Morphometric analysis	SNT	Ferreira et al., 2014
Sholl Analysis	ImageJ	N/A
Co-localizatioin	Coloc2	https://imagej.net/Coloc_2
Proteome discoverer 2.2 software	Thermo Fisher	https://www.thermofisher.com/order/catalog/product/IQLAAEGABSFAKJMAUH RRID:SCR_014477
SwissProt Database Mouse	NCBI Protein	https://www.ncbi.nlm.nih.gov/protein RRID:SCR_003257
mitoCARTA 2.0 database	Calvo et al., 2016)	N/A
Perseus Software	Perseus	http://maxquant.net/perseus/ RRID:SCR_015753
GraphPad Prism 7.0	GraphPad Software	https://www.graphpad.com:443/ RRID:SCR_002798
Adobe Illustrator	Adobe Illustrator	https://www.adobe.com/de/products/catalog.html RRID:SCR_010279
Zeiss AxioVision 4.7 software	Zeiss	http://www.zeiss.com/microscopy/us/products/microscope-software/zen-core.html?vaURL=www.zeiss.com/microscopy/us/products/microscope-software/axiovision.html
Microsoft Excel	Microsoft Excel	https://www.microsoft.com/en-gb/ RRID:SCR_016137
Seahorse Wave	Agilent Technologies	https://www.agilent.com/en-us/products/cell-analysis-(seahorse)/software-download-for-wave-desktop RRID:SCR_014526
RStudio		https://rstudio.com
	DHARMa	https://cran.r-project.org/web/packages/DHARMa/vignettes/DHARMa.html
	DEP	https://www.bioconductor.org/packages/release/bioc/html/DEP.html
	ggplot2	https://ggplot2.tidyverse.org
	Pheatmap	https://www.bioconductor.org/packages/release/bioc/html/heatmaps.html
	fgsea	https://bioconductor.org/packages/release/bioc/html/fgsea.html
	TopGo	https://bioconductor.org/packages/release/bioc/html/topGO.html
Other		
Aqua Poly/Mount	Polysciences	Cat# 18606-20

RESOURCE AVAILABILITY

Lead Contact

Further information and requests for resources and reagents should be directed to and will be fulfilled by the Lead Contact, Prof. Magdalena Götz (magdalena.goetz@helmholtz-muenchen.de).

Materials Availability

- Plasmids generated in this study are available upon request.
- gRNA sequences used to activate gene-specific loci are listed in Methods S1.
- Aldh1-Cre transgenic mice are available at Jackson Lab (stock n.023748).
- There are restrictions to the availability of dCAM mice due to MTA request.

Data and Code Availability

- Mass spectrometry proteomics data have been deposited to the ProteomeXchange Consortium via the PRIDE, partner repository, with dataset identifier PXD014886.

EXPERIMENTAL MODEL AND SBJECT DETAILS

Wild-type mice (Primary Cell culture, Proteomics, IHC)

All experimental procedures in this study, done at the LMU München, were performed in accordance with German and European Union guidelines and were approved by the government of Upper Bavaria. For most of the experiments, primary cultures of astrocytes were obtained from brains of C57BL/6J mice of 5-7 days of age; no specific gender was considered. Primary cultures of cortical neurons were obtained from brains of C57BL/6J embryos at 14.5 days post conception (14.5 dpc or E14.5). Mice were fed *ad libitum* and housed with 12/12 h light and dark cycle and kept under specific-pathogen-free (SPF) conditions.

Aldh1-Cre and Cre-inducible dCas9-VPR mice

The activation of specific mitochondria-coding genes was performed in primary cultures of astrocytes obtained from Aldh1l1-Cre (Tien et al., 2012) crossed with dCAM mice (Rosa26-loxP-Stop-LoxP-dCas9VPR-SAM mice (J.G.-S., unpublished data). Both strains were used as heterozygotes. The background strain of the mice was C57BL/6.

Primary cultures of cortical astrocytes

Astrocytes were isolated and cultured as previously described, with small changes (Heins et al., 2002). After removal of the meninges, gray matter tissue from cerebral cortex of C57BL/6J mice at postnatal day 5-7 (P5–P7) was dissected and dissociated mechanically. Subsequently, cells were centrifuged for 5 min at 1,300 rpm, re-suspended, and plated in a T25 flask in medium consisting of DMEM/F12 (1:1), 10% fetal bovine serum (FBS), penicillin /streptomycin, and 1x B27 serum-free-supplement, 10 ng/ml epidermal growth factor (EGF), and 10 ng/ml basic fibroblast growth factor (bFGF) (astro-medium). Cells were passaged at 80%–90% confluency after 7-10 days using trypsin/EDTA and plated on poly-D-lysine coated glass coverslips at a density of 50,000-60,000 cells per coverslip (in 24-well plates) in fresh astro-medium. The vast majority of the cells (> 90%) in these cultures were positive for glial fibrillary acidic protein (Gfap) as previously described. Primary cultures of astrocytes were maintained in an incubator for 6-8 days at 37°C and 5% CO_2.

Cells undergoing direct neuronal conversion

One day after transduction or transfection, astro-medium was replaced with fresh medium consisting of DMEM/F12 (1:1), penicillin/streptomycin, supplemented with 1x B27 and Glutamax, but not FBS, EGF and FGF (differentiation medium). Small molecules were added once, at the time of medium replacement (24h after transduction or transfection). Cultures were maintained in an incubator for 6-8 days at 37°C and 9% CO_2.

Primary cultures of cortical neurons

Cerebral cortices were dissected from embryonic day (E) 14 mice as described before (Hartfuss et al., 2001; Walcher et al., 2013). Cortices were isolated, meninges removed and samples mechanically dissociated in 1x HBSS medium containing 10mM HEPES, on ice. Subsequently, cells were digested for 15 min in trypsin-EDTA (0.05%) and centrifuged for 5 min at 1,000 rpm. The pellet was resuspended in medium containing 10% FBS to stop trypsin, then centrifuged again and resuspended in 1x Neurobasal Medium, supplemented with 1x Glutamax, penicillin/streptomycin, and 1x B27. Cells were counted and plated at a density of 600,000 cells per well in 6-well plates, pre-coated with poly-D-lysine. After one week in culture the cells had mostly differentiated into neurons, with a high purity and little contamination by other cell types.

METHOD DETAILS

Transfection and Transduction

For transfection, DNA-liposome complexes were prepared in OptiMem medium using the retroviral plasmids described below and Lipofectamine 2000. Astrocytic cultures, plated the day before in 24-well plates at a density of 60,000-80,000 cells per well, were transfected with DNA-liposome complexes composed of 0.6 μg total DNA, mixed with 0,75μl of Lipofectamine2000 per well, in 400μl of OptiMem medium for 4 hours. Then, transfection medium was replaced by a solution composed to 1:1 ratio of fresh astro-medium and astro-medium collected from the same cells before the transfection (and filtered). One day later, the medium was replaced with differentiation medium and cells maintained in culture until 6-7 days post-transfection in 9% CO_2 incubator. For FACSorting, RNA extraction and RT-PCR, astrocytes were plated in 6-well plates pre-coated with PDL at a concentration of 350,000 cells per well. The following day, cells were transfected with DNA-liposome complexes containing 1μg total DNA and 1,25μl Lipofectamine 2000 per 1ml of OptiMem medium for 4 hours and cultured in astro-medium for 48hours before sorting. For STAgR experiments, primary cultures of astrocytes, obtained from double positive Aldh1l1-Cre dCAM mice (Rosa26-loxP-Stop-LoxP-dCas9VPR-SAM mice (Giehrl-Schwab J. et al., in revision), were transfected with plasmids encoding the indicated STAgR and Ascl1 with a molar ratio 1:1. For transduction, astrocytes were infected with 1μl of virus per well one day after plating. The viruses used are listed in the key resource table and were produced as previously described (Gascón et al., 2016).

Fluorescence-activated Cell Sorting

WT astrocytes were transfected with gRNAs-GFP and dCas9-VPR-DsRed plasmids. Cells were collected 48 hours after transfection and sorted for RFP^+/GFP^+, using the FACSAria III (BD Bioscience) system at high purity mode and a flow rate lower than 600 cells per second. Alternatively, astrocytes obtained from Aldh1l1-Cre x dCAM transgenic mice were transfected only with gRNA-expressing plasmids and subjected to FACS analysis at 48 hours, collecting GFP+ cells. Cells were washed twice with 1x PBS, treated with trypsin (0,05% in EDTA) for 5%, then astro-medium was added. Cells were harvested by centrifugation (1,000 rpm, 5min, 4°C), washed twice with 1x PBS and, then, resuspended in 400μl of DMEM/F12 (1:1), phenol-red-free. Single cell suspension was filtrated using a 70-μm cell strainer. Cells were sorted using the FACS Aria III (BD). Gates were set by using un-transfected cells, as well cells expressing GFP or DsRed as positive control. 15,000 cells were sorted directly in extraction buffer (Picopure RNA isolation kit) to enhance RNA quality and efficiency, for subsequent extraction and qRT-PCR.

Mitochondria isolation

Mitochondria isolation from cultured astrocytes and neurons was performed as previously described (Schmitt et al., 2013) using the pump-controlled cell (PCC) rupture method; a cell homogenizer (Isobiotec, Germany) combined with 1 mL Luer Lock Gas-Tight Syringes (4.608 mm i.d., SGE Supelco, USA) and a high-precision pump (Pump 11, Harvard Apparatus, USA). The homogenizer was pre-cooled on ice to ensure cooling of the samples during the isolation, the tungsten carbide ball (6um diameter) was inserted and the homogenizer was equilibrated with isolation buffer (300 mM sucrose, 5 mM TES, and 200 μM ethyleneglycoltetraacetic acid [EGTA], pH 7.2). The sample of dissociated astrocytes or neurons was added to 1 mL of isolation buffer and passed three (neurons) to six (astrocytes) times through the system at a constant rate (700 μl/min). To recover the homogenate, the system was rinsed once with 1 mL of isolation buffer. The sample preparation and the tunable parameters of the PCC, such as the clearance and the number of strokes, were optimized for each sample. Yield and functionality (mitochondrial transmembrane potential, $\Delta\psi_m$) of the isolated mitochondria were used to assess the optimal parameters. Around 1 million astrocytes and neurons respectively were used to obtain a sufficient amount of mitochondria for further processing. The pooled homogenate was cleared from cell debris and nuclei by centrifugation (800 × *g*, 5 min at 4°C), and mitochondria were pelleted at 9000 × *g* (10 min at 4°C). After the isolation, syringes were rinsed 3-4 times with double distilled water (ddH_2O). The tungsten carbide ball and the cell homogenizer were cleaned with isopropanol followed by ddH_2O to allow processing of the next sample without contamination.

Characterization of isolated mitochondria

The functional analysis of isolated mitochondria was performed by measuring Rhodamine 123 (Rh123) fluorescence quenching in order to determine $\Delta\psi_m$, as well as measuring the absorbance change at 540nm (Synergy 2, BioTek, USA) to determine mitochondrial swelling, as described previously (Schmitt et al., 2013). Protein concentrations were determined by the Bradford assay. For immunoblotting analysis, 10 μg of protein was subjected to sodium dodecyl sulfate-polyacrylamide gel electrophoresis (SDS-PAGE), and separated proteins were transferred onto PVDF membrane. Equal protein loading and proper transfer were controlled by Ponceau red staining. The primary and secondary antibodies used for Western Blot analysis are listed in the Key Resource table.

Electron microscopy analysis of the isolated mitochondria was done as described previously (Zischka et al., 2008). ZE-FFE-separated mitochondrial fractions were immediately pelleted, fixed in 2.5% glutaraldehyde, post-fixed with 1% osmium tetroxide, dehydrated with ethanol and embedded in Epon. Ultrathin sections were negatively stained with uranyl acetate and lead citrate and then analyzed on a Zeiss EM 10 CR electron microscope.

Seahorse experiments

Primary cortical astrocytes or neurons were plated onto XF24 V3 PET cell culture microplates from Seahorse biosciences, pre-coated with PDL, and analyzed the day after plating. Cells were seeded at 20,000, 30,000, 50,000 for neurons; and 15,000, 25,000 or 40,000 for astrocytes. The final cell number was assessed by counting $DAPI^+$ nuclei and measuring DNA content to normalize the data to μg DNA or 1000 cells. Before measuring cellular respiration, cells were washed twice with assay medium (XF DMEM + 25 mM glucose) and then incubated in 750 μL of assay medium for 10 min in an air incubator without CO_2 at 37°C. The XF24 plate was then transferred to the XF24 Extracellular Fluxanalyzer (Seahorse Bioscience). Basal respiration was determined with 4-5 assay cycles (2 min. mix, 2 min. measuring), and all parameters were obtained after the respective drug application. Basal OCR and PPR were measured prior to oligomycin treatment. For the measurement of different mitochondrial respiration states, oligomycin A (Oligo, 5 μg/ml) was used to inhibit the ATP synthase, followed by Carbonyl cyanide-*4*-(trifluoromethoxy)phenylhydrazone (FCCP, 1 μM) to induce maximal substrate oxidation capacity, and a cocktail containing rotenone (Rot, 5 μM) and antimycin A (Ant, 2 μM) to inhibit ETC activity and determine non-mitochondrial oxygen uptake. Finally, 2-deoxyglucose (2-DG, 100mM) was added to block glycolysis. Extracellular acidification rate (ECAR) was converted to proton production rate (PPR) based on machine algorithms and the buffer capacity of the medium. The OCR/PPR ratio was calculated over the averaged basal values. Each value is calculated averaging 3-5 time points from 3 technical replicates.

Proteome analysis

Isolated mitochondria (10 μg) were used per biological replicate. SDS was added to a final concentration of 2% for efficient solubilization, prior to tryptic protein digest using a modified FASP protocol (Wiśniewski et al., 2009). Proteomic measurements were performed on a Q-Exactive HF mass spectrometer (Thermo Scientific) online coupled to an Ultimate 3000 nano-RSLC (Dionex). Peptides

were separated on a C18 nanoEase MZ HSS T3 column (100Å, 1.8 μm, 75 μm x 250 mm; Waters) in a 95 min non-linear acetonitrile gradient. Precursor (scan range 300 – 1500 m/z) and TOP10 fragment spectra of charges 2-7 were acquired in the orbitrap mass detector of the mass spectrometer, at resolutions of 60,000 and 15,000 respectively with a maximum injection time of 50 ms and a dynamic exclusion of 30 s for each one. The individual raw-files were loaded to the Proteome discoverer 2.2 software (Thermo scientific) allowing for peptide identification and label-free quantification using the Minora node. Searches were performed using Sequest HT as a search engine in the Swissprot mouse database with the following search settings: 10 ppm precursor tolerance, 0.02 Da fragment tolerance, two missed cleavages allowed, carbamidomethyl on cysteine as fixed modification, deamidation of glutamine and asparagine allowed as variable modification, as well as oxidation of methionine and Met-loss combined with acetylation at the N terminus of the protein. Proteins were quantified by summing up the abundances of allocated unique and razor peptides; resulting protein abundances are given in Table S1. Mitochondrial proteins were classified using the mitoCARTA 2.0 database (Calvo et al., 2016). Data were analyzed in RStudio (version 3.5.3), using the package DEP (Zhang et al., 2018). First, we filtered for proteins identified in all replicates of at least one condition; then, data were normalized using variance stabilizing transformation (vsn). Differential enrichment analysis was performed based on linear model. Identified proteins were considered as enriched in neurons if the log2(fold-change value) was > 1 and enriched in astrocytes if the log2(fold-change value) was < −1 and pvalue < 0.05 (according to DEP output). Differentially enriched proteins (DEP) data are provided in Table S1. *T*-Distributed Stochastic Neighbor Embedding (*t*-SNE) was computed from data normalized in DEP package in RStudio, as well as the heatmap of all considered proteins and the distance matrix including hierarchical clustering. Gene Ontology analysis was performed in RStudio using the package "TopGO," using exact Fisher test. Proteins were considered differentially enriched if log2(fold-change) > |1| and pval < 0.05. Complete list of GO term is provided in Table S2. For Gene Set Enrichment Analysis (GSEA) the package "fgsea" in Rstudio was employed (Korotkevich et al., 2019). Complete list of GSEA term is provided in Table S2*E*.

Western Blot Analysis

Primary cultures of astrocytes or neurons were collected and lysed in RIPA buffer. Protein concentration was evaluated with RC DC Protein assay (Bio-Rad Laboratories); 60μg of lysate was loaded in sodium dodecyl sulfate-polyacrylamide gel electrophoresis (SDS-PAGE) and transferred onto a polyvinylidene fluoride (PVDF) membrane. Depending on the size of the protein analyzed, different gel concentration was used. The primary and secondary antibodies used for Western Blot analysis are listed in Key Resources Table.

Immunocytochemistry

Cells were fixed in 4% paraformaldehyde (PFA) in PBS1X for 10 min. at room temperature, washed in PBS1X twice for 5 minutes, and stored up to a month at 4°C before staining. For Prdx2 staining, cells were fixed in ice-cold Methanol 20% for 10 minutes, washed twice in PBS1X for 10 minutes, and subsequently stored and treated as other samples. Specimen were incubated in primary antibodies (for concentration see Key Resources Table) in PBS1X containing 3% Bovine Serum Albumin (BSA) and 0.5% Triton X-100 for 2 hours at room temperature or overnight at 4°C. After washing twice for 5 minutes with PBS, cells were incubated with the appropriate species- or subclass-specific secondary antibodies, with or without DAPI to label nuclei (blue), diluted 1:10000, for 1 hour in the dark at room temperature. Optionally, after incubating with primary antibodies and washing with PBS, biotin-labeled secondary antibodies were used at a dilution of 1:200 for 1 hour, followed by streptavidin-coupled fluorophores (1:500) for another hour. Coverslips were then mounted with Aqua Poly/Mount (Polysciences, Warrington, PA). Samples were imaged at the LSM710 laser-scanning confocal or Axio Observer Z1 epifluorescence microscope (Carl Zeiss). Digital images were acquired using the ZEN software (Carl Zeiss) at 80X, 40X or 25x.

RNA extraction, retro-transcription and Real Time Quantitative PCR (qRT-PCR)

RNA was extracted using Arcturus PicoPure RNA Isolation Kit (Thermo Fisher Scientific) according to the manufacturer's instructions, including removal of genomic DNA. 100ng RNA was reverse transcribed using the ThermoFisher cDNA first strand kit. Each cDNA sample was diluted 1:5. qPCR reactions were performed on an Applied Biosystems QuantStudio 6 Flex Real-Time PCR System, or Roche LightCycler 480. Each 10 μL reaction consisted of 5 μL of PowerUp SYBR Green Master Mix (Thermo Fisher), 0.05 μL of forward and reverse primer (100 μM) and 5 μL of DNA appropriately diluted. qRT-PCR primers can be found in Key Resource table. The expression of each gene was analyzed in triplicate. Data were subjected to normalization by using *Gapdh* as housekeeping genes and expressed as mRNA fold change compared to control. Quantification was performed on 3 independent biological samples, each time as technical triplicate. Off targets were selected from the UCSC genome browser, potentially targeting intergenic as well as exon regions. Primers are listed in Methods S1.

STAgR cloning

For generation of STAgR cloning fragments, we followed previously published protocols (Breunig et al., 2018a, 2018b; Gibson, 2011). In particular, we generated individual cloning fragments for Gibson assembly by PCRs on 10 ng of vector templates (STAgR_Neo, STAGR_gRNAScaffold_hU6, STAGR_gRNAScaffold_hH1, STAGR_gRNAScaffold_h7SK and/or STAGR_gRNAScaffold_mU6). The mix contained 10 μl of high fidelity (HF) buffer, 1 μl of 10 mM dNTPs, 0.25 μl of overhang-primers (see key resources), 0.5 μl of HF polymerase, 1.5 μl of dimethyl sulfoxide (DMSO) and enough H_2O to reach a final volume of 50 μl. Reactions were incubated on a thermocycler as follows: 1 cycle of 98°C for 1 min 30 s; 38 cycles of 98°C for 10 s, 59°C (for gRNA scaffold)/ 68°C (for SAM loop) for 10 s, 72°C for 30 s (for inserts) / 1 min 30 s (for vectors); 1 cycle of 72°C for 10 min. 44.5 μl of the PCR reaction were mixed

with 0.5 μl of DpnI enzyme (10 units) and 5 μl of buffer, then incubated for 1 h at 37°C. DNA purification was achieved through incubation with 90 μl of magnetic beads for 2 min at room temperature (RT). Beads were pelleted through a magnet and washed twice with 70% ethanol without complete resuspension. The pellet was then dissolved in 20μl H_2O and separated from the beads. DNA concentration was measured using a spectrophotometer. Gibson Assembly has been performed following a homemade Gibson assembly mix. The 5x isothermal reaction buffer is composed as follows: 1 M Tris (Tris(hydroxymethyl)aminomethane)-HCl (pH 7.5), 300 μl of 1 M MgCl, 60μl of 100 mM dGTP (deoxyguanosine triphosphate), 60 μl of 100 mM dATP (deoxyadenosine triphosphate), 60 μl of 100 mM dTTP (deoxythymidine triphosphate), 60 μl of 100 mM dCTP (deoxycytidine triphosphate), 300 μl of 1 M DTT (dithiothreitol), 1.5 g of PEG-8000 (polyethylene glycol), 300 μl of 100 mM NAD (nicotinamide adenine dinucleotide) and enough H_2O to obtain 6 ml. For the assembly master mix, 320 μl of 5x isothermal reaction buffer was combined with 697 μl of H_2O, 3 μl of 10 U/μl T5 exonuclease, 20 μl of 2 U/μl DNA polymerase and 160 μl of 40 U/μl Taq DNA ligase. 7.5 μl of assembly master mix have been mixed with 2.5 μl of insert and vector. A vector to insert ratio of 1:3 was used. Samples were incubated at 50°C for 60 min and subsequently transformed into *E. Coli*. Resulting plasmids have been sequenced by the Sanger sequencing method with the following primers: StAgR_seq_fwd1 (GAGTTAGGGGCGGGACTATG), StAgR_seq_fwd2 (ACTGGATCCGGTACCAAGG) and StAgR_seq_rev (TTACGGTTCCTGGCCTTTTG). Verified inserts have been cut with KpnI and subcloned into pCDNA-miniCMV-GFP. Primers for gRNA are listed in Methods S1 table.

Live-Imaging Microscopy

Continuous live imaging was performed with a Cell Observer (Zeiss) at a constant temperature of 37°C and at 5% CO_2. Phase-contrast images were acquired every 10 min and fluorescence pictures every 4 hours for 6 days using a 10x phase contrast objective (Zeiss) and an AxioCam HRm camera with a self-written VBA module remote controlling Zeiss AxioVision 4.7 software (TAT, Prof. Dr. Timm Schroeder). Movies were assembled and analyzed using ImageJ (NIH) software, as also described in Gascón et al. (2016). In Figure 4B data are shown as pool of five independent biological replicates; in Figures 4C–4G all cells considered from all biological replicates are shown, indicated by different colors; statistics was performed on the 5 biological replicates using linear regression in Rstudio (see below).

QUANTIFICATION AND STATISTICAL ANALYSIS

When virus was used to induce neuronal conversion (Figure 1; Figure S2; Figure 3; Figure S3; Figure 4), astrocytes were fixed at the days after transduction, as indicated in the figures. Quantification for neuronal cells was based on β-III-tubulin immunoreactivity and morphological parameters, e.g., appearance of processes longer than 3x the cell soma as in Gascón et al. (2016). Astrocytes were quantified based on morphological features and Gfap expression, though Gfap is downregulated following direct conversion. For quantification in Figure 2 and Figure S2, we selected 10 transduced cells per each condition (DsRed, Ascl1-ires-DsRed at day 1 and day 3, and DsRed, Ascl1-ires-DsRed with neuronal morphology or astrocytic morphology at day 5 and 7). ImageJ (v1.52p) was used to define a region of interest (ROI) outlining a selected cell in order to measure the signal intensity for a given protein. To prevent a possible bias due to the different mitochondrial content in astrocytes and neurons, we also evaluated the intensity of Tomm20, a pan-mitochondrial protein. For each ROI, after subtracting the background value, we divided the intensity of the protein of interest by the corresponding Tomm20 expression, and log transformed the value. The colocalization analysis was conducted using the Coloc2 plugin for ImageJ.

For time-lapse experiment quantifications (Figure 4 and Figure S4), cells were tracked in every frame of the movie. $GFP^+/DsRed^+$ cells acquiring neuronal morphology, with processes longer than 3x the cell soma, were quantified among the total $GFP^+/DsRed^+$ cells, as previously published (Gascón et al., 2016). In total, 158 cells were tracked in controls and 177 in Ascl1+Prdx2-Sod1 over n = 5 biological replicates.

Morphological analysis of reprogrammed neuronal cells (Figures 3F–3H) was performed with the ImageJ plugin SNT (simple Neurite tracer) (Ferreira et al., 2014) and different parameters were measured. Sholl analysis, also in ImageJ, was performed on each of the traced neurons: a step size of 10μm was maintained constant, with the first radius defined according to the soma of each cell. We evaluated 3-4 neurons per condition, in 4 biological replicates. Data were analyzed with Microsoft Excel, GraphPad Prism 7.0 software and linear regression using "lm" function (R Stats package) in RStudio. Evaluation of the residuals for fitted linear models was performed with the package "DHARMa" (Hartig and Lohse, 2020) in RStudio.

Statistics on the reprogramming efficiency in Figure S2 and Figure 4 was performed as follows: reprogramming efficiency was log2 transformed, in order to reduce differences in variance across experiments and to fit the data to a normal distribution. Then, linear regression model was used, together with "DHARMa" package to evaluate the residuals. Statistics on Figure 2 and Figure S3 was perfomerd log2-transformed ratio. Statistics on Figure 4 was evaluated using paired t test. The number of biological replicates is indicated in the corresponding Figure legends. Data are plotted as mean ± standard error of the mean (SEM). Significance is based on the p value indicated on the graphs as * $p \leq 0.05$, ** $p \leq 0.01$, ***$p \leq 0.001$.

Cell Stem Cell, Volume *28*

Supplemental Information

CRISPR-Mediated Induction of Neuron-Enriched Mitochondrial Proteins Boosts Direct Glia-to-Neuron Conversion

Gianluca L. Russo, Giovanna Sonsalla, Poornemaa Natarajan, Christopher T. Breunig, Giorgia Bulli, Juliane Merl-Pham, Sabine Schmitt, Jessica Giehrl-Schwab, Florian Giesert, Martin Jastroch, Hans Zischka, Wolfgang Wurst, Stefan H. Stricker, Stefanie M. Hauck, Giacomo Masserdotti, and Magdalena Götz

Figure S1

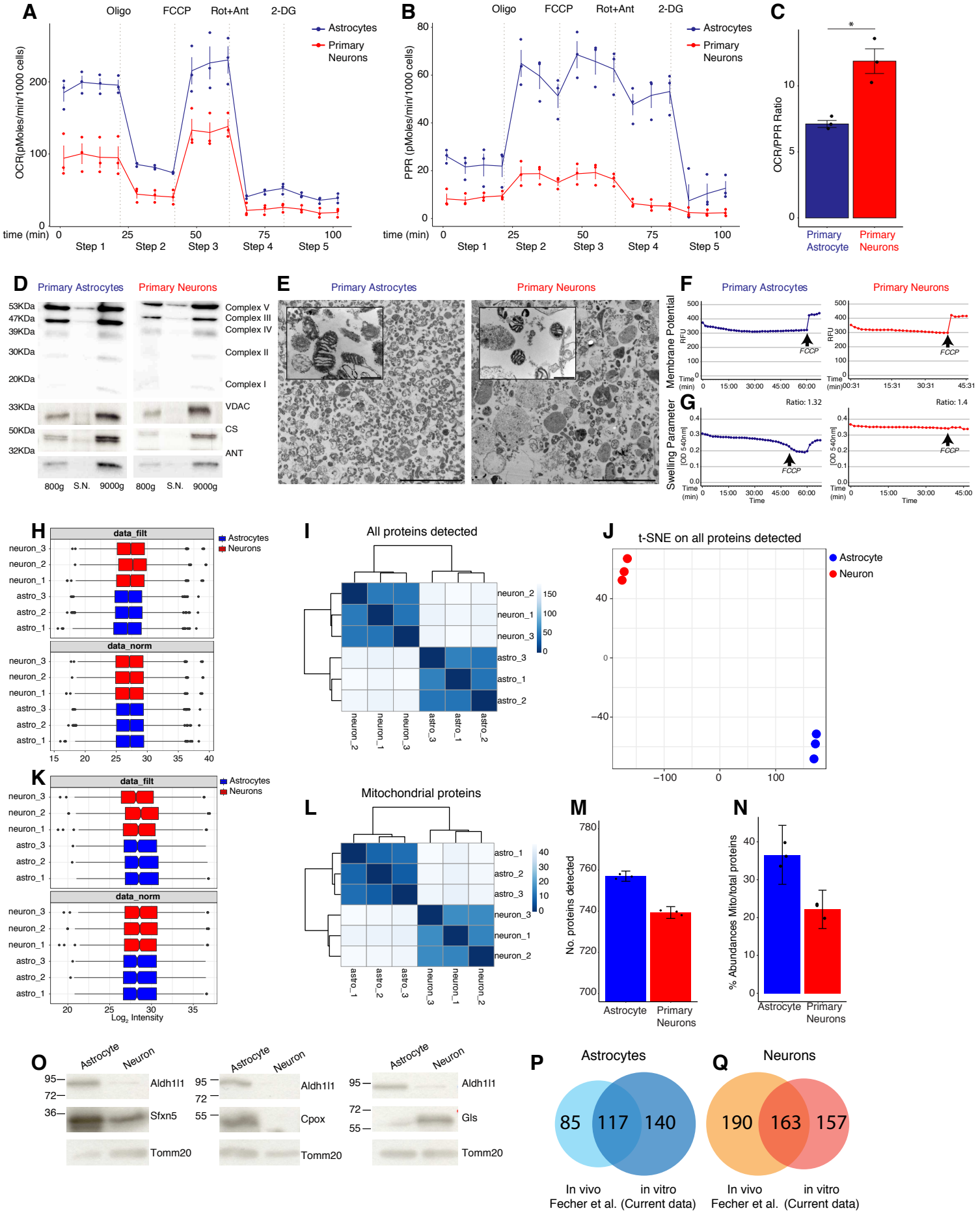
A
Oligo
FCCP
Rot+Ant
2-DG
Astrocytes
Primary Neurons
OCR(pMoles/min/1000 cells)
time (min)
Step 1
Step 2
Step 3
Step 4
Step 5
B
PPR (pMoles/min/1000 cells)
C
OCR/PPR Ratio
Primary Astrocyte
Primary Neurons
D
Primary Astrocytes
Primary Neurons
53KDa
47KDa
39KDa
30KDa
20KDa
33KDa
50KDa
32KDa
Complex V
Complex III
Complex IV
Complex II
Complex I
VDAC
CS
ANT
800g
S.N.
9000g
E
F
Membrane Potential
RFU
FCCP
G
Swelling Parameter
Ratio: 1.32
Ratio: 1.4
H
data_filt
data_norm
Astrocytes
Neurons
I
All proteins detected
J
t-SNE on all proteins detected
Astrocyte
Neuron
K
Log2 Intensity
L
Mitochondrial proteins
M
No. proteins detected
N
% Abundances Mito/total proteins
O
Aldh1l1
Sfxn5
Cpox
Gls
Tomm20
P
Astrocytes
85
117
140
In vivo Fecher et al.
in vitro (Current data)
Q
Neurons
190
163
157

SUPPLEMENTAL MATERIAL

Figure S1, related to Figure 1. Astrocytes and neurons from cerebral cortex differ in mitochondrial function

(**A-B**) Longitudinal traces of extracellular flux analysis measured by Seahorse XF analyzer, comparing the Oxygen Consumption Rate (**A**) and the Proton Production Rate (**B**) of astrocytes (blue) versus neurons (red) over time, after challenging the cells with different ETC inhibitors. Values are normalized per 1000 cells. Each time point is shown as mean ± SD. n=3 experimental batches for each group.

(C) Barplot showing OCR/PPR ratio in cultures of primary astrocytes versus neurons, as measured by Seahorse XF analyzer. * $p \leq 0.05$. n=3 for each group.

(D) Immunoblot detection of mitochondrial proteins in different fractions (800g, nuclear; S.N., cytosolic; 9000g, mitochondria and other organelles) isolated from astrocytes or neurons.

(E) Electron Microscopy images of mitochondria isolated from astrocyte and neuron cultures. Scale bar: 5µm. Magnifications scale bar: 500nm.

(**F**) Graphs showing the membrane potential of mitochondria isolated from astrocytes (*upper panel*) and neurons (*lower panel*) measured by Rhodamine 123 assay, indicating their healthy functional state.

(**G**) Graphs showing the swelling parameter of mitochondria isolated from astrocytes (*upper panel*) and neurons (*lower panel*) by absorbance at 540nm indicating their healthy functional state.

(H) Boxplot depicting abundances of all proteins before (*upper panel*) and after (*lower panel*) normalization.

(I) Unsupervised cluster analysis of the samples considering all quantified proteins.

(J) *t*-SNE of the samples, based on all proteins after normalization.

(K) Boxplot depicting abundances of mitochondrial proteins selected according to mitoCarta before (*upper panel*) and after (*lower panel*) normalization.

(L) Unsupervised cluster analysis of the samples considering only mitochondrial proteins.

(M) Barplot showing the number of mitochondrial proteins identified by mass spec in astrocytes (blue) and neurons (red). Each dot represents a biological replicate.

(N) Barplot depicting the percentage of mitochondrial protein abundance over total protein abundance in astrocytes (blue) and neurons (red). Each dot represents a biological replicate.

(**O**) Western blots of total lysates from cultured astrocytes or neurons confirming the selective cell enrichment by high amounts of Adlh1l1 in astrocyte lysates, equal mitochondrial protein loading by Tomm20 and the higher amount of Sfxn5 and Cpox in astrocytes and Gls in neurons.

(**P,Q**) Venn Diagrams of all astrocyte-enriched (**I**) and neuron-enriched (**J**) mitochondrial proteins detected by Fecher et al. and our analysis showing a high degree of overlap given that mitochondrial proteins were isolated at different stages (adult versus postnatal), from different regions (cerebellum versus cortex) and in different conditions *(in vivo* versus *in vitro*).

Figure S2

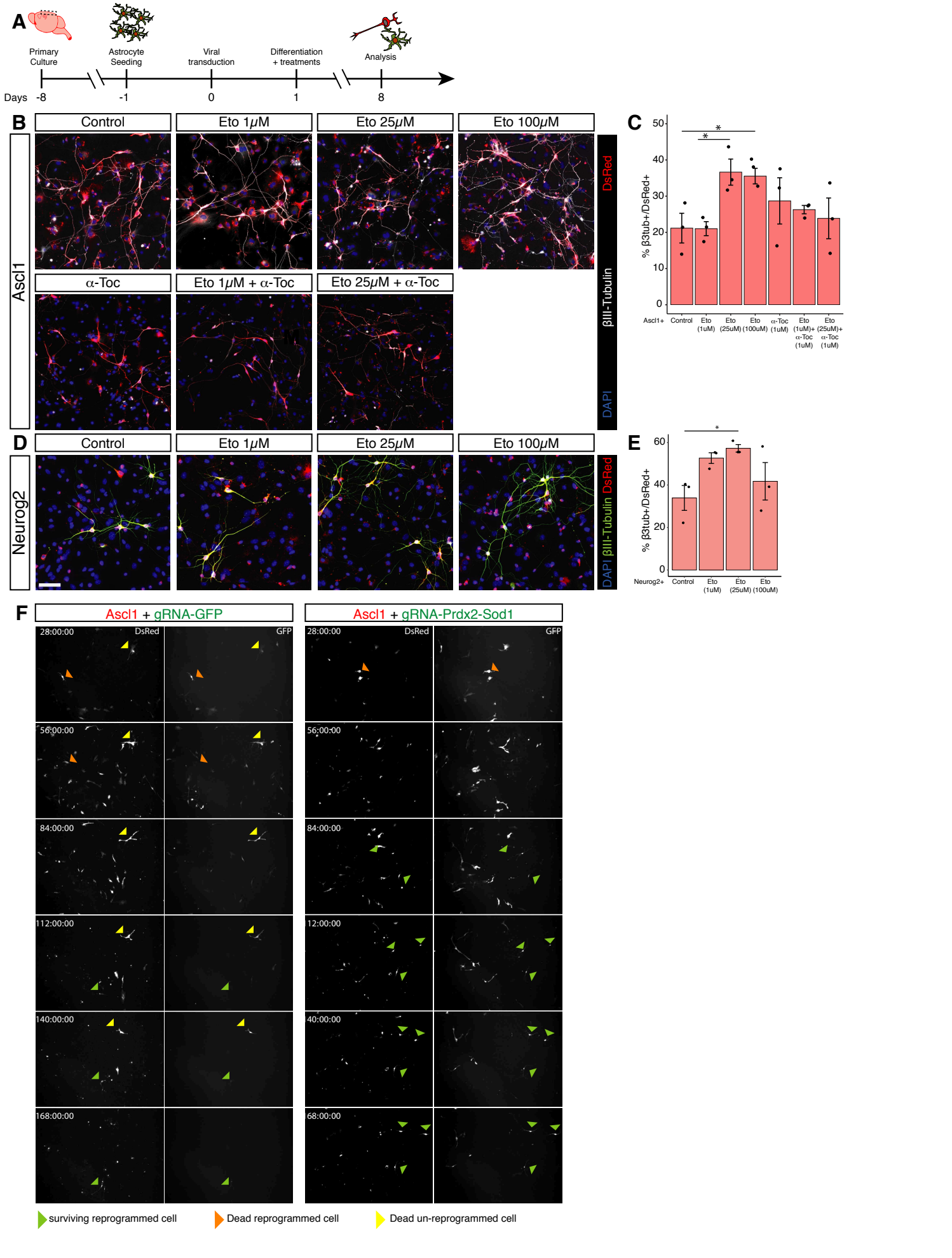
A
Primary Culture
Astrocyte Seeding
Viral transduction
Differentiation + treatments
Analysis
Days -8 -1 0 1 8
B
Control
Eto 1μM
Eto 25μM
Eto 100μM
α-Toc
Eto 1μM + α-Toc
Eto 25μM + α-Toc
Ascl1
DsRed
βIII-Tubulin
DAPI
C
% β3tub+/DsRed+
Ascl1+ Control Eto (1uM) Eto (25uM) Eto (100uM) α-Toc (1uM) Eto (1uM)+ α-Toc (1uM) Eto (25uM)+ α-Toc (1uM)
D
Neurog2
E
Neurog2+ Control Eto (1uM) Eto (25uM) Eto (100uM)
F
Ascl1 + gRNA-GFP
Ascl1 + gRNA-Prdx2-Sod1
28:00:00
56:00:00
84:00:00
112:00:00
140:00:00
168:00:00
surviving reprogrammed cell
Dead reprogrammed cell
Dead un-reprogrammed cell

Figure S2, related to Figure 1 and 4. Etomoxir treatment improves direct neuronal reprogramming.

(**A**) Schematic drawing of the experimental setup.

(B) Micrographs showing the Ascl1-transduced cells (DsRed+) that are βIII-tubulin+ neurons (in white), nuclei labeled in DAPI (Blue), in the treatment conditions indicated. Scale bar: 50µm.

(C) Histogram depicting the percent of βIII-tubulin+ cells amongst Ascl1-transduced DsRed^{+} cells at 8 DPI. Data are shown as mean±SEM. Each dot represents a biological replicate (n=3 for experimental condition). *$p \leq 0.05$

(**D**) Micrographs showing the efficiency of neuronal conversion in upon Neurog2 expression together with treatment of different concentration of Etomoxir. Reprogrammed neurons (DsRed+) are βIII-tubulin+ (in white). Nuclei labeled in DAPI (Blue). Scale bar: 50µm.

(**E**) Histogram depicting the percentage of βIII-tubulin+ cells amongst Neurog2-transduced DsRed^{+} cells at 8 DPI. Data are shown mean±SEM. Each dot represents a biological replicate (n=3 for experimental condition). *$p \leq 0.05$

(F) Example of fluorescent pictures acquired during the imaging and used for analysis (related to **Figure 4**).

Figure S3

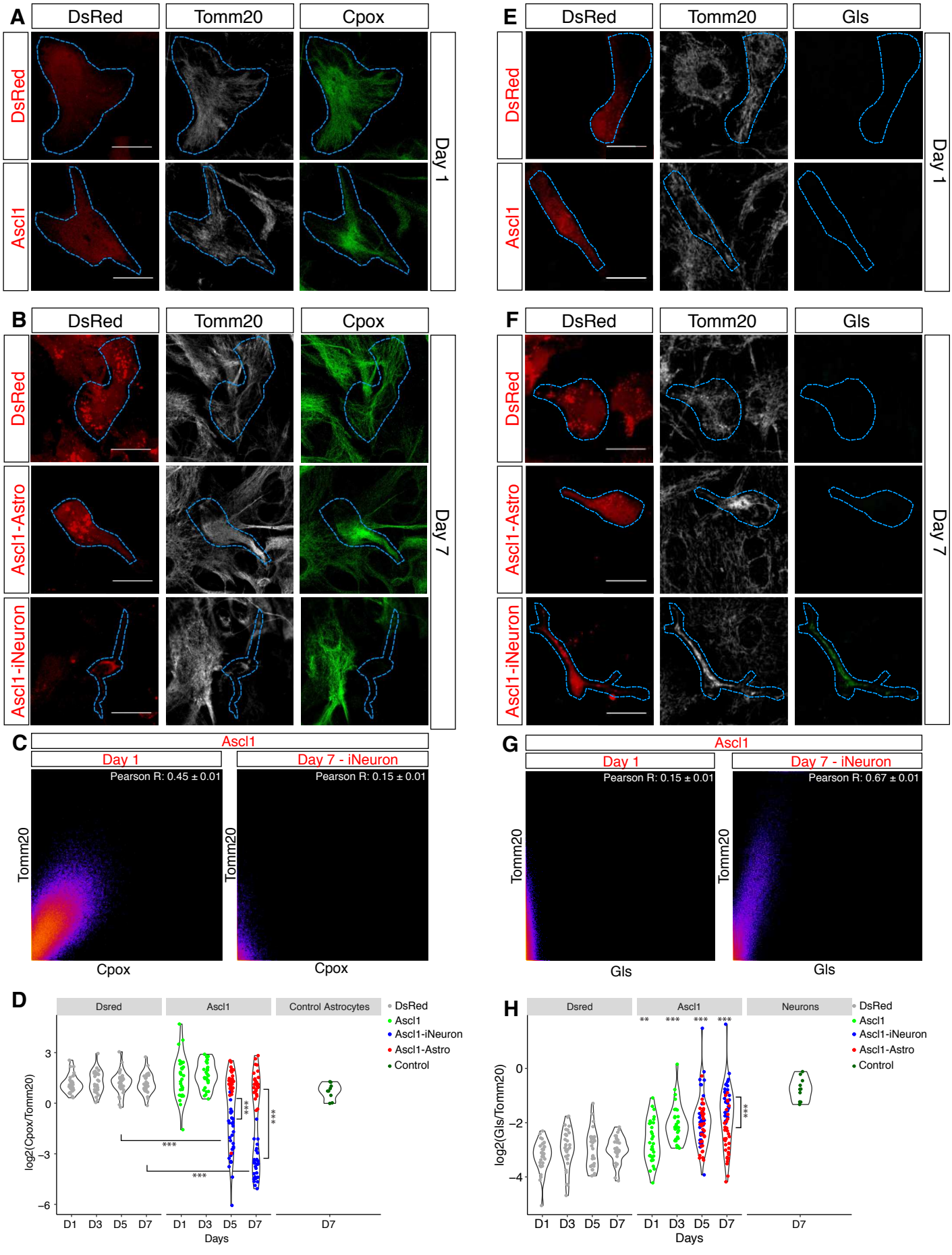
A
DsRed
Tomm20
Cpox
DsRed
Ascl1
Day 1
E
DsRed
Tomm20
Gls
DsRed
Ascl1
Day 1
B
DsRed
Tomm20
Cpox
DsRed
Ascl1-Astro
Ascl1-iNeuron
Day 7
F
DsRed
Tomm20
Gls
DsRed
Ascl1-Astro
Ascl1-iNeuron
Day 7
C
Ascl1
Day 1
Pearson R: 0.45 ± 0.01
Day 7 - iNeuron
Pearson R: 0.15 ± 0.01
Tomm20
Cpox
G
Ascl1
Day 1
Pearson R: 0.15 ± 0.01
Day 7 - iNeuron
Pearson R: 0.67 ± 0.01
Tomm20
Gls
D
Dsred
Ascl1
Control Astrocytes
log2(Cpox/Tomm20)
Days
DsRed
Ascl1
Ascl1-iNeuron
Ascl1-Astro
Control
H
Dsred
Ascl1
Neurons
log2(Gls/Tomm20)
Days
DsRed
Ascl1
Ascl1-iNeuron
Ascl1-Astro
Control

Figure S3, related to Figure 2. Mitochondrial protein changes during astrocyte-to-neuron reprogramming

(**A, B**) Micrographs showing immunostainings of the astrocyte-enriched mitochondrial protein Cpox in astrocytes transduced with DsRed (control) or Ascl1-ires-DsRed at 1 (**A**) or 7 (**B**) DPI as indicated. Mitochondria are identified by the expression of Tomm20. Scale bar: 20µm.

(**C**) Example of scatter plot of the pixel intensity correlation between Tomm20 and Cpox in Ascl1-transduced cells at 1 (*left panel*) and 7 (*right panel*) DPI. Pearson's coefficient as average of 3 cells/biological replicate; n=3 biological replicates.

(**D**) Violin plot depicting the log2-ratio of the intensity of the expression of Cpox versus Tomm20 over time (D1, D3, D5, D7) and in cortical astrocyte cultures at day 7. Each dot represents 1 analyzed cell. 10 cells analyzed per biological replicate, each condition. n=3 biological replicates; ***$p \leq 0.001$.

(**E, F**) Micrographs showing the expression of the neuron-specific mitochondrial protein Prdx2 in astrocytes transduced with DsRed (control) or Ascl1-ires-DsRed at 1 (**E**) and 7 (**F**) DPI. Mitochondria are identified by the expression of Tomm20. Scale bar: 20µm.

(**G**) Example of scatter plot of the pixel intensity correlation between Tomm20 and Gls in Ascl1-transduced cells at 1 (left panel) and 7 (right panel) DPI. Pearson's coefficient as average of 3 cells/biological replicate; n=3 biological replicates.

(**H**) Violin plot depicting the log2-ratio of the intensity of the expression of Gls versus Tomm20 over time (D1, D3, D5, D7) and in E14 cortex-derived cultures at 7 days in vitro. Each dot represents 1 analyzed cell. 10 cells analyzed per biological replicate, each condition. n=3 biological replicates; ***$p \leq 0.001$.

Figure S4

A

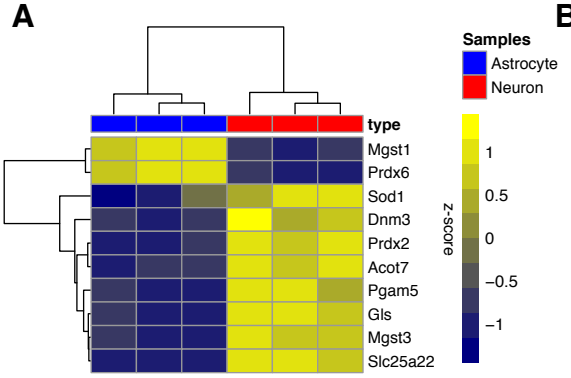

B

Genes	gRNA-ctl	gRNA-Prdx2-Sod1	gRNA-Arg2-Gls	gRNA-AD
GAPDH	27	25,88333333	25,29666667	27,04666667
Prdx2	30,06666667	25,85333333		
Sod1	26,91333333	24,23		
Arg2	40,54333333		28,22333333	29,36666667
Gls	34,59666667		31,34333333	
Dnm3	37,68			33,71666667

Genes	gRNA-ctl	gRNA-Acot7	gRNA-Slc25a22	gRNA-Pgam5	gRNA-Prdx6	gRNA-Mgst1	gRNA-Mgst3
gapdh	27,46	26,9225	30,845	29,4725	27,8425	28,215	29,575
Acot7	33,745	30,38666667					
Mgst1	33,325					32,02	
Mgst3	35,15666667						36,8
Pgam5	33,73666667			35,69333333			
Prdx6	32,8975				32,35666667		
Pgam5	33,73666667			35,69333333			
Slc25a22	35,565		36,63				

C

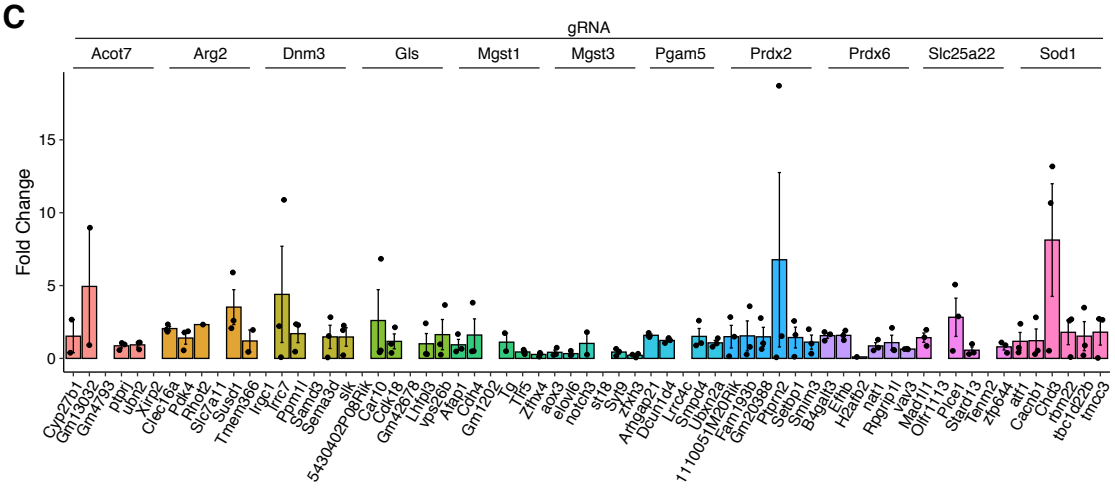

D

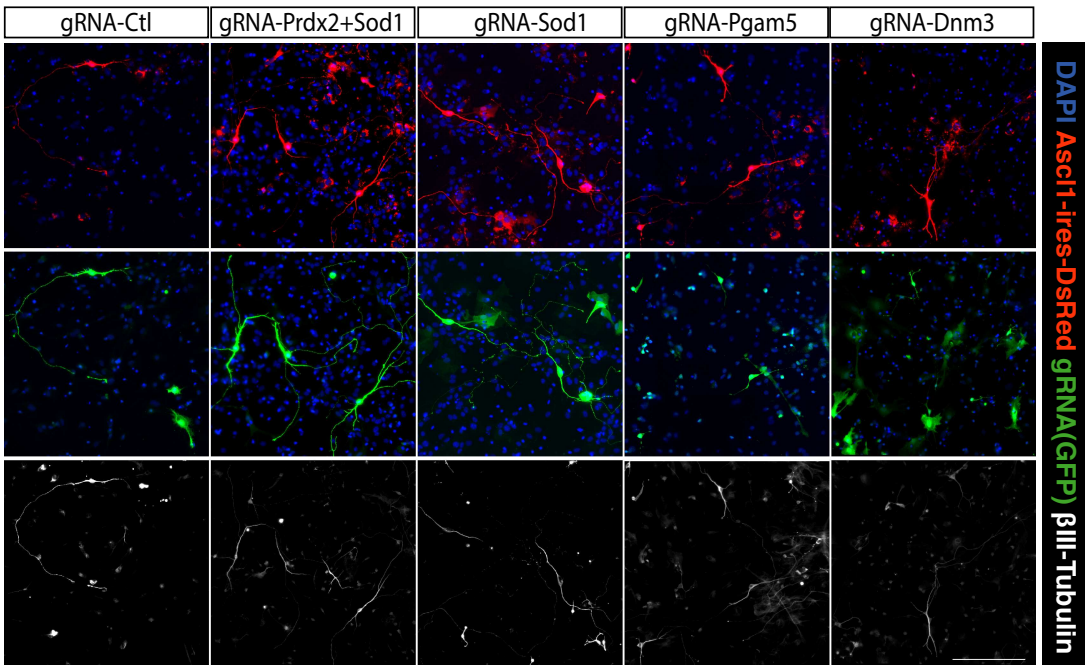

Figure S4, related to Figure 3. Characterization of selected candidates

(**A**) Unsupervised heatmap depicting the relative expression of the selected candidates.

(**B**) Graphs depicting the log2-normalized abundance of the astrocyte-enriched (blue dots) and neuron-enriched (red dots) candidates, as analyzed in Figure 2. Each dot represents a biological replicate.

(**C**) Real Time quantitative PCR (RT-qPCR) showing the fold change of putative off-targets following the transfection of gene-specific gRNA. Data are shown as fold change over the gRNA-scramble control (mean ± SEM). None of this is significant over Paired t-test used. control. n=3 biological replicates for each group.

(**D**) Single channel immunofluorescence images showing reprogrammed neurons (βIII-tubulin^{+}-DsRed^{+}-GFP^{+}) transfected by Ascl1-ires-DsRed (red) and different STAgR constructs (green). Scale bar: 100μm.

2.2 Aim of the Study II

The aim of the second study was to investigate the role of mitochondrial metabolism in the direct neuronal reprogramming of human cells and discover potential treatments to improve reprogramming as well as treat mitochondrial dysfunction.

Mitochondrial deficiency limits the direct neuronal reprogramming of human cells

Giovanna Sonsalla, Therese Riedemann, Mirjana Gusic, Ejona Rusha, Micha Drukker, Sonia Najas, Aleks Janjic, Wolfgang Enard, Pawel Smialowski, Holger Prokisch, Magdalena Götz, and Giacomo Masserdotti

For this paper, being the first author, I performed most of the experiments except for the electrophysiology, and I analyzed the data with the exception of the RNAseq analysis which was conducted by Giacomo Masserdotti. I wrote and revised the first draft of the manuscript with Magdalena Götz and Giacomo Masserdotti.

This project is finalized in a manuscript that will be submitted to Cell Stem Cell in June 2021

Mitochondrial deficiency limits the direct neuronal reprogramming of human cells

Giovanna Sonsalla[1,2,3], Therese Riedemann[1], Mirjana Gusic[4], Ejona Rusha[2], Micha Drukker[2], Sonia Najas[1,2], Aleks Janjic[5], Wolfgang Enard[5], Pawel Smialowski[1,2], Holger Prokisch[4], Magdalena Götz[1,2*], and Giacomo Masserdotti[1,2*]

[1]Physiological Genomics, Biomedical Center, Ludwig-Maximilians-Universität, Planegg-Martinsried, Germany

[2]Institute for Stem Cell Research, Helmholtz Center Munich, Neuherberg, Germany

[3]Graduate School of Systemic Neurosciences, Ludwig-Maximilians-Universität, Planegg-Martinsried, Germany

[4]Institute of Neurogenomics, Helmholtz Center Munich, Neuherberg, Germany

[5]Anthropology and Human Genomics, Department Biology II, Ludwig-Maximilians-Universität, Planegg-Martinsried, Germany

[*]Co-last authors.

Abstract

Direct neuronal reprogramming is a powerful tool for replacing neurons lost in disease or traumatic injury, and is ultimately being developed for use in human patients. However, major barriers identified in murine cell reprogramming remain unexplored in human glia to neuron conversion. Mitochondria play a major role in the conversion process, as well as in neurodevelopmental and neurological disease, and differ profoundly between glia and neurons. Here we show that even common components of the mitochondria, such as Complex I function, are limiting in the conversion to neurons, by using iPSC-derived glia from patients with a Complex I mutation (Leigh syndrome). We further identify treatments to overcome this hurdle, most surprisingly blockers of the unfolded protein response, which highlight mitochondria-ER communication as a key event in the reprogramming of both control and patient cells. Taken together, disease modeling using patient cells for glia to neuron reprogramming unraveled novel pathways to improve the metabolic hurdles in this process and achieve high efficiencies in human glia cell reprogramming.

Introduction

Restoring the loss of functional neurons resulting from brain injury or neurodegenerative disease is of paramount importance, as disease due to neuron loss cannot currently be treated causally. A particularly promising approach for brain repair involves the recruitment and direct neuronal reprogramming of endogenous cells already present in the brain (Barker et al., 2018; Vignoles et al., 2019). This therapeutic strategy has been pioneered in 2002 (Heins et al., 2002) and been successfully improved over many years enlisting glial cells *in vitro* (Berninger et al., 2007; Heinrich et al., 2010; Masserdotti et al., 2015) and *in vivo* with mouse models (Heinrich et al., 2014; Torper et al., 2015; Mattugini et al., 2019). However, there are many hurdles to direct neuronal reprogramming that prevent a high reprogramming efficiency and full neuronal maturation, including neuronal repressors (e.g., RE-1 transcription repressor complex (REST); Masserdotti et al., 2015) and the chromatin context (Wapinski et al., 2013; Smith et al., 2016).

In particular, mitochondria have been identified as a major barrier to the reprogramming of glia to neurons, due to the metabolic conversion from glycolysis to oxidative phosphorylation (oxphos) that occurs in parallel (Gascón et al., 2016; Camandola & Mattson, 2017). Indeed, neuronal reprogramming even after brain injury *in vivo* can be significantly improved by alleviating the stress associated with the shifted metabolism, such as by the application of antioxidants or Bcl2 (Gascón et al., 2016). Furthermore, we recently demonstrated that the mitochondrial proteome differs profoundly between glia and neurons and neuron-enriched proteins appear only late in reprogramming (Russo et al., 2021). Accordingly, the early activation of only 1 or 2 neuron-enriched mitochondrial proteins from the start of the reprogramming process could potently improve the neuronal conversion (Russo et al., 2021). However, it is unknown to which extent mitochondrial proteins present in all cells, such as Complexes I-IV (CI-IV) of the electron transport chain (ETC), would affect neuronal reprogramming. Blocking oxphos by oligomycin A treatment completely abolished the reprogramming of murine astrocytes into neurons (Gascón et al., 2016), but whether this is a general phenotype is unknown. Conversely, oxphos itself can have limiting effects on reprogramming, such as through the generation of reactive oxygen species (ROS), which are deleterious for direct neuronal reprogramming in murine glia (Gascón et al., 2016; Russo et al., 2021). We were therefore interested to determine the effects of CI mutations in the conversion process of human glial cells to neurons. Indeed, very little is known about the role of

mitochondria in the reprogramming of human cells. Although some studies have investigated the reprogramming potential of glial cells of human origin (Zhang et al., 2015; Nolbrant et al., 2020), nothing is known about the metabolic hurdles as this area is still vastly understudied and is hampered by lengthy protocols and low reprogramming efficiencies.

Understanding the role of mitochondrial metabolism is not only important for neuronal reprogramming, but is also essential for directly treating neurodegenerative diseases, as mitochondrial dysfunction is one of their main hallmarks (Watts et al., 2018; Stanga et al., 2020). Indeed, mitochondria are not only relevant in the aging context but also play a major role in early-onset diseases, such as Leigh syndrome (LS) (Rahman et al., 1996; Hong et al., 2020). The direct neuronal reprogramming of human cells can thus be used as a valuable tool, not only for neuronal replacement strategies, but also in the context of disease modeling and novel treatment discovery. Therefore, cells from patients with a mutation in NDUFS4, a subunit of CI, were investigated and compared to cells from control donors. The cells were studied not only in resting conditions, but also under stress during direct neuronal reprogramming. Interestingly, treatments targeting underlying mechanisms of mitochondrial impairment did not only lead to improvements in patient cell reprogramming, but also in control cells, and led to the novel discovery of the unfolded protein response as a major barrier in the conversion process.

Results

Comparable astrocyte differentiation of NDUFS4-patients and controls

We aimed at investigating the role of metabolism in the direct neuronal reprogramming of human glial cells by studying patients with a mitochondrial deficiency. To this end, control donor and NDUFS4-mutant patient iPSCs were successfully differentiated into glial progenitor cells (GPCs) and astrocytes following a protocol adapted from Santos et al., 2017 (Fig. S1A). There were no detectable differences between the patient and control cells over the course of astrocyte differentiation based on immunocytochemistry analysis (Fig. S1B). To ensure our results were not biased by one specific mutation, we analyzed iPSCs from three separate patients, each containing unique mutations in NDUFS4 (Fig. S1C; #114107, #87971, #79787). Transcriptome analysis of the three patient and three control cell lines further demonstrated the loss of pluripotency markers and accumulation of markers for astrocytes over time (Fig. S1D).

There were few genes differentially expressed between patient and control cells, demonstrating that astrocyte differentiation is much less impaired than neuronal differentiation, as was shown by patient iPSCs from other LS patients (Inak et al., 2021) However, gene set enrichment (GSEA) analysis revealed functional transcriptome differences, such as the downregulation of genes related to inflammation (Fig. S1E), as well as mitochondrial biogenesis (Fig. S1F) in patient cells compared to controls.

Interestingly, the functionality of the cells in basal conditions appeared similar, as determined through a glutamate uptake assay (Fig. S1G) and the measured oxygen consumption rate at resting basal condition (Fig. S1H). However, when the cells were challenged by different ETC inhibitors, control GPCs showed a significantly higher maximal respiration and spare respiratory capacity compared to patient GPCs (Fig. S1H). The mitochondrial metabolic deficit demonstrated in these results in NDUFS4-mutant GPCs is consistent with previously published data on NDUFS4-mutant fibroblasts (Catania et al., 2019), and cells from LS patients with other mutations in CI or CIV (Inak et al., 2021).

Mitochondrial deficiency impairs direct neuronal reprogramming of GPCs

Since a defect in mitochondrial metabolism could be detected in the patients at the GPC stage, we decided to focus on this cell stage for the neuronal reprogramming experiments conducted according to the paradigm illustrated in Figure 1A. Control and patient GPCs were transduced with a retrovirus encoding either the red fluorescent protein (DsRed) as a control condition, or different proneural transcription factors, including the well-established factors Neurogenin-2 (Neurog2) and Achaete-scute homolog 1 (Ascl1) (Berninger et al., 2007; Heinrich et al., 2010; Gascón et al., 2016; Rivetti di Val Cervo et al., 2017; Russo et al., 2021). We also tested the phospho-mutant versions of Neurog2 and Ascl1 (hereby referred to as pMutNeurog2 and pMutAscl1), because of their enhanced neurogenic activity *in vivo* (Ali et al., 2011; 2014). Interestingly, GPCs differentiated from control donor-iPSCs showed a significantly higher reprogramming efficiency (Neurog2 median = 49.25, IQR = 13.05; pMutNeurog2 median = 61.88, IQR = 15.89) than GPCs obtained from patient-derived iPSCs (Neurog2 median = 32.39, IQR = 12.75; pMutNeurog2 median = 36.96, IQR = 14.77) upon the expression of either Neurog2 or pMutNeurog2 (Fig. 1B, 1C). Although pMutNeurog2 further increased the reprogramming efficiency of control cells compared to wild type Neurog2, supporting the notion of its enhanced neurogenic capability, there was no parallel increase seen with the patient cells. In contrast, both Ascl1 and pMutAscl1 conditions led to a lot of cell death in both

genotypes, with very few infected cells surviving to day 20, although controls were still reprogrammed more efficiently than patients (control: Ascl1 median = 33.33, IQR = 29.65; pMutAscl1 median = 30, IQR = 31.52; patient: Ascl1 median = 7.14, IQR = 25; pMutAscl1 median = 3.33, IQR = 13.51) (Fig. 1B, 1C). Such transcription factor preference is consistent with previous studies that showed that Neurog2 is more effective in astrocytic cells than Ascl1 (Berninger et al., 2007).

As Bcl2 has a positive effect in the neuronal reprogramming of murine astrocytes through its reduction of oxidative stress (Gascón et al., 2016), we tested its expression in combination with each of the above-mentioned four proneural factors (Fig. 1D, 1E). Green fluorescence protein (GFP) was included with DsRed as a double-transduction control. Bcl2 further enhanced the reprogramming efficiency of control cells, both in the Neurog2 (median = 50.37, IQR = 12.98) and pMutNeurog2 (median = 64.16, IQR = 21.12) conditions. Surprisingly, Bcl2 did not significantly affect the reprogramming efficiency of NDUFS4-mutant cells either in Neurog2 (median = 34.15, IQR = 13.16) or pMutNeurog2 (median = 38.89, IQR = 11.17) conditions. Similar to the single factor conditions, Bcl2 combined with Ascl1 did not have a synergistic effect in the GPCs, regardless of donor type (control: Ascl1 median = 7.14, IQR = 13.28; pMutAscl1 median = 12.5, IQR = 13.35; patient: Ascl1 median = 17.44, IQR = 18.66; pMutAscl1 median = 13.33, IQR = 22.5) (Fig. 1D, 1E). This could indicate that apoptosis and ferroptosis, triggered by excessive ROS levels, and decreased by Bcl2 (Gascón et al., 2016) are not a limitation in this reprogramming paradigm – neither for patient nor control cells.

Therefore, although differences between control and mitochondrial-deficient GPCs were not detected at resting conditions, once the cells were challenged by conversion towards a neuronal fate significant differences became apparent.

Treatments alleviating different aspects of mitochondrial dysfunction rescue the reprogramming of NDUFS4-mutant GPCs

Given the differences between murine and human glial cells, and the need to alleviate the deficits of the patient cells, we explored the effects of manipulating several pathways – the ETC and ROS, the mitochondria turn-over and the unfolded protein response.

To do so, the neuronal reprogramming paradigm was conducted as before, except that the cells were treated with different compounds during the first media change at Day 2. Control and patient GPCs were either treated with Oligomycin A (OligoA), a blocker of the ATP synthase in the ETC, or with α-tocopherol, an analog of Vitamin E and a ROS scavenger. The cells were then fixed at day 20 and the proportion of neurons amongst the transduced GPCs was evaluated. Both control and patient GPCs had their reprogramming blocked by treatment with OligoA (Fig. 2A, 2B), as was the case for murine astrocytes (Gascón et al., 2016). Intriguingly, α-tocopherol did not significantly improve the neuronal reprogramming, neither of control nor patient GPCs, demonstrating important differences between human and murine glial cells.

Since neither Bcl2 nor α-tocopherol improved the patient GPCs reprogramming, reducing oxidative stress was not sufficient to rescue their conversion. Therefore, we decided to explore other aspects of metabolic stress and selected compounds that target different branches of mitochondrial dysfunction (Russel et al., 2020) (Fig. 2C-E). Mutations in CI can interfere with its ability to pass electrons down the ETC; therefore idebenone, a ubiquinone analog, was included to pass electrons in place of CI, albeit without restoring the proton pump function of CI (Haefeli et al., 2011). We also tested the mitophagy activator Urolithin A (UA) to address the possible accumulation of dysfunctional mitochondria that can be toxic for the cell (Ryu et al., 2016). Idebenone caused a mild improvement (control: median = 61.67, IQR = 7.06; patient: median = 49.71, IQR = 17.34). The mitophagy activator had the least effect on the neuronal reprogramming (control: median = 48.55, IQR = 6.58; patient: median = 46.66, IQR = 15.72), suggesting that mitochondrial turn-over is not a major roadblock. The NAD^+ precursor nicotinamide riboside (NR) was chosen to address the NAD^+/NADH redox balance, which is disrupted in NDUFS4-mutant patients (Lee et al., 2019). Remarkably, NR significantly improved the reprogramming efficiency of both mutant (median = 66.55, IQR = 22.51), and control GPCs (median = 71.02, IQR = 6.17), thus supporting mitochondrial oxidative metabolism (Cantó et al., 2012) as a limiting factor in direct reprogramming.

Due to the proximity and functional interaction that occurs between the mitochondria and the endoplasmic reticulum (ER) (Moltedo et al., 2019), we tested the possibility that the ER stress pathway known as the unfolded protein response (UPR) is involved during reprogramming. To this end, we inhibited two different branches of the UPR pathway, the IRE1 branch by treatment with STF-083010 (STF) and the PERK branch with AMG-PERK 44 (AMG) (Li et al., 2020).

The IRE1 branch triggers the generation of chaperones by activation of XBP-1, and the PERK branch inhibits translation, among other things, through the activation of eukaryotic translation initiation factor 2 alpha (eIF2α) (Wang & Kaufman, 2016). Interestingly, both UPR inhibitors had a significant improvement on the reprogramming efficiency of the cells compared to the Neurog2 alone condition (Fig. 2C-D). Once again, the control GPCs (STF median = 76.32, IQR = 6.64; AMG median = 74.52, IQR = 6.46) had augmented neuronal reprogramming reaching almost 80% efficiency. Strikingly, blocking the UPR with either inhibitor also allowed the patient GPCs to achieve a very high proportion of neurons reaching almost 70 % (STF median = 67.85, IQR = 9.14; AMG median = 66.1, IQR = 15.7). These data indicate that the normally beneficial UPR response is a hurdle in neuronal reprogramming and patient cells can indeed convert to neurons efficiently upon blocking the UPR.

A prominent role for ER stress and the redox status of the cell are thus implicated in metabolic function and reprogramming. We next wanted to determine if enhanced cell survival accounted for the differences observed in the treatment conditions.

Reprogramming dynamics are influenced, and neuronal functionality is rescued upon UPR treatment of NDUFS4-mutant cells

Previous work showed that cell death is a major limiting factor in direct neuronal reprogramming (Gascón et al., 2016; Russo et al., 2021) and an excessive UPR response elicits cell death (Hetz et al., 2012; 2020). We therefore aimed to monitor if and when this may be the case in human GPC reprogramming and to detect any differences between control and patient cells, and upon treatment. To elucidate the reprogramming dynamics in control and patient GPCs, we followed their conversion process over time by live imaging in 3 different time windows across the 20-day reprogramming protocol: days 4-8, 8-12 and 13-17 (Fig. S2A).

We had hypothesized that the low reprogramming efficiency of patient cells could be due to cell death occurring at early stages of the reprogramming process, as the stress from their oxphos deficit prevented them from fully converting and instead triggered cell death pathways. Thus, we investigated the number of transduced cells at early time points of reprogramming and normalized the results to the control DsRed condition. Interestingly, there was no overall difference in cell death between the control and patient cells (Fig. S2B-D), although there was a difference in timing, as more patient cell death occurred in the second block (days 8-12) versus more control cell death in the third block (days 13-17). Neither the treatment with α-tocopherol nor STF had an effect on cell survival.

We also investigated the appearance of neuronal cells in the reprogramming process, focusing on days 13-17 (Fig. S2E). A higher reprogramming efficiency was observed in the control GPCs compared to patient GPCs at this late time interval, despite their increased cell death, further strengthening the notion that late cell death is a byproduct of successful reprogramming (Gascón et al., 2016). Both α-tocopherol and STF enhanced the reprogramming efficiency and control cells were always more efficient than patient cells (Fig, S2E).

To assess whether the UPR treatments not only improved the reprogramming efficiency, but also had a positive effect on the activity of reprogrammed cells, we performed electrophysiological analysis on neuronal cells derived from control or patient GPCs, either with or without UPR-inhibitor treatment. To achieve functionally mature neurons cells were plated on an astrocyte feeder layer as described before (Mertens et al., 2015) (Fig. 3A). Both control and patient GPCs were transduced with Neurog2+Bcl2 and cultured for ~ 60 days. A greater percentage of control derived neurons (65%) were able to fire an action potential compared to patient-derived neurons (45%) (Fig. 3C). Therefore, the mitochondrial deficiency of the patient cells not only hinders their reprogramming efficiency, but also reduces the functionality of the resulting reprogrammed neurons. Remarkably, double the amount of patient-derived neuronal cells showed action potentials following treatment with the UPR inhibitor AMG (88%) similar to control-derived neurons. The rescue of patient cells upon AMG treatment not only increased the proportion of recorded cells that fired an action potential, but also led to increased amplitude and decreased duration of the recorded APs (Fig. 3D, 3E), suggestive of improved neuronal maturation.

Furthermore, spontaneous AP firing was recorded from a patient cell treated with AMG, and this was not detected in any of the other control or patient cells. Thus, the UPR inhibition not only led to a significant increase in control and patient GPC reprogramming ability, but also improved the percentage of reprogrammed neurons showing an action potential and their electrophysiological properties. It is therefore a novel major hurdle in direct neuronal reprogramming and even allows the deficits of the patient cells in neuronal conversion to be overcome.

Fibroblasts with a mitochondrial deficiency can also be rescued by targeting the UPR

To test if the above-described effects and results are cell type-specific, we investigated direct reprogramming of a different human starter cell type, namely fibroblasts. The fibroblasts were obtained from three control donors and three NDUFS4-mutant patients, two of which were used to generate iPSCs (#79787, #114107). The fibroblasts were reprogrammed with the same factors and protocol employed for the GPCs direct conversion (Figure 1A). Intriguingly, neither the control (Neurog2 median = 5.23, IQR = 1.34; pMutNeurog2 median = 15.91, IQR = 6.16) nor patient fibroblasts (Neurog2 median = 3.95, IQR = 3.66; pMutNeurog2 median = 6.42, IQR = 12.54) showed a high reprogramming efficiency when transduced with Neurog2 or pMutNeurog2, in stark contrast to the GPCs (Fig. 4A, 4B) and in line with previous observations (Liu et al., 2013). Likewise, Ascl1 alone had a relatively low reprogramming efficiency with the human fibroblasts, as was previously reported (Pang et al., 2011). Conversely, pMutAscl1 significantly increased the proportion of induced neurons from both the control (Ascl1 median = 12, IQR = 7.69; pMutAscl1 median = 36.97, IQR = 14.72) and patient cells (Ascl1 median = 8.33, IQR = 11.81; pMutAscl1 median = 35.14, IQR = 14.13). Remarkably, the co-expression of Bcl2 improved pMutAscl1-mediated neuronal conversion, but only in control fibroblasts (Fig. 4C, 4D). Indeed, these results, consistent over 3 different cell lines, suggest that NDUFS4-mutant fibroblasts can be reprogrammed to a certain efficiency, which cannot be further improved by established neurogenic factors, thus implying the presence of additional limiting hurdles in the process.

As the NDUFS4-mutant fibroblasts showed a similar reprogramming deficit as the GPCs, we tested if the same treatments improving GPC-to-neuron conversion were also successful for the patient-derived fibroblasts. Fibroblasts were transduced with Neurog2 and treated during the first media change on day 2, then fixed on day 20 for analysis. Despite the very low reprogramming efficiency induced by Neurog2, some treatments were still able to significantly increase the neuronal conversion in both control and patient cells (Fig. S3). Intriguingly, only the UPR inhibitor AMG had a significant improvement on both control (median = 13.17, IQR = 2.66) and patient (median = 9.77, IQR = 2) cells (though not completely rescuing the efficiency to the levels of the control), thus implicating PERK-mediated UPR stress as a hurdle to direct neuronal reprogramming in fibroblasts. Furthermore, STF also significantly improved patient cell (median = 5.62, IQR = 5) reprogramming, even rescuing the patient fibroblast reprogramming to within control cell reprogramming levels (median = 7.69, IQR = 10.95). Interestingly, NR and idebenone increased the neuronal conversion in control (NR median =

11.91, IQR.= 1.39; idebenone median = 12.3, IQR = 8.7), but not patient cells (NR median = 4.74, IQR = 1.62; idebenone median = 3.57, IQR = 5.12), highlighting some key differences in their response, as between GPC and fibroblast neuronal reprogramming.

Together, these data reinforce the observation that pharmacological treatments, aimed at regulating either metabolic mediators (NR) or cellular stress (AMG, STF), can indeed improve the direct neuronal conversion process, irrespective of the starter cells.

Discussion

Here we unraveled three major findings using a glia-to-neuron reprogramming paradigm. Most importantly, we discovered a novel pathway, the unfolded protein response, as a major hurdle in this reprogramming process. We further show that blocking this pathway is sufficient to almost completely rescue the neuronal conversion deficits of LS patient-derived glial cells, and we demonstrate that differentiation into the astrocyte lineage is virtually unaffected by the LS mutation in the CI protein NDUFS4.

We differentiated iPSCs carrying three different mutations in the NDUFS4 gene into GPCs in parallel with iPSCs from control donors and observed no major differences in astrocyte markers, glutamate up-take or a comprehensive RNA-seq analysis. Also, we did not observe maintenance of proliferation signatures as previously described for LS-patient cells with mutations in the CIV protein SURF1 (Inak et al., 2021). While the SURF1 mutation results in defective neural stem cells, gliogenesis, neurogenesis, and neuronal differentiation (Inak et al., 2021), our three NDUFS4-mutant iPSC lines differentiated in a comparable manner to control cells towards the astrocyte lineage. This was the case despite deficits in mitochondrial function as detected by the seahorse analysis of GPCs or fibroblasts, namely lower maximal respiration and spare respiratory capacity. There are similarities not only in the pathology of the LS patients carrying mutations in different ETC complex genes (Gerards et al., 2016; Hong et al., 2020), but also at the cellular and molecular level. Neurogenesis and neuronal differentiation were shown to be defective in all LS patient-derived iPSC differentiation paradigms tested so far (Lorenz et al., 2017; Galera-Monge et al., 2020; Inak et al., 2021) and this deficiency was also prominent in the glia-to-neuron fate conversion tested here. Patient GPCs could convert

into functional neurons, but with a reduced efficiency not exceeding ~40% without additional treatments. Moreover, the NDUFS4-mutant GPCs showed similar deficits at the transcriptome level as those observed in SURF1-mutant NPCs. For example, there was a reduced expression of genes involved in regulating inflammation in patient GPCs compared to controls (Fig. S1E), as well as downregulation of PPARGC1A (Fig S1F), which encodes for PGC-1α, a known modulator of mitochondrial biogenesis (Liang & Ward, 2006), as was observed in SURF1-mutant NPCs (Inak et al., 2021). Conversely, we did not observe maintenance of proliferation or pluripotency genes when differentiating the NDUFS4 patient cells into GPCs, highlighting important differences and similarities in the cellular and molecular phenotype of LS patient-derived iPSCs during differentiation into different lineages.

One of the main aims of this and previous studies is to identify possible novel treatment options for LS patients, and also to improve human glia-to-neuron reprogramming for patients suffering from stroke or neurodegeneration. Mitochondrial conversion is a major hurdle in glia-to-neuron reprogramming due to the slow turn-over of mitochondrial proteins (Russo et al., 2021) and excessive ROS production (Gascón et al., 2016). We expected GPCs from LS patients to struggle even more with this mitochondrial adaptation, due to generally increased ROS levels (Verkaart et al., 2007; Valsecchi et al., 2013) and reduced PGC-1α expression, which indicates lower mitochondrial biogenesis. However, treatment with a ROS scavenger (α-tocopherol), re-establishing the transfer of electrons by the ubiquinone analog idebenone or increasing mitochondrial turn-over by Urolithin A, did not have a strong effect on reprogramming – neither for patient- nor control-derived cells. For control cells this shows a notable difference to the results obtained with murine astrocytes (Gascón et al., 2016), highlighting the species and cell-type specificity of the conversion process. These results are also consistent with the antioxidant treatment of SURF1-mutant cells, as little improvement upon treatment was shown in SURF1 NPCs or neurogenesis (Inak et al., 2021). Conversely, SURF1-mutant neurogenesis was improved by increasing mitochondrial mass using the PPAR agonist bezafibrate (Inak et al., 2021), while removing defective mitochondria and increasing turn-over failed to improve neuronal conversion of both control and LS patient cells in our study.

CI converts NADH to NAD^+, and most LS patient cells show reduced NAD^+ levels and NAD^+/NADH ratio (Thompson Legault et al., 2015; Iannetti et al., 2018; Inak et al., 2021). Accordingly, restoring this balance through NR treatment has been a therapeutic strategy in

mouse models (Khan et al., 2014), and has also proved to be effective in improving the reprogramming deficit, not only of patient cells, but, remarkably, it had a strong effect also in the control cells. One possible explanation is that when cells are undergoing forced neuronal conversion and switch from favoring a glycolytic metabolism to oxphos, the redox energy of the cell can become unbalanced. The correct level of NAD^+ is crucial for cellular function, as it has been shown to be involved in mitochondrial biogenesis (Bai et al., 2011) and the regulation of proteins, including histone acetylation via Sirtuins (Karamanlidis et al., 2013; Lee et al., 2019; Chakrabarty and Chandel, 2021). Thus, adequate NAD^+ levels may help gene activation processes during the course of reprogramming.

The most surprising and novel finding was the identification of the UPR as a major roadblock in direct reprogramming, with its inhibition achieving a very high efficiency of conversion into neurons. The UPR is activated in the ER upon accumulation of misfolded proteins and in the presence of high ROS levels (Li et al., 2020; Cao et al., 2014; Hetz et al., 2020). The UPR coordinates the increased expression of chaperones, reduced translation rates and mounts an antioxidant response (Wang & Kaufman, 2016), all designed to improve the rate of adequately folded proteins. During prolonged activation, the UPR elicits cell death, typically via apoptosis (Rutkowski et al., 2006; Tabas & Ron, 2011). We had previously observed a high expression of genes associated with the UPR in the scRNA-seq of murine astrocytes converting to neurons (Najas et al., unpublished data) and therefore tested if UPR inhibition could enhance the direct neuronal reprogramming of human cells. Indeed, inhibitors targeting two separate branches of the UPR pathway (i.e., PERK and IRE1) profoundly increased the reprogramming efficiency and maturation of the induced neurons of both control and NDUFS4-patient derived cells. Strikingly, live imaging of the conversion process did not reveal a major difference in cell death, suggesting other UPR-mediated processes as hurdles in reprogramming. One intriguing possibility is that the reduced global translation rate due to UPR activation is deleterious to the conversion process during which many new proteins are required. Indeed, our recent work showed a difference of ~20% of the mitochondria proteins between astrocytes and neurons that needs to be adapted during the conversion process (Russo et al., 2021), in addition to the need of many new functional channels, receptors, cytoskeletal changes, and much more. A reduced translation rate could thus be a major limitation in this process and would also fit to the PERK-eIF2a pathway inhibitor being most effective in our study. Interestingly, the UPR response can also be elicited in development by interfering with codon translation speed resulting in a

reduced generation of neurons (Laguesse et al., 2015) and is elicited by Zika virus infections blocking neurogenesis (Alfano et al., 2019).

Moreover, the tight interconnection between the ER and mitochondria coordinates key cellular functions such as calcium homeostasis, inflammation signaling and autophagy, among others (Missiroli et al., 2018). For example, it has been shown that ER stress instigates mitochondrial Ca^{2+} influx to provide energy for protein folding (Rossi et al., 2019). However, the subsequently increased ROS generation can in turn further enhance ER stress and lead to the activation of apoptotic pathways (Martucciello et al., 2020). Therefore, blocking this feedback loop between the organelles can be a possible explanation for the positive effect of the UPR inhibitors on reprogramming efficiency. Similar to how mitochondrial dysfunction has been linked to neurodegenerative diseases, protein accumulation and the activated UPR pathway have also been tied to these disorders (Hetz et al., 2017). Most excitingly, blocking the UPR also allowed a very high efficiency of neuronal induction from patient GPCs, as they reached a proportion of more than 60% neurons, identifying the UPR as a novel pathway responsible for limiting neuron generation in this paradigm.

In conclusion, this work revealed a new major hurdle in neuronal reprogramming, the unfolded protein response, allowing efficient conversion of human glial cells even from LS patients. This highlights not only the validity of using direct neuronal reprogramming to model mitochondrial disease, but also unravels therapeutic strategies aimed at replacing functional neurons by direct reprogramming, as well as for treating mitochondrial disorders.

Acknowledgements

We are very grateful to Andrea Steiner for virus production; to Tatiana Simon-Ebert for primary mouse astrocyte cultures; to Pawel Smialowski for RNAseq analysis input; to Kalina Draganova for advice on human iPSC culture; and to Alicia Kemble for advice on human astrocyte differentiation. This work was funded by the German Research Foundation (SPP 1757, SFB 870 and TR 274), and the German Excellence Cluster SyNergy.

Author contributions

M.G. and G.M. conceived and designed the project. G.S., G.M., and M.G. developed the project, and G.S. performed experiments and analyzed the results. T.R. conducted the electrophysiology experiments. M.G. provided expertise on metabolism and the Seahorse Assay. E.R. and M.D. generated the iPSC cell lines used in the study. S.N. provided initial evidence of UPR in reprogramming. A.J. prepared bulk-adapted mcscrb-seq libraries and W.E. provided expertise. H.P. provided the NDUFS4-mutant patient cell lines, and expertise regarding the patients and metabolism. G.M. analyzed the RNAseq data and provided expertise and training of G.S. regarding direct neuronal reprogramming. P.S. demultiplexed and aligned the RNA-seq libraries. G.M and M.G. co-directed the project. G.S., G.M., and M.G. wrote the manuscript. All authors contributed to corrections and comments.

Declarations of Interests

The authors declare no competing interests.

Materials and Methods

EXPERIMENTAL MODEL AND SUBJECT DETAILS

Human iPSCs and fibroblasts

The control fibroblast cell line NDHFneo was obtained from Lonza (Cat. No. CC-2509). The other two control fibroblast cell lines (#47041, #61691) and the three NDUFS4-mutant patient fibroblast cell lines (#79787, #114107, #114106) were obtained from skin biopsies of patients with signed informed consent. The cell line #79787 belongs to a patient with the homozygous frameshift mutation c.462delA (p.Lys154fs) within the *NDUFS4* gene. The cell lines #114107 and #114106 belong to patients with a substitution mutation in the *NDUFS4* gene, at c.119G>A (p.Trp40) and at c.316C>T (p.Arg106) respectively.

The control iPSC cell line UKERi82a-R1-002 was obtained as part of the ForIPS research consortium. The ethics approval is No. 4120, FAU Erlangen-Nuernberg, Germany. Detailed genetic information can be found in Popp et al., 2018. The other two control iPSC cell lines (#1 and HMGU12) and the three patient iPSC cell lines (#87971, #79787, #114107) were generated by the iPSC core unit (headed by Micha Drukker) at the Helmholtz Zentrum München.

Primary cultures of mouse cortical astrocytes

Astrocytes were isolated and cultured as previously described, with small changes (Heins et al., 2002; Heinrich et al., 2011). The meninges was removed, and then the grey matter tissue from the cerebral cortex of C57BL/6J mice at postnatal day 5-7 (P5–P7) was dissected and mechanically dissociated. The dissociated cells were centrifuged at 1,400rpm for 5min, re-suspended and plated in a T25 flask in mouse astrocyte medium (DMEM/F12 (1:1) plus Glutamax, 10% fetal bovine serum (FBS), penicillin /streptomycin (P/S), 1x B27 serum-free-supplement, 10 ng/ml epidermal growth factor (EGF), and 10 ng/ml basic fibroblast growth factor (bFGF)). The cells reached ~80% confluency after 7 days and were then passaged using trypsin/EDTA and subsequently plated on poly-D-lysine coated glass coverslips in a 24-well dish. Fresh mouse astrocyte medium was used to plate the cells at a density of 45,000-55,000 cells per coverslip. The primary mouse astrocytes were maintained in an incubator at 37ºC and with 5% CO_2.

Human iPSC culture

iPSCs were cultured on Geltrex™ LDEV-Free, Reduced Growth Factor Basement Membrane Matrix coated 6-well plates in mTESR1 medium containing 1× mTESR1 supplement. Media was changed every day. For passaging, the cells were incubated with Collagenase Type IV for 5–7 minutes at 37°C. The collagenase was aspirated and fresh mTESR1 (with supplement) medium was added to each well. A cell scraper was used to collect the cells, and they were subsequently plated on a fresh 6-well plate at the desired dilution.

Generation of human GPCs and Astrocytes

Glial progenitor cells (GPCs) and astrocytes were generated as previously described with modifications (Santos et al., 2017). Briefly, confluent iPSC cultures were dissociated with collagenase, collected with a cell scraper and then cultured in suspension to form embryoid bodies. The first 24hrs the cells were cultured in mTESR1 with 1× mTESR1 supplement and 10 μM Rock Inhibitor Y-27632. For the next two weeks the cells were cultured in Astrocyte medium (AM) supplemented with 20ng/ml Noggin and 10ng/mL PDGFAA, and an additional week with only PDGFAA. The embryoid bodies were then manually dissociated by pipetting and the resulting GPCs were plated on poly-L-ornithine (PO) and laminin-coated dishes in AM supplemented with 10ng/ml bFGF and 10ng/ml EGF. Upon reaching ~80% confluency, the GPCs were passaged using Accutase. The GPCs were maintained in culture until ~day 45-50 of glial differentiation, and then astrocytes were differentiated from the GPCs in AM supplemented with 10ng/ml LIF. The media was changed every second day.

Human fibroblast culture

The human fibroblasts were cultured in T75 flasks with fibroblast media consisting of DMEM plus Glutamax, P/S (1:100), and FBS 10%. Upon reaching ~80% confluency the fibroblasts were passaged using Trypsin/EDTA. The media was changed every second day.

METHODS DETAILS

Direct neuronal reprogramming

Two days post-transduction, GPC media or fibroblast media was replaced with fresh neuronal differentiation media consisting of DMEM/F12 and Neurobasal media (1:1), 1x P/S, 1x B27 supplement, 1x N2 supplement and 1x MEM non-essential amino acids (NEAA) solution. The media was supplemented with growth factors and small molecules (adapted from the media used in Drouin-Ouellet et al., 2017) at the following concentrations: LDN-193189 (0.5 μM), LM-22A4 (2 μM), GDNF (2 ng/ml), CHIR99021 (2 μM), NT3 (10 ng/μl), SB-431542 (10 μM), db-cAMP (0.1 μg/ml), and Noggin (50 ng/ml), as well as valproic acid sodium salt (VPA; 1 mM). The media was partially changed every second day. From day seventeen post-transduction until the end of the experiment, the neuronal media was only supplemented with growth factors (GDNF, LM-22A4, NT3, and db-cAMP). At day twenty post-transduction the cells were fixed with 4% paraformaldehyde (PFA) for 10min, and then stored in 1xPBS at 4ºC for further analysis. During reprogramming the cultures were maintained in an incubator at 37ºC, 5% O_2 and 5% CO_2.

Bulk RNA sequencing and analysis

Cells at iPSC, GPC and astrocyte stages were collected and RNA was isolated on column using the PicPure™ RNAextraction kit (Applied Biosystems). RNA quality and concentration were

evaluated with an Agilent BioAnalyzer 2100 (Agilent). All included samples had a RIN>9. 10ng of RNA from each sample was used to generate the RNA-seq libraries using bulk-adapted mcSCRB-seq protocol (Bagnoli et al., 2018): cDNA was generated by oligo-dT primers containing well-specific (e.g. sample specific) barcodes and unique molecular identifiers (UMIs). Unincorporated barcode primers were digested using Exonuclease I (Thermo Fisher). cDNA was pre-amplified using KAPA HiFi HotStart polymerase (Roche) and pooled before Nextera libraries were constructed from 0.8 ng of pre-amplified cleaned up cDNA using Nextera XT Kit (Illumina). 3' ends were enriched with a custom P5 primer (P5NEXTPT5, IDT) and libraries were size selected using 2% E6 Gel Agarose EX Gels (Life Technologies), cut out in the range of 300–800 bp, and extracted using the Monarch DNA Gel Extraction Kit (New England Biolabs) according to manufacturer's recommendations. Libraries were paired end sequenced on an Illumina HiSeq 1500 instrument. Sixteen bases were sequenced within the first read to obtain cellular and molecular barcodes, and 50 bases were sequenced in the second read into the cDNA fragment. An additional eight bases were sequenced to obtain the i7 barcode. On average, we sequence around 20 million read/sample. Gene-based transcripts counts were obtained by running the zUMI pipeline (Parekh et al., 2018) (version 0.0.2) using Ensembl annotation release 81 (hg38_Oct2017/ensembl90). We analyzed 3 biological replicates per stage per cell line. One sample (#87971, iPSC stage) was analyzed twice.

The analysis was performed using R (3.5.3) and RStudio (version 1.2.1335). Differential gene expression analysis was performed using DESEQ2 package (Love et al., "Moderated estimation of fold change and dispersion for RNA-seq data with DESeq2", 2014): 3 main stages were considered (iPSC, GPC and Astrocytes) belonging to 2 different donors (Control and Patient). Gene Ontology enrichment on Biological Process (BP) analysis was performed using the package "TopGO": differentially expressed genes (Log2FC>1, pvalue<0.05 or Log2FC<-1, pvalue<0.05) were provided as input, while the list of the genes with a pvalue were used as background. Top 20 GO terms, ranked based on Exact Fisher score (<0.01), were selected; GO terms were then ranked for the enrichment, obtained by diving the number of detected genes versus the number of expected genes, and top 5 were plotted. Gene Set Enrichment Analysis (Subramanian et al., 2005) was performed using the package "fgsea" in Rstudio (Sergushichev A (2016). "An algorithm for fast pre-ranked gene set enrichment analysis using cumulative statistic calculation").

Cell cycle score was generated by summing the normalized gene expression, obtained from DESeq2, of the genes listed in Tirosh (Tirosh et al, Science 2016) for G1/S and G2/M. Genes plotted in Figure S1D were selected based on pluripotent stem cell markers (Giulitti et al, Nature Cell Biology, 2019, figure 3A) and known astrocytic markers (e.g. Sox9) and markers identified in Barbar (Barbar et al., Neuron, 2020, Figures 2D and 2E).

Plasmids and viral production

The plasmids containing *Ascl1* or *Neurog2* cDNA were previously described (Heinrich et al., 2010). Briefly, the coding sequence of the reprogramming factors was cloned downstream of a CAG promoter and followed by an intra-ribosome-entry-site (IRES) together with DsRed coding gene. The plasmid containing Bcl2 was previously described (Gascón et al., 2016). The phospho-incompetent forms of Neurog2 and Ascl1 were a kind gift of Prof. Anna Philpott. cDNA of these phospho-mutants was cloned in the same plasmid used for the wild type forms of Neurog2 and Ascl1. Viral vectors were produced as described (Heinrich et al., 2011).

Transduction

The GPCs were plated on PO/laminin-coated glass coverslips, and the fibroblasts were plated on 0.1% gelatin-coated glass coverslips, in 24-well plates at a density of 40,000 cells per well. The day after plating the cells were transduced with 1µl of virus per well. Once the cells were transduced, they were placed in an incubator at 37ºC, 5% O_2 and 5% CO_2. Two days post-transduction the cells had their media changed to neuronal differentiation media, as is described above.

Pharmacological treatment

The pharmacological treatment of the GPCs and fibroblasts undergoing reprogramming was conducted during the first media change, at two days post-transduction. The cells were treated once with each compound at the following concentrations: α-tocopherol (10 µM), Oligomycin A (1 µg/ml), Urolithin A (2 µg/ml), Nicotinamide riboside (10 µM), Idebenone (1 µg/ml), AMG PERK-44 (10 µM), and STF-083010 (10 µM).

Glutamate Uptake Assay

The iPSCs, GPCs and astrocytes were plated on 6-well plates, and upon reaching confluency the cells were treated with glutamate to reach a final concentration of 10µM, 100µM or they were left untreated. The cells were incubated for 30min, and then the supernatant was removed from the cells across the different conditions. The glutamate concentration of each supernatant was subsequently analyzed using the Glutamate Assay Kit (ab83389) from Abcam. The Glutamate Assay Kit instructions were followed as described in the Abcam protocol booklet.

Seahorse experiments

Human fibroblasts, iPSC-derived GPCs and iPSC-derived astrocytes were plated on XF96 V3-PS 96-well cell culture microplates from Seahorse Bioscience and analyzed the day after plating. The cells were seeded at a density of 20,000 cells per well, and the four corner wells contained only media for background correction. Before the Seahorse analysis, cells were washed once with un-buffered media, and then incubated with 180µl of the bicarbonate-free DMEM in an air incubator without CO_2 at 37°C for 30 min. The XF96 plate was then placed in the XF96 Extracellular Flux

Analyzer (Seahorse Bioscience) and the oxygen consumption rates (OCR) were measured. The OCR was first measured with no additions, and then again after adding various compounds to obtain measurements of different respiration states. First, Oligomycin A (1 μM) was added to inhibit ATP synthase, followed by carbonyl cyanide 4-(trifluoromethoxy) phenylhydrazone (FCCP, 0.4 μM) to determine the maximal oxidation capacity, and finally a combination of rotenone (2 μM) and Antimycin A (2.5 μM) to block ETC activity. The OCR was measured at three time points for each measurement condition, and ~16-24 technical replicate wells were plated for each cell line. After the Seahorse Assay finished, the normalization for the number of cells in each well was conducted using the CyQuant Assay.

Three biological replicates were conducted for the Seahorse data in Figure S1. The parameters depicted in Figure S1 are from OCR measurements in different conditions: Basal respiration is calculated from the OCR measurements before the first compound injection; ATP-linked respiration is calculated from the OCR before oligomycin injection minus OCR after oligomycin injection; Maximal respiration is calculated from the OCR after FCCP injection; Spare respiratory capacity is calculated from maximal respiration minus basal respiration.

Immunocytochemistry

Cells were fixed with 4% PFA for 10 min. at room temperature, and then stored in 1xPBS at 4°C before staining. The cells were incubated in blocking solution (1xPBS plus 3% Bovine Serum Albumin (BSA) and 0.5% Triton X-100) for 30min, and were subsequently incubated with primary antibodies diluted in blocking solution for 2 hours at room temperature or overnight at 4°C. After washing 3x for 5 minutes each with 1xPBS, the cells were incubated with the correct species-specific secondary antibodies at a dilution of 1:1000 for 1hr in the dark at room temperature. DAPI was also added during this step to label the nuclei, diluted at 1:10,000 in blocking solution. The cells were washed 3x for 5 minutes each with 1xPBS, and then the coverslips were mounted with Aqua Poly/Mount. The cells were imaged at the Axio Observer Z1 epifluorescence microscope (Carl Zeiss) or the LSM710 laser-scanning confocal. Digital images were acquired using the ZEN software (Carl Zeiss) at 20X, 25X or 40X.

The following primary and secondary antibodies were used:

Species	**Primary Antibodies**	**Dilution**	**Company**	**Catalog number**
Rabbit	FGFR3	1:200	Santa Cruz	sc-123
Mouse IgG1	S100β	1:200	Sigma	S2532
Rat IgG2a	RFP	1:200	Helmholtz Facility	5F8
Chicken	GFP	1:300	Aves Labs	GFP-1020
Mouse IgG1	MAP2	1:200	Sigma	M4403
Guinea Pig	β-III-tubulin	1:300	Synaptic Systems	302304
Reactivity	**Secondary Antibodies**	**Dilution**	**Company**	**Catalog number**

Chicken	Alexa Fluor 488	1:1000	Thermo Fisher	A11039
Rat	Alexa Fluor 546	1:1000	Thermo Fisher	A11081
Guinea Pig	Alexa Fluor 647	1:1000	Thermo Fisher	A21450
Mouse IgG1	Alexa Fluor 488	1:1000	Thermo Fisher	A21121
Rabbit	Cy3	1:1000	Jackson Laboratory	711-165-152

Co-culture for electrophysiology

Human GPCs were plated on 6-well plates at ~210,000 cells per well. The following day the cells were transduced with 5 µl of virus per well. Two days post-transduction the GPCs were washed twice with 1xPBS and plated on top of the mouse astrocytes (that had been plated the day before in 24-well plates). The co-culture cells were maintained in mouse astrocyte conditioned media (media taken from T75 flasks of mouse astrocyte cultures after 3-4 days and supplemented with the neuronal reprogramming media factors plus 10 µM Rock Inhibitor Y-27632. The media was partially changed every second day.

Whole-cell patch-clamp recordings

Whole-cell patch-clamp measurements were performed as previously described (Schieweck et al., accepted, Riedemann et al., 2018). Briefly, coverslips with cultured iNeurons were transferred to an organ bath mounted on the stage of an upright microscope (BX-RFA-1-5, Olympus, Japan). A single coverslip was continuously perfused with artificial cerebro-spinal fluid (ASCF) containing (in mM): NaCl (125), KCl (3), NaH_2PO_4 (1.25), $NaHCO_3$ (25), $CaCl_2$ (2), $MgCl_2$ (2) and D-Glucose (25 mM). The ACSF was saturated with 95% O_2 / 5% CO_2 to maintain a pH of 7.4. The osmolarity of the ACSF ranged between 305 to 318 mOsmol. The perfusion rate with ACSF was set to 3 mL / min and recordings were performed at 28°C. Cultured cells were visualized with a Dodt contrast tube (DGC, Scientifica, UK) that was attached to the microscope. Successfully transduced neurons were identified by DsRed expression with the help of a fluorescence lamp (pE-300, CooLED, UK) and epifluorescence optics for red fluorescence (filter: ZT635dcrb, Chroma Technology, USA). Images were taken and displayed using a software-operated microscope camera (Evolve 512 Delta, Teledyne Photometrics, USA). The electrodes for whole cell patch-clamp recordings were fabricated from borosilicate glass capillaries (OD: 1.5 mm, ID: 0.86 mm, Hugo Sachs Elektronik-Harvard Apparatus, March-Hugstetten, Germany) and filled with a solution composed of (in mM): K-gluconate (135), KCl (4), NaCl (2), EGTA (0.2), HEPES (10), Mg-ATP (4), Na-GTP (0.5), and phosphocreatine (10). The osmolarity ranged between 288-295 mOsmol, the pH was adjusted to 7.3. The electrodes (resistance: 3 – 5 M□) were connected to the headstage of a npi ELC-03XS amplifier (npi, Tamm, Germany). The recorded signals were amplified (x20), filtered at 20 kHz, digitized at a sampling rate of 50 kHz and stored on a computer for off-line analysis. Data acquisition was performed by means of a CED 1401 Power 3 system in conjunction with the

Signal6 data acquisition software (Cambridge electronic design, Cambridge, England). The input resistance was determined by injecting at least 10 small hyperpolarizing current steps (500 ms, 1-10 pA) into the cells and by determining the averaged voltage deflection in response to the current injection. The input resistance was then calculated according to Ohm's law (R= V/I). The properties of single action potentials (AP) were obtained from recordings in which action potentials were elicited by means of just suprathreshold current steps or current ramps (duration: 50 ms). The following AP parameters were analyzed: AP amplitude, AP duration, AP threshold, AP rising slope. The amplitude was determined as the difference between the resting membrane potential and the AP peak voltage. Duration, rising slope and spike threshold were determined according to methods given by Bean (2007): Single spikes were differentiated, and the spike duration corresponded to the temporal difference between the maximum and the minimum of the differentiated spike. The rising slope was equal to the maximum of the first spike derivative. For the spike threshold analysis, the differentiated spike was plotted as a function of the membrane voltage. In this phase plane, the threshold corresponded to the point where the rising slope of the membrane voltage displayed a sudden increase. To test whether an iNeuron was able to fire repetitive action potentials, at least 20 current steps with increasing amplitudes (duration: 1 s) were injected into the cells. Depending on a cell's input resistance, these current steps ranged between 1-10 pA. Data analysis was performed using IGOR Pro 6 together with the Neuromatic IGOR plugin (Rothman and Silver, 2018).

Live-Imaging Microscopy

Continuous live imaging was performed with a Cell Observer (Zeiss) microscope and the cells were maintained in a chamber with 37°C temperature and with 5% CO_2. The imaging was conducted over 5 days, with phase-contrast images being acquired every 10 min and fluorescence pictures every 4 hours using a 10x phase contrast objective (Zeiss) and an AxioCam HRm camera with a self-written VBA module remote controlling Zeiss AxioVision 4.7 software (TAT, Prof. Dr. Timm Schroeder). The images were analyzed using ImageJ (NIH) software (as described in Gascón et al., 2016).

QUANTIFICATION AND STATISTICS

The efficiency of neuronal reprogramming for both GPCs and fibroblasts across conditions was analyzed at day 20 post-transduction. The quantification of neuronal-like cells was conducted as previously described (Gascón et al., 2016): in essence, morphological parameters such as the length of processes and β-III-tubulin immunoreactivity were assessed.

The continuous live imaging experiments were analyzed at 4 time points across the 5 days (0hrs, 48hrs, 80hrs and 100hrs). The number of $DsRed^+$ cells was calculated for each time point to

determine the amount of transduced-cell death occurring over the experiment. The reprogramming efficiency was analyzed as detailed above.

Data were analyzed with Microsoft Excel, GraphPad Prism 7.0 software and linear regression using “lm” function (R Stats package) in RStudio. Evaluation of the residuals for fitted linear models was performed with the package “DHARMa” (Florian Hartig (2020). DHARMa: Residual Diagnostics for Hierarchical (Multi-Level / Mixed) Regression Models. R package version 0.3.2.0. https://CRAN.R-project.org/package=DHARMa) in RStudio.

The number of biological replicates is detailed in the Figure Legends, and the data are plotted as either median ± interquartile range (IQR) or mean ± SEM. The significance illustrated in the graphs belong to the corresponding p-values: * $p \leq 0.05$, ** $p \leq 0.01$, *** $p \leq 0.001$.

References

Alfano, C., Gladwyn-Ng, I., Couderc, T., Lecuit, M., & Nguyen, L. (2019). The Unfolded Protein Response: A Key Player in Zika Virus-Associated Congenital Microcephaly. *Frontiers in cellular neuroscience*, *13*, 94. https://doi.org/10.3389/fncel.2019.00094

Ali, F., Hindley, C., McDowell, G., Deibler, R., Jones, A., Kirschner, M., Guillemot, F., & Philpott, A. (2011). Cell cycle-regulated multi-site phosphorylation of Neurogenin 2 coordinates cell cycling with differentiation during neurogenesis. *Development)*, *138*(19), 4267–4277. https://doi.org/10.1242/dev.067900

Ali, F. R., Cheng, K., Kirwan, P., Metcalfe, S., Livesey, F. J., Barker, R. A., & Philpott, A. (2014). The phosphorylation status of Ascl1 is a key determinant of neuronal differentiation and maturation in vivo and in vitro. *Development*, *141*(11), 2216–2224. https://doi.org/10.1242/dev.106377

Bagnoli, J. W., Ziegenhain, C., Janjic, A., Wange, L. E., Vieth, B., Parekh, S., Geuder, J., Hellmann, I., & Enard, W. (2018). Sensitive and powerful single-cell RNA sequencing using mcSCRB-seq. *Nature communications*, *9*(1), 2937. https://doi.org/10.1038/s41467-018-05347-6

Bai, P., Cantó, C., Oudart, H., Brunyánszki, A., Cen, Y., Thomas, C., Yamamoto, H., Huber, A., Kiss, B., Houtkooper, R. H., Schoonjans, K., Schreiber, V., Sauve, A. A., Menissier-de Murcia, J., & Auwerx, J. (2011). PARP-1 inhibition increases mitochondrial metabolism through SIRT1 activation. *Cell metabolism*, *13*(4), 461–468. https://doi.org/10.1016/j.cmet.2011.03.004

Barbar, L., Jain, T., Zimmer, M., Kruglikov, I., Sadick, J. S., Wang, M., Kalpana, K., Rose, I., Burstein, S. R., Rusielewicz, T., Nijsure, M., Guttenplan, K. A., di Domenico, A., Croft, G., Zhang, B., Nobuta, H., Hébert, J. M., Liddelow, S. A., & Fossati, V. (2020). CD49f Is a Novel Marker of Functional and Reactive Human iPSC-Derived Astrocytes. *Neuron*, *107*(3), 436–453.e12. https://doi.org/10.1016/j.neuron.2020.05.014

Barker, R. A., Götz, M., & Parmar, M. (2018). New approaches for brain repair-from rescue to reprogramming. *Nature*, *557*(7705), 329–334. https://doi.org/10.1038/s41586-018-0087-1

Bean B. P. (2007). The action potential in mammalian central neurons. *Nature reviews. Neuroscience*, *8*(6), 451–465. https://doi.org/10.1038/nrn2148

Berninger, B., Costa, M. R., Koch, U., Schroeder, T., Sutor, B., Grothe, B., & Götz, M. (2007). Functional properties of neurons derived from in vitro reprogrammed postnatal astroglia. *The Journal of neuroscience: the official journal of the Society for Neuroscience*, *27*(32), 8654–8664. https://doi.org/10.1523/JNEUROSCI.1615-07.2007

Camandola, S., & Mattson, M. P. (2017). Brain metabolism in health, aging, and neurodegeneration. *The EMBO journal*, *36*(11), 1474–1492. https://doi.org/10.15252/embj.201695810

Cantó, C., Houtkooper, R. H., Pirinen, E., Youn, D. Y., Oosterveer, M. H., Cen, Y., Fernandez-Marcos, P. J., Yamamoto, H., Andreux, P. A., Cettour-Rose, P., Gademann, K., Rinsch, C., Schoonjans, K., Sauve, A. A., & Auwerx, J. (2012). The NAD(+) precursor nicotinamide riboside enhances oxidative metabolism and protects against high-fat diet-induced obesity. *Cell metabolism*, *15*(6), 838–847. https://doi.org/10.1016/j.cmet.2012.04.022

Cao, S. S., & Kaufman, R. J. (2014). Endoplasmic reticulum stress and oxidative stress in cell fate decision and human disease. *Antioxidants & redox signaling*, *21*(3), 396–413. https://doi.org/10.1089/ars.2014.5851

Catania, A., Iuso, A., Bouchereau, J., Kremer, L. S., Paviolo, M., Terrile, C., Bénit, P., Rasmusson, A. G., Schwarzmayr, T., Tiranti, V., Rustin, P., Rak, M., Prokisch, H., & Schiff, M. (2019). Arabidopsis thaliana alternative dehydrogenases: a potential therapy for mitochondrial complex I deficiency?

Perspectives and pitfalls. *Orphanet journal of rare diseases*, *14*(1), 236. https://doi.org/10.1186/s13023-019-1185-3

Chakrabarty, R. P., & Chandel, N. S. (2021). Mitochondria as Signaling Organelles Control Mammalian Stem Cell Fate. *Cell stem cell*, *28*(3), 394–408. https://doi.org/10.1016/j.stem.2021.02.011

Drouin-Ouellet, J., Lau, S., Brattås, P. L., Rylander Ottosson, D., Pircs, K., Grassi, D. A., Collins, L. M., Vuono, R., Andersson Sjöland, A., Westergren-Thorsson, G., Graff, C., Minthon, L., Toresson, H., Barker, R. A., Jakobsson, J., & Parmar, M. (2017). REST suppression mediates neural conversion of adult human fibroblasts via microRNA-dependent and -independent pathways. *EMBO molecular medicine*, *9*(8), 1117–1131. https://doi.org/10.15252/emmm.201607471

Galera-Monge, T., Zurita-Díaz, F., Canals, I., Hansen, M. G., Rufián-Vázquez, L., Ehinger, J. K., Elmér, E., Martin, M. A., Garesse, R., Ahlenius, H., & Gallardo, M. E. (2020). Mitochondrial Dysfunction and Calcium Dysregulation in Leigh Syndrome Induced Pluripotent Stem Cell Derived Neurons. *International journal of molecular sciences*, *21*(9), 3191. https://doi.org/10.3390/ijms21093191

Gascón, S., Murenu, E., Masserdotti, G., Ortega, F., Russo, G. L., Petrik, D., Deshpande, A., Heinrich, C., Karow, M., Robertson, S. P., Schroeder, T., Beckers, J., Irmler, M., Berndt, C., Angeli, J. P., Conrad, M., Berninger, B., & Götz, M. (2016). Identification and Successful Negotiation of a Metabolic Checkpoint in Direct Neuronal Reprogramming. *Cell stem cell*, *18*(3), 396–409. https://doi.org/10.1016/j.stem.2015.12.003

Gerards, M., Sallevelt, S. C., & Smeets, H. J. (2016). Leigh syndrome: Resolving the clinical and genetic heterogeneity paves the way for treatment options. *Molecular genetics and metabolism*, *117*(3), 300–312. https://doi.org/10.1016/j.ymgme.2015.12.004

Giulitti, S., Pellegrini, M., Zorzan, I., Martini, P., Gagliano, O., Mutarelli, M., Ziller, M. J., Cacchiarelli, D., Romualdi, C., Elvassore, N., & Martello, G. (2019). Direct generation of human naive induced pluripotent stem cells from somatic cells in microfluidics. *Nature cell biology*, *21*(2), 275–286. https://doi.org/10.1038/s41556-018-0254-5

Haefeli, R. H., Erb, M., Gemperli, A. C., Robay, D., Courdier Fruh, I., Anklin, C., Dallmann, R., & Gueven, N. (2011). NQO1-dependent redox cycling of idebenone: effects on cellular redox potential and energy levels. *PloS one*, *6*(3), e17963. https://doi.org/10.1371/journal.pone.0017963

Hartig, F. & Lohse, L. (2020). DHARMa: Residual Diagnostics for Hierarchical (Multi-Level/Mixed) Regression Models. R package version 0.3.2.0. https://cran.r-project.org/web/packages/DHARMa/index.html

Heinrich, C., Blum, R., Gascón, S., Masserdotti, G., Tripathi, P., Sánchez, R., Tiedt, S., Schroeder, T., Götz, M., & Berninger, B. (2010). Directing astroglia from the cerebral cortex into subtype specific functional neurons. *PLoS biology*, *8*(5), e1000373. https://doi.org/10.1371/journal.pbio.1000373

Heinrich, C., Gascón, S., Masserdotti, G., Lepier, A., Sanchez, R., Simon-Ebert, T., Schroeder, T., Götz, M., & Berninger, B. (2011). Generation of subtype-specific neurons from postnatal astroglia of the mouse cerebral cortex. *Nature protocols*, *6*(2), 214–228. https://doi.org/10.1038/nprot.2010.188

Heinrich, C., Bergami, M., Gascón, S., Lepier, A., Viganò, F., Dimou, L., Sutor, B., Berninger, B., & Götz, M. (2014). Sox2-mediated conversion of NG2 glia into induced neurons in the injured adult cerebral cortex. *Stem cell reports*, *3*(6), 1000–1014. https://doi.org/10.1016/j.stemcr.2014.10.007

Heins, N., Malatesta, P., Cecconi, F., Nakafuku, M., Tucker, K. L., Hack, M. A., Chapouton, P., Barde, Y. A., & Götz, M. (2002). Glial cells generate neurons: the role of the transcription factor Pax6. *Nature neuroscience*, *5*(4), 308–315. https://doi.org/10.1038/nn828

Hetz C. (2012). The unfolded protein response: controlling cell fate decisions under ER stress and beyond. *Nature reviews. Molecular cell biology*, *13*(2), 89–102. https://doi.org/10.1038/nrm3270

Hetz, C., & Saxena, S. (2017). ER stress and the unfolded protein response in neurodegeneration. *Nature reviews. Neurology*, *13*(8), 477–491. https://doi.org/10.1038/nrneurol.2017.99

Hetz, C., Zhang, K., & Kaufman, R. J. (2020). Mechanisms, regulation and functions of the unfolded protein response. *Nature reviews. Molecular cell biology*, *21*(8), 421–438. https://doi.org/10.1038/s41580-020-0250-z

Hong, C. M., Na, J. H., Park, S., & Lee, Y. M. (2020). Clinical Characteristics of Early-Onset and Late-Onset Leigh Syndrome. *Frontiers in neurology*, *11*, 267. https://doi.org/10.3389/fneur.2020.00267

Iannetti, E. F., Smeitink, J., Willems, P., Beyrath, J., & Koopman, W. (2018). Rescue from galactose-induced death of Leigh Syndrome patient cells by pyruvate and NAD. *Cell death & disease*, *9*(11), 1135. https://doi.org/10.1038/s41419-018-1179-4

Inak, G., Rybak-Wolf, A., Lisowski, P., Pentimalli, T. M., Jüttner, R., Glažar, P., Uppal, K., Bottani, E., Brunetti, D., Secker, C., Zink, A., Meierhofer, D., Henke, M. T., Dey, M., Ciptasari, U., Mlody, B., Hahn, T., Berruezo-Llacuna, M., Karaiskos, N., Di Virgilio, M., … Prigione, A. (2021). Defective metabolic programming impairs early neuronal morphogenesis in neural cultures and an organoid model of Leigh syndrome. *Nature communications*, *12*(1), 1929. https://doi.org/10.1038/s41467-021-22117-z

Karamanlidis, G., Lee, C. F., Garcia-Menendez, L., Kolwicz, S. C., Jr, Suthammarak, W., Gong, G., Sedensky, M. M., Morgan, P. G., Wang, W., & Tian, R. (2013). Mitochondrial complex I deficiency increases protein acetylation and accelerates heart failure. *Cell metabolism*, *18*(2), 239–250. https://doi.org/10.1016/j.cmet.2013.07.002

Khan, N. A., Auranen, M., Paetau, I., Pirinen, E., Euro, L., Forsström, S., Pasila, L., Velagapudi, V., Carroll, C. J., Auwerx, J., & Suomalainen, A. (2014). Effective treatment of mitochondrial myopathy by nicotinamide riboside, a vitamin B3. *EMBO molecular medicine*, *6*(6), 721–731. https://doi.org/10.1002/emmm.201403943

Laguesse, S., Creppe, C., Nedialkova, D. D., Prévot, P. P., Borgs, L., Huysseune, S., Franco, B., Duysens, G., Krusy, N., Lee, G., Thelen, N., Thiry, M., Close, P., Chariot, A., Malgrange, B., Leidel, S. A., Godin, J. D., & Nguyen, L. (2015). A Dynamic Unfolded Protein Response Contributes to the Control of Cortical Neurogenesis. *Developmental cell*, *35*(5), 553–567. https://doi.org/10.1016/j.devcel.2015.11.005

Lee, C. F., Caudal, A., Abell, L., Nagana Gowda, G. A., & Tian, R. (2019). Targeting NAD^+ Metabolism as Interventions for Mitochondrial Disease. *Scientific reports*, *9*(1), 3073. https://doi.org/10.1038/s41598-019-39419-4

Li, A., Song, N. J., Riesenberg, B. P., & Li, Z. (2020). The Emerging Roles of Endoplasmic Reticulum Stress in Balancing Immunity and Tolerance in Health and Diseases: Mechanisms and Opportunities. *Frontiers in immunology*, *10*, 3154. https://doi.org/10.3389/fimmu.2019.03154

Liang, H., & Ward, W. F. (2006). PGC-1alpha: a key regulator of energy metabolism. *Advances in physiology education*, *30*(4), 145–151. https://doi.org/10.1152/advan.00052.2006

Liu, M. L., Zang, T., Zou, Y., Chang, J. C., Gibson, J. R., Huber, K. M., & Zhang, C. L. (2013). Small molecules enable neurogenin 2 to efficiently convert human fibroblasts into cholinergic neurons. *Nature communications*, *4*, 2183. https://doi.org/10.1038/ncomms3183

Lorenz, C., Lesimple, P., Bukowiecki, R., Zink, A., Inak, G., Mlody, B., Singh, M., Semtner, M., Mah, N., Auré, K., Leong, M., Zabiegalov, O., Lyras, E. M., Pfiffer, V., Fauler, B., Eichhorst, J., Wiesner, B., Huebner, N., Priller, J., Mielke, T., … Prigione, A. (2017). Human iPSC-Derived Neural Progenitors Are an Effective Drug Discovery Model for Neurological mtDNA Disorders. *Cell stem cell*, *20*(5), 659–674.e9. https://doi.org/10.1016/j.stem.2016.12.013

Love, M. I., Huber, W., & Anders, S. (2014). Moderated estimation of fold change and dispersion for RNA-seq data with DESeq2. *Genome biology*, *15*(12), 550. https://doi.org/10.1186/s13059-014-0550-8

Martucciello, S., Masullo, M., Cerulli, A., & Piacente, S. (2020). Natural Products Targeting ER Stress, and the Functional Link to Mitochondria. *International journal of molecular sciences*, *21*(6), 1905. https://doi.org/10.3390/ijms21061905

Masserdotti, G., Gillotin, S., Sutor, B., Drechsel, D., Irmler, M., Jørgensen, H. F., Sass, S., Theis, F. J., Beckers, J., Berninger, B., Guillemot, F., & Götz, M. (2015). Transcriptional Mechanisms of Proneural Factors and REST in Regulating Neuronal Reprogramming of Astrocytes. *Cell stem cell*, *17*(1), 74–88. https://doi.org/10.1016/j.stem.2015.05.014

Mattugini, N., Bocchi, R., Scheuss, V., Russo, G. L., Torper, O., Lao, C. L., & Götz, M. (2019). Inducing Different Neuronal Subtypes from Astrocytes in the Injured Mouse Cerebral Cortex. *Neuron*, *103*(6), 1086–1095.e5. https://doi.org/10.1016/j.neuron.2019.08.009

Mertens, J., Paquola, A., Ku, M., Hatch, E., Böhnke, L., Ladjevardi, S., McGrath, S., Campbell, B., Lee, H., Herdy, J. R., Gonçalves, J. T., Toda, T., Kim, Y., Winkler, J., Yao, J., Hetzer, M. W., & Gage, F. H. (2015). Directly Reprogrammed Human Neurons Retain Aging-Associated Transcriptomic Signatures and Reveal Age-Related Nucleocytoplasmic Defects. *Cell stem cell*, *17*(6), 705–718. https://doi.org/10.1016/j.stem.2015.09.001

Missiroli, S., Patergnani, S., Caroccia, N., Pedriali, G., Perrone, M., Previati, M., Wieckowski, M. R., & Giorgi, C. (2018). Mitochondria-associated membranes (MAMs) and inflammation. *Cell death & disease*, *9*(3), 329. https://doi.org/10.1038/s41419-017-0027-2

Moltedo, O., Remondelli, P., & Amodio, G. (2019). The Mitochondria-Endoplasmic Reticulum Contacts and Their Critical Role in Aging and Age-Associated Diseases. *Frontiers in cell and developmental biology*, *7*, 172. https://doi.org/10.3389/fcell.2019.00172

Nolbrant, S., Giacomoni, J., Hoban, D. B., Bruzelius, A., Birtele, M., Chandler-Militello, D., Pereira, M., Ottosson, D. R., Goldman, S. A., & Parmar, M. (2020). Direct Reprogramming of Human Fetal- and Stem Cell-Derived Glial Progenitor Cells into Midbrain Dopaminergic Neurons. *Stem cell reports*, *15*(4), 869–882. https://doi.org/10.1016/j.stemcr.2020.08.013

Pang, Z. P., Yang, N., Vierbuchen, T., Ostermeier, A., Fuentes, D. R., Yang, T. Q., Citri, A., Sebastiano, V., Marro, S., Südhof, T. C., & Wernig, M. (2011). Induction of human neuronal cells by defined transcription factors. *Nature*, *476*(7359), 220–223. https://doi.org/10.1038/nature10202

Parekh, S., Ziegenhain, C., Vieth, B., Enard, W., & Hellmann, I. (2018). zUMIs - A fast and flexible pipeline to process RNA sequencing data with UMIs. *GigaScience*, *7*(6), giy059. https://doi.org/10.1093/gigascience/giy059

Popp, B., Krumbiegel, M., Grosch, J., Sommer, A., Uebe, S., Kohl, Z., Plötz, S., Farrell, M., Trautmann, U., Kraus, C., Ekici, A. B., Asadollahi, R., Regensburger, M., Günther, K., Rauch, A., Edenhofer, F., Winkler, J., Winner, B., & Reis, A. (2018). Need for high-resolution Genetic Analysis in iPSC: Results and Lessons from the ForIPS Consortium. *Scientific reports*, *8*(1), 17201. https://doi.org/10.1038/s41598-018-35506-0

Rahman, S., Blok, R. B., Dahl, H. H., Danks, D. M., Kirby, D. M., Chow, C. W., Christodoulou, J., & Thorburn, D. R. (1996). Leigh syndrome: clinical features and biochemical and DNA abnormalities. *Annals of neurology*, *39*(3), 343–351. https://doi.org/10.1002/ana.410390311

Riedemann, T., Straub, T., & Sutor, B. (2018). Two types of somatostatin-expressing GABAergic interneurons in the superficial layers of the mouse cingulate cortex. *PloS one*, *13*(7), e0200567. https://doi.org/10.1371/journal.pone.0200567

Rossi, A., Pizzo, P., & Filadi, R. (2019). Calcium, mitochondria and cell metabolism: A functional triangle in bioenergetics. *Biochimica et biophysica acta. Molecular cell research*, *1866*(7), 1068–1078. https://doi.org/10.1016/j.bbamcr.2018.10.016

Rothman, J. S., & Silver, R. A. (2018). NeuroMatic: An Integrated Open-Source Software Toolkit for Acquisition, Analysis and Simulation of Electrophysiological Data. *Frontiers in neuroinformatics*, *12*, 14. https://doi.org/10.3389/fninf.2018.00014

Russell, O. M., Gorman, G. S., Lightowlers, R. N., & Turnbull, D. M. (2020). Mitochondrial Diseases: Hope for the Future. *Cell*, *181*(1), 168–188. https://doi.org/10.1016/j.cell.2020.02.051

Russo, G. L., Sonsalla, G., Natarajan, P., Breunig, C. T., Bulli, G., Merl-Pham, J., Schmitt, S., Giehrl-Schwab, J., Giesert, F., Jastroch, M., Zischka, H., Wurst, W., Stricker, S. H., Hauck, S. M., Masserdotti, G., & Götz, M. (2021). CRISPR-Mediated Induction of Neuron-Enriched Mitochondrial Proteins Boosts Direct Glia-to-Neuron Conversion. *Cell stem cell*, *28*(3), 524–534.e7. https://doi.org/10.1016/j.stem.2020.10.015

Rutkowski, D. T., Arnold, S. M., Miller, C. N., Wu, J., Li, J., Gunnison, K. M., Mori, K., Sadighi Akha, A. A., Raden, D., & Kaufman, R. J. (2006). Adaptation to ER stress is mediated by differential stabilities of pro-survival and pro-apoptotic mRNAs and proteins. *PLoS biology*, *4*(11), e374. https://doi.org/10.1371/journal.pbio.0040374

Ryu, D., Mouchiroud, L., Andreux, P. A., Katsyuba, E., Moullan, N., Nicolet-Dit-Félix, A. A., Williams, E. G., Jha, P., Lo Sasso, G., Huzard, D., Aebischer, P., Sandi, C., Rinsch, C., & Auwerx, J. (2016). Urolithin A induces mitophagy and prolongs lifespan in C. elegans and increases muscle function in rodents. *Nature medicine*, *22*(8), 879–888. https://doi.org/10.1038/nm.4132

Santos, R., Vadodaria, K. C., Jaeger, B. N., Mei, A., Lefcochilos-Fogelquist, S., Mendes, A., Erikson, G., Shokhirev, M., Randolph-Moore, L., Fredlender, C., Dave, S., Oefner, R., Fitzpatrick, C., Pena, M., Barron, J. J., Ku, M., Denli, A. M., Kerman, B. E., Charnay, P., Kelsoe, J. R., … Gage, F. H. (2017). Differentiation of Inflammation-Responsive Astrocytes from Glial Progenitors Generated from Human Induced Pluripotent Stem Cells. *Stem cell reports*, *8*(6), 1757–1769. https://doi.org/10.1016/j.stemcr.2017.05.011

Smith, D. K., Yang, J., Liu, M. L., & Zhang, C. L. (2016). Small Molecules Modulate Chromatin Accessibility to Promote NEUROG2-Mediated Fibroblast-to-Neuron Reprogramming. *Stem cell reports*, *7*(5), 955–969. https://doi.org/10.1016/j.stemcr.2016.09.013

Stanga, S., Caretto, A., Boido, M., & Vercelli, A. (2020). Mitochondrial Dysfunctions: A Red Thread across Neurodegenerative Diseases. *International journal of molecular sciences*, *21*(10), 3719. https://doi.org/10.3390/ijms21103719

Sergushichev A (2016). "An algorithm for fast preranked gene set enrichment analysis using cumulative statistic calculation." *bioRxiv*. doi: 10.1101/060012, http://biorxiv.org/content/early/2016/06/20/060012.

Subramanian, A., Tamayo, P., Mootha, V. K., Mukherjee, S., Ebert, B. L., Gillette, M. A., Paulovich, A., Pomeroy, S. L., Golub, T. R., Lander, E. S., & Mesirov, J. P. (2005). Gene set enrichment analysis: a knowledge-based approach for interpreting genome-wide expression profiles. *Proceedings of the National Academy of Sciences of the United States of America*, *102*(43), 15545–15550. https://doi.org/10.1073/pnas.0506580102

Tabas, I., & Ron, D. (2011). Integrating the mechanisms of apoptosis induced by endoplasmic reticulum stress. *Nature cell biology*, *13*(3), 184–190. https://doi.org/10.1038/ncb0311-184

Thompson Legault, J., Strittmatter, L., Tardif, J., Sharma, R., Tremblay-Vaillancourt, V., Aubut, C., Boucher, G., Clish, C. B., Cyr, D., Daneault, C., Waters, P. J., LSFC Consortium, Vachon, L., Morin, C., Laprise, C., Rioux, J. D., Mootha, V. K., & Des Rosiers, C. (2015). A Metabolic Signature of Mitochondrial Dysfunction Revealed through a Monogenic Form of Leigh Syndrome. *Cell reports*, *13*(5), 981–989. https://doi.org/10.1016/j.celrep.2015.09.054

Tirosh, I., Izar, B., Prakadan, S. M., Wadsworth, M. H., 2nd, Treacy, D., Trombetta, J. J., Rotem, A., Rodman, C., Lian, C., Murphy, G., Fallahi-Sichani, M., Dutton-Regester, K., Lin, J. R., Cohen, O., Shah, P., Lu, D., Genshaft, A. S., Hughes, T. K., Ziegler, C. G., Kazer, S. W., … Garraway, L. A. (2016). Dissecting the multicellular ecosystem of metastatic melanoma by single-cell RNA-seq. *Science (New York, N.Y.)*, *352*(6282), 189–196. https://doi.org/10.1126/science.aad0501

Torper, O., Ottosson, D. R., Pereira, M., Lau, S., Cardoso, T., Grealish, S., & Parmar, M. (2015). In Vivo Reprogramming of Striatal NG2 Glia into Functional Neurons that Integrate into Local Host Circuitry. *Cell reports*, *12*(3), 474–481. https://doi.org/10.1016/j.celrep.2015.06.040

Valsecchi, F., Grefte, S., Roestenberg, P., Joosten-Wagenaars, J., Smeitink, J. A., Willems, P. H., & Koopman, W. J. (2013). Primary fibroblasts of NDUFS4(-/-) mice display increased ROS levels and aberrant mitochondrial morphology. *Mitochondrion*, *13*(5), 436–443. https://doi.org/10.1016/j.mito.2012.12.001

Verkaart, S., Koopman, W. J., van Emst-de Vries, S. E., Nijtmans, L. G., van den Heuvel, L. W., Smeitink, J. A., & Willems, P. H. (2007). Superoxide production is inversely related to complex I activity in inherited complex I deficiency. *Biochimica et biophysica acta*, *1772*(3), 373–381. https://doi.org/10.1016/j.bbadis.2006.12.009

Vignoles, R., Lentini, C., d'Orange, M., & Heinrich, C. (2019). Direct Lineage Reprogramming for Brain Repair: Breakthroughs and Challenges. *Trends in molecular medicine*, *25*(10), 897–914. https://doi.org/10.1016/j.molmed.2019.06.006

Wang, M., & Kaufman, R. J. (2016). Protein misfolding in the endoplasmic reticulum as a conduit to human disease. *Nature*, *529*(7586), 326–335. https://doi.org/10.1038/nature17041

Wapinski, O. L., Vierbuchen, T., Qu, K., Lee, Q. Y., Chanda, S., Fuentes, D. R., Giresi, P. G., Ng, Y. H., Marro, S., Neff, N. F., Drechsel, D., Martynoga, B., Castro, D. S., Webb, A. E., Südhof, T. C., Brunet, A., Guillemot, F., Chang, H. Y., & Wernig, M. (2013). Hierarchical mechanisms for direct reprogramming of fibroblasts to neurons. *Cell*, *155*(3), 621–635. https://doi.org/10.1016/j.cell.2013.09.028

Watts, M. E., Pocock, R., & Claudianos, C. (2018). Brain Energy and Oxygen Metabolism: Emerging Role in Normal Function and Disease. *Frontiers in molecular neuroscience*, *11*, 216. https://doi.org/10.3389/fnmol.2018.00216

Zhang, L., Yin, J. C., Yeh, H., Ma, N. X., Lee, G., Chen, X. A., Wang, Y., Lin, L., Chen, L., Jin, P., Wu, G. Y., & Chen, G. (2015). Small Molecules Efficiently Reprogram Human Astroglial Cells into Functional Neurons. *Cell stem cell*, *17*(6), 735–747. https://doi.org/10.1016/j.stem.2015.09.012

Figure Legends

Figure 1: NDUFS4-mutant glial cells exhibit impaired neuronal reprogramming.

(**A**) Schematic of the experimental protocol used for direct neuronal reprogramming.

(**B**) Micrographs showing immunostaining of control and patient GPCs transduced with one transcription factor at day 20 of neuronal reprogramming. Scale bars, 50μm.

(**C**) Boxplot of reprogramming efficiency of control and patient GPCs across the single transcription factor conditions. Efficiency is defined as the ratio of βIII-tubulin$^+$/DsRed$^+$ to DsRed$^+$ cells. Data are shown as median ± IQR. $^*p \leq 0.05$, $^{**}p \leq 0.01$. n = 5 per experimental condition.

(**D**) Micrographs of control and patient GPCs transduced with two transcription factors at day 20 of neuronal reprogramming. Scale bars, 50μm.

(**E**) Boxplot of reprogramming efficiency of control and patient GPCs across double transduction conditions. Data are shown as median ± IQR. $^{***}p \leq 0.001$. n = 5 per experimental condition.

Figure 2: Neuronal reprogramming deficit of patient GPCs can be rescued and control GPCs reprogramming further improved with pharmacological treatments

(**A**) Micrographs of control and patient GPCs transduced with Neurog2 alone or in combination with OligoA and α-tocopherol treatment. Scale bars, 50 μm.

(**B**) Boxplot of reprogramming efficiency of control and patient GPCs across the different treatment conditions. Data are shown as median ± IQR. $^{**}p \leq 0.01$. n = 3 per experimental condition.

(**C**) Micrographs of control and patient GPCs transduced with Neurog2 alone or in combination with Nicotinamide Riboside (NR), Urolithin A (UA), Idebenone, STF-083010 (STF) or AMG-PERK 44 (AMG) treatment. Scale bars, 50 μm.

(**D**) Boxplot of reprogramming efficiency of control and patient GPCs treated with AMG, STF or untreated. Significant differences between control and patient GPC reprogramming are indicated, as well as the significance of treated control and patient conditions relative to their respective untreated condition. Data are shown as median ± IQR. $^*p \leq 0.05$, $^{***}p \leq 0.001$. n = 3 per experimental condition (HMGU12, #79787, #114107), n = 2 per experimental condition (#1, #87971).

(**E**) Boxplot of reprogramming efficiency of control and patient GPCs treated with Idebenone, NR, Urolithin A, or untreated. Significant differences between control and patient GPC reprogramming are indicated, as well as the significance of treated control and patient conditions relative to their respective untreated condition. Data are shown as median ± IQR. $^*p \leq 0.05$, $^{**}p \leq 0.01$, $^{***}p \leq 0.001$. n = 3 per experimental condition (HMGU12, #79787, #114107), n = 2 per experimental condition (#1, #87971).

Figure 3: Patient reprogrammed neurons display impaired functionality that can be rescued upon UPR inhibitor treatment.

(**A**) Schematic of the mouse astrocyte co-culture paradigm used to obtain recordings from reprogrammed neurons.

(**B**) Representative traces of recordings from the three conditions.

(**C**) Histogram showing the percentage of recorded reprogrammed neurons across different conditions that fired or did not fire an action potential. Control (n = 17, 65% AP, 34% no AP), Patient (n = 11, 45% AP, 55% no AP), Patient plus AMG (n = 8, 88% AP, 12% no AP).

(**D**) Boxplot of action potential amplitude recorded from the three conditions. Data are shown as median ± IQR.

(**E**) Boxplot of action potential duration recorded from the three conditions. Data are shown as median ± IQR.

Figure 4: Reprogramming deficiency verified with NDUFS4-mutant fibroblasts

(**A**) Micrographs of control and patient fibroblasts transduced with one transcription factor at day 20 of neuronal reprogramming. Scale bars, 50 μm.

(**B**) Boxplot of reprogramming efficiency of control and patient fibroblasts across the different transcription factor conditions. Data are shown as median ± IQR. $^{**}p \leq 0.01$. n = 3 per experimental condition.

(**C**) Micrographs of control and patient fibroblasts transduced with two transcription factors at day 20 of neuronal reprogramming. Scale bars, 50 μm.

(**D**) Boxplot of reprogramming efficiency of control and patient fibroblasts across double transduction conditions. Data are shown as median ± IQR. $^{***}p \leq 0.001$. n = 3 per experimental condition.

Supplementary Figure 1: NDUFS4-mutant iPSCs can be differentiated into glial cells comparable to control donor iPSCs.

(**A**) Schematic of the differentiation protocol used to obtain iPSC-derived glial cells.

(**B**) Micrographs of control and patient cells at two different stages of glial differentiation. Scale bars, 50 μm.

(**C**) Schematic of the NDUFS4 gene demonstrating the location of each mutation for the respective patient cell lines. (iPSCs: #114107, #87971, #79787). (Fibroblasts: #114107, #114106, #79787).

(**D**) Heatmap analysis of different pluripotent and astrocyte markers across control and patient cells at three different stages of differentiation (iPSC, GPC and Astrocyte). The color scale indicates Z score.

(**E**) Barplot showing the log2(fold change) of genes involved in the chemokine mediated signaling pathway, identified by gene set enrichment analysis (GSEA) analysis

(**F**) Barplot showing the log2(fold change) of the main genes involved in fatty acid metabolic process, identified by GSEA analysis.

(**G**) Histogram of the glutamate concentration present in the media after glutamate treatment, used as an indicator of residual glutamate that was not taken up by the cells. Data are shown as mean from 3 technical replicates. n = 1 per experimental condition.

(**H**) Histogram of four different parameters obtained from measurement by the Seahorse XF analyzer, comparing between control and patient cells at the GPC stage. Data are shown as mean ± SEM. $^{*}p \leq 0.05$, n = 3 per experimental condition.

(**I**) Histogram of four different parameters obtained from measurement by the Seahorse XF analyzer, comparing between control and patient cells at the astrocyte stage. Data are shown as mean ± SEM. n = 3 per experimental condition.

Supplementary Figure 2: Time course analysis of reprogramming reveals different patterns of cell death in control and patient GPCs

(**A**) Schematic of the neuronal reprogramming paradigm, with three different time blocks indicated for the time course analysis.

(**B**) Time course analysis of the percentage of transduced cells at the indicated time points (Days 4-8). Results normalized to the DsRed condition. Data are shown as mean ± SEM, n =2.

(**C**) Time course analysis of the percentage of transduced cells at the indicated time points (Days 8-12). Results normalized to the DsRed condition. Data are shown as mean ± SEM, n = 2.

(**D**) Time course analysis of the percentage of transduced cells at the indicated time points (Days 13-17). Results normalized to the DsRed condition. Data are shown as mean, n = 1.

(**E**) Time course analysis of the percentage of cells acquiring neuronal morphology over transduced cells at the indicated time points (Days 13-17). Data are shown as mean, n = 1.

Supplementary Figure 3: Patient fibroblasts reprogramming efficiency can also be partially rescued by blocking the UPR pathway.

(**A**) Micrographs of control and patient fibroblasts transduced with Neurog2 alone or in combination with Nicotinamide Riboside (NR), Urolithin A (UA), Idebenone, STF-083010 (STF) or AMG-PERK 44 (AMG) treatment. Scale bars, 50 μm.

(**B**) Boxplot of reprogramming efficiency of control and patient fibroblasts across the different treatment conditions. Significant differences between control and patient fibroblast reprogramming are indicated, as well as the significance of treated control and patient conditions relative to their

respective untreated condition. Data are shown as median ± IQR. $^{*}p \leq 0.05$, $^{***}p \leq 0.001$. n = 3 per experimental condition.

FIGURE 1

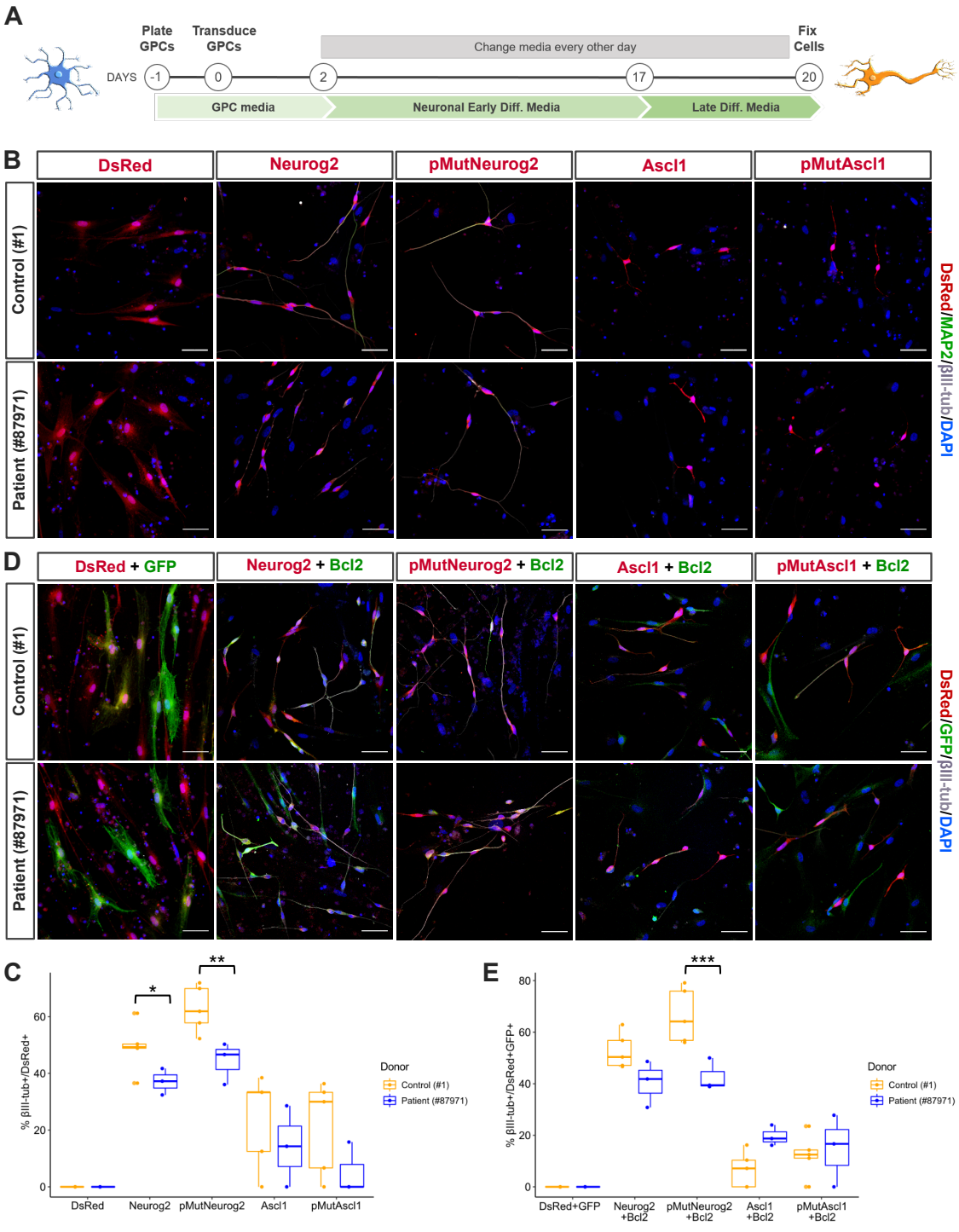
A
Plate GPCs
Transduce GPCs
Change media every other day
Fix Cells
DAYS
-1
0
2
17
20
GPC media
Neuronal Early Diff. Media
Late Diff. Media
B
DsRed
Neurog2
pMutNeurog2
Ascl1
pMutAscl1
Control (#1)
Patient (#87971)
DsRed/MAP2/βIII-tub/DAPI
D
DsRed + GFP
Neurog2 + Bcl2
pMutNeurog2 + Bcl2
Ascl1 + Bcl2
pMutAscl1 + Bcl2
Control (#1)
Patient (#87971)
DsRed/GFP/βIII-tub/DAPI
C
% βIII-tub+/DsRed+
DsRed
Neurog2
pMutNeurog2
Ascl1
pMutAscl1
Donor
Control (#1)
Patient (#87971)
E
% βIII-tub+/DsRed+GFP+
DsRed+GFP
Neurog2 +Bcl2
pMutNeurog2 +Bcl2
Ascl1 +Bcl2
pMutAscl1 +Bcl2
Donor
Control (#1)
Patient (#87971)

FIGURE 2

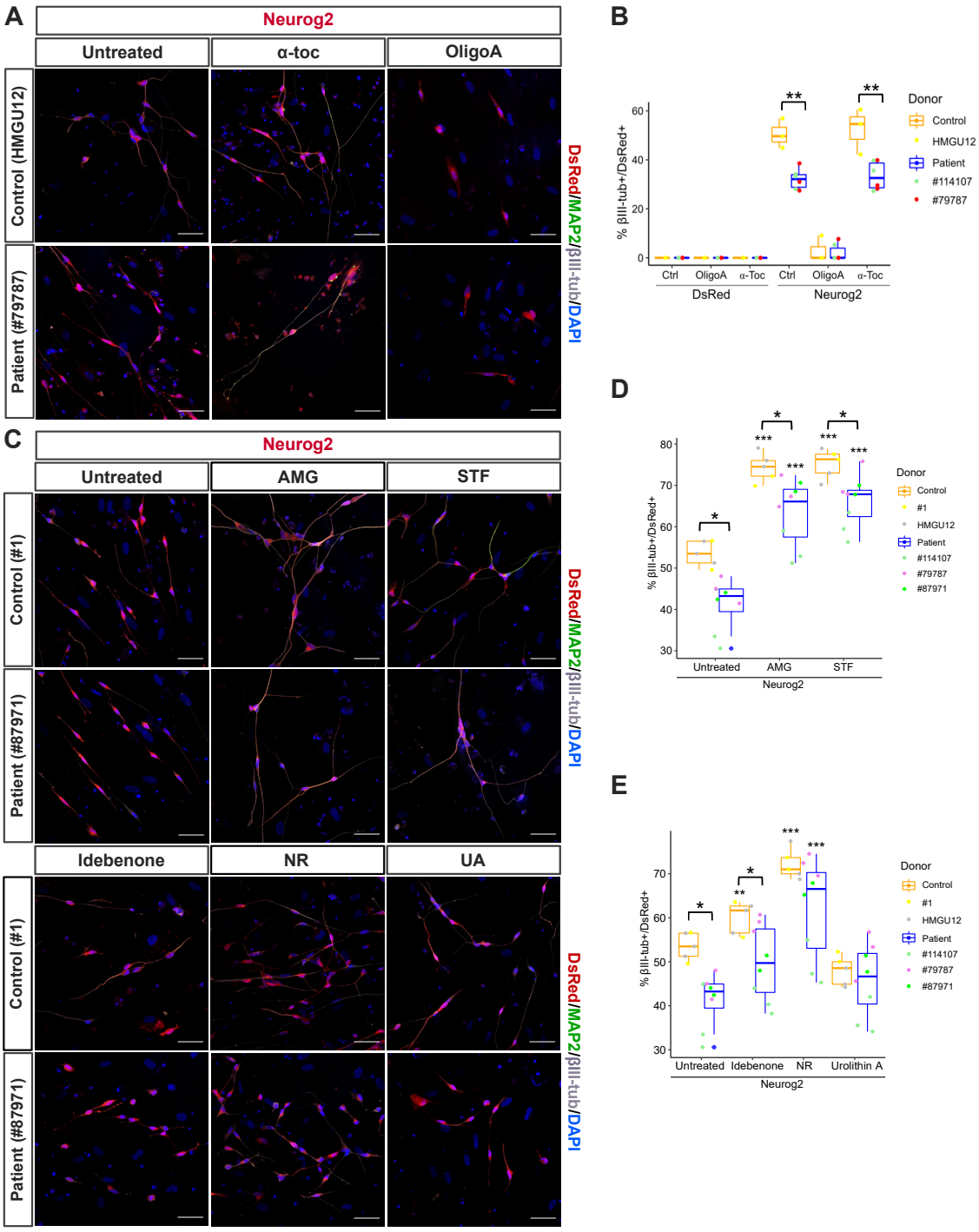
A
Neurog2
Untreated
α-toc
OligoA
Control (HMGU12)
Patient (#79787)
DsRed/MAP2/βIII-tub/DAPI
B
% βIII-tub+/DsRed+
Donor
Control
HMGU12
Patient
#114107
#79787
Ctrl
OligoA
α-Toc
DsRed
Neurog2
C
Neurog2
Untreated
AMG
STF
Control (#1)
Patient (#87971)
DsRed/MAP2/βIII-tub/DAPI
D
% βIII-tub+/DsRed+
Donor
Control
#1
HMGU12
Patient
#114107
#79787
#87971
Untreated
AMG
STF
Neurog2
Idebenone
NR
UA
E
% βIII-tub+/DsRed+
Donor
Control
#1
HMGU12
Patient
#114107
#79787
#87971
Untreated
Idebenone
NR
Urolithin A
Neurog2

FIGURE 3

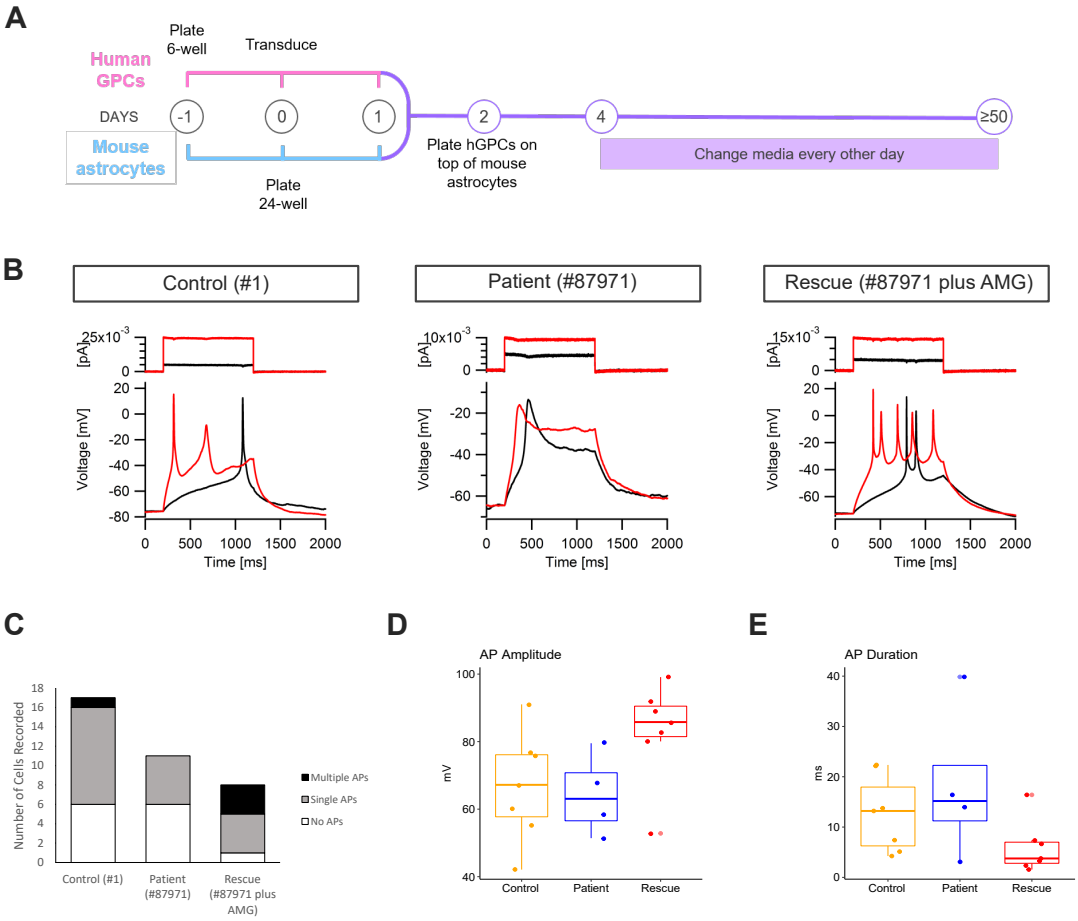
A
Plate
6-well
Transduce
Human
GPCs
DAYS
-1
0
1
2
4
≥50
Mouse
astrocytes
Plate
24-well
Plate hGPCs on
top of mouse
astrocytes
Change media every other day
B
Control (#1)
Patient (#87971)
Rescue (#87971 plus AMG)
[pA]
Voltage [mV]
Time [ms]
C
Number of Cells Recorded
Multiple APs
Single APs
No APs
Control (#1)
Patient
(#87971)
Rescue
(#87971 plus
AMG)
D
AP Amplitude
mV
Control
Patient
Rescue
E
AP Duration
ms
Control
Patient
Rescue

FIGURE 4

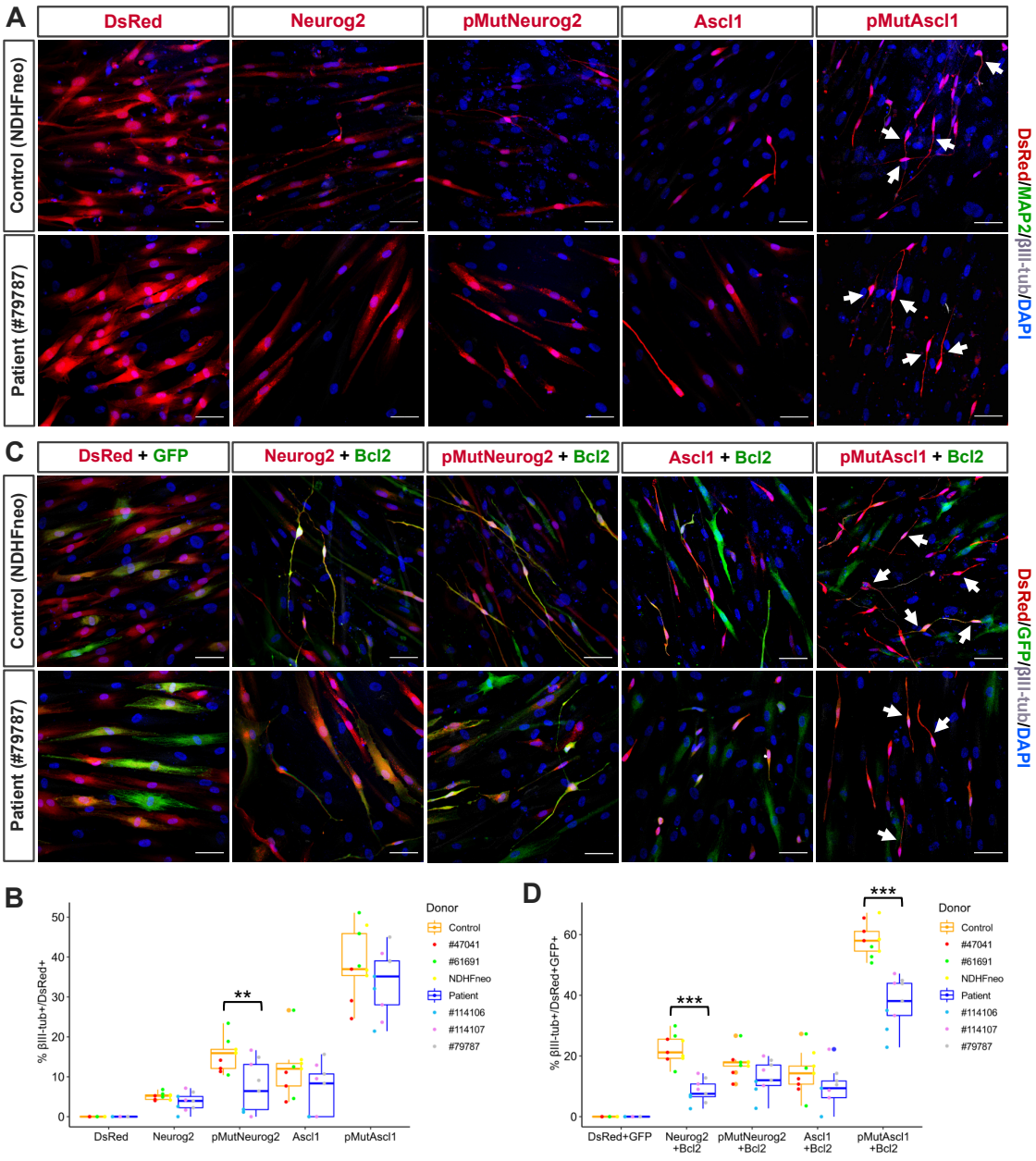
A
DsRed
Neurog2
pMutNeurog2
Ascl1
pMutAscl1
Control (NDHFneo)
Patient (#79787)
DsRed/MAP2/βIII-tub/DAPI
C
DsRed + GFP
Neurog2 + Bcl2
pMutNeurog2 + Bcl2
Ascl1 + Bcl2
pMutAscl1 + Bcl2
Control (NDHFneo)
Patient (#79787)
DsRed/GFP/βIII-tub/DAPI
B
% βIII-tub+/DsRed+
**
DsRed
Neurog2
pMutNeurog2
Ascl1
pMutAscl1
Donor
Control
#47041
#61691
NDHFneo
Patient
#114106
#114107
#79787
D
% βIII-tub+/DsRed+GFP+
***
***
DsRed+GFP
Neurog2 +Bcl2
pMutNeurog2 +Bcl2
Ascl1 +Bcl2
pMutAscl1 +Bcl2
Donor
Control
#47041
#61691
NDHFneo
Patient
#114106
#114107
#79787

SUPPLEMENTARY FIGURE 1

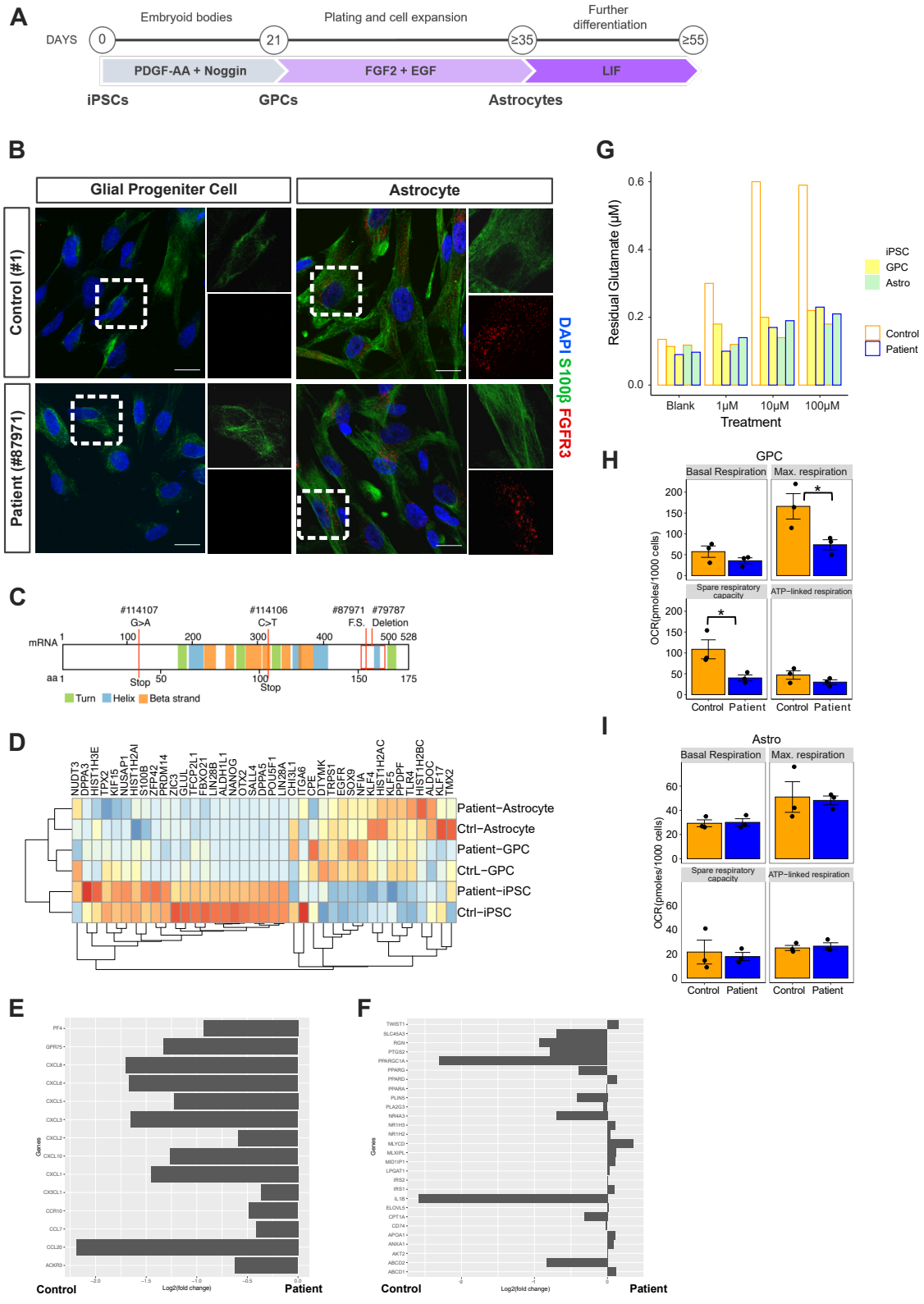

SUPPLEMENTARY FIGURE 2

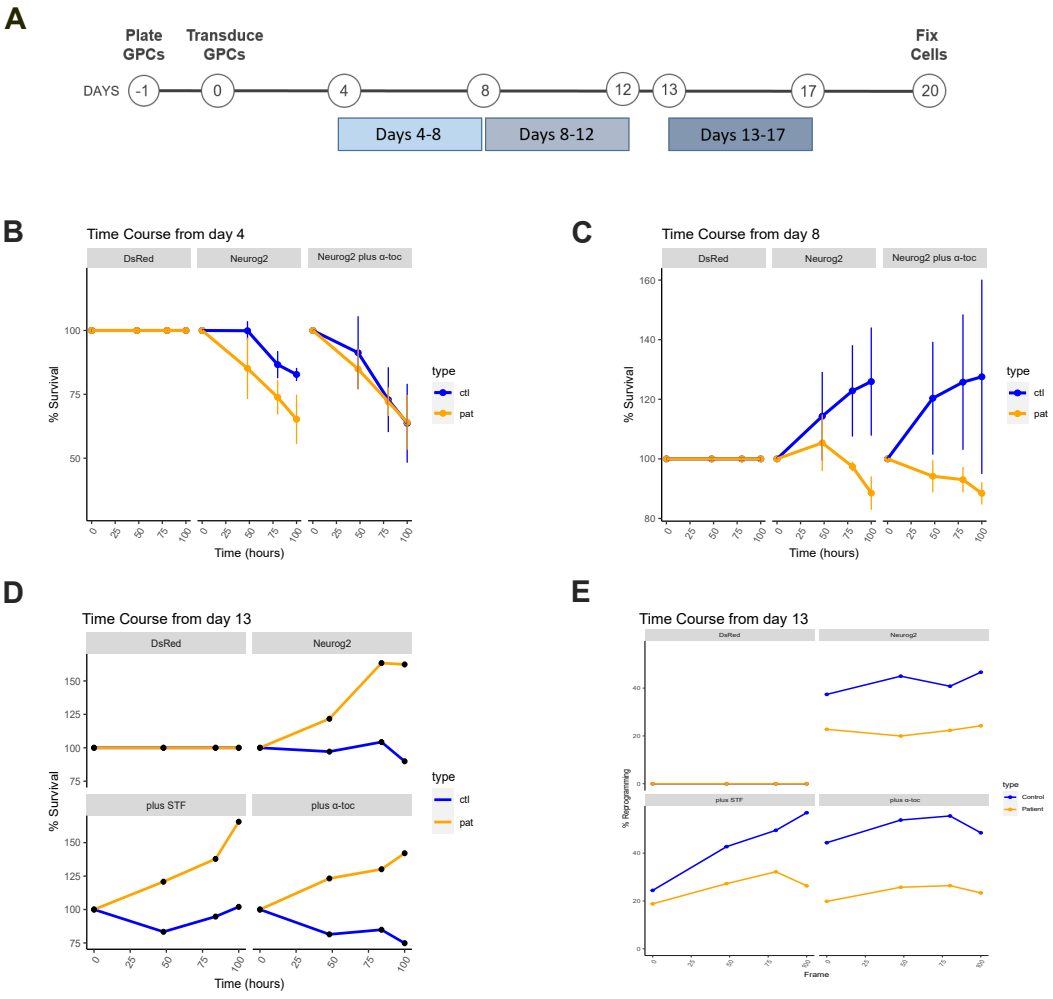

SUPPLEMENTARY FIGURE 3

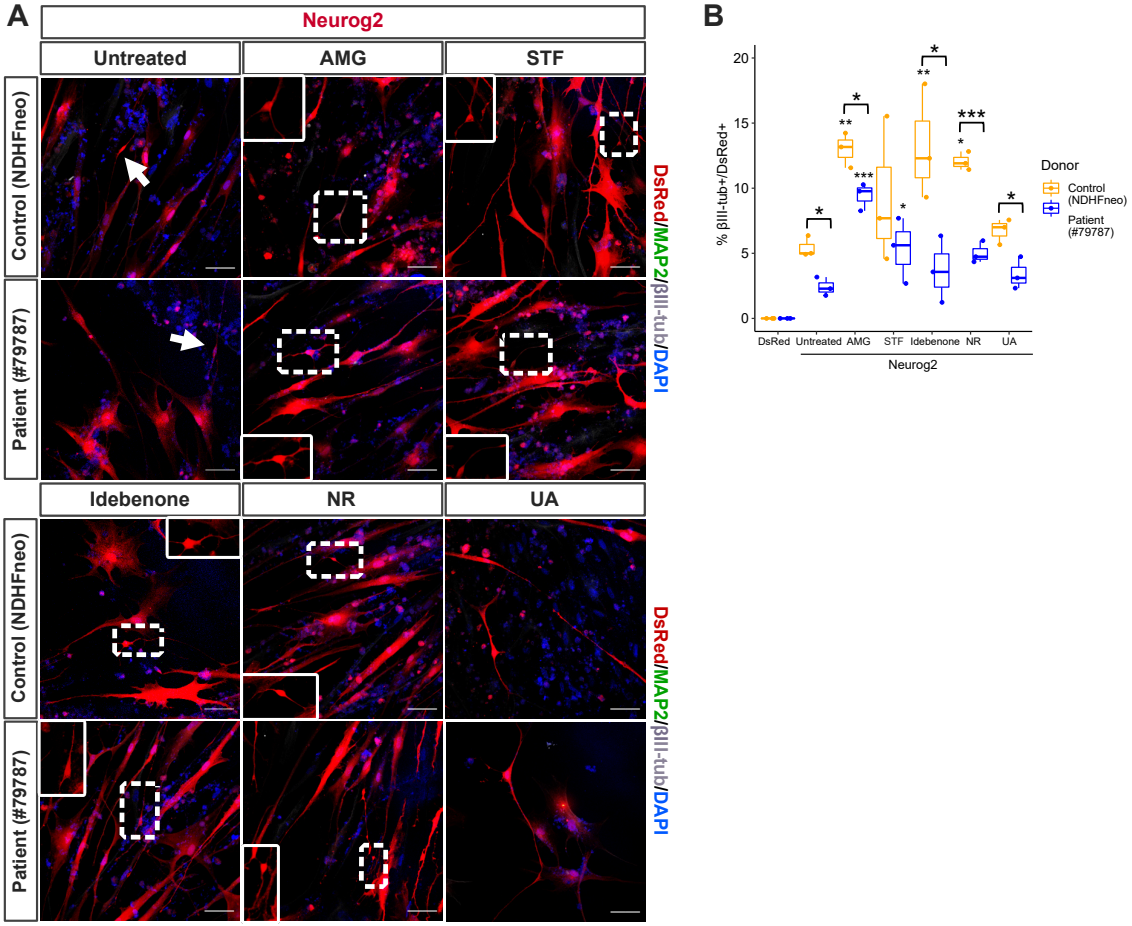

Discussion

3. Discussion

My PhD projects focused on the role of metabolism in direct neuronal reprogramming. In Russo et al. (2021) the mitochondrial proteomes of murine astrocytes and neurons were investigated, further revealing the metabolic differences between the cell types. This information was utilized to express neuron-enriched mitochondrial proteins during the process of neuronal reprogramming. Intriguingly, priming the astrocyte mitochondria for their neuronal fate led to a significant increase in reprogramming efficiency. Therefore, the role of the mitochondria as an essential driver during murine cell reprogramming was established. However, the role of mitochondria in human cell reprogramming is much less well understood. As such, in Sonsalla et al. human cells were obtained from control donors and patients with a mitochondrial deficiency. The cells were differentiated into astrocytes and then their neuronal reprogramming ability was investigated. Clear differences were observed in the reprogramming of control versus patient cells, thus highlighting the importance of functioning oxphos metabolism for neuronal conversion. The UPR pathway was identified as a novel player in the reprogramming process, as its inhibition led to improvements in both the patient and control cells. Different aspects of mitochondrial function in reprogramming were therefore revealed in my PhD studies, with implications for therapeutic applications.

3.1 Project 1: Murine astrocyte direct neuronal reprogramming is enhanced by the manipulation of mitochondrial proteins

The role of mitochondria in reprogramming is important to understand, as mitochondria are not only involved in the regulation of metabolic pathways, but they also play a prominent role in regulating transcription and the synthesis of macromolecules. During endogenous cell fate conversion, it is known that mitochondria change to match the requirements of the new cell identity. For example, transcriptional studies have shown a downregulation of genes related to aerobic glycolysis and upregulation of genes related to oxphos in neural progenitor cells during neuronal differentiation (Agostini et al., 2016; Zheng et al., 2016). Furthermore, a mitochondrial protein knockout inhibiting the use of oxphos by neural stem cells *in vivo* resulted in reduced neurogenesis and defects in cortical development (Khacho et al., 2017). We wanted to investigate if the metabolic plasticity of mitochondria in reprogramming is consistent with their role in endogenous cellular differentiation.

In Russo et al. (2021), the mitochondrial differences between astrocytes and neurons were investigated and established. Murine cortical astrocytes and E14-derived cortical neurons were used as *in vitro* models. Seahorse analysis demonstrated functional metabolic differences, such as the ability of astrocytes to utilize both oxphos and glycolysis for energy generation, whereas neurons rely more on oxphos. During neuronal reprogramming, a switch in mitochondrial metabolism was detected through morphological analysis, as murine astrocytes had elongated mitochondria, while smaller mitochondria were present in Ascl1-induced neurons; consistent with previous reports of neurons (Misgeld & Schwarz, 2017) and astrocytes (Motori et al., 2013). We then investigated the metabolic profile of astrocytes and neurons at the molecular level by conducting proteomic analysis on isolated mitochondria from the two cell types. The higher metabolic plasticity of astrocytes was reflected by their gene ontology (GO) terms, as well as by their enrichment of the fatty acid oxidation pathway. In contrast, mitochondria from neurons had enrichment for RNA metabolism. Considering that mitochondrial morphology was shown to change over the course of reprogramming, we also wanted to examine how cell-specific mitochondrial protein expression was altered during forced cell fate change. Interestingly, the astrocyte-enriched proteins Sfxn5 and Cpox were downregulated in cells that successfully reprogrammed into induced neurons, whereas transduced cells that remained astrocytic retained a higher expression of these proteins. The shift in protein expression occurred late in the conversion process, and this was also reflected in the delayed acquisition of the neuron-enriched mitochondrial proteins Prdx2 and Gls. Since the change in mitochondrial proteins was only detected in induced neurons, we wanted to explore if we could enhance neuronal reprogramming by harnessing the expression of proteins related to neuronal metabolism. To this end, we crossed the astrocyte-specific ALDH1L1:Cre mouse line with a transgenic mouse line where transcriptional activators were fused to catalytically inactive Cas9 (dCas9). The resulting primary mouse astrocyte cultures were then transfected with the neurogenic factor Ascl1, as well as guide RNAs (gRNA) that targeted specific neuron-enriched proteins. Notably, the initiation of neuron mitochondrial gene expression during neuronal reprogramming did indeed increase the reprogramming efficiency. In particular, the gene *Sod1* alone or in combination with *Prdx2* led to a strong increase in efficiency, possibly due to their antioxidant activity. Interestingly, genes with antioxidant function but enriched in astrocytes did not have the same effect on reprogramming. The induction of Sod1 and Prdx2 also led to an improvement in the morphology of the reprogrammed neurons and was found to speed up

the conversion process and reduce cell death. Therefore, we clearly illustrated the functional relevance of the shift in mitochondrial proteins during forced cell fate conversion.

The specialization of the mitochondria across different cell types is important to understand not only in regard to its role in cellular bioenergetics, but also due to its involvement in signaling events, generation of metabolic precursors, and epigenetic modifications (Matilainen et al., 2017; Spinelli & Haigis, 2018). Indeed, disease pathologies influencing the mitochondria of specific cell types further support the need for greater understanding in this field (Suomalainen & Battersby, 2018). Although it can be useful to compare mitochondria in pathological/treated and healthy conditions at the whole tissue level (Chou et al., 2011; Nilsen et al., 2007), the impact of individual cell types on the respective conditions is lost. The mitochondrial proteome across organs has been investigated (Mootha et al., 2003; Pagliarini et al., 2008), as has the molecular diversity of mitochondria in brain cells (Fecher et al., 2019; Graham et al., 2017; Völgyi et al., 2015), however, the relevance of these findings for forced neuronal cell fate conversion has not previously been established.

Metabolic plasticity in neuronal reprogramming

In our study, we further elucidated the metabolic differences underlying astrocytes and neurons and applied our findings to neuronal reprogramming. The GO term analysis of mitochondrial astrocytes showed enrichment for fatty acid β-oxidation and lipid metabolism, which is supported at the transcriptional level by previous results in murine astrocytes (van Deijk et al., 2017) and through *in situ* lipid tracing (Hofmann et al., 2017). Interestingly, lipid metabolism also regulates the activity of neural stem cells (NSCs) (Knobloch et al., 2017) and is involved in hematopoietic stem cell maintenance (Ito et al., 2012). There is a reduced reliance on lipid metabolism for energy generation as NSCs differentiate into neurons during endogenous neurogenesis (Llorens-Bobadilla et al., 2015), and we show that these results are mirrored during the direct reprogramming of astrocytes into induced neurons. For example, when fatty acid β-oxidation was blocked in murine astrocytes during neuronal reprogramming using etomoxir, there was an increase in the reprogramming efficiency (Russo et al., 2021).

The benefit of harnessing cellular metabolism during reprogramming has previously been established not in the neuronal context, but for the generation of pluripotent stem cells (Wu et al., 2016). When somatic cells undergo forced cell fate conversion into a pluripotent fate, they

switch to favoring glycolysis for energy generation as shown by upregulation of glycolytic genes and concomitant downregulation of genes related to the ETC (Folmes et al., 2011). Indeed, assisting the metabolic switch by blocking oxphos with ETC inhibitor treatment (Son et al., 2013) or stimulating glycolysis through PS48 treatment (Zhu et al., 2010) increased the pluripotent reprogramming efficiency. Thus, understanding the role of metabolism in cell fate transition is not only beneficial for directly replacing neuronal loss upon injury or disease, but also for tissue repair by inducing differentiated cells back into a pluripotent state.

Morphological changes occur in parallel to mitochondrial metabolism alterations

The metabolic transition during cell fate change does not only occur at the functional level but is also reflected in mitochondrial structural changes. The reduction of proteins implicated in mitochondrial fusion dynamics (mitofusin 1 and 2) led to the more fragmented mitochondria favored by stem cells and thus increased pluripotent reprogramming efficiency (Son et al., 2015). Stem cells have smaller and rounder mitochondria with poorly developed cristae (Prigione et al., 2010), and upon pluripotent reprogramming fibroblasts have been shown to lose their mature mitochondrial morphology and adopt that reminiscent of stem cells (Prigione et al., 2011).

We used electron microscopy to examine the isolated mitochondria from astrocytes and neurons. Our results are consistent with previous reports of neuronal mitochondria having smaller and less branched morphology in order to provide energy to the axons (Misgeld & Schwarz, 2017). The extended network of mitochondria in astrocytes was further confirmed *in vivo* (Motori et al., 2013). The importance of cell-type-specific mitochondrial morphology has also been established *in vivo* in relation to endogenous neurogenesis, as inhibition of the fission factor Drp1 caused developmental abnormalities and death (Ishihara et al., 2009), and also impeded adult neurogenesis (Steib et al., 2014). Indeed, the structural changes accompanying the bioenergetic transition are not limited to morphology adjustments, but can also require mitochondrial turnover such as mitophagy, a specific form of autophagy. Sequestosome 1 (SQSTM1/p62), which is linked to mitophagy (Park et al., 2014), is required for successful neuronal differentiation (Calvo-Garrido et al., 2019). Specifically, the metabolic shift from glycolysis to oxphos was blocked upon p62 KO in neuroepithelial stem cells through, among other things, upregulation of the glycolytic gene lactate dehydrogenase A (LDHA) (Calvo-Garrido et al., 2019). Interestingly, in Sonsalla et al., the neuronal reprogramming efficiency

of human cells was not improved when they were treated with the mitophagy activator Urolithin A. Therefore, although mitophagy can assist the shift of metabolic machinery, enhanced activation is not necessarily beneficial for neuronal fate acquisition.

Expression of neuron-enriched proteins significantly improves neuronal reprogramming efficiency

We found that the unique metabolic program of astrocytes and neurons is further defined by their mitochondrial proteome, with one-fifth of proteins found to be significantly different between the two cell types. Intriguingly, the failure of a cell to both downregulate astrocyte-enriched and acquire neuron-enriched mitochondrial proteins was mirrored by its unsuccessful reprogramming. Therefore, we influenced this metabolic conversion and see if there was a concomitant increase in reprogramming efficiency. To this end, 8 neuron-enriched mitochondrial proteins were chosen to have their expression induced through the use of gene-specific gRNAs. In order to test the collaborative effects of inducing multiple enriched genes at once, we used the multiplexed CRISPR technique known as string assembly gRNA cloning (STAgR) (Breunig et al., 2018). As was previously mentioned, the genes *Sod1* and *Prdx2,* which protect against oxidative stress, were included. Interestingly, Prdx2 alone did not have a beneficial effect on the cellular conversion, in contrast to Sod1, indicating that regardless of their functional relevance, not all enriched proteins are sufficient by themselves to enhance the reprogramming process. Sod1 has been shown to protect cells against superoxide radical damage and has been implicated in neurodegenerative disease (Brasil et al., 2019; Gill et al., 2019; Pharaoh et al., 2019). A synergistic effect was demonstrated with the combination of Sod1 and Prdx2, in line with the known neuroprotective role of Prdx2 in injury paradigms (Boulos et al., 2007). The elevated oxidative stress in converting astrocytes can lead to cell death (Gascón et al., 2016), and thus preempting the heightened ROS by early induction of antioxidant proteins could reduce this effect.

Induction of enriched genes unrelated to antioxidative roles, such as *Pgam5* and *Slc25a22*, still led to a significant increase in reprogramming efficiency. Mitochondrial homeostasis is monitored by the mitochondrial phosphatase Pgam5 through its role in mitochondrial dynamics and cell death pathways (Cheng et al., 2021; Lu et al., 2016; Ma et al., 2020; Wang et al., 2012). Therefore, the function of Pgam5 in regulating mitochondrial biogenesis and fission could account for its advantageous effect in neuronal reprogramming. On the other hand, the

glutamate transporter Slc25a22 is imperative to prevent the build-up of intracellular glutamate (Goubert et al., 2017), which can result, among other things, in impaired mitochondrial metabolism. Indeed, the importance of these proteins for cellular function is reflected by their prominent positions in injury and disease; for both Pgam5 (Cheng et al., 2021; Lu et al., 2014) and Slc25a22 (Molinari et al., 2009; Molinari et al., 2005; Palmieri et al., 2020). Strikingly, when proteins were induced that were associated with antioxidant function but enriched in astrocytes rather than neurons, there was no favorable effect detected. Thus, although proteins can have similar functions, there are clearly other factors that make them especially suited for specific cellular environments, and so the enrichment of different antioxidative proteins is not superfluous.

The speed of metabolic conversion seems to be an important factor in successful reprogramming. Although changes in transcription have been detected already at 48h after neuronal induction, metabolic genes, such as those related to lipid metabolism, were not yet altered (Masserdotti et al., 2015). Therefore, there appears to be a delay in the transition of the metabolic machinery. Interestingly, when the mitochondria structure was influenced to promote glycolysis through depletion of mitofusin-1 and -2, the enhanced pluripotent reprogramming was matched by an early upregulation during the reprogramming process of genes related to glycolysis (Son et al., 2015). Our findings further support these conclusions, as the induction of the neuron-enriched mitochondrial proteins Sod1 and Prdx2 over time course analysis not only increased the number of reprogrammed cells surviving, but also increased their conversion speed.

The activation of genes by CRISPR/Cas9-based transcriptional activators is an exciting avenue for cellular reprogramming, as the DNA of the cell is directly manipulated by targeting endogenous genes, in contrast to the traditional viral vector-based method of introducing exogenous transgenes (Chakraborty et al., 2014). The CRISPR system allows for the simultaneous manipulation of multiple target genes (McCarty et al., 2020), and it has been utilized successfully both *in vitro* (Black et al., 2016; Rubio et al., 2016) and *in vivo* (Zhou et al., 2018; 2020). Genome-wide screens using CRISPR technology can also provide valuable information regarding the impact of specific transcription factors on the cell-fate determination (Black et al., 2020; Liu et al., 2018) and can be used to further identify pertinent proteins for reprogramming. Indeed, we were able to use CRISPR to harness neuron-enriched mitochondrial proteins, and further highlight the importance of mitochondrial metabolism in

reprogramming. Considering the wide-spread functions of mitochondrial proteins and metabolites, both in regulating cellular bioenergetics and epigenetics, much can be learned from studying their role in cell fate determination.

Our work has established a solid foundation that we can build on by continuing to investigate the metabolic hurdles underlying reprogramming and ultimately increase conversion efficiencies. To make these results relevant for therapeutic applications, it will be necessary to verify the results not only in our *in vitro* paradigm but also in the *in vivo* context. Although the changes in some mitochondria proteins were analyzed during reprogramming through immunocytochemistry, full proteome analysis of the mitochondria at different stages of reprogramming would provide a great deal of valuable information, especially regarding the reprogramming-resistant cells. In comparison to murine cells, very little is known about the role of mitochondria in human cell direct reprogramming, and therefore this was the focus of my second PhD project.

3.2 Project 2: Direct neuronal reprogramming of human cells is hindered by oxphos deficit

While we established the prominent role of metabolism as a hurdle and a driver in direct neuronal reprogramming (Gascón et al., 2016; Russo et al., 2021), these findings were mainly limited to murine cells. In order to apply neuronal reprogramming as a therapeutic strategy in human patients, the conversion of human cells needs to be optimized. Thus, we decided to study the metabolic switch that has been demonstrated in murine cell reprogramming as well as during endogenous neurogenesis. Understanding the role of mitochondria in human cells is also important because mitochondrial dysfunction has been implicated in aging, as well as in various diseases (Stanga et al., 2020; Watts et al., 2018). To this end, we obtained human cells from control donors and from patients with a mitochondrial mutation in CI of the ETC.

In Sonsalla et al., human iPSCs from control donors and NDUFS4-mutant patients were differentiated into glial progenitor cells (GPCs) and astrocytes. Patient cells were able to differentiate in a manner comparable to controls, although differences could be detected when the ETC was challenged, such as during oxygen consumption analysis. Transcriptomic analysis demonstrated that both patient and control cells upregulated astrocyte marker expression in a

similar manner, however, unique pathways were upregulated in their respective GO term analysis. In order to assess the impact of the oxphos defect on the cell's ability to adopt a neuronal identity, we took GPCs from control and patient cells and transduced them with different combinations of proneural transcription factors. Interestingly, the patient GPCs converted at a significantly lower efficiency compared to the control GPCs. Not only was their efficiency affected, but also the functionality of the patient cells was altered, as evidenced by the fewer action potentials elicited from the patient compared to control induced neurons. We wanted to understand what aspects of mitochondrial function were most critical for a successful cell fate conversion, and thus various treatments were tested, including α-tocopherol (ROS scavenger), NR (NAD^+/NADH balance), idebenone (ubiquinone analog), UA (mitophagy activator), and STF/AMG (inhibitors of the UPR pathway). Intriguingly, NR and the UPR inhibitors (STF and AMG) significantly improved the reprogramming efficiency of not only the patient cells, but also the control cells. The treatment with AMG also rescued the functionality of the patient cells, as demonstrated by their improved action potential activity. We confirmed that the influence of the oxphos deficit on neuronal reprogramming was not limited to glial cell conversion but was also relevant for other somatic cells. Patient and control fibroblasts underwent reprogramming, and once again confirmed the reprogramming impairment of patient cells that could be alleviated upon UPR inhibitor treatment. Therefore, the importance of a functioning oxphos metabolic machinery was established for direct neuronal reprogramming, and possible treatments for enhancing the neuronal conversion were identified.

Differential gene expression and features of CI dysfunction

Although both control and patient cells obtained astrocyte-specific genes in a similar manner during glial differentiation, differential gene expression was still detected between the two donor types. For example, the gene PPARGC1A, which encodes for the protein PGC-1α, was upregulated in control cells compared to NDUFS4-mutant patients. PGC-1α is known to stimulate oxphos and mitochondrial biogenesis, as well as to maintain mitochondrial homeostasis through the modulation of ROS production (Handschin & Spiegelman, 2006; Lin et al., 2005; Wu et al., 1999). Due to the essential role of PGC-1α in mitochondrial function, it has unsurprisingly been associated with various neurodegenerative diseases (Rudenok et al., 2020; Soyal et al., 2012, 2019). The reduced expression of PPARGC1A in patient cells thus possibly reflects the mitochondrial dysfunction present as a result of their NDUFS4 mutation.

Consistent with our results, downregulation of PPARGC1A was also observed in NPCs from LS patients with a mutation in SURF1 (Inak et al., 2021). Interestingly, the inflammatory response was also upregulated in control cells compared to patient cells. The ability of control cells to more effectively utilize oxphos for energy generation compared to patient cells could mean that a parallel increase in ROS levels occurs, and ROS is known to be involved in inflammation-signaling pathways (Forrester et al., 2018; Zhou et al., 2011). Indeed, ROS can lead to the activation of the NLRP3 inflammasome, which in turn leads to the secretion of inflammatory cytokines such as IL-1β (Zhou et al., 2011), which was shown to be differentially upregulated in the control cells. Therefore, although patient cells were able to compensate for their metabolic defects and successfully differentiate into astrocytes, distinct transcriptome signatures were still revealed between control and patient cells.

A deficit in the oxidative respiration of patient GPCs was revealed when the ETC was pressured during Seahorse analysis. The metabolic plasticity of glial cells compared to neurons, especially their ability to more readily compensate with glycolysis for energy production, probably accounts for the otherwise comparable functionality between control and patient glial cells. However, when the cells were forced to favor the oxphos metabolic pathway during direct neuronal reprogramming, significant differences were revealed in the abilities of the control and patient cells. The impact of mitochondrial dysfunction on neuronal fate acquisition was recently investigated using patient cells containing a mutation in SURF1, which is involved in the assembly of CIV of the ETC (Inak et al., 2021). The SURF1-mutant cells displayed defective neuronal maturation, including reduced oxphos bioenergetics. Furthermore, multi-omics analysis revealed that the patient cells were detained in a glycolytic and proliferative state, which hindered their ability to obtain a neuronal identity. Stimulating mitochondrial biogenesis through bezafibrate treatment enhanced the neuronal differentiation of SURF1-mutant cells (Inak et al., 2021). Therefore, a functional oxphos metabolism is instrumental for endogenous neuronal conversion, consistent with the results from Sonsalla et al. regarding neuronal fate acquisition during direct reprogramming. We investigated diverse features of mitochondrial metabolism to better understand their relative contribution to mitochondrial dysfunction, as well as their role in the metabolic switch.

CI has three main roles in mitochondrial metabolism; the transfer of electrons along the ETC, the oxidation of NADH to NAD^+, and maintaining the mitochondrial membrane potential through its proton pumping activity (Hirst, 2013). Therefore, CI deficiency can lead to various

aberrations in mitochondrial function. For example, failure to properly pass electrons along the ETC can lead to the increased release of free electrons, which are then able to react with oxygen and amplify the ROS generation. Additionally, if the oxidation of NADH by CI is disrupted it can lead to disequilibrium of the $NADH/NAD^+$ ratio, the repercussions of which include the buildup of lactate. Finally, a reduction in ATP synthesis can result from the compromised proton pumping ability of CI and the subsequently diminished membrane potential (Hirst, 2013). In order to address the reprogramming deficiency observed in the patient cells, as well as to possibly enhance control cell reprogramming, we treated multiple aspects of mitochondrial metabolism, including the ones described above.

The role of ROS in mitochondrial dysfunction and the metabolic switch

First, we decided to target oxidative stress, since not only was enhanced ROS generation known to be a potential side effect of CI defects, but alleviating ROS levels had previously proven beneficial in the neuronal reprogramming of murine astrocytes (Gascón et al., 2016). We treated oxidative stress using α-tocopherol (α-toc), which is an analog of Vitamin E and a ROS scavenger. Unexpectedly, α-toc treatment did not lead to a significant improvement in the reprogramming efficiency of either the control or patient cells. This was against our predictions, since mitochondrial oxphos metabolism, in addition to generating a large amount of metabolic energy, also concomitantly generates a great deal of ROS. Even in healthy cells, the electron transfer that occurs at CI and CIII is leaky, and thus instead of being passed down the ETC, some electrons react directly with oxygen and form superoxide (Marchi et al., 2012). Mitochondrial superoxide dismutase (SOD) can then dismutate superoxide into hydrogen peroxide, or superoxide can also react with nitric oxide and generate reactive nitrogen species (RNS) (Marchi et al., 2012). The damage resulting from this ROS production is wide-ranging, involving mtDNA and mitochondrial protein impairment as well as lipid peroxidation (Marchi et al., 2012). However, it is important to note that ROS also has favorable functions, for example as a mediator of mitochondrial dynamics (Cid-Castro et al., 2018), and as an essential signaling molecule (Vicente-Gutiérrez et al., 2021). Indeed, elevated ROS is actually a normal and functional component of endogenous neuronal differentiation (Hou et al., 2013; Khacho et al., 2017; Rharass et al., 2014) and it also occurs transiently during the pluripotent reprogramming of somatic cells into iPSCs (Ying et al., 2016). Interestingly, during mouse adult hippocampal neurogenesis, the fluctuation of ROS levels were shown to be inversed, as the quiescent neural precursor cells (NPCs) had higher ROS levels that actually decreased as

the cells shifted toward neuronal lineage differentiation (Adusumilli et al., 2021). Therefore, although imbalanced ROS levels can be detrimental to the cell, ROS dynamics have also been shown to be an integral component of cell fate conversion. These factors could thus account for the lack of reprogramming improvement we observed with ROS scavenger treatment.

Nonetheless, the lack of benefit from the α-toc treatment was an especially surprising result for the NDUFS4-mutant patient cells, since increased ROS levels have previously been reported in patient cells (Breuer et al., 2013; Distelmaier et al., 2009a), and antioxidants have even been investigated as a therapeutic treatment (De Haas et al., 2017; Distelmaier et al., 2009b). One possible explanation for the absence of detected improvement is that the cells used for our reprogramming experiments were incubated at oxygen levels comparable to those present in the physiological brain, i.e., ~5% O_2 (Carreau et al., 2011). Low oxygen conditions have previously been shown to be beneficial for neuronal reprogramming (Davila et al., 2013) and they allowed us to make our reprogramming experiments more similar to the *in vivo* environment. In hypoxic conditions the transcription of glycolytic genes, such as LDHA, is activated by hypoxia-inducible factor 1α (HIF-1α), and this stimulation of glycolysis enhances iPSC reprogramming (Yoshida et al., 2009). Although it seems counterintuitive that triggering glycolysis would assist neuronal reprogramming, forcibly slowing down the oxphos metabolic switch might allow the cell to upregulate other neuron-enriched mitochondrial proteins in the meantime and better handle the new metabolic pressures. Curtailing oxidative metabolism early in the reprogramming process would also reduce the concomitant spike of ROS that normally occurs, and in that case treating with ROS scavengers would be unnecessary. Interestingly, hypoxia has been shown to have protective functions in mitochondrial disease (Ferrari et al., 2017; Jain et al., 2016). Another explanation is that although the α-toc treatment might have helped, its beneficial effect was undetected because it was insufficient to overcome the other reprogramming hurdles the cell faced. In corroboration of our results, antioxidant treatment was also unsuccessful at improving the defective neuronal morphogenesis of SURF1 NPCs (Inak et al., 2021). Thus, we decided to instead target other features of mitochondrial metabolism that have also been highlighted in mitochondrial disease (Russell et al., 2020).

Investigating electron transfer, mitophagy and NAD^+ in relation to mitochondrial metabolism

The disruption of electron transfer along the ETC not only leads to increased ROS, but also hampers ATP production. To address this issue, we used the synthetic quinone, idebenone,

which has an antioxidant function, but is also able to pass electrons down the ETC and partially rescue ATP generation (Haefeli et al., 2011). However, idebenone did not lead to a strong improvement in our control or patient cells during reprogramming. Consistent with our results, there was only a mild improvement when idebenone was given to patients with the mitochondrial disorder known as Leber's hereditary optic neuropathy (Klopstock et al., 2011), and when idebenone was tested in clinical trials for MS it did not significantly hinder the disease progression (Kosa et al., 2020). Another possible target for treating mitochondrial dysfunction is the process of mitophagy, a specific form of autophagy that was first described in 1998 (Scott & Klionsky, 1998). Mitophagy is essential for cell maintenance and functionality, and disruption of this pathway has been linked to multiple neurodegenerative diseases (Martinez-Vicente, 2017; Rodolfo et al., 2018; Youle & Narendra, 2011). However, increasing mitophagy during reprogramming by treatment with the mitophagy activator Urolithin A (UA) did not have a significant effect on the neuronal conversion of control or patient cells. Although UA treatment has led to improvements in mouse models of aging (Ryu et al., 2016), as well as in elderly individuals (Andreux et al., 2019), boosting mitophagy is not advantageous to cell fate change in our paradigm. Therefore, partially rescuing the electron transfer along the ETC or stimulating mitophagy were not sufficient to overcome reprogramming hurdles or alleviate the oxphos deficit.

Intriguingly, treatment with the NAD^+ precursor, nicotinamide riboside (NR), during reprogramming led to a significant improvement in the reprogramming efficiency of both control and patient cells. The altered ratio of NAD^+ to NADH is a known side-effect of mitochondrial dysfunction (Gomes et al., 2013; Lautrup et al., 2019), and reduced NAD^+ was detected in iPSC-derived neurons from patients with a mitochondrial deficiency (Inak et al., 2021). In accordance with our results, treatment with NR has led to increased mitochondrial biogenesis and boosted oxidative capacity in mouse skeletal muscle (Cantó et al., 2012; Khan et al., 2014). Furthermore, a NAD^+ redox imbalance was demonstrated in a mouse model of LS, but the symptoms could be improved upon administration of the exogenous NAD^+ precursor nicotinamide mononucleotide (NMN) (Lee et al., 2019). Indeed, NAD^+ is not only involved in cellular bioenergetics but is also a crucial substrate for many enzymes, such as poly ADP-ribose polymerases (PARPs), cyclic ADP-ribose (cADPR) synthases, and sirtuin deacetylases (Katsyuba & Auwerx, 2017; Yang & Sauve, 2016). Thus, NAD^+ may also assist cellular reprogramming through its involvement in the modification of transcription factors.

Interaction between the ER and mitochondria: UPR pathway

The most striking improvement to direct neuronal reprogramming in both the patient and control cells was observed with the inhibition of the unfolded protein response (UPR), which is an endoplasmic reticulum (ER) stress response pathway. The identification of the UPR pathway as a major obstacle to reprogramming was an engrossing and unexpected result, which highlights an important role for the ER in reprogramming that we had not previously considered.

Similar to mitochondrial dysfunction, ER stress and the UPR have been implicated in diabetes and cancer, as well as in various neurodegenerative diseases (Remondelli & Renna, 2017; Xiang et al., 2017; Zhao & Ackerman, 2006). Interestingly, the mitochondria and the ER have many integrated signaling pathways and even have designated regions of close physical association, known as mitochondria-associated membranes (MAMs). These areas allow for the efficient coordination of calcium homeostasis, inflammation signaling, and autophagy, among others (Missiroli et al., 2018). Indeed, a constant low-level calcium transfer from the ER to the mitochondria through the inositol trisphosphate receptor ($InsP_3R$) calcium release channel is essential to sustain oxphos levels (Cárdenas et al., 2010). On the other hand, an overload of calcium can lead to cell death through the parallel increase in ROS along with oxphos stimulation and opening of the permeability transition pore (PTP) in the mitochondria, which leads to swelling and apoptosis (Hajnóczky et al., 2006). Indeed, the interactions between the ER and mitochondria do not occur only as part of normal cellular function but are also influenced during times of dysfunction. In order to restore homeostasis during times of ER stress, one cellular response is to activate the UPR (Senft & Ronai, 2015; Xiang et al., 2017). As illustrated in Figure 3, there are three different branches of the UPR: double-stranded RNA-activated protein kinase (PKR)-like ER kinase (PERK), inositol-requiring enzyme 1 (IRE1), and activating transcription factor 6 (ATF6) (Li et al., 2020). The three transmembrane proteins listed above each carry out specific functions. Protein translation is inhibited by PERK through the phosphorylation of eukaryotic translation initiation factor 2 alpha (eIF2α) (Senft & Ronai, 2015). In addition, ATF4 is upregulated, which leads to the increased expression of chaperones to assist in protein folding, as well as proteins related to the antioxidant response. IRE1 stimulates the production of chaperones by activating the transcription factor XBP-1, and it also fosters mRNA degradation. Finally, ATF6 translocates to the Golgi, where it is cleaved, and subsequently activates transcription factors in the nucleus, such as C/EBP homologous

protein (CHOP). The UPR can ultimately result in the activation of cell death pathways if the cell is unable to re-establish homeostasis (Senft & Ronai, 2015).

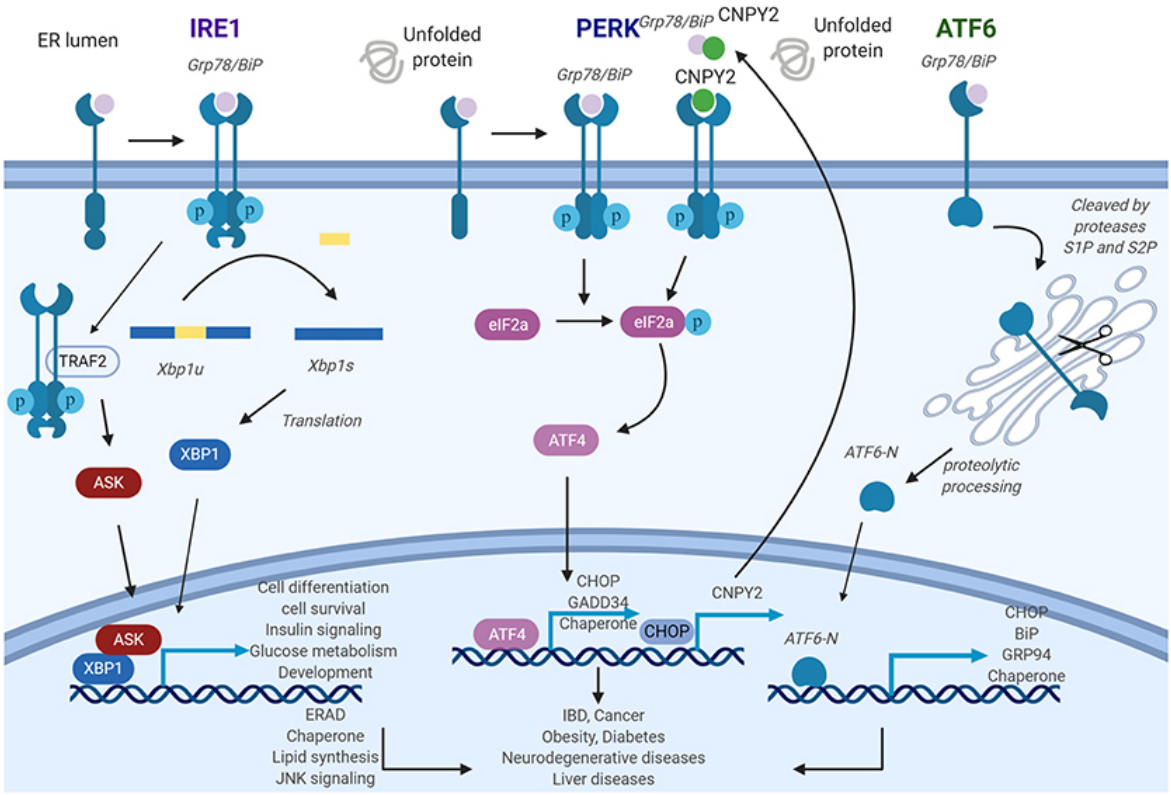

Figure 3: *The three transmembrane sensors of the UPR pathway*. The downstream functions of protein kinase (PKR)-like ER kinase (PERK), inositol-requiring enzyme 1 (IRE1), and activating transcription factor 6 (ATF6) are illustrated (Li et al., 2020; this is an open access article distributed under the terms of the Creative Commons Attribution License)

Strikingly, we observed a significantly increased neuronal reprogramming efficiency in both control and NDUFS4-mutant cells upon inhibition of either the IRE1 (STF-083010 inhibitor) or PERK (AMG PERK 44 inhibitor) branch of the UPR. This was very intriguing, as the UPR is initially activated in a protective manner to re-equilibrate cellular homeostasis, such as through stimulating the transcription of chaperones to assist with the management of misfolded proteins and through the reduction of global protein translation (Wang & Kaufman, 2016). The UPR can also directly benefit the mitochondria, as PERK-mediated activation of ATF4 leads to the upregulation of parkin, which can prevent mitochondrial damage (Bouman et al., 2011). However, once the UPR has been chronically active it becomes detrimental to the cell and

ultimately leads to cell death (Wang & Kaufman, 2016). Therefore, one possibility is that during times of prolonged cellular stress, such as during forced cell fate conversion, the UPR can activate cell death pathways and thus be a hurdle to reprogramming. The close association between the mitochondria and the ER implies that the ER is influenced by the mitochondrial switch in metabolic profile, and in addition mitochondria stress itself has been shown to activate the UPR pathway (Bouman et al., 2011). Interestingly, ER stress has also been linked directly to the regulation of NDUFS4 localization. The ER membrane protein B cell receptor–associated protein 31 (BAP31) forms a complex with translocase of the outer mitochondrial membrane 40 (Tom40) (Namba, 2019). This BAP31-Tom40 complex is involved in the translocation of NDUFS4 from the cytosol into the mitochondria. It was shown that ER stress caused this BAP31-Tom40 complex to dissociate, thus reducing the amount of NDUFS4 that could join CI. This reduction resulted in disrupted mitochondria homeostasis and reduced oxygen consumption (Namba, 2019). Therefore, although ER stress can be neuroprotective, it can also have many adverse effects on cellular function.

Intriguingly, inhibition of two separate branches of the UPR led to improved reprogramming. The beneficial effect we observed by targeting the IRE1 branch of the UPR could be due to its upregulation of pro-apoptotic and pro-inflammatory proteins during extended periods of ER stress (Chen & Brandizzi, 2013; Lerner et al., 2012). Furthermore, IRE1 has been shown to mediate a reduction in glycolysis and mitochondrial respiration during UPR activation (van der Harg et al., 2017), and this decreased metabolism could hinder cell fate conversion. The PERK branch, on the other hand, reduces the protein load on the cell by attenuating translation (Harding et al., 2000). This reduction of translation could be detrimental to the cells undergoing reprogramming, as the change in cell identity would require the generation of new proteins. Indeed, activation of the PERK-mediated UPR during murine cortical neurogenesis led to a disruption in the generation of neurons (Laguesse et al., 2015). A notable and novel role for the UPR pathway as a significant obstacle in direct neuronal reprogramming is thus established.

In this study, new aspects of mitochondrial function related to direct neuronal reprogramming in human cells were revealed, markedly the relevance of redox equilibrium and the UPR pathway. Interestingly, the ROS scavenger treatment found to be beneficial during murine cell reprogramming (Gascón et al., 2016) did not have a significant effect on the human cells. In order to better understand the role of ROS in human cell reprogramming, and in relation to cells with a mitochondrial deficiency, oxidative stress should be monitored in cells at different

stages of the reprogramming process, for instance through CellRox treatment. It would also be interesting to assess specific features of ROS damage, such as lipid peroxidation. Transcriptomic analysis has previously been done on murine cells undergoing reprogramming to elucidate the transcriptional changes occurring at the early stages of the reprogramming process (Masserdotti et al., 2015). To complement our understanding of reprogramming and increase its relevance for therapeutic applications, it would be important to conduct scRNA-seq analysis on human cells early in the reprogramming paradigm. Comparing control and patient cells would reveal valuable information regarding the metabolic switch and also provide insights into mitochondrial disease. Furthermore, the induction of the UPR pathway has previously been observed by us in murine astrocytes undergoing reprogramming (Najas et al., unpublished data), however we still need to confirm the presence of UPR activation during the neuronal reprogramming of human cells. It would be interesting to include the UPR inhibitor treatment in the scRNA-seq experiment, as that would further elucidate the underlying influence of our novel finding on neuronal reprogramming.

3.3 Concluding remarks

In conclusion, my PhD studies highlighted the importance of the mitochondria as a driver not only in the neuronal reprogramming of murine cells, but also in regard to human cell reprogramming paradigms. Forced cell fate conversion causes the cells to change their metabolic phenotype at a greater speed than required during endogenous neurogenesis, thus leading to increased stress and cell death. Supporting the cells through the switch, such as by upregulating specific neuron-enriched proteins, can be a useful strategy for increasing reprogramming efficiencies and improving the quality of the resulting induced neurons. Alleviating mitochondrial stress is also relevant for directly treating the mitochondrial dysfunction observed in neurodegenerative disease. Investigating cells from human control donors and NDUFS4-mutant patients emphasized the importance of the redox balance homeostasis in mitochondrial function and revealed the UPR as a new pathway relevant for direct neuronal reprogramming. The underlying mechanisms responsible for this role of the UPR, as well as the impact of other mitochondrial features, remain to be discovered.

4. References

Adusumilli, V. S., Walker, T. L., Overall, R. W., Klatt, G. M., Zeidan, S. A., Zocher, S., Kirova, D. G., Ntitsias, K., Fischer, T. J., Sykes, A. M., Reinhardt, S., Dahl, A., Mansfeld, J., Rünker, A. E., & Kempermann, G. (2021). ROS Dynamics Delineate Functional States of Hippocampal Neural Stem Cells and Link to Their Activity-Dependent Exit from Quiescence. *Cell Stem Cell*, *28*(2), 300-314.e6. https://doi.org/10.1016/j.stem.2020.10.019

Agostini, M., Romeo, F., Inoue, S., Niklison-Chirou, M. V., Elia, A. J., Dinsdale, D., Morone, N., Knight, R. A., Mak, T. W., & Melino, G. (2016). Metabolic reprogramming during neuronal differentiation. *Cell Death and Differentiation*, *23*(9), 1502–1514. https://doi.org/10.1038/cdd.2016.36

Akram, M. (2014). Citric Acid Cycle and Role of its Intermediates in Metabolism. *Cell Biochemistry and Biophysics*, *68*(3), 475–478. https://doi.org/10.1007/s12013-013-9750-1

Almeida, A., Almeida, J., Bolañ, J. P., & Moncada, S. (2001). Different responses of astrocytes and neurons to nitric oxide: The role of glycolytically generated ATP in astrocyte protection. *Proceedings of the National Academy of Sciences of the United States of America*, *98*(26), 15294–15299. www.pnas.orgcgidoi10.1073pnas.261560998

Almeida, A., Moncada, S., & Bolaños, J. P. (2004). Nitric oxide switches on glycolysis through the AMP protein kinase and 6-phosphofructo-2-kinase pathway. *Nature Cell Biology*, *6*(1), 45–51. https://doi.org/10.1038/ncb1080

Amaral, A. I., Meisingset, T. W., Kotter, M. R., & Sonnewald, U. (2013). Metabolic aspects of Neuron-Oligodendrocyte-Astrocyte interactions. In *Frontiers in Endocrinology* (Vol. 4, Issue MAY). https://doi.org/10.3389/fendo.2013.00054

Andreux, P. A., Blanco-Bose, W., Ryu, D., Burdet, F., Ibberson, M., Aebischer, P., Auwerx, J., Singh, A., & Rinsch, C. (2019). The mitophagy activator urolithin A is safe and induces a molecular signature of improved mitochondrial and cellular health in humans. *Nature Metabolism*, *1*(6), 595–603. https://doi.org/10.1038/s42255-019-0073-4

Assouline, Z., Jambou, M., Rio, M., Bole-Feysot, C., de Lonlay, P., Barnerias, C., Desguerre, I., Bonnemains, C., Guillermet, C., Steffann, J., Munnich, A., Bonnefont, J. P., Rötig, A., & Lebre, A. S. (2012). A constant and similar assembly defect of mitochondrial respiratory chain complex I allows rapid identification of NDUFS4 mutations in patients with Leigh syndrome. *Biochimica et Biophysica Acta - Molecular Basis of Disease*, *1822*(6), 1062–1069. https://doi.org/10.1016/j.bbadis.2012.01.013

Attwell, D., Buchan, A. M., Charpak, S., Lauritzen, M., MacVicar, B. A., & Newman, E. A. (2010). Glial and neuronal control of brain blood flow. In *Nature* (Vol. 468, Issue 7321, pp. 232–243). https://doi.org/10.1038/nature09613

Baertling, F., Rodenburg, R. J., Schaper, J., Smeitink, J. A., Koopman, W. J. H., Mayatepek, E., Morava, E., & Distelmaier, F. (2014). A guide to diagnosis and treatment of Leigh syndrome. *Journal of Neurology, Neurosurgery and Psychiatry*, *85*(3), 257–265. https://doi.org/10.1136/jnnp-2012-304426

Bélanger, M., Allaman, I., & Magistretti, P. J. (2011). Brain energy metabolism: Focus on Astrocyte-neuron metabolic cooperation. In *Cell Metabolism* (Vol. 14, Issue 6, pp. 724–738). https://doi.org/10.1016/j.cmet.2011.08.016

Berninger, B., Costa, M. R., Koch, U., Schroeder, T., Sutor, B., Grothe, B., & Götz, M. (2007). Functional properties of neurons derived from in vitro reprogrammed postnatal astroglia. *Journal of Neuroscience*, *27*(32), 8654–8664. https://doi.org/10.1523/JNEUROSCI.1615-07.2007

Berridge, M. V., Schneider, R. T., & McConnell, M. J. (2016). Mitochondrial Transfer from Astrocytes to Neurons following Ischemic Insult: Guilt by Association? In *Cell Metabolism* (Vol. 24, Issue 3, pp. 376–378). Cell Press. https://doi.org/10.1016/j.cmet.2016.08.023

Bertrand, N., Castro, D. S., & Guillemot, F. (2002). Proneural genes and the specification of neural cell types. *Nature Reviews Neuroscience*, *3*(7), 517–530. https://doi.org/10.1038/nrn874

Bittar, P. G., Charnay, Y., Pellerin, T., Bouras, C., & Magistretti, J. (1996). Selective Distribution of Lactate Dehydrogenase Isoenzymes in Neurons and Astrocytes of Human Brain. *Journal of Cerebral Blood Flow*, *16*, 1079–1089. https://doi.org/https://doi.org/10.1097/00004647-199611000-00001

Black, J. B., Adler, A. F., Wang, H. G., D'Ippolito, A. M., Hutchinson, H. A., Reddy, T. E., Pitt, G. S., Leong, K. W., & Gersbach, C. A. (2016). Targeted Epigenetic Remodeling of Endogenous Loci by CRISPR/Cas9-Based Transcriptional Activators Directly Converts Fibroblasts to Neuronal Cells. *Cell Stem Cell*, *19*(3), 406–414. https://doi.org/10.1016/j.stem.2016.07.001

Black, J. B., McCutcheon, S. R., Dube, S., Barrera, A., Klann, T. S., Rice, G. A., Adkar, S. S., Soderling, S. H., Reddy, T. E., & Gersbach, C. A. (2020). Master Regulators and Cofactors of Human Neuronal Cell Fate Specification Identified by CRISPR Gene Activation Screens. *Cell Reports*, *33*(9). https://doi.org/10.1016/j.celrep.2020.108460

Blum, R., Heinrich, C., Sánchez, R., Lepier, A., Gundelfinger, E. D., Berninger, B., & Götz, M. (2011). Neuronal network formation from reprogrammed early postnatal rat cortical glial cells. *Cerebral Cortex*, *21*(2), 413–424. https://doi.org/10.1093/cercor/bhq107

Bolaños, J. P., Almeida, A., & Moncada, S. (2010). Glycolysis: a bioenergetic or a survival pathway? In *Trends in Biochemical Sciences* (Vol. 35, Issue 3, pp. 145–149). https://doi.org/10.1016/j.tibs.2009.10.006

Boulos, S., Meloni, B. P., Arthur, P. G., Bojarski, C., & Knuckey, N. W. (2007). Peroxiredoxin 2 overexpression protects cortical neuronal cultures from ischemic and oxidative injury but not glutamate excitotoxicity, whereas Cu/Zn superoxide dismutase 1 overexpression protects only against oxidative injury. *Journal of Neuroscience Research*, *85*(14), 3089–3097. https://doi.org/10.1002/jnr.21429

Bouman, L., Schlierf, A., Lutz, A. K., Shan, J., Deinlein, A., Kast, J., Galehdar, Z., Palmisano, V., Patenge, N., Berg, D., Gasser, T., Augustin, R., Trümbach, D., Irrcher, I., Park, D. S., Wurst, W., Kilberg, M. S., Tatzelt, J., & Winklhofer, K. F. (2011). Parkin is transcriptionally regulated by ATF4: Evidence for an interconnection between mitochondrial stress and ER stress. *Cell Death and Differentiation*, *18*(5), 769–782. https://doi.org/10.1038/cdd.2010.142

Boumezbeur, F., Mason, G. F., De Graaf, R. A., Behar, K. L., Cline, G. W., Shulman, G. I., Rothman, D. L., & Petersen, K. F. (2010). Altered brain mitochondrial metabolism in healthy aging as assessed by in vivo magnetic resonance spectroscopy. *Journal of Cerebral Blood Flow and Metabolism*, *30*(1), 211–221. https://doi.org/10.1038/jcbfm.2009.197

Brasil, A. de A., de Carvalho, M. D. C., Gerhardt, E., Queiroz, D. D., Pereira, M. D., Outeiro, T. F., & Eleutherio, E. C. A. (2019). Characterization of the activity, aggregation, and toxicity of heterodimers of WT and ALS-associated mutant Sod1. *Proceedings of the National Academy of Sciences*, *116*(51).

https://doi.org/10.1073/pnas.1902483116

Breuer, M. E., Willems, P. H. G. M., Smeitink, J. A. M., Koopman, W. J. H., & Nooteboom, M. (2013). Cellular and animal models for mitochondrial complex i deficiency: A focus on the NDUFS4 subunit. In *IUBMB Life* (Vol. 65, Issue 3, pp. 202–208). https://doi.org/10.1002/iub.1127

Breunig, C. T., Durovic, T., Neuner, A. M., Baumann, V., Wiesbeck, M. F., Köferle, A., Götz, M., Ninkovic, J., & Stricker, S. H. (2018). One step generation of customizable gRNA vectors for multiplex CRISPR approaches through string assembly gRNA cloning (STAgR). *PLoS ONE*, *13*(4). https://doi.org/10.1371/journal.pone.0196015

Brown, A. M. (2004). Brain glycogen re-awakened. In *Journal of Neurochemistry* (Vol. 89, Issue 3, pp. 537–552). Blackwell Publishing Ltd. https://doi.org/10.1111/j.1471-4159.2004.02421.x

Budde, S. M. S., van den Heuvel, L. P. W. J., Smeets, R. J. P., Skladal, D., Mayr, J. A., Boelen, C., Petruzzella, V., Papa, S., & Smeitink, J. A. M. (2003). Clinical heterogeneity in patients with mutations in the NDUFS4 gene of mitochondrial complex I. In *Journal of Inherited Metabolic Disease* (Vol. 26, Issue 8, pp. 813–815). https://doi.org/10.1023/B:BOLI.0000010003.14113.af

Buffo, A., Vosko, M. R., Ertü rk, D., Hamann, G. F., Jucker, M., Rowitch, D., & Gö tz, M. (2005). *Expression pattern of the transcription factor Olig2 in response to brain injuries: Implications for neuronal repair*. www.pnas.orgcgidoi10.1073pnas.0506535102

Cai, L., Morrow, E. M., & Cepko, C. L. (2000). Misexpression of basic helix-loop-helix genes in the murine cerebral cortexaffects cell fate choices and neuronal survival. *Development*, *127*, 3021–3030. http://axon.med.harvard.edu/~cepko/protocol/xgalplap-

Caiazzo, M., Dell'Anno, M. T., Dvoretskova, E., Lazarevic, D., Taverna, S., Leo, D., Sotnikova, T. D., Menegon, A., Roncaglia, P., Colciago, G., Russo, G., Carninci, P., Pezzoli, G., Gainetdinov, R. R., Gustincich, S., Dityatev, A., & Broccoli, V. (2011). Direct generation of functional dopaminergic neurons from mouse and human fibroblasts. In *Nature* (Vol. 476, Issue 7359, pp. 224–227). https://doi.org/10.1038/nature10284

Calvaruso, M. A., Willems, P., Van den brand, M., Valsecchi, F., Kruse, S., Palmiter, R., Smeitink, J., & Nijtmans, L. (2012). Mitochondrial complex III stabilizes complex I in the absence of NDUFS4 to provide partial activity. *Human Molecular Genetics*, *21*(1), 115–120. https://doi.org/10.1093/hmg/ddr446

Calvo-Garrido, J., Maffezzini, C., Schober, F. A., Clemente, P., Uhlin, E., Kele, M., Stranneheim, H., Lesko, N., Bruhn, H., Svenningsson, P., Falk, A., Wedell, A., Freyer, C., & Wredenberg, A. (2019). SQSTM1/p62-Directed Metabolic Reprogramming Is Essential for Normal Neurodifferentiation. *Stem Cell Reports*, *12*(4), 696–711. https://doi.org/10.1016/j.stemcr.2019.01.023

Camandola, S., & Mattson, M. P. (2017). Brain metabolism in health, aging, and neurodegeneration. *The EMBO Journal*, *36*(11), 1474–1492. https://doi.org/10.15252/embj.201695810

Cantó, C., Houtkooper, R. H., Pirinen, E., Youn, D. Y., Oosterveer, M. H., Cen, Y., Fernandez-Marcos, P. J., Yamamoto, H., Andreux, P. A., Cettour-Rose, P., Gademann, K., Rinsch, C., Schoonjans, K., Sauve, A. A., & Auwerx, J. (2012). The NAD+ precursor nicotinamide riboside enhances oxidative metabolism and protects against high-fat diet-induced obesity. *Cell Metabolism*, *15*(6), 838–847. https://doi.org/10.1016/j.cmet.2012.04.022

Cárdenas, C., Miller, R. A., Smith, I., Bui, T., Molgó, J., Müller, M., Vais, H., Cheung, K. H., Yang, J., Parker,

I., Thompson, C. B., Birnbaum, M. J., Hallows, K. R., & Foskett, J. K. (2010). Essential Regulation of Cell Bioenergetics by Constitutive InsP3 Receptor Ca2+ Transfer to Mitochondria. *Cell*, *142*(2), 270–283. https://doi.org/10.1016/j.cell.2010.06.007

Carreau, A., Hafny-Rahbi, B. El, Matejuk, A., Grillon, C., & Kieda, C. (2011). Why is the partial oxygen pressure of human tissues a crucial parameter? Small molecules and hypoxia. *Journal of Cellular and Molecular Medicine*, *15*(6), 1239–1253. https://doi.org/10.1111/j.1582-4934.2011.01258.x

Casarosa, S., Fode, C., & Guillemot, F. (1999). Mash1 regulates neurogenesis in the ventral telencephalon. *Development*, *126*, 525–534.

Chakraborty, S., Ji, H., Kabadi, A. M., Gersbach, C. A., Christoforou, N., & Leong, K. W. (2014). A CRISPR/Cas9-based system for reprogramming cell lineage specification. *Stem Cell Reports*, *3*(6), 940–947. https://doi.org/10.1016/j.stemcr.2014.09.013

Chanda, S., Ang, C. E., Davila, J., Pak, C., Mall, M., Lee, Q. Y., Ahlenius, H., Jung, S. W., Südhof, T. C., & Wernig, M. (2014). Generation of induced neuronal cells by the single reprogramming factor ASCL1. *Stem Cell Reports*, *3*(2), 282–296. https://doi.org/10.1016/j.stemcr.2014.05.020

Chen, B., Hui, J., Montgomery, K. S., Gella, A., Bolea, I., Sanz, E., Palmiter, R. D., & Quintana, A. (2017). Loss of mitochondrial Ndufs4 in striatal medium spiny neurons mediates progressive motor impairment in a mouse model of leigh syndrome. *Frontiers in Molecular Neuroscience*, *10*. https://doi.org/10.3389/fnmol.2017.00265

Chen, W., Zhang, X., & Huang, W. J. (2016). Role of neuroinflammation in neurodegenerative diseases (Review). *Molecular Medicine Reports*, *13*(4), 3391–3396. https://doi.org/10.3892/mmr.2016.4948

Chen, Y., & Brandizzi, F. (2013). IRE1: ER stress sensor and cell fate executor. In *Trends in Cell Biology* (Vol. 23, Issue 11, pp. 547–555). https://doi.org/10.1016/j.tcb.2013.06.005

Cheng, M., Lin, N., Dong, D., Ma, J., Su, J., & Sun, L. (2021). PGAM5: A crucial role in mitochondrial dynamics and programmed cell death. In *European Journal of Cell Biology* (Vol. 100, Issue 1). Elsevier GmbH. https://doi.org/10.1016/j.ejcb.2020.151144

Choi, W. S., Kim, H. W., Tronche, F., Palmiter, R. D., Storm, D. R., & Xia, Z. (2017). Conditional deletion of Ndufs4 in dopaminergic neurons promotes Parkinson's disease-like non-motor symptoms without loss of dopamine neurons. *Scientific Reports*, *7*. https://doi.org/10.1038/srep44989

Chou, J. L., Shenoy, D. V., Thomas, N., Choudhary, P. K., LaFerla, F. M., Goodman, S. R., & Breen, G. A. M. (2011). Early dysregulation of the mitochondrial proteome in a mouse model of Alzheimer's disease. *Journal of Proteomics*, *74*(4), 466–479. https://doi.org/10.1016/j.jprot.2010.12.012

Chouchani, E. T., Methner, C., Buonincontri, G., Hu, C. H., Logan, A., Sawiak, S. J., Murphy, M. P., & Krieg, T. (2014). Complex I deficiency due to selective loss of Ndufs4 in the mouse heart results in severe hypertrophic cardiomyopathy. *PLoS ONE*, *9*(4). https://doi.org/10.1371/journal.pone.0094157

Chung, W. S., Allen, N. J., & Eroglu, C. (2015). Astrocytes control synapse formation, function, and elimination. *Cold Spring Harbor Perspectives in Biology*, *7*(9). https://doi.org/10.1101/cshperspect.a020370

Cid-Castro, C., Hernández-Espinosa, D. R., & Morán, J. (2018). ROS as Regulators of Mitochondrial Dynamics in Neurons. In *Cellular and Molecular Neurobiology* (Vol. 38, Issue 5, pp. 995–1007). Springer New York LLC. https://doi.org/10.1007/s10571-018-0584-7

Clason, T., Ruiz, T., Schägger, H., Peng, G., Zickermann, V., Brandt, U., Michel, H., & Radermacher, M. (2010). The structure of eukaryotic and prokaryotic complex I. *Journal of Structural Biology*, *169*(1), 81–88. https://doi.org/10.1016/j.jsb.2009.08.017

Colasante, G., Lignani, G., Rubio, A., Medrihan, L., Yekhlef, L., Sessa, A., Massimino, L., Giannelli, S. G., Sacchetti, S., Caiazzo, M., Leo, D., Alexopoulou, D., Dell'Anno, M. T., Ciabatti, E., Orlando, M., Studer, M., Dahl, A., Gainetdinov, R. R., Taverna, S., … Broccoli, V. (2015). Rapid Conversion of Fibroblasts into Functional Forebrain GABAergic Interneurons by Direct Genetic Reprogramming. *Cell Stem Cell*, *17*(6), 719–734. https://doi.org/10.1016/j.stem.2015.09.002

Cooper, M. L., Pasini, S., Lambert, W. S., D'Alessandro, K. B., Yao, V., Risner, M. L., & Calkins, D. J. (2020). Redistribution of metabolic resources through astrocyte networks mitigates neurodegenerative stress. *Proceedings of the National Academy of Sciences*, *117*(31), 18810–18821. https://doi.org/10.1073/PNAS.2009425117

Davila, J., Chanda, S., Ang, C. E., Südhof, T. C., & Wernig, M. (2013). Acute reduction in oxygen tension enhances the induction of neurons from human fibroblasts. *Journal of Neuroscience Methods*, *216*(2), 104–109. https://doi.org/10.1016/j.jneumeth.2013.03.020

Davis, C. O., Kim, K.-Y., Bushong, E. A., Mills, E. A., Boassa, D., Shih, T., Kinebuchi, M., Phan, S., Zhou, Y., Bihlmeyer, N. A., Nguyen, J. V., Jin, Y., Ellisman, M. H., & Marsh-Armstrong, N. (2014). Transcellular degradation of axonal mitochondria. *Proceedings of the National Academy of Sciences*, *111*(26), 9633–9638. https://doi.org/10.1073/PNAS.1404651111

De Araújo Brasil, A., Dias Castela De Carvalho, M., Gerhardt, E., Dias Queiroz, D., Dias Pereira, M., Outeiro, F., Cristina, E., & Eleutherio, A. (n.d.). *Characterization of the activity, aggregation, and toxicity of heterodimers of WT and ALS-associated mutant Sod1*. https://doi.org/https://doi.org/10.1073/pnas.1902483116

de Barcelos, I. P., Troxell, R. M., & Graves, J. S. (2019). Mitochondrial dysfunction and multiple sclerosis. *Biology*, *8*(2). https://doi.org/10.3390/biology8020037

De Haas, R., Das, D., Garanto, A., Renkema, H. G., Greupink, R., Van Den Broek, P., Pertijs, J., Collin, R. W. J., Willems, P., Beyrath, J., Heerschap, A., Russel, F. G., & Smeitink, J. A. (2017). Therapeutic effects of the mitochondrial ROS-redox modulator KH176 in a mammalian model of Leigh Disease. *Scientific Reports*, *7*(1). https://doi.org/10.1038/s41598-017-09417-5

Dienel, G. A. (2019). Brain Glucose Metabolism: Integration of Energetics with Function. *Physiol Rev*, *99*, 949–1045. https://doi.org/10.1152/phys

Distelmaier, F., Koopman, W. J. H., Van Den Heuvel, L. P., Rodenburg, R. J., Mayatepek, E., Willems, P. H. G. M., & Smeitink, J. A. M. (2009). Mitochondrial complex i deficiency: From organelle dysfunction to clinical disease. In *Brain* (Vol. 132, Issue 4, pp. 833–842). Oxford University Press. https://doi.org/10.1093/brain/awp058

Distelmaier, F., Visch, H. J., Smeitink, J. A. M., Mayatepek, E., Koopman, W. J. H., & Willems, P. H. G. M. (2009). The antioxidant Trolox restores mitochondrial membrane potential and Ca2+-stimulated ATP production in human complex i deficiency. *Journal of Molecular Medicine*, *87*(5), 515–522. https://doi.org/10.1007/s00109-009-0452-5

Divakaruni, A. S., Wallace, M., Buren, C., Martyniuk, K., Andreyev, A. Y., Li, E., Fields, J. A., Cordes, T.,

Reynolds, I. J., Bloodgood, B. L., Raymond, L. A., Metallo, C. M., & Murphy, A. N. (2017). Inhibition of the mitochondrial pyruvate carrier protects from excitotoxic neuronal death. *Journal of Cell Biology*, *216*(4), 1091–1105. https://doi.org/10.1083/jcb.201612067

Dringen, R., Gebhardt, R., & Hamprecht, B. (1993). Glycogen in astrocytes: possible function as lactate supply for neighboring cells *. In *Brain Research* (Vol. 623).

Drouin-Ouellet, J., Pircs, K., Barker, R. A., Jakobsson, J., & Parmar, M. (2017). Direct neuronal reprogramming for disease modeling studies using patient-derived neurons: What have we learned? In *Frontiers in Neuroscience* (Vol. 11, Issue SEP). Frontiers Media S.A. https://doi.org/10.3389/fnins.2017.00530

Drukarch, B., Schepens, E., Stoof, J. C., Langeveld, C. H., & Van Muiswinkel, F. L. (1998). Astrocyte-Enhanced Neuronal Survival is Mediated by Scavenging of Extracellular Reactive Oxygen Species. *Free Radical Biology and Medicine*, *25*(2), 217–220.

Fang, D., Qing, Y., Yan, S., Chen, D., & Yan, S. S. Du. (2016). Development and Dynamic Regulation of Mitochondrial Network in Human Midbrain Dopaminergic Neurons Differentiated from iPSCs. *Stem Cell Reports*, *7*(4), 678–692. https://doi.org/10.1016/j.stemcr.2016.08.014

Fecher, C., Trovò, L., Müller, S. A., Snaidero, N., Wettmarshausen, J., Heink, S., Ortiz, O., Wagner, I., Kühn, R., Hartmann, J., Karl, R. M., Konnerth, A., Korn, T., Wurst, W., Merkler, D., Lichtenthaler, S. F., Perocchi, F., & Misgeld, T. (2019). Cell-type-specific profiling of brain mitochondria reveals functional and molecular diversity. *Nature Neuroscience*, *22*(10), 1731–1742. https://doi.org/10.1038/s41593-019-0479-z

Ferrari, M., Jain, I. H., Goldberger, O., Rezoagli, E., Thoonen, R., Chen, K. H., Sosnovik, D. E., Scherrer-Crosbie, M., Mootha, V. K., & Zapol, W. M. (2017). Hypoxia treatment reverses neurodegenerative disease in a mouse model of Leigh syndrome. *Proceedings of the National Academy of Sciences of the United States of America*, *114*(21), E4241–E4250. https://doi.org/10.1073/pnas.1621511114

Fiedorczuk, K., & Sazanov, L. A. (2018). Mammalian Mitochondrial Complex I Structure and Disease-Causing Mutations. In *Trends in Cell Biology* (Vol. 28, Issue 10, pp. 835–867). Elsevier Ltd. https://doi.org/10.1016/j.tcb.2018.06.006

Filosto, M., Scarpelli, M., Cotelli, M. S., Vielmi, V., Todeschini, A., Gregorelli, V., Tonin, P., Tomelleri, G., & Padovani, A. (2011). The role of mitochondria in neurodegenerative diseases. *Journal of Neurology*, *258*(10), 1763–1774. https://doi.org/10.1007/s00415-011-6104-z

Fode, C., Gradwohl, G., Morin, X., Dierich, A., LeMeur, M., Goridis, C., & Guillemot, F. (1998). The bHLH Protein NEUROGENIN 2 Is a Determination Factor for Epibranchial Placode-Derived Sensory Neurons. *Neuron*, *20*, 483–494.

Fode, Carol, Ma, Q., Casarosa, S., Ang, S.-L., Anderson, D. J., & Ois Guillemot, F. (2000). A role for neural determination genes in specifying the dorsoventral identity of telencephalic neurons. *Genes and Development*, *14*. www.genesdev.org

Folmes, C. D. L., Nelson, T. J., Martinez-Fernandez, A., Arrell, D. K., Lindor, J. Z., Dzeja, P. P., Ikeda, Y., Perez-Terzic, C., & Terzic, A. (2011). Somatic oxidative bioenergetics transitions into pluripotency-dependent glycolysis to facilitate nuclear reprogramming. *Cell Metabolism*, *14*(2), 264–271. https://doi.org/10.1016/j.cmet.2011.06.011

Forrester, S. J., Kikuchi, D. S., Hernandes, M. S., Xu, Q., & Griendling, K. K. (2018). Reactive oxygen species

in metabolic and inflammatory signaling. In *Circulation Research* (Vol. 122, Issue 6, pp. 877–902). Lippincott Williams and Wilkins. https://doi.org/10.1161/CIRCRESAHA.117.311401

Friedrich, T., & Böttcher, B. (2004). The gross structure of the respiratory complex I: A Lego System. In *Biochimica et Biophysica Acta - Bioenergetics* (Vol. 1608, Issue 1, pp. 1–9). Elsevier. https://doi.org/10.1016/j.bbabio.2003.10.002

Galera-Monge, T., Zurita-Díaz, F., Canals, I., Hansen, M. G., Rufián-Vázquez, L., Ehinger, J. K., Elmér, E., Martin, M. A., Garesse, R., Ahlenius, H., & Gallardo, M. E. (2020). Mitochondrial dysfunction and calcium dysregulation in leigh syndrome induced pluripotent stem cell derived neurons. *International Journal of Molecular Sciences*, *21*(9). https://doi.org/10.3390/ijms21093191

Gan, L., Cookson, M. R., Petrucelli, L., & La Spada, A. R. (2018). Converging pathways in neurodegeneration, from genetics to mechanisms. In *Nature Neuroscience* (Vol. 21, Issue 10, pp. 1300–1309). Nature Publishing Group. https://doi.org/10.1038/s41593-018-0237-7

Gao, L., Guan, W., Wang, M., Wang, H., Yu, J., Liu, Q., Qiu, B., Yu, Y., Ping, Y., Bian, X., Shen, L., & Pei, G. (2017). Direct Generation of Human Neuronal Cells from Adult Astrocytes by Small Molecules. *Stem Cell Reports*, *8*(3), 538–547. https://doi.org/10.1016/j.stemcr.2017.01.014

Gascón, S., Masserdotti, G., Russo, G. L., & Götz, M. (2017). Direct Neuronal Reprogramming: Achievements, Hurdles, and New Roads to Success. In *Cell Stem Cell* (Vol. 21, Issue 1, pp. 18–34). Cell Press. https://doi.org/10.1016/j.stem.2017.06.011

Gascón, S., Murenu, E., Masserdotti, G., Ortega, F., Russo, G. L., Petrik, D., Deshpande, A., Heinrich, C., Karow, M., Robertson, S. P., Schroeder, T., Beckers, J., Irmler, M., Berndt, C., Angeli, J. P. F., Conrad, M., Berninger, B., & Götz, M. (2016). Identification and Successful Negotiation of a Metabolic Checkpoint in Direct Neuronal Reprogramming. *Cell Stem Cell*, *18*(3), 396–409. https://doi.org/10.1016/j.stem.2015.12.003

Gibbs, M. E., Anderson, D. G., & Hertz, L. (2006). Inhibition of glycogenolysis in astrocytes interrupts memory consolidation in young chickens. *GLIA*, *54*(3), 214–222. https://doi.org/10.1002/glia.20377

Gill, C., Phelan, J. P., Hatzipetros, T., Kidd, J. D., Tassinari, V. R., Levine, B., Wang, M. Z., Moreno, A., Thompson, K., Maier, M., Grimm, J., Gill, A., & Vieira, F. G. (2019). SOD1-positive aggregate accumulation in the CNS predicts slower disease progression and increased longevity in a mutant SOD1 mouse model of ALS. *Scientific Reports*, *9*(1). https://doi.org/10.1038/s41598-019-43164-z

Gomes, A. P., Price, N. L., Ling, A. J. Y., Moslehi, J. J., Montgomery, M. K., Rajman, L., White, J. P., Teodoro, J. S., Wrann, C. D., Hubbard, B. P., Mercken, E. M., Palmeira, C. M., De Cabo, R., Rolo, A. P., Turner, N., Bell, E. L., & Sinclair, D. A. (2013). Declining NAD+ induces a pseudohypoxic state disrupting nuclear-mitochondrial communication during aging. *Cell*, *155*(7), 1624–1638. https://doi.org/10.1016/j.cell.2013.11.037

Goubert, E., Mircheva, Y., Lasorsa, F. M., Melon, C., Profilo, E., Sutera, J., Becq, H., Palmieri, F., Palmieri, L., Aniksztejn, L., & Molinari, F. (2017). Inhibition of the mitochondrial glutamate carrier SLC25A22 in astrocytes leads to intracellular glutamate accumulation. *Frontiers in Cellular Neuroscience*, *11*. https://doi.org/10.3389/fncel.2017.00149

Graham, L. C., Eaton, S. L., Brunton, P. J., Atrih, A., Smith, C., Lamont, D. J., Gillingwater, T. H., Pennetta, G., Skehel, P., & Wishart, T. M. (2017). Proteomic profiling of neuronal mitochondria reveals modulators

of synaptic architecture. *Molecular Neurodegeneration*, *12*(1). https://doi.org/10.1186/s13024-017-0221-9

Guillemot, F., Lo, L.-C., Johnson, J. E., Auerbach, A., Anderson, D. J., & Joyner, A. L. (1993). Mammalian achaete-scute Homolog 1 Is Required for the Early Development of Olfactory and Autonomic Neurons. In *Cell* (Vol. 75).

Gusic, M., & Prokisch, H. (2021). Genetic basis of mitochondrial diseases. In *FEBS Letters*. John Wiley and Sons Inc. https://doi.org/10.1002/1873-3468.14068

Haefeli, R. H., Erb, M., Gemperli, A. C., Robay, D., Fruh, I., Anklin, C., Dallmann, R., & Gueven, N. (2011). NQo1-dependent redox cycling of idebenone: Effects on cellular redox potential and energy levels. *PLoS ONE*, *6*(3). https://doi.org/10.1371/journal.pone.0017963

Hajnóczky, G., Csordás, G., Das, S., Garcia-Perez, C., Saotome, M., Sinha Roy, S., & Yi, M. (2006). Mitochondrial calcium signalling and cell death: Approaches for assessing the role of mitochondrial Ca2+ uptake in apoptosis. *Cell Calcium*, *40*(5–6), 553–560. https://doi.org/10.1016/j.ceca.2006.08.016

Handschin, C., & Spiegelman, B. M. (2006). Peroxisome proliferator-activated receptor γ coactivator 1 coactivators, energy homeostasis, and metabolism. *Endocrine Reviews*, *27*(7), 728–735. https://doi.org/10.1210/er.2006-0037

Harding, H. P., Novoa, I., Zhang, Y., Zeng, H., Wek, R., Schapira, M., & Ron, D. (2000). Our present understanding of mammalian eIF2 ki. In *Molecular Cell* (Vol. 6).

Harris, J. J., Jolivet, R., & Attwell, D. (2012). Synaptic Energy Use and Supply. In *Neuron* (Vol. 75, Issue 5, pp. 762–777). https://doi.org/10.1016/j.neuron.2012.08.019

Hayakawa, K., Esposito, E., Wang, X., Terasaki, Y., Liu, Y., Xing, C., Ji, X., & Lo, E. H. (2016). Transfer of mitochondria from astrocytes to neurons after stroke. *Nature*, *535*(7613), 551–555. https://doi.org/10.1038/nature18928

Heinrich, C., Bergami, M., Gascón, S., Lepier, A., Viganò, F., Dimou, L., Sutor, B., Berninger, B., & Götz, M. (2014). Sox2-mediated conversion of NG2 glia into induced neurons in the injured adult cerebral cortex. *Stem Cell Reports*, *3*(6), 1000–1014. https://doi.org/10.1016/j.stemcr.2014.10.007

Heinrich, C., Blum, R., Gascón, S., Masserdotti, G., Tripathi, P., Sánchez, R., Tiedt, S., Schroeder, T., Götz, M., & Berninger, B. (2010). Directing astroglia from the cerebral cortex into subtype specific functional neurons. *PLoS Biology*, *8*(5). https://doi.org/10.1371/journal.pbio.1000373

Heinrich, C., Gascón, S., Masserdotti, G., Lepier, A., Sanchez, R., Simon-Ebert, T., Schroeder, T., Ğtz, M., & Berninger, B. (2011). Generation of subtype-specific neurons from postnatal astroglia of the mouse cerebral cortex. *Nature Protocols*, *6*(2), 214–228. https://doi.org/10.1038/nprot.2010.188

Heins, N., Malatesta, P., Cecconi, F., Nakafuku, M., Tucker, K. L., Hack, M. A., Chapouton, P., Barde, Y. A., & Goötz, M. (2002). Glial cells generate neurons: The role of the transcription factor Pax6. *Nature Neuroscience*, *5*(4), 308–315. https://doi.org/10.1038/nn828

Herrero-Mendez, A., Almeida, A., Fernández, E., Maestre, C., Moncada, S., & Bolaños, J. P. (2009). The bioenergetic and antioxidant status of neurons is controlled by continuous degradation of a key glycolytic enzyme by APC/C-Cdh1. *Nature Cell Biology*, *11*(6), 747–752. https://doi.org/10.1038/ncb1881

Hirst, J. (2013). Mitochondrial complex i. In *Annual Review of Biochemistry* (Vol. 82, pp. 551–575). https://doi.org/10.1146/annurev-biochem-070511-103700

Hofmann, K., Rodriguez-Rodriguez, R., Gaebler, A., Casals, N., Scheller, A., & Kuerschner, L. (2017).

Astrocytes and oligodendrocytes in grey and white matter regions of the brain metabolize fatty acids. *Scientific Reports*, *7*(1). https://doi.org/10.1038/s41598-017-11103-5

Hou, Y., Mattson, M. P., & Cheng, A. (2013). Permeability Transition Pore-Mediated Mitochondrial Superoxide Flashes Regulate Cortical Neural Progenitor Differentiation. *PLoS ONE*, *8*(10). https://doi.org/10.1371/journal.pone.0076721

Hu, W., Qiu, B., Guan, W., Wang, Q., Wang, M., Li, W., Gao, L., Shen, L., Huang, Y., Xie, G., Zhao, H., Jin, Y., Tang, B., Yu, Y., Zhao, J., & Pei, G. (2015). Direct Conversion of Normal and Alzheimer's Disease Human Fibroblasts into Neuronal Cells by Small Molecules. *Cell Stem Cell*, *17*(2), 204–212. https://doi.org/10.1016/j.stem.2015.07.006

Hu, X., Qin, S., Huang, X., Yuan, Y., Tan, Z., Gu, Y., Cheng, X., Wang, D., Lian, X. F., He, C., & Su, Z. (2019). Region-Restrict Astrocytes Exhibit Heterogeneous Susceptibility to Neuronal Reprogramming. *Stem Cell Reports*, *12*(2), 290–304. https://doi.org/10.1016/j.stemcr.2018.12.017

Iadecola, C., & Nedergaard, M. (2007). Glial regulation of the cerebral microvasculature. In *Nature Neuroscience* (Vol. 10, Issue 11, pp. 1369–1376). https://doi.org/10.1038/nn2003

Inak, G., Lorenz, C., Lisowski, P., Zink, A., Mlody, B., & Prigione, A. (2017). Concise Review: Induced Pluripotent Stem Cell-Based Drug Discovery for Mitochondrial Disease. In *Stem Cells* (Vol. 35, Issue 7, pp. 1655–1662). Wiley-Blackwell. https://doi.org/10.1002/stem.2637

Inak, G., Rybak-Wolf, A., Lisowski, P., Pentimalli, T. M., Jüttner, R., Glažar, P., Uppal, K., Bottani, E., Brunetti, D., Secker, C., Zink, A., Meierhofer, D., Henke, M. T., Dey, M., Ciptasari, U., Mlody, B., Hahn, T., Berruezo-Llacuna, M., Karaiskos, N., … Prigione, A. (2021). Defective metabolic programming impairs early neuronal morphogenesis in neural cultures and an organoid model of Leigh syndrome. *Nature Communications*, *12*(1). https://doi.org/10.1038/s41467-021-22117-z

Ioannou, M. S., Jackson, J., Sheu, S. H., Chang, C. L., Weigel, A. V., Liu, H., Pasolli, H. A., Xu, C. S., Pang, S., Matthies, D., Hess, H. F., Lippincott-Schwartz, J., & Liu, Z. (2019). Neuron-Astrocyte Metabolic Coupling Protects against Activity-Induced Fatty Acid Toxicity. *Cell*, *177*(6), 1522-1535.e14. https://doi.org/10.1016/j.cell.2019.04.001

Ishihara, N., Nomura, M., Jofuku, A., Kato, H., Suzuki, S. O., Masuda, K., Otera, H., Nakanishi, Y., Nonaka, I., Goto, Y. I., Taguchi, N., Morinaga, H., Maeda, M., Takayanagi, R., Yokota, S., & Mihara, K. (2009). Mitochondrial fission factor Drp1 is essential for embryonic development and synapse formation in mice. *Nature Cell Biology*, *11*(8), 958–966. https://doi.org/10.1038/ncb1907

Ito, K., Carracedo, A., Weiss, D., Arai, F., Ala, U., Avigan, D. E., Schafer, Z. T., Evans, R. M., Suda, T., Lee, C. H., & Pandolfi, P. P. (2012). A PML-PPAR-δ pathway for fatty acid oxidation regulates hematopoietic stem cell maintenance. *Nature Medicine*, *18*(9), 1350–1358. https://doi.org/10.1038/nm.2882

Itoh, Y., Esaki, T., Shimoji, K., Cook, M., Law, M. J., Kaufman, E., & Sokoloff, L. (2003). Dichloroacetate effects on glucose and lactate oxidation by neurons and astroglia in vitro and on glucose utilization by brain in vivo. *Proceedings of the National Academy of Sciences* , *100*(8), 4879–4884. www.pnas.orgcgidoi10.1073pnas.0831078100

Jain, I. H., Zazzeron, L., Goli, R., Alexa, K., Schatzman-Bone, S., Dhillon, H., Goldberger, O., Peng, J., Shalem, O., Sanjana, N. E., Zhang, F., Goessling, W., Zapol, W. M., & Mootha, V. K. (2016). Hypoxia as a therapy for mitochondrial disease. *Science*, *352*(6281), 54–61. https://doi.org/10.1126/science.aad9642

Jimenez-Blasco, D., Santofimia-Castanõ, P., Gonzalez, A., Almeida, A., & Bolanõs, J. P. (2015). Astrocyte NMDA receptors' activity sustains neuronal survival through a Cdk5-Nrf2 pathway. *Cell Death and Differentiation*, *22*(11), 1877–1889. https://doi.org/10.1038/cdd.2015.49

Kandimalla, R., Manczak, M., Yin, X., Wang, R., & Reddy, P. H. (2018). Hippocampal phosphorylated tau induced cognitive decline, dendritic spine loss and mitochondrial abnormalities in a mouse model of Alzheimer's disease. *Human Molecular Genetics*, *27*(1), 30–40. https://doi.org/10.1093/hmg/ddx381

Karow, M., Gray Camp, J., Falk, S., Gerber, T., Pataskar, A., Gac-Santel, M., Kageyama, J., Brazovskaja, A., Garding, A., Fan, W., Riedemann, T., Casamassa, A., Smiyakin, A., Schichor, C., Götz, M., Tiwari, V. K., Treutlein, B., & Berninger, B. (2018). Direct pericyte-to-neuron reprogramming via unfolding of a neural stem cell-like program. *Nature Neuroscience*, *21*(7), 932–940. https://doi.org/10.1038/s41593-018-0168-3

Karow, M., Sánchez, R., Schichor, C., Masserdotti, G., Ortega, F., Heinrich, C., Gascón, S., Khan, M. A., Lie, D. C., Dellavalle, A., Cossu, G., Goldbrunner, R., Götz, M., & Berninger, B. (2012). Reprogramming of pericyte-derived cells of the adult human brain into induced neuronal cells. *Cell Stem Cell*, *11*(4), 471–476. https://doi.org/10.1016/j.stem.2012.07.007

Kasischke, K. A., Vishwasrao, H. D., Fisher, P. J., Zipfel, W. R., & Webb, W. W. (2004). Neural Activity Triggers Neuronal Oxidative Metabolism Followed by Astrocytic Glycolysis. *Science*, *305*(5680), 99–103.

Katsyuba, E., & Auwerx, J. (2017). Modulating NAD + metabolism, from bench to bedside . *The EMBO Journal*, *36*(18), 2670–2683. https://doi.org/10.15252/embj.201797135

Keller, J. N., Schmitt, F. A., Scheff, S. W., Ding, Q., Chen, Q., Butterfield, D. A., & Markesbery, W. R. (2005). Evidence of increased oxidative damage in subjects with mild cognitive impairment. *Neurology* , *64*(7).

Khacho, M., Clark, A., Svoboda, D. S., MacLaurin, J. G., Lagace, D. C., Park, D. S., & Slack, R. S. (2017). Mitochondrial dysfunction underlies cognitive defects as a result of neural stem cell depletion and impaired neurogenesis. *Human Molecular Genetics*, *26*(17), 3327–3341. https://doi.org/10.1093/hmg/ddx217

Khan, N. A., Auranen, M., Paetau, I., Pirinen, E., Euro, L., Forsström, S., Pasila, L., Velagapudi, V., Carroll, C. J., Auwerx, J., & Suomalainen, A. (2014). Effective treatment of mitochondrial myopathy by nicotinamide riboside, a vitamin B3. *EMBO Molecular Medicine*, *6*(6), 721–731. https://doi.org/10.1002/emmm.201403943

Kim, J. A., Wei, Y., & Sowers, J. R. (2008). Role of mitochondrial dysfunction in insulin resistance. In *Circulation Research* (Vol. 102, Issue 4, pp. 401–414). https://doi.org/10.1161/CIRCRESAHA.107.165472

Klopstock, T., Yu-Wai-Man, P., Dimitriadis, K., Rouleau, J., Heck, S., Bailie, M., Atawan, A., Chattopadhyay, S., Schubert, M., Garip, A., Kernt, M., Petraki, D., Rummey, C., Leinonen, M., Metz, G., Griffiths, P. G., Meier, T., & Chinnery, P. F. (2011). A randomized placebo-controlled trial of idebenone in Leber's hereditary optic neuropathy. *Brain*, *134*(9), 2677–2686. https://doi.org/10.1093/brain/awr170

Knobloch, M., Pilz, G. A., Ghesquière, B., Kovacs, W. J., Wegleiter, T., Moore, D. L., Hruzova, M., Zamboni, N., Carmeliet, P., & Jessberger, S. (2017). A Fatty Acid Oxidation-Dependent Metabolic Shift Regulates Adult Neural Stem Cell Activity. *Cell Reports*, *20*(9), 2144–2155. https://doi.org/10.1016/j.celrep.2017.08.029

Kondo, T., Funayama, M., Tsukita, K., Hotta, A., Yasuda, A., Nori, S., Kaneko, S., Nakamura, M., Takahashi, R., Okano, H., Yamanaka, S., & Inoue, H. (2014). Focal transplantation of human iPSC-derived glial-rich neural progenitors improves lifespan of ALS mice. *Stem Cell Reports*, *3*(2), 242–249. https://doi.org/10.1016/j.stemcr.2014.05.017

Koopman, W. J. H., Distelmaier, F., Smeitink, J. A. M., & Willems, P. H. G. M. (2013). OXPHOS mutations and neurodegeneration. In *EMBO Journal* (Vol. 32, Issue 1, pp. 9–29). https://doi.org/10.1038/emboj.2012.300

Koopman, W. J. H., Willems, P. H. G. M., & Smeitink, J. A. M. (2012). Monogenic Mitochondrial Disorders. *N Engl J Med*, *366*, 1132–1173.

Kosa, P., Wu, T., Phillips, J., Leinonen, M., Masvekar, R., Komori, M., Wichman, A., Sandford, M., & Bielekova, B. (2020). Idebenone does not inhibit disability progression in primary progressive MS. *Multiple Sclerosis and Related Disorders*, *45*. https://doi.org/10.1016/j.msard.2020.102434

Kruse, S. E., Watt, W. C., Marcinek, D. J., Kapur, R. P., Schenkman, K. A., & Palmiter, R. D. (2008). Mice with Mitochondrial Complex I Deficiency Develop a Fatal Encephalomyopathy. *Cell Metabolism*, *7*(4), 312–320. https://doi.org/10.1016/j.cmet.2008.02.004

Laguesse, S., Creppe, C., Nedialkova, D. D., Prévot, P. P., Borgs, L., Huysseune, S., Franco, B., Duysens, G., Krusy, N., Lee, G., Thelen, N., Thiry, M., Close, P., Chariot, A., Malgrange, B., Leidel, S. A., Godin, J. D., & Nguyen, L. (2015). A Dynamic Unfolded Protein Response Contributes to the Control of Cortical Neurogenesis. *Developmental Cell*, *35*(5), 553–567. https://doi.org/10.1016/j.devcel.2015.11.005

Lautrup, S., Sinclair, D. A., Mattson, M. P., & Fang, E. F. (2019). NAD+ in Brain Aging and Neurodegenerative Disorders. In *Cell Metabolism* (Vol. 30, Issue 4, pp. 630–655). Cell Press. https://doi.org/10.1016/j.cmet.2019.09.001

Lazarou, M., McKenzie, M., Ohtake, A., Thorburn, D. R., & Ryan, M. T. (2007). Analysis of the Assembly Profiles for Mitochondrial- and Nuclear-DNA-Encoded Subunits into Complex I. *Molecular and Cellular Biology*, *27*(12), 4228–4237. https://doi.org/10.1128/mcb.00074-07

Lee, C. F., Caudal, A., Abell, L., Nagana Gowda, G. A., & Tian, R. (2019). Targeting NAD + Metabolism as Interventions for Mitochondrial Disease. *Scientific Reports*, *9*(1). https://doi.org/10.1038/s41598-019-39419-4

Lee, M., Sim, H., Ahn, H., Ha, J., Baek, A., Jeon, Y. J., Son, M. Y., & Kim, J. (2019). Direct reprogramming to human induced neuronal progenitors from fibroblasts of familial and sporadic parkinson's disease patients. *International Journal of Stem Cells*, *12*(3), 474–483. https://doi.org/10.15283/ijsc19075

Lerner, A. G., Upton, J. P., Praveen, P. V. K., Ghosh, R., Nakagawa, Y., Igbaria, A., Shen, S., Nguyen, V., Backes, B. J., Heiman, M., Heintz, N., Greengard, P., Hui, S., Tang, Q., Trusina, A., Oakes, S. A., & Papa, F. R. (2012). IRE1α induces thioredoxin-interacting protein to activate the NLRP3 inflammasome and promote programmed cell death under irremediable ER stress. *Cell Metabolism*, *16*(2), 250–264. https://doi.org/10.1016/j.cmet.2012.07.007

Letts, J. A., & Sazanov, L. A. (2017). Clarifying the supercomplex: The higher-order organization of the mitochondrial electron transport chain. In *Nature Structural and Molecular Biology* (Vol. 24, Issue 10, pp. 800–808). Nature Research. https://doi.org/10.1038/nsmb.3460

Li, A., Song, N. J., Riesenberg, B. P., & Li, Z. (2020). The Emerging Roles of Endoplasmic Reticulum Stress in

Balancing Immunity and Tolerance in Health and Diseases: Mechanisms and Opportunities. In *Frontiers in Immunology* (Vol. 10). Frontiers Media S.A. https://doi.org/10.3389/fimmu.2019.03154

Li, X., Zuo, X., Jing, J., Ma, Y., Wang, J., Liu, D., Zhu, J., Du, X., Xiong, L., Du, Y., Xu, J., Xiao, X., Wang, J., Chai, Z., Zhao, Y., & Deng, H. (2015). Small-Molecule-Driven Direct Reprogramming of Mouse Fibroblasts into Functional Neurons. *Cell Stem Cell*, *17*(2), 195–203. https://doi.org/10.1016/j.stem.2015.06.003

Liang, X. G., Tan, C., Wang, C. K., Tao, R. R., Huang, Y. J., Ma, K. F., Fukunaga, K., Huang, M. Z., & Han, F. (2018). Myt1l induced direct reprogramming of pericytes into cholinergic neurons. *CNS Neuroscience and Therapeutics*, *24*(9), 801–809. https://doi.org/10.1111/cns.12821

Liang, X., Kristiansen, C. K., Vatne, G. H., Hong, Y., & Bindoff, L. A. (2020). Patient-specific neural progenitor cells derived from induced pluripotent stem cells offer a promise of good models for mitochondrial disease. In *Cell and Tissue Research* (Vol. 380, Issue 1, pp. 15–30). Springer. https://doi.org/10.1007/s00441-019-03164-x

Liddelow, S. A., & Barres, B. A. (2017). Reactive Astrocytes: Production, Function, and Therapeutic Potential. In *Immunity* (Vol. 46, Issue 6, pp. 957–967). Cell Press. https://doi.org/10.1016/j.immuni.2017.06.006

Lin, J., Handschin, C., & Spiegelman, B. M. (2005). Metabolic control through the PGC-1 family of transcription coactivators. In *Cell Metabolism* (Vol. 1, Issue 6, pp. 361–370). https://doi.org/10.1016/j.cmet.2005.05.004

Lin, M. T., & Beal, M. F. (2006). Mitochondrial dysfunction and oxidative stress in neurodegenerative diseases. *Nature* , *443*, 787–795.

Liu, F., Zhang, Y., Chen, F., Yuan, J., Li, S., Han, S., Lu, D., Geng, J., Rao, Z., Sun, L., Xu, J., Shi, Y., Wang, X., & Liu, Y. (2021). Neurog2 directly converts astrocytes into functional neurons in midbrain and spinal cord. *Cell Death & Disease*, *12*(3), 225. https://doi.org/10.1038/s41419-021-03498-x

Liu, X., Li, F., Stubblefield, E. A., Blanchard, B., Richards, T. L., Larson, G. A., He, Y., Huang, Q., Tan, A. C., Zhang, D., Benke, T. A., Sladek, J. R., Zahniser, N. R., & Li, C. Y. (2012). Direct reprogramming of human fibroblasts into dopaminergic neuron-like cells. *Cell Research*, *22*(2), 321–332. https://doi.org/10.1038/cr.2011.181

Liu, Y., Yu, C., Daley, T. P., Wang, F., Cao, W. S., Bhate, S., Lin, X., Still, C., Liu, H., Zhao, D., Wang, H., Xie, X. S., Ding, S., Wong, W. H., Wernig, M., & Qi, L. S. (2018). CRISPR Activation Screens Systematically Identify Factors that Drive Neuronal Fate and Reprogramming. *Cell Stem Cell*, *23*(5), 758-771.e8. https://doi.org/10.1016/j.stem.2018.09.003

Llorens-Bobadilla, E., Zhao, S., Baser, A., Saiz-Castro, G., Zwadlo, K., & Martin-Villalba, A. (2015). Single-Cell Transcriptomics Reveals a Population of Dormant Neural Stem Cells that Become Activated upon Brain Injury. *Cell Stem Cell*, *17*(3), 329–340. https://doi.org/10.1016/j.stem.2015.07.002

Lopez-Fabuel, I., Douce, J. Le, Logan, A., James, A. M., Bonvento, G., Murphy, M. P., Almeida, A., & Bolaños, J. P. (2016). Complex I assembly into supercomplexes determines differential mitochondrial ROS production in neurons and astrocytes. *Proceedings of the National Academy of Sciences*, *113*(46), 13063–13068. https://doi.org/10.1073/PNAS.1613701113

Lorenz, C., Lesimple, P., Bukowiecki, R., Zink, A., Inak, G., Mlody, B., Singh, M., Semtner, M., Mah, N., Auré, K., Leong, M., Zabiegalov, O., Lyras, E. M., Pfiffer, V., Fauler, B., Eichhorst, J., Wiesner, B.,

Huebner, N., Priller, J., … Prigione, A. (2017). Human iPSC-Derived Neural Progenitors Are an Effective Drug Discovery Model for Neurological mtDNA Disorders. *Cell Stem Cell*, *20*(5), 659-674.e9. https://doi.org/10.1016/j.stem.2016.12.013

Lu, W., Karuppagounder, S. S., Springer, D. A., Allen, M. D., Zheng, L., Chao, B., Zhang, Y., Dawson, V. L., Dawson, T. M., & Lenardo, M. (2014). Genetic deficiency of the mitochondrial protein PGAM5 causes a Parkinsons-like movement disorder. *Nature Communications*, *5*. https://doi.org/10.1038/ncomms5930

Lu, W., Sun, J., Yoon, J. S., Zhang, Y., Zheng, L., Murphy, E., Mattson, M. P., & Lenardo, M. J. (2016). Mitochondrial protein PGAM5 regulates mitophagic protection against cell necroptosis. *PLoS ONE*, *11*(1). https://doi.org/10.1371/journal.pone.0147792

Lu, Y. L., & Yoo, A. S. (2018). Mechanistic insights into MicroRNA-induced neuronal reprogramming of human adult fibroblasts. In *Frontiers in Neuroscience* (Vol. 12, Issue AUG). Frontiers Media S.A. https://doi.org/10.3389/fnins.2018.00522

Ma, H., Folmes, C. D. L., Wu, J., Morey, R., Mora-Castilla, S., Ocampo, A., Ma, L., Poulton, J., Wang, X., Ahmed, R., Kang, E., Lee, Y., Hayama, T., Li, Y., Van Dyken, C., Gutierrez, N. M., Tippner-Hedges, R., Koski, A., Mitalipov, N., … Mitalipov, S. (2015). Metabolic rescue in pluripotent cells from patients with mtDNA disease. *Nature*, *524*(7564), 234–238. https://doi.org/10.1038/nature14546

Ma, K., Zhang, Z., Chang, R., Cheng, H., Mu, C., Zhao, T., Chen, L., Zhang, C., Luo, Q., Lin, J., Zhu, Y., & Chen, Q. (2020). Dynamic PGAM5 multimers dephosphorylate BCL-xL or FUNDC1 to regulate mitochondrial and cellular fate. *Cell Death and Differentiation*, *27*(3), 1036–1051. https://doi.org/10.1038/s41418-019-0396-4

Magistretti, P. J., & Allaman, I. (2015). A Cellular Perspective on Brain Energy Metabolism and Functional Imaging. In *Neuron* (Vol. 86, Issue 4, pp. 883–901). Cell Press. https://doi.org/10.1016/j.neuron.2015.03.035

Magistretti, P. J., & Allaman, I. (2018). Lactate in the brain: From metabolic end-product to signalling molecule. In *Nature Reviews Neuroscience* (Vol. 19, Issue 4, pp. 235–249). Nature Publishing Group. https://doi.org/10.1038/nrn.2018.19

Marchi, S., Giorgi, C., Suski, J. M., Agnoletto, C., Bononi, A., Bonora, M., De Marchi, E., Missiroli, S., Patergnani, S., Poletti, F., Rimessi, A., Duszynski, J., Wieckowski, M. R., & Pinton, P. (2012). Mitochondria-Ros Crosstalk in the Control of Cell Death and Aging. *Journal of Signal Transduction*, *2012*, 1–17. https://doi.org/10.1155/2012/329635

Martinez-Vicente, M. (2017). Neuronal mitophagy in neurodegenerative diseases. In *Frontiers in Molecular Neuroscience* (Vol. 10). Frontiers Research Foundation. https://doi.org/10.3389/fnmol.2017.00064

Masserdotti, G., Gillotin, S., Sutor, B., Drechsel, D., Irmler, M., Jørgensen, H. F., Sass, S., Theis, F. J., Beckers, J., Berninger, B., Guillemot, F., & Götz, M. (2015). Transcriptional Mechanisms of Proneural Factors and REST in Regulating Neuronal Reprogramming of Astrocytes. *Cell Stem Cell*, *17*(1), 74–88. https://doi.org/10.1016/j.stem.2015.05.014

Mathiisen, T. M., Lehre, K. P., Danbolt, N. C., & Ottersen, O. P. (2010). The perivascular astroglial sheath provides a complete covering of the brain microvessels: An electron microscopic 3D reconstruction. *GLIA*, *58*(9), 1094–1103. https://doi.org/10.1002/glia.20990

Matilainen, O., Quirós, P. M., & Auwerx, J. (2017). Mitochondria and Epigenetics – Crosstalk in Homeostasis

and Stress. In *Trends in Cell Biology* (Vol. 27, Issue 6, pp. 453–463). Elsevier Ltd. https://doi.org/10.1016/j.tcb.2017.02.004

Mattugini, N., Bocchi, R., Scheuss, V., Russo, G. L., Torper, O., Lao, C. L., & Götz, M. (2019). Inducing Different Neuronal Subtypes from Astrocytes in the Injured Mouse Cerebral Cortex. *Neuron*, *103*(6), 1086-1095.e5. https://doi.org/10.1016/j.neuron.2019.08.009

McCarty, N. S., Graham, A. E., Studená, L., & Ledesma-Amaro, R. (2020). Multiplexed CRISPR technologies for gene editing and transcriptional regulation. In *Nature Communications* (Vol. 11, Issue 1). Nature Research. https://doi.org/10.1038/s41467-020-15053-x

McKenna, M. C. (2013). Glutamate pays its own way in astrocytes. In *Frontiers in Endocrinology* (Vol. 4, Issue DEC). Frontiers Media SA. https://doi.org/10.3389/fendo.2013.00191

McKenna, M. C. (2007). The glutamate-glutamine cycle is not stoichiometric: Fates of glutamate in brain. *Journal of Neuroscience Research*, *85*(15), 3347–3358. https://doi.org/10.1002/jnr.21444

McKenna, M. C., Stridh, M. H., McNair, L. F., Sonnewald, U., Waagepetersen, H. S., & Schousboe, A. (2016). Glutamate oxidation in astrocytes: Roles of glutamate dehydrogenase and aminotransferases. In *Journal of Neuroscience Research* (Vol. 94, Issue 12, pp. 1561–1571). John Wiley and Sons Inc. https://doi.org/10.1002/jnr.23908

Mederos, S., González-Arias, C., & Perea, G. (2018). Astrocyte–Neuron Networks: A Multilane Highway of Signaling for Homeostatic Brain Function. *Frontiers in Synaptic Neuroscience*, *10*. https://doi.org/10.3389/fnsyn.2018.00045

Melcher, M., Danhauser, K., Seibt, A., Degistirici, Ö., Baertling, F., Kondadi, A. K., Reichert, A. S., Koopman, W. J. H., Willems, P. H. G. M., Rodenburg, R. J., Mayatepek, E., Meisel, R., & Distelmaier, F. (2017). Modulation of oxidative phosphorylation and redox homeostasis in mitochondrial NDUFS4 deficiency via mesenchymal stem cells. *Stem Cell Research and Therapy*, *8*(1). https://doi.org/10.1186/s13287-017-0601-7

Mergenthaler, P., Lindauer, U., Dienel, G. A., & Meisel, A. (2013). Sugar for the brain: The role of glucose in physiological and pathological brain function. In *Trends in Neurosciences* (Vol. 36, Issue 10, pp. 587–597). https://doi.org/10.1016/j.tins.2013.07.001

Mertens, J., Marchetto, M. C., Bardy, C., & Gage, F. H. (2016). Evaluating cell reprogramming, differentiation and conversion technologies in neuroscience. *Nature Reviews Neuroscience*, *17*(7), 424–437. https://doi.org/10.1038/nrn.2016.46

Misgeld, T., & Schwarz, T. L. (2017). Mitostasis in Neurons: Maintaining Mitochondria in an Extended Cellular Architecture. In *Neuron* (Vol. 96, Issue 3, pp. 651–666). Cell Press. https://doi.org/10.1016/j.neuron.2017.09.055

Mishra, P., & Chan, D. C. (2014). Mitochondrial dynamics and inheritance during cell division, development and disease. In *Nature Reviews Molecular Cell Biology* (Vol. 15, Issue 10, pp. 634–646). Nature Publishing Group. https://doi.org/10.1038/nrm3877

Missiroli, S., Genovese, I., Perrone, M., Vezzani, B., Vitto, V. A. M., & Giorgi, C. (2020). The Role of Mitochondria in Inflammation: From Cancer to Neurodegenerative Disorders. *Journal of Clinical Medicine*, *9*(3), 740. https://doi.org/10.3390/jcm9030740

Missiroli, S., Patergnani, S., Caroccia, N., Pedriali, G., Perrone, M., Previati, M., Wieckowski, M. R., & Giorgi,

C. (2018). Mitochondria-associated membranes (MAMs) and inflammation. *Cell Death and Disease*, *9*(3). https://doi.org/10.1038/s41419-017-0027-2

Molinari, F., Kaminska, A., Fiermonte, G., Boddaert, N., Raas-Rothschild, A., Plouin, P., Palmieri, L., Brunelle, F., Palmieri, F., Dulac, O., Munnich, A., & Colleaux, L. (2009). Mutations in the mitochondrial glutamate carrier SLC25A22 in neonatal epileptic encephalopathy with suppression bursts. *Clinical Genetics*, *76*(2), 188–194. https://doi.org/10.1111/j.1399-0004.2009.01236.x

Molinari, Florence, Raas-Rothschild, A., Ne Rio, M., Fiermonte, G., Encha-Razavi, F., Palmieri, L., Palmieri, F., Ben-Neriah, Z., Kadhom, N., Vekemans, M., Attié-Bitach, T., Munnich, A., Rustin, P., & Colleaux, L. (2005). Impaired Mitochondrial Glutamate Transport in Autosomal Recessive Neonatal Myoclonic Epilepsy. In *Am. J. Hum. Genet* (Vol. 76).

Mootha, V. K., Bunkenborg, J., Olsen, J. V, Hjerrild, M., Wisniewski, J. R., Stahl, E., Bolouri, M. S., Ray, H. N., Sihag, S., Kamal, M., Patterson, N., Lander, E. S., & Mann, M. (2003). Integrated Analysis of Protein Composition, Tissue Diversity, and Gene Regulation in Mouse Mitochondria ates the majority of cellular reactive oxygen species. In *Cell* (Vol. 115). http://mips.gsf.de/proj/medgen/mitop/

Morales, I., Sanchez, A., Puertas-Avendaño, R., Rodriguez-Sabate, C., Perez-Barreto, A., & Rodriguez, M. (2020). Neuroglial transmitophagy and Parkinson's disease. *GLIA*, *68*(11), 2277–2299. https://doi.org/10.1002/glia.23839

Morita, M., Ikeshima-Kataoka, H., Kreft, M., Vardjan, N., Zorec, R., & Noda, M. (2019). Metabolic plasticity of astrocytes and aging of the brain. In *International Journal of Molecular Sciences* (Vol. 20, Issue 4). MDPI AG. https://doi.org/10.3390/ijms20040941

Motori, E., Puyal, J., Toni, N., Ghanem, A., Angeloni, C., Malaguti, M., Cantelli-Forti, G., Berninger, B., Conzelmann, K. K., Götz, M., Winklhofer, K. F., Hrelia, S., & Bergami, M. (2013). Inflammation-induced alteration of astrocyte mitochondrial dynamics requires autophagy for mitochondrial network maintenance. *Cell Metabolism*, *18*(6), 844–859. https://doi.org/10.1016/j.cmet.2013.11.005

Nagoshi, N., & Okano, H. (2018). iPSC-derived neural precursor cells: potential for cell transplantation therapy in spinal cord injury. In *Cellular and Molecular Life Sciences* (Vol. 75, Issue 6, pp. 989–1000). Birkhauser Verlag AG. https://doi.org/10.1007/s00018-017-2676-9

Nakada, Y., Hunsaker, T. L., Henke, R. M., & Johnson, J. E. (2004). Distinct domains within Mash1 and Math1 are required for function in neuronal differentiation versus neuronal cell-type specification. In *Development* (Vol. 131, Issue 6, pp. 1319–1330). https://doi.org/10.1242/dev.01008

Namba, T. (2019). BAP31 regulates mitochondrial function via interaction with Tom40 within ER-mitochondria contact sites. *Namba, Sci. Adv*, *5*, 1386–1398.

Nelson, S. R., Schulz, D. W., Passonneau, J. V., & Lowry, O. H. (1968). Control of glycogen levels in brain. *Journal of Neurochemistry*, *15*, 1271–1279.

Nilsen, J., Irwin, R. W., Gallaher, T. K., & Brinton, R. D. (2007). Estradiol in vivo regulation of brain mitochondrial proteome. *Journal of Neuroscience*, *27*(51), 14069–14077. https://doi.org/10.1523/JNEUROSCI.4391-07.2007

Nissen, J. D., Pajecka, K., Stridh, M. H., Skytt, D. M., & Waagepetersen, H. S. (2015). Dysfunctional TCA-Cycle Metabolism in Glutamate Dehydrogenase Deficient Astrocytes. *GLIA*, *63*(12), 2313–2326. https://doi.org/10.1002/glia.22895

Okita, K., Ichisaka, T., & Yamanaka, S. (2007). Generation of germline-competent induced pluripotent stem cells. *Nature*, *448*(7151), 313–317. https://doi.org/10.1038/nature05934

Ortigoza-Escobar, J. D., Oyarzabal, A., Montero, R., Artuch, R., Jou, C., Jiménez, C., Gort, L., Briones, P., Muchart, J., López-Gallardo, E., Emperador, S., Pesini, E. R., Montoya, J., Pérez, B., Rodríguez-Pombo, P., & Pérez-Dueñas, B. (2016). Ndufs4 related Leigh syndrome: A case report and review of the literature. In *Mitochondrion* (Vol. 28, pp. 73–78). Elsevier B.V. https://doi.org/10.1016/j.mito.2016.04.001

Pagliarini, D. J., Calvo, S. E., Chang, B., Sheth, S. A., Vafai, S. B., Ong, S. E., Walford, G. A., Sugiana, C., Boneh, A., Chen, W. K., Hill, D. E., Vidal, M., Evans, J. G., Thorburn, D. R., Carr, S. A., & Mootha, V. K. (2008). A Mitochondrial Protein Compendium Elucidates Complex I Disease Biology. *Cell*, *134*(1), 112–123. https://doi.org/10.1016/j.cell.2008.06.016

Palmieri, F., Scarcia, P., & Monné, M. (2020). Diseases caused by mutations in mitochondrial carrier genes SLC25: A review. In *Biomolecules* (Vol. 10, Issue 4). MDPI AG. https://doi.org/10.3390/biom10040655

Pang, Z. P., Yang, N., Vierbuchen, T., Ostermeier, A., Fuentes, D. R., Yang, T. Q., Citri, A., Sebastiano, V., Marro, S., Südhof, T. C., & Wernig, M. (2011). Induction of human neuronal cells by defined transcription factors. In *Nature* (Vol. 476, Issue 7359, pp. 220–223). https://doi.org/10.1038/nature10202

Panov, A., Orynbayeva, Z., Vavilin, V., & Lyakhovich, V. (2014). Fatty acids in energy metabolism of the central nervous system. In *BioMed Research International* (Vol. 2014). Hindawi Publishing Corporation. https://doi.org/10.1155/2014/472459

Papa, S., Rasmo, D. De, Technikova-Dobrova, Z., Panelli, D., Signorile, A., Scacco, S., Petruzzella, V., Papa, F., Palmisano, G., Gnoni, A., Micelli, L., & Sardanelli, A. M. (2012). Respiratory chain complex I, a main regulatory target of the cAMP/PKA pathway is defective in different human diseases. In *FEBS Letters* (Vol. 586, Issue 5, pp. 568–577). https://doi.org/10.1016/j.febslet.2011.09.019

Park, S., Choi, S. G., Yoo, S. M., Son, J. H., & Jung, Y. K. (2014). Choline dehydrogenase interacts with SQSTM1/p62 to recruit LC3 and stimulate mitophagy. *Autophagy*, *10*(11), 1906–1920. https://doi.org/10.4161/auto.32177

Pellerin, L, & Magistretti, P. J. (1994). Glutamate uptake into astrocytes stimulates aerobic glycolysis: a mechanism coupling neuronal activity to glucose utilization. *Proceedings of the National Academy of Sciences of the United States of America*, *91*(22), 10625–10629. https://doi.org/10.1073/pnas.91.22.10625

Pellerin, Luc, Pellegri, G., Bittar, P. G., Charnay, Y., Bouras, C., Martin, J.-L., Stella, N., & Magistretti, P. J. (1998). Astrocyte-Neuron Metabolic Pathways Evidence Supporting the Existence of an Activity-Dependent Astrocyte-Neuron Lactate Shuttle. *Developmental Neuroscience*, *20*, 291–299. https://doi.org/https://doi.org/10.1159/000017324

Perevoshchikova, I. V., Quinlan, C. L., Orr, A. L., Gerencser, A. A., & Brand, M. D. (2013). Sites of superoxide and hydrogen peroxide production during fatty acid oxidation in rat skeletal muscle mitochondria. *Free Radical Biology and Medicine*, *61*, 298–309. https://doi.org/10.1016/j.freeradbiomed.2013.04.006

Petruzzella, V., Vergari, R., Puzziferri, I., Boffoli, D., Lamantea, E., Zeviani, M., & Papa, S. (2001). A nonsense mutation in the NDUFS4 gene encoding the 18 kDa (AQDQ) subunit of complex I abolishes assembly and activity of the complex in a patient with Leigh-like syndrome. In *Human Molecular Genetics* (Vol. 10, Issue 5).

Pfeiffer-Guglielmi, B., Fleckenstein, B., Jung, G., & Hamprech, B. (2003). Immunocytochemical localization of

glycogen phosphorylase isozymes in rat nervous tissues by using isozyme-specific antibodies. *Journal of Neurochemistry*, *85*(1), 73–81. https://doi.org/10.1046/j.1471-4159.2003.01644.x

Pfisterer, U., Kirkeby, A., Torper, O., Wood, J., Nelander, J., Dufour, A., Björklund, A., Lindvall, O., Jakobsson, J., & Parmar, M. (2011). Direct conversion of human fibroblasts to dopaminergic neurons. *Proceedings of the National Academy of Sciences of the United States of America*, *108*(25), 10343–10348. https://doi.org/10.1073/pnas.1105135108

Pharaoh, G., Sataranatarajan, K., Street, K., Hill, S., Gregston, J., Ahn, B., Kinter, C., Kinter, M., & Van Remmen, H. (2019). Metabolic and stress response changes precede disease onset in the spinal cord of mutant SOD1 ALS mice. *Frontiers in Neuroscience*, *13*(MAY). https://doi.org/10.3389/fnins.2019.00487

Polyzos, A. A., Lee, D. Y., Datta, R., Hauser, M., Budworth, H., Holt, A., Mihalik, S., Goldschmidt, P., Frankel, K., Trego, K., Bennett, M. J., Vockley, J., Xu, K., Gratton, E., & McMurray, C. T. (2019). Metabolic Reprogramming in Astrocytes Distinguishes Region-Specific Neuronal Susceptibility in Huntington Mice. *Cell Metabolism*, *29*(6), 1258-1273.e11. https://doi.org/10.1016/j.cmet.2019.03.004

Porporato, P. E., Filigheddu, N., Pedro, J. M. B. S., Kroemer, G., & Galluzzi, L. (2018). Mitochondrial metabolism and cancer. In *Cell Research* (Vol. 28, Issue 3, pp. 265–280). Nature Publishing Group. https://doi.org/10.1038/cr.2017.155

Prigione, A., Fauler, B., Lurz, R., Lehrach, H., & Adjaye, J. (2010). The senescence-related mitochondrial/oxidative stress pathway is repressed in human induced pluripotent stem cells. *Stem Cells*, *28*(4), 721–733. https://doi.org/10.1002/stem.404

Prigione, A., Hossini, A. M., Lichtner, B., Serin, A., Fauler, B., Megges, M., Lurz, R., Lehrach, H., Makrantonaki, E., Zouboulis, C. C., & Adjaye, J. (2011). Mitochondrial-Associated cell death mechanisms are reset to an Embryonic-Like state in aged Donor-Derived iPS cells harboring chromosomal aberrations. *PLoS ONE*, *6*(11). https://doi.org/10.1371/journal.pone.0027352

Quintana, A., Kruse, S. E., Kapur, R. P., Sanz, E., & Palmiter, R. D. (2010). Complex I deficiency due to loss of Ndufs4 in the brain results in progressive encephalopathy resembling Leigh syndrome. *Proceedings of the National Academy of Sciences of the United States of America*, *107*(24), 10996–11001. https://doi.org/10.1073/pnas.1006214107

Rahman, S., Blok, R. B., Dahl, H.-H. M., Danks, D. M., Kirby, D. M., Chow, C. W., Christodoulou, J., & Thorburn, D. R. (1996). Leigh Syndrome: Clinical Features and Biochemical and DNA Abnormalities. *Annals of Neurology*, *39*(3), 343–351.

Remondelli, P., & Renna, M. (2017). The endoplasmic reticulum unfolded protein response in neurodegenerative disorders and its potential therapeutic significance. In *Frontiers in Molecular Neuroscience* (Vol. 10). Frontiers Media S.A. https://doi.org/10.3389/fnmol.2017.00187

Ren, D., Zheng, P., Zou, S., Gong, Y., Wang, Y., Duan, J., Deng, J., Chen, H., Feng, J., Zhong, C., & Chen, W. (2021). GJA1-20K Enhances Mitochondria Transfer from Astrocytes to Neurons via Cx43-TnTs After Traumatic Brain Injury. *Cellular and Molecular Neurobiology*. https://doi.org/10.1007/s10571-021-01070-x

Rharass, T., Lemcke, H., Lantow, M., Kuznetsov, S. A., Weiss, D. G., & Panáková, D. (2014). Ca2+-mediated Mitochondrial Reactive Oxygen Species Metabolism Augments Wnt/β-Catenin Pathway Activation to Facilitate Cell Differentiation. *Journal of Biological Chemistry*, *289*(40), 27937–27951.

https://doi.org/10.1074/jbc.m114.573519

Rich, L. R., Harris, W., & Brown, A. M. (2019). The Role of Brain Glycogen in Supporting Physiological Function. In *Frontiers in Neuroscience* (Vol. 13). Frontiers Media S.A. https://doi.org/10.3389/fnins.2019.01176

Rivetti Di Val Cervo, P., Romanov, R. A., Spigolon, G., Masini, D., Martín-Montañez, E., Toledo, E. M., La Manno, G., Feyder, M., Pifl, C., Ng, Y. H., Sánchez, S. P., Linnarsson, S., Wernig, M., Harkany, T., Fisone, G., & Arenas, E. (2017). Induction of functional dopamine neurons from human astrocytes in vitro and mouse astrocytes in a Parkinson's disease model. *Nature Biotechnology*, *35*(5), 444–452. https://doi.org/10.1038/nbt.3835

Rodolfo, C., Campello, S., & Cecconi, F. (2018). Mitophagy in neurodegenerative diseases. *Neurochemistry International*, *117*. https://doi.org/10.1016/j.neuint.2017.08.004

Rosenberg, P. A., & Aizenman, E. (1989). Hundred-fold increase in neuronal vulnerability to glutamate toxicity in astrocyte-poor cultures of rat cerebral cortex. *Neuroscience Letters*, *103*(2), 162–168.

Rothstein, J. D., Dykes-Hoberg, M., Pardo, C. a., Bristol, L. a., Jin, L., Kuncl, R. W., Kanai, Y., Hediger, M. a., Wang, Y., Schielke, J. P., & Welty, D. F. (1996). Knockout of glutamate transporters reveals a major role for astroglial transport in excitotoxicity and clearance of glutamate. *Neuron*, *16*(3), 675–686. https://doi.org/10.1016/S0896-6273(00)80086-0

Rubio, A., Luoni, M., Giannelli, S. G., Radice, I., Iannielli, A., Cancellieri, C., Di Berardino, C., Regalia, G., Lazzari, G., Menegon, A., Taverna, S., & Broccoli, V. (2016). Rapid and efficient CRISPR/Cas9 gene inactivation in human neurons during human pluripotent stem cell differentiation and direct reprogramming. *Scientific Reports*, *6*. https://doi.org/10.1038/srep37540

Rudenok, M. M., Alieva, A. K., Starovatykh, J. S., Nesterov, M. S., Stanishevskaya, V. A., Kolacheva, A. A., Ugryumov, M. V., Slominsky, P. A., & Shadrina, M. I. (2020). Expression analysis of genes involved in mitochondrial biogenesis in mice with MPTP-induced model of Parkinson's disease. *Molecular Genetics and Metabolism Reports*, *23*. https://doi.org/10.1016/j.ymgmr.2020.100584

Russell, O. M., Gorman, G. S., Lightowlers, R. N., & Turnbull, D. M. (2020). Mitochondrial Diseases: Hope for the Future. In *Cell* (Vol. 181, Issue 1, pp. 168–188). Cell Press. https://doi.org/10.1016/j.cell.2020.02.051

Russo, G. L., Sonsalla, G., Natarajan, P., Breunig, C. T., Bulli, G., Merl-Pham, J., Schmitt, S., Giehrl-Schwab, J., Giesert, F., Jastroch, M., Zischka, H., Wurst, W., Stricker, S. H., Hauck, S. M., Masserdotti, G., & Götz, M. (2021). CRISPR-Mediated Induction of Neuron-Enriched Mitochondrial Proteins Boosts Direct Glia-to-Neuron Conversion. *Cell Stem Cell*, *28*(3), 524-534.e7. https://doi.org/10.1016/j.stem.2020.10.015

Ryu, D., Mouchiroud, L., Andreux, P. A., Katsyuba, E., Moullan, N., Nicolet-Dit-Félix, A. A., Williams, E. G., Jha, P., Lo Sasso, G., Huzard, D., Aebischer, P., Sandi, C., Rinsch, C., & Auwerx, J. (2016). Urolithin A induces mitophagy and prolongs lifespan in C. elegans and increases muscle function in rodents. *Nature Medicine*, *22*(8), 879–888. https://doi.org/10.1038/nm.4132

Sadeghian, M., Mastrolia, V., Rezaei Haddad, A., Mosley, A., Mullali, G., Schiza, D., Sajic, M., Hargreaves, I., Heales, S., Duchen, M. R., & Smith, K. J. (2016). Mitochondrial dysfunction is an important cause of neurological deficits in an inflammatory model of multiple sclerosis. *Scientific Reports*, *6*. https://doi.org/10.1038/srep33249

Scacco, S., Petruzzella, V., Budde, S., Vergari, R., Tamborra, R., Panelli, D., Van den Heuvel, L. P., Smeitink,

J. A., & Papa, S. (2003). Pathological Mutations of the Human NDUFS4 Gene of the 18-kDa (AQDQ) Subunit of Complex I Affect the Expression of the Protein and the Assembly and Function of the Complex. *Journal of Biological Chemistry*, *278*(45), 44161–44167. https://doi.org/10.1074/jbc.M307615200

Schlieben, L. D., & Prokisch, H. (2020). The Dimensions of Primary Mitochondrial Disorders. In *Frontiers in Cell and Developmental Biology* (Vol. 8). Frontiers Media S.A. https://doi.org/10.3389/fcell.2020.600079

Schmukler, E., Solomon, S., Simonovitch, S., Goldshmit, Y., Wolfson, E., Michaelson, D. M., & Pinkas-Kramarski, R. (2020). Altered mitochondrial dynamics and function in APOE4-expressing astrocytes. *Cell Death and Disease*, *11*(7). https://doi.org/10.1038/s41419-020-02776-4

Schönfeld, P., & Reiser, G. (2013). Why does brain metabolism not favor burning of fatty acids to provide energy-Reflections on disadvantages of the use of free fatty acids as fuel for brain. In *Journal of Cerebral Blood Flow and Metabolism* (Vol. 33, Issue 10, pp. 1493–1499). https://doi.org/10.1038/jcbfm.2013.128

Schousboe, A. (2019). Metabolic signaling in the brain and the role of astrocytes in control of glutamate and GABA neurotransmission. In *Neuroscience Letters* (Vol. 689, pp. 11–13). Elsevier Ireland Ltd. https://doi.org/10.1016/j.neulet.2018.01.038

Scott, S. V, & Klionsky, D. J. (1998). Delivery of proteins and organelles to the vacuole from the cytoplasm. *Current Opinion in Cell Biology*, *10*, 523–529. http:/Ibiomednet.com/elecref/0955067401000523

Senft, D., & Ronai, Z. A. (2015). UPR, autophagy, and mitochondria crosstalk underlies the ER stress response. In *Trends in Biochemical Sciences* (Vol. 40, Issue 3, pp. 141–148). Elsevier Ltd. https://doi.org/10.1016/j.tibs.2015.01.002

Sharma, A., Sances, S., Workman, M. J., & Svendsen, C. N. (2020). Multi-lineage Human iPSC-Derived Platforms for Disease Modeling and Drug Discovery. In *Cell Stem Cell* (Vol. 26, Issue 3, pp. 309–329). Cell Press. https://doi.org/10.1016/j.stem.2020.02.011

Sickmann, H. M., Walls, A. B., Schousboe, A., Bouman, S. D., & Waagepetersen, H. S. (2009). Functional significance of brain glycogen in sustaining glutamatergic neurotransmission. *Journal of Neurochemistry*, *109*(SUPPL. 1), 80–86. https://doi.org/10.1111/j.1471-4159.2009.05915.x

Singh, V. K., Kalsan, M., Kumar, N., Saini, A., & Chandra, R. (2015). Induced pluripotent stem cells: Applications in regenerative medicine, disease modeling, and drug discovery. In *Frontiers in Cell and Developmental Biology* (Vol. 3, Issue FEB). Frontiers Media S.A. https://doi.org/10.3389/fcell.2015.00002

Smeitink, J., Sengers, R., Trijbels, F., & Van Den Heuvel, L. (2001). Human NADH:Ubiquinone Oxidoreductase. *Journal of Bioenergetics and Biomembranes*, *33*(3).

Smeitink J, van den Heuvel L, & DiMauro S. (2001). The genetics and pathology of oxidative phosphorylation. *Nature Reviews Genetics*, *2*, 342–352. www.nature.com/reviews/genetics

Son, M. J., Kwon, Y., Son, M. Y., Seol, B., Choi, H. S., Ryu, S. W., Choi, C., & Cho, Y. S. (2015). Mitofusins deficiency elicits mitochondrial metabolic reprogramming to pluripotency. *Cell Death and Differentiation*, *22*(12), 1957–1969. https://doi.org/10.1038/cdd.2015.43

Son, Myung Jin, Jeong, B. R., Kwon, Y., & Cho, Y. S. (2013). Interference with the mitochondrial bioenergetics fuels reprogramming to pluripotency via facilitation of the glycolytic transition. *The International Journal of Biochemistry & Cell Biology*, *45*(11). https://doi.org/10.1016/j.biocel.2013.07.023

Soyal, S. M., Felder, T. K., Auer, S., Hahne, P., Oberkofler, H., Witting, A., Paulmichl, M., Landwehrmeyer, G. B., Weydt, P., & Patsch, W. (2012). A greatly extended PPARGC1A genomic locus encodes several new brain-specific isoforms and influences Huntington disease age of onset. *Human Molecular Genetics*, *21*(15), 3461–3473. https://doi.org/10.1093/hmg/dds177

Soyal, S. M., Zara, G., Ferger, B., Felder, T. K., Kwik, M., Nofziger, C., Dossena, S., Schwienbacher, C., Hicks, A. A., Pramstaller, P. P., Paulmichl, M., Weis, S., & Patsch, W. (2019). The PPARGC1A locus and CNS-specific PGC-1α isoforms are associated with Parkinson's Disease. *Neurobiology of Disease*, *121*, 34–46. https://doi.org/10.1016/j.nbd.2018.09.016

Spinelli, J. B., & Haigis, M. C. (2018). The multifaceted contributions of mitochondria to cellular metabolism. In *Nature Cell Biology* (Vol. 20, Issue 7, pp. 745–754). Nature Publishing Group. https://doi.org/10.1038/s41556-018-0124-1

Srivastava, S. (2017). The mitochondrial basis of aging and age-related disorders. In *Genes* (Vol. 8, Issue 12). MDPI AG. https://doi.org/10.3390/genes8120398

Stanga, S., Caretto, A., Boido, M., & Vercelli, A. (2020). Mitochondrial dysfunctions: A red thread across neurodegenerative diseases. In *International Journal of Molecular Sciences* (Vol. 21, Issue 10). MDPI AG. https://doi.org/10.3390/ijms21103719

Steib, K., Schäffner, I., Jagasia, R., Ebert, B., & Chichung Lie, D. (2014). Mitochondria modify exercise-induced development of stem cell-derived neurons in the adult brain. *Journal of Neuroscience*, *34*(19), 6624–6633. https://doi.org/10.1523/JNEUROSCI.4972-13.2014

Suomalainen, A., & Battersby, B. J. (2018). Mitochondrial diseases:the contribution of organellestress responses to pathology. *Nature Reviews Molecular Cell Biology*, *19*, 77–92. https://doi.org/https://doi.org/10.1038/nrm.2017.66

Supplie, L. M., Düking, T., Campbell, G., Diaz, F., Moraes, C. T., Götz, M., Hamprecht, B., Boretius, S., Mahad, D., & Nave, K. A. (2017). Respiration-Deficient Astrocytes Survive As Glycolytic Cells In Vivo. *The Journal of Neuroscience : The Official Journal of the Society for Neuroscience*, *37*(16), 4231–4242. https://doi.org/10.1523/JNEUROSCI.0756-16.2017

Suzuki, A., Stern, S. A., Bozdagi, O., Huntley, G. W., Walker, R. H., Magistretti, P. J., & Alberini, C. M. (2011). Astrocyte-neuron lactate transport is required for long-term memory formation. *Cell*, *144*(5), 810–823. https://doi.org/10.1016/j.cell.2011.02.018

Swanson, R. A., & Choi, D. W. (1993). Glial Glycogen Stores Affect Neuronal Survival During Glucose Deprivation In Vitro. *Journal of Cerebral Blood Flow and Metabolism*, *13*, 162–169.

Takahashi, K., Tanabe, K., Ohnuki, M., Narita, M., Ichisaka, T., Tomoda, K., & Yamanaka, S. (2007). Induction of Pluripotent Stem Cells from Adult Human Fibroblasts by Defined Factors. *Cell*, *131*(5), 861–872. https://doi.org/10.1016/j.cell.2007.11.019

Takahashi, K., & Yamanaka, S. (2006). Induction of Pluripotent Stem Cells from Mouse Embryonic and Adult Fibroblast Cultures by Defined Factors. *Cell*, *126*(4), 663–676. https://doi.org/10.1016/j.cell.2006.07.024

Tan, J., Wagner, M., Stenton, S. L., Strom, T. M., Wortmann, S. B., Prokisch, H., Meitinger, T., Oexle, K., & Klopstock, T. (2020). Lifetime risk of autosomal recessive mitochondrial disorders calculated from genetic databases. *EBioMedicine*, *54*. https://doi.org/10.1016/j.ebiom.2020.102730

Thorens, B., & Mueckler, M. (2010). Glucose transporters in the 21st Century. *Am J Physiol Endocrinol Metab*,

298, 141–145. https://doi.org/10.1152/ajpendo.00712.2009.-The

Tzoulis, C., Tran, G. T., Coxhead, J., Bertelsen, B., Lilleng, P. K., Balafkan, N., Payne, B., Miletic, H., Chinnery, P. F., & Bindoff, L. A. (2014). Molecular pathogenesis of polymerase gamma-related neurodegeneration. *Annals of Neurology*, *76*(1), 66–81. https://doi.org/10.1002/ana.24185

van Deijk, A. L. F., Camargo, N., Timmerman, J., Heistek, T., Brouwers, J. F., Mogavero, F., Mansvelder, H. D., Smit, A. B., & Verheijen, M. H. G. (2017). Astrocyte lipid metabolism is critical for synapse development and function in vivo. *GLIA*, *65*(4), 670–682. https://doi.org/10.1002/glia.23120

Van Den Heuvel, L., Ruitenbeek, W., Smeets, R., Gelman-Kohan, Z., Elpeleg, O., Loeffen, J., Trijbels, F., Mariman, E., De Bruijn, D., & Smeitink, J. (1998). Demonstration of a new pathogenic mutation in human complex I deficiency: A 5-bp duplication in the nuclear gene encoding the 18-kD (AQDQ) subunit. *American Journal of Human Genetics*, *62*(2), 262–268. https://doi.org/10.1086/301716

van der Harg, J. M., van Heest, J. C., Bangel, F. N., Patiwael, S., van Weering, J. R. T., & Scheper, W. (2017). The UPR reduces glucose metabolism via IRE1 signaling. *Biochimica et Biophysica Acta - Molecular Cell Research*, *1864*(4), 655–665. https://doi.org/10.1016/j.bbamcr.2017.01.009

Verkhratsky, A., & Nedergaard, M. (2018). PHYSIOLOGY OF ASTROGLIA. *Physiology of Astroglia. Physiol Rev*, *98*, 239–389. https://doi.org/10.1152/physrev.00042.2016.-Astro

Vicente-Gutiérrez, C., Jiménez-Blasco, D., & Quintana-Cabrera, R. (2021). Intertwined ROS and Metabolic Signaling at the Neuron-Astrocyte Interface. *Neurochemical Research*, *46*(1), 23–33. https://doi.org/10.1007/s11064-020-02965-9

Vierbuchen, T., Ostermeier, A., Pang, Z. P., Kokubu, Y., Südhof, T. C., & Wernig, M. (2010). Direct conversion of fibroblasts to functional neurons by defined factors. *Nature*, *463*(7284), 1035–1041. https://doi.org/10.1038/nature08797

Vierbuchen, T., & Wernig, M. (2011). Direct lineage conversions: Unnatural but useful? In *Nature Biotechnology* (Vol. 29, Issue 10, pp. 892–907). https://doi.org/10.1038/nbt.1946

Vilchez, D., Ros, S., Cifuentes, D., Pujadas, L., Vallès, J., García-Fojeda, B., Criado-García, O., Fernández-Sánchez, E., Medrão-Fernández, I., Domínguez, J., García-Rocha, M., Soriano, E., Rodríguez De Córdoba, S., & Guinovart, J. J. (2007). Mechanism suppressing glycogen synthesis in neurons and its demise in progressive myoclonus epilepsy. *Nature Neuroscience*, *10*(11), 1407–1413. https://doi.org/10.1038/nn1998

Vogel, R. O., Smeitink, J. A. M., & Nijtmans, L. G. J. (2007). Human mitochondrial complex I assembly: A dynamic and versatile process. In *Biochimica et Biophysica Acta - Bioenergetics* (Vol. 1767, Issue 10, pp. 1215–1227). https://doi.org/10.1016/j.bbabio.2007.07.008

Völgyi, K., Gulyássy, P., Háden, K., Kis, V., Badics, K., Kékesi, K. A., Simor, A., Györffy, B., Tóth, E. A., Lubec, G., Juhász, G., & Dobolyi, A. (2015). Synaptic mitochondria: A brain mitochondria cluster with a specific proteome. *Journal of Proteomics*, *120*. https://doi.org/10.1016/j.jprot.2015.03.005

Voloboueva, L. A., Suh, S. W., Swanson, R. A., & Giffard, R. G. (2007). Inhibition of mitochondrial function in astrocytes: implications for neuroprotection. *Journal of Neurochemistry*, *0*(0), 070508225918005-??? https://doi.org/10.1111/j.1471-4159.2007.4634.x

Wade, J. J., McDaid, L. J., Harkin, J., Crunelli, V., & Kelso, J. A. S. (2011). Bidirectional coupling between astrocytes and neurons mediates learning and dynamic coordination in the brain: A multiple modeling

approach. *PLoS ONE*, *6*(12). https://doi.org/10.1371/journal.pone.0029445

Wang, M., & Kaufman, R. J. (2016). Protein misfolding in the endoplasmic reticulum as a conduit to human disease. In *Nature* (Vol. 529, Issue 7586, pp. 326–335). Nature Publishing Group. https://doi.org/10.1038/nature17041

Wang, Z., Jiang, H., Chen, S., Du, F., & Wang, X. (2012). The mitochondrial phosphatase PGAM5 functions at the convergence point of multiple necrotic death pathways. *Cell*, *148*(1–2), 228–243. https://doi.org/10.1016/j.cell.2011.11.030

Wapinski, O. L., Lee, Q. Y., Chen, A. C., Li, R., Corces, M. R., Ang, C. E., Treutlein, B., Xiang, C., Baubet, V., Suchy, F. P., Sankar, V., Sim, S., Quake, S. R., Dahmane, N., Wernig, M., & Chang, H. Y. (2017). Rapid Chromatin Switch in the Direct Reprogramming of Fibroblasts to Neurons. *Cell Reports*, *20*(13), 3236–3247. https://doi.org/10.1016/j.celrep.2017.09.011

Wapinski, O. L., Vierbuchen, T., Qu, K., Lee, Q. Y., Chanda, S., Fuentes, D. R., Giresi, P. G., Ng, Y. H., Marro, S., Neff, N. F., Drechsel, D., Martynoga, B., Castro, D. S., Webb, A. E., Südhof, T. C., Brunet, A., Guillemot, F., Chang, H. Y., & Wernig, M. (2013). Hierarchical mechanisms for direct reprogramming of fibroblasts to neurons. *Cell*, *155*(3), 621. https://doi.org/10.1016/j.cell.2013.09.028

Watts, M. E., Pocock, R., & Claudianos, C. (2018). Brain energy and oxygen metabolism: Emerging role in normal function and disease. *Frontiers in Molecular Neuroscience*, *11*. https://doi.org/10.3389/fnmol.2018.00216

Wernig, M., Meissner, A., Foreman, R., Brambrink, T., Ku, M., Hochedlinger, K., Bernstein, B. E., & Jaenisch, R. (2007). In vitro reprogramming of fibroblasts into a pluripotent ES-cell-like state. *Nature*, *448*, 318–325.

Wilson, D. F. (2017). Oxidative phosphorylation: regulation and role in cellular and tissue metabolism. In *Journal of Physiology* (Vol. 595, Issue 23, pp. 7023–7038). Blackwell Publishing Ltd. https://doi.org/10.1113/JP273839

Windrem, M. S., Osipovitch, M., Liu, Z., Bates, J., Chandler-Militello, D., Zou, L., Munir, J., Schanz, S., McCoy, K., Miller, R. H., Wang, S., Nedergaard, M., Findling, R. L., Tesar, P. J., & Goldman, S. A. (2017). Human iPSC Glial Mouse Chimeras Reveal Glial Contributions to Schizophrenia. *Cell Stem Cell*, *21*(2), 195-208.e6. https://doi.org/10.1016/j.stem.2017.06.012

Wirth, C., Brandt, U., Hunte, C., & Zickermann, V. (2016). Structure and function of mitochondrial complex i. *Biochimica et Biophysica Acta - Bioenergetics*, *1857*(7), 902–914. https://doi.org/10.1016/j.bbabio.2016.02.013

Wu, J., Ocampo, A., & Belmonte, J. C. I. (2016). Cellular Metabolism and Induced Pluripotency. In *Cell* (Vol. 166, Issue 6, pp. 1371–1385). Cell Press. https://doi.org/10.1016/j.cell.2016.08.008

Wu, Z., Puigserver, P., Andersson, U., Zhang, C., Adelmant, G., Mootha, V., Troy, A., Cinti, S., Lowell, B., Scarpulla, R. C., & Spiegelman, B. M. (1999). Mechanisms Controlling Mitochondrial Biogenesis and Respiration through the Thermogenic Coactivator PGC-1. *Cell*, *98*(1). https://doi.org/10.1016/S0092-8674(00)80611-X

Xiang, C., Wang, Y., Zhang, H., & Han, F. (2017). The role of endoplasmic reticulum stress in neurodegenerative disease. In *Apoptosis* (Vol. 22, Issue 1). Springer New York LLC. https://doi.org/10.1007/s10495-016-1296-4

Xie, H., Hou, S., Jiang, J., Sekutowicz, M., Kelly, J., & Bacskai, B. J. (2013). Rapid cell death is preceded by amyloid plaque-mediated oxidative stress. *Proceedings of the National Academy of Sciences of the United States of America*, *110*(19), 7904–7909. https://doi.org/10.1073/pnas.1217938110

Yang, Yaming, Chen, R., Wu, X., Zhao, Y., Fan, Y., Xiao, Z., Han, J., Sun, L., Wang, X., & Dai, J. (2019). Rapid and Efficient Conversion of Human Fibroblasts into Functional Neurons by Small Molecules. *Stem Cell Reports*, *13*(5), 862–876. https://doi.org/10.1016/j.stemcr.2019.09.007

Yang, Yue, & Sauve, A. A. (2016). NAD+ metabolism: Bioenergetics, signaling and manipulation for therapy. In *Biochimica et Biophysica Acta - Proteins and Proteomics* (Vol. 1864, Issue 12, pp. 1787–1800). Elsevier B.V. https://doi.org/10.1016/j.bbapap.2016.06.014

Yao, J., Irwin, R. W., Zhao, L., Nilsen, J., Hamilton, R. T., & Brinton, R. D. (2009). Mitochondrial bioenergetic deficit precedes Alzheimer's pathology in female mouse model of Alzheimer's disease. *Proceedings of the National Academy of Sciences*, *106*(34), 14670–14675. https://doi.org/10.1073/PNAS.0903563106

Yin, J. C., Zhang, L., Ma, N. X., Wang, Y., Lee, G., Hou, X. Y., Lei, Z. F., Zhang, F. Y., Dong, F. P., Wu, G. Y., & Chen, G. (2019). Chemical Conversion of Human Fetal Astrocytes into Neurons through Modulation of Multiple Signaling Pathways. *Stem Cell Reports*, *12*(3), 488–501. https://doi.org/10.1016/j.stemcr.2019.01.003

Ying, Z., Chen, K., Zheng, L., Wu, Y., Li, L., Wang, R., Long, Q., Yang, L., Guo, J., Yao, D., Li, Y., Bao, F., Xiang, G., Liu, J., Huang, Q., Wu, Z., Hutchins, A. P., Pei, D., & Liu, X. (2016). Transient Activation of Mitoflashes Modulates Nanog at the Early Phase of Somatic Cell Reprogramming. *Cell Metabolism*, *23*(1), 220–226. https://doi.org/10.1016/j.cmet.2015.10.002

Yoshida, Y., Takahashi, K., Okita, K., Ichisaka, T., & Yamanaka, S. (2009). Hypoxia Enhances the Generation of Induced Pluripotent Stem Cells. In *Cell Stem Cell* (Vol. 5, Issue 3, pp. 237–241). https://doi.org/10.1016/j.stem.2009.08.001

Youle, R. J., & Narendra, D. P. (2011). Mechanisms of mitophagy. *Nature Reviews Molecular Cell Biology*, *12*(1), 9–14. https://doi.org/10.1038/nrm3028

Zhang, L., Yin, J. C., Yeh, H., Ma, N. X., Lee, G., Chen, X. A., Wang, Y., Lin, L., Chen, L., Jin, P., Wu, G. Y., & Chen, G. (2015). Small Molecules Efficiently Reprogram Human Astroglial Cells into Functional Neurons. *Cell Stem Cell*, *17*(6), 735–747. https://doi.org/10.1016/j.stem.2015.09.012

Zhang, Y., Chen, K., Sloan, S. A., Bennett, M. L., Scholze, A. R., O'Keeffe, S., Phatnani, H. P., Guarnieri, P., Caneda, C., Ruderisch, N., Deng, S., Liddelow, S. A., Zhang, C., Daneman, R., Maniatis, T., Barres, B. A., & Wu, J. Q. (2014). An RNA-sequencing transcriptome and splicing database of glia, neurons, and vascular cells of the cerebral cortex. *Journal of Neuroscience*, *34*(36), 11929–11947. https://doi.org/10.1523/JNEUROSCI.1860-14.2014

Zhao, L., & Ackerman, S. L. (2006). Endoplasmic reticulum stress in health and disease. In *Current Opinion in Cell Biology* (Vol. 18, Issue 4, pp. 444–452). https://doi.org/10.1016/j.ceb.2006.06.005

Zheng, X., Boyer, L., Jin, M., Mertens, J., Kim, Y., Ma, L., Ma, L., Hamm, M., Gage, F. H., & Hunter, T. (2016). Metabolic reprogramming during neuronal differentiation from aerobic glycolysis to neuronal oxidative phosphorylation. *ELife*, *5*. https://doi.org/10.7554/eLife.13374

Zhou, H., Liu, J., Zhou, C., Gao, N., Rao, Z., Li, H., Hu, X., Li, C., Yao, X., Shen, X., Sun, Y., Wei, Y., Liu, F., Ying, W., Zhang, J., Tang, C., Zhang, X., Xu, H., Shi, L., … Yang, H. (2018). In vivo simultaneous

transcriptional activation of multiple genes in the brain using CRISPR-dCas9-activator transgenic mice. *Nature Neuroscience*, *21*(3), 440–446. https://doi.org/10.1038/s41593-017-0060-6

Zhou, H., Su, J., Hu, X., Zhou, C., Li, H., Chen, Z., Xiao, Q., Wang, B., Wu, W., Sun, Y., Zhou, Y., Tang, C., Liu, F., Wang, L., Feng, C., Liu, M., Li, S., Zhang, Y., Xu, H., … Yang, H. (2020). Glia-to-Neuron Conversion by CRISPR-CasRx Alleviates Symptoms of Neurological Disease in Mice. *Cell*, *181*(3), 590-603.e16. https://doi.org/10.1016/j.cell.2020.03.024

Zhou, R., Yazdi, A. S., Menu, P., & Tschopp, J. (2011). A role for mitochondria in NLRP3 inflammasome activation. *Nature*, *469*(7329), 221–226. https://doi.org/10.1038/nature09663

Zhu, S., Li, W., Zhou, H., Wei, W., Ambasudhan, R., Lin, T., Kim, J., Zhang, K., & Ding, S. (2010). Reprogramming of human primary somatic cells by OCT4 and chemical compounds. In *Cell Stem Cell* (Vol. 7, Issue 6, pp. 651–655). Cell Press. https://doi.org/10.1016/j.stem.2010.11.015

Zielke, H. R., Zielke, C. L., & Baab, P. J. (2009). Direct measurement of oxidative metabolism in the living brain by microdialysis: A review. *Journal of Neurochemistry*, *109*(SUPPL. 1), 24–29. https://doi.org/10.1111/j.1471-4159.2009.05941.x

List of publications

- Russo, G. L., Sonsalla, G., Natarajan, P., Breunig, C. T., Bulli, G., Merl-Pham, J., Schmitt, S., Giehrl-Schwab, J., Giesert, F., Jastroch, M., Zischka, H., Wurst, W., Stricker, S. H., Hauck, S. M., Masserdotti, G., & Götz, M. (2021)
  CRISPR-Mediated Induction of Neuron-Enriched Mitochondrial Proteins Boosts Direct Glia-to-Neuron Conversion.
  Cell Stem Cell, 28(3): 524–534.e7.

- Sonsalla, G., Riedemann, T., Gusic, M., Rusha, E., Drukker, M., Najas, S., Janjic, A., Enard, W., Smialowski, P., Prokisch, H., Götz, M. & Masserdotti, G.
  Mitochondrial deficiency limits the direct neuronal reprogramming of human cells
  Manuscript in preparation

Acknowledgements

First of all, I am very thankful to my supervisor Magdalena Götz for the opportunity to work and study as a PhD student in her lab. **Thank you, Magdalena**, not only for the fascinating projects and the many stimulating discussions, but also for supporting me and pushing me to become better, both scientifically and personally. The invigorating scientific environment you foster provided me with many growth experiences over the years. I am grateful for your continued encouragement and, without a doubt, the time I have spent in your lab has been incredibly rewarding.

Many thanks to my co-supervisor Giacomo Masserdotti, who spent countless hours teaching me various scientific techniques and discussing my projects. **Thank you, Giacomo**, for your steadfast support, whether that be conversing about science, untangling some gnarly RNAseq data, or driving my cells to different labs around Munich. I greatly appreciate all of the time and energy you spent, not only on helping me with experimental designs, but also with practicing my many presentations. Your constant guidance has been an instrumental part of my PhD, thank you!

I am very grateful that I was surrounded by such an amazing group of colleagues, who provided both indispensable scientific feedback, as well as emotional support. Thank you very much to Judith T. (PhD buddy extraordinaire), Gianluca (social butterfly with the best hugs), Elisa (co-conspirator, the best advice and pizza), Manja (constant help and laughs), Matteo (provider of both fabulous Italian food and drama), Sergio, Amel, Chu Lan, Steffi, Ilaria, Riccardo, Allwyn, Bob, Poornemaa, Sonia, Miriam, Giorgia and Florencia. Also special thanks to the iPSC group members (Kalina, Giulia, and Adam), who helped share the load of daily cell culture over the years and provided constant invaluable input. Throughout the stress of the PhD I was always happy to come to the lab because there was such an awesome environment of support. We managed to work hard but also create the all-important moments of fun, both inside and outside of the lab. Finally, thank you to the lab members and technicians whose essential contribution maintained a well-functioning lab: Tatiana, Martina, Elsa, Judith F., Ines, Andrea, Detlef, Gül, and all others. I am beyond thankful for the chance to have worked in such a great group!

A big thank you to the GSN, who provided a great network of support during my studies. I am also grateful to my TAC members Silvia Cappello and Holger Prokisch for their essential expertise throughout the years of my PhD studies. The GSN fast-track preparatory year was a great foundation for my PhD, and the many activities and retreats organized by the GSN established some great friendships. Thanks to my GSN colleagues with whom I have created a lot of unforgettable memories, especially Tobi, Nejc, Inanna, Alicia, Duncan, Sandra, Sophie, Mike, and Sebastian. These last few years would not have been the same without the incredible support from, in particular, Nadya (my kindred-spirit and fellow bookworm) and Dóra (amazing girls nights, salsa dancing, and drama).

A special thanks to my wonderful friends around the world who have supported me both virtually and in person throughout my studies. Thanks to the crew from the University of St. Andrews, especially Ellen, Carl, Ondrej, Akie, Albina, Yukiko and Anne Marie. Also, a big shout-out to my friends from back home, Danica (20 years of friendship and going strong) and Nikki (the best New Year's Eve partner), who continue to follow me on my escapades.

Most of all, thank you very much to my family for their immense love and support! Thank you to my parents, who always encourage me to embrace new adventures. Thank you to my sister, the best partner in crime who never fails to make me laugh. Thank you to my Sonsalla and Boduch grandparents, who have provided an indispensable stream of love, prayers, and care packages. I am so grateful that despite my travels around the world we still maintain such strong relationships.

Finally, thank you, Dominic, for the endless support and love you have provided during these stressful years of my PhD studies. Thank you for your patience and advice, and for making heaps of delicious food. I am very lucky to have had you by my side during this journey.

Declaration of Author Contribution

1. Russo, G. L., **Sonsalla, G.,** Natarajan, P., Breunig, C. T., Bulli, G., Merl-Pham, J., Schmitt, S., Giehrl-Schwab, J., Giesert, F., Jastroch, M., Zischka, H., Wurst, W., Stricker, S. H., Hauck, S. M., Masserdotti, G.*, & Götz, M.* (2021)
   "CRISPR-Mediated Induction of Neuron-Enriched Mitochondrial Proteins Boosts Direct Glia-to-Neuron Conversion"
   Cell Stem Cell, 28(3): 524–534.e7.

   *Co-last author

   M.G. conceived and designed the project. G.L.R. and G.M. shaped the project, and G.L.R. performed experiments and analysis. ***G.S. contributed to the time course analysis.*** P.N. performed and analyzed the experiment with etomoxir, gRNA, and continuous live imaging. C.T.B. and S.H.S. provided CRISPR-Cas expertise and developed and designed the STAgR approach, and C.T.B. helped with cloning of the constructs. G.B. performed western blots. J.M.-P. and S.M.H. providedproteomics expertise and performed experiments and analysis. S.S. and H.Z. performed mitochondrial isolation and electron microscopy. J.G.-S., F.G., and W.W. generated and provided dCAM transgenic mice. M.J. provided expertise regarding metabolism and Seahorse analysis. G.M. analyzed the data; provided expertise and training of G.L.R., G.S., P.N., and G.B. regarding reprogramming; and co-directed the project together with M.G. G.L.R., G.M., and M.G. wrote the manuscript, ***and all authors contributed to corrections and comments***.

2. **Sonsalla, G.,** Riedemann, T., Gusic, M., Rusha, E., Drukker, M., Najas, S., Janjic, A., Enard, W., Smialowski, P., Prokisch, H., Götz, M.* & Masserdotti, G.*

   "Mitochondrial deficiency limits the direct neuronal reprogramming of human cells"

   Manuscript ready for submission

   *Co-last author

   M.G. and G.M. conceived and designed the project. ***G.S., G.M., and M.G. developed the project, and G.S. performed experiments and analyzed the results.*** T.R. conducted the electrophysiology experiments. M.G. provided expertise on metabolism and the Seahorse Assay. E.R. and M.D. generated the iPSC cell lines used in the study. S.N. provided initial evidence of UPR in reprogramming. A.J. prepared bulk-adapted mcscrb-seq libraries and W.E. provided expertise. H.P. provided the NDUFS4-mutant patient cell lines, and expertise

regarding the patients andmetabolism. G.M. analyzed the RNAseq data and provided expertise and training of G.S. regarding direct neuronal reprogramming. P.S. demultiplexed and aligned the RNA-seq libraries. G.M and M.G. co-directed the project. ***G.S., G.M., and M.G. wrote the manuscript.*** All authors contributed to corrections and comments.

Signature Prof. Dr. Magdalena Götz

Signature Dr. Gianluca Russo

Signature Giovanna Sonsalla

Affidavit

Eidesstattliche Versicherung/Affidavit

Hiermit versichere ich an Eides statt, dass ich die vorliegende Dissertation **"The Role of Mitochondria in Direct Neuronal Reprogramming and its Relevance for Disease"** selbstständig angefertigt habe, mich außer der angegebenen keiner weiteren Hilfsmittel bedient und alle Erkenntnisse, die aus dem Schrifttum ganz oder annähernd übernommen sind, als solche kenntlich gemacht und nach ihrer Herkunft unter Bezeichnung der Fundstelle einzeln nachgewiesen habe.

I hereby confirm that the dissertation **"The Role of Mitochondria in Direct Neuronal Reprogramming and its Relevance for Disease"** is the result of my own work and that I have only used sources or materials listed and specified in the dissertation.

München, den Munich, date	Unterschrift Signature
Munich, 28.05.2021	Giovanna Rose Sonsalla